Development and preclinical assessment of novel therapies for Epilepsy. Exploring the potential of human-derived cell lines and glial cell line-derived neurotrophic factor for network inhibition.

Waloschkova, Eliska

2022

Document Version:
Publisher's PDF, also known as Version of record

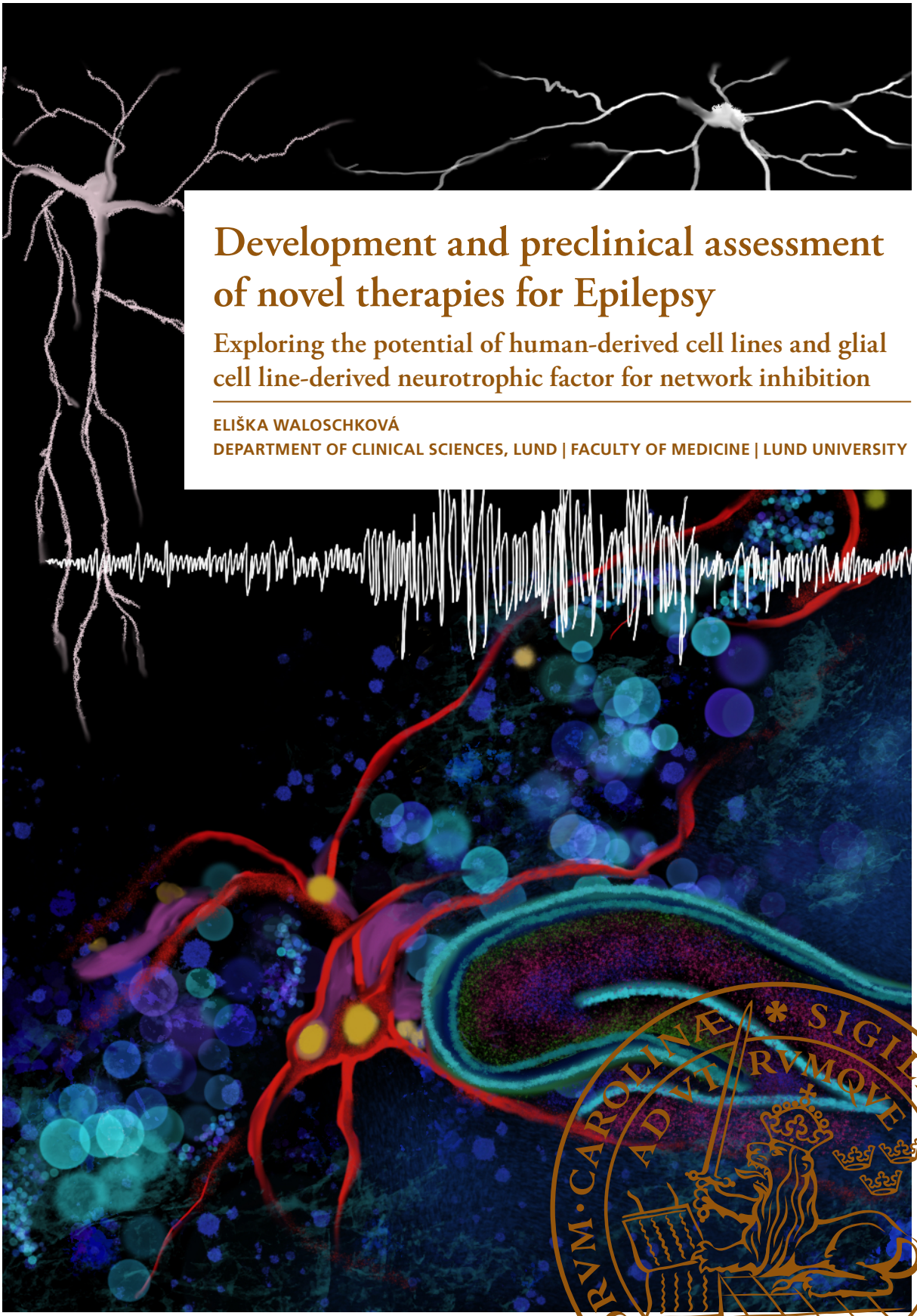

Development and preclinical assessment of novel therapies for Epilepsy

Exploring the potential of human-derived cell lines and glial cell line-derived neurotrophic factor for network inhibition

ELIŠKA WALOSCHKOVÁ
DEPARTMENT OF CLINICAL SCIENCES, LUND | FACULTY OF MEDICINE | LUND UNIVERSITY

Development and preclinical assessment of novel therapies for Epilepsy

Exploring the potential of human-derived cell lines and glial cell line-derived neurotrophic factor for network inhibition

Eliška Waloschková

LUND
UNIVERSITY

DOCTORAL DISSERTATION

by due permission of the Faculty of Medicine, Lund University, Sweden.
To be defended at GK-salen, BMC I11, on Friday the 22nd of April 2022 at 9.15.

Faculty opponent
Professor **William Gray** MD, PhD
Neuroscience & Mental Health Research Institute, School of Medicine
Cardiff University, United Kingdom

Organization	Document name
LUND UNIVERSITY Faculty of Medicine Department of Clinical Sciences Epilepsy Centre	DOCTORAL DISSERTATION **Date of issue** 2022-04-22
Author Eliška Waloschková	Sponsoring organization

Title and subtitle

Development and preclinical assessment of novel therapies for Epilepsy: Exploring the potential of human-derived cell lines and glial cell line-derived neurotrophic factor for network inhibition

Abstract

Epilepsy is one of the leading neurological disorders affecting not only patients who suffer from seizures but also people around them and society in general. The striking one third of patients not responding to pharmacological treatments implies the necessity of developing alternative options for controlling seizures in these individuals. Moreover, the possibility to stop the progression of the disease before seizures occur would pose a viable option in the future. A rising treatment approach targeting focal epilepsies, such as temporal lobe epilepsy (TLE), commonly diagnosed as pharmacoresistant, is cell therapy. The results presented in this thesis, reflect the efforts to suppress seizures in the chronic phase of epilepsy by transplanting inhibitory GABAergic interneurons, and to ameliorate the outcomes of epileptogenesis after a brain-damaging insult by transplanting mesenchymal stem cells (MSCs) alone or modified to release glial cell line-derived neurotrophic factor (GDNF). These studies were performed in the post-status epilepticus (SE) rat model of TLE induced by systemic kainic acid injections.

Using electrophysiology and optogenetics, the maturation and synaptic integration of human embryonic stem cell-derived GABAergic interneurons (hdInts) was confirmed *in vitro* in human neuronal networks and *in vivo* in the hippocampi of the rat TLE model. In both cases the cells differentiated mostly into calretinin and calbindin interneuron subtypes confirmed by immunohistochemistry. In hippocampal slices from the epileptic animals the optogenetic activation of these cells reduced epileptiform activity and with video monitoring, fewer seizures were detected in animals treated with hdInts.

GDNF has reported anti-seizure effects in animal epilepsy models. The mechanism of this inhibitory potential was investigated, specifically how GDNF acts on principal neurons in the mouse and human hippocampus. An increase in frequency and amplitude of inhibitory postsynaptic currents was observed electrophysiologically. Additionally, this effect was attributed to the GDNF family receptor alpha-1 and the transmembrane receptor tyrosine kinase signalling pathway using electrophysiology and western blot.

Next, the use of GDNF was combined with the use of MSCs as carriers. This approach was implemented to modify epileptogenesis by transplanting either naïve MSCs or GDNF-releasing MSCs into the hippocampi of rats one day after SE. Both cell types altered the progress of epileptogenesis as seen by analysing 35 days of continuous video-EEG recordings, the MSCs alone reducing seizure occurrence and the GDNF-MSCs prolonging the intervals between seizures. Some behavioural alterations of the epileptic animals were partially corrected after 5 weeks of monitoring, however, the elevated microglia activation was not changed by either of the cell types.

In summary, the data presented in this thesis contribute to the development of the growing field of novel therapeutic approaches for epilepsy which may in the future benefit those patients whose seizures cannot be controlled by conventional drugs, or even prevent seizures from occurring.

Key words

Epilepsy, epileptogenesis, inhibition, cell therapy, GABAergic interneurons, mesenchymal stem cells, GDNF

Classification system and/or index terms (if any)

Supplementary bibliographical information		**Language** English
ISSN and key title 1652-8220		**ISBN** 978-91-8021-216-8
Recipient's notes	**Number of pages** 91	Price
	Security classification	

Signature  Date 2022-03-15

Development and preclinical assessment of novel therapies for Epilepsy

Exploring the potential of human-derived cell lines and glial cell line-derived neurotrophic factor for network inhibition

Eliška Waloschková

LUND
UNIVERSITY

Cover artwork by Lucie Niebauerová Waloschková

Faculty of Medicine
Department of Clinical Sciences, Lund

ISBN 978-91-8021-216-8
ISSN 1652-8220
Lund University, Faculty of Medicine Doctoral Dissertation Series 2022:55

Printed in Sweden by Media-Tryck, Lund University
Lund 2022

To my family

"Don't panic."
Douglas Adams, The Hitchhiker's Guide to the Galaxy

Table of Contents

Summary

Epilepsy is an often-stigmatized condition affecting the brain. Patients with epilepsy do not only suffer from seizures but also often experience difficulties within society. However, in most patients, seizures can be suppressed by anti-seizure medication. Still, despite this, about one third of them do not respond to this treatment and they suffer from uncontrollable seizures. These patients in the majority of cases suffer from focal epilepsies, meaning that the seizures originate from a specific location in the brain. In some cases, surgical resection of the epileptic focus is an effective remedy, but this is not available for everyone and often does not completely stop seizure occurrence. Therefore, other treatment options are being developed for these patients, including cell and gene therapies.

In temporal lobe epilepsy (TLE), a type of focal epilepsy where seizures originate from this specific brain region, the hippocampus, a structure responsible, e.g., for memory formation and navigation, is often affected. This can be caused by a brain-damaging insult where cellular and molecular alterations in the hippocampus after a certain time result in hyperexcitability of the tissue and a reduced seizure threshold. Possible therapeutic interventions could therefore be introduced even before the patient develops spontaneous seizures, i.e., during the latent period after the insult called epileptogenesis. In this thesis, we used animal models of TLE and tried to increase inhibition in the hippocampus to either suppress spontaneous seizures in chronic epilepsy or modify the epileptogenesis processes.

For this purpose, we generated inhibitory neurons, so-called GABAergic interneurons, from human embryonic stem cells (hESCs). These cells are capable of inhibiting other neurons due to their release of gamma-aminobutyric acid (GABA), which is the main inhibitory neurotransmitter of the brain. The hESC-derived cells functionally matured *in vitro* into GABAergic interneurons capable of forming inhibitory synapses onto other human neurons either derived from foetal brains or located in tissue resected from patients with epilepsy. These results encouraged us to move forward to examine the potential of these cells *in vivo*. For this, we utilised a rat model of TLE. We induced status epilepticus (SE) in rats by systemically injecting kainic acid, and four weeks after the SE, transplanted hESC-derived GABAergic precursors into the hippocampi of these animals. The transplanted cells were able to survive in the host tissue and mature into functional GABAergic interneurons over time. Their formation of functional

inhibitory synapses towards the host neurons was also confirmed and we assumed this resulted in the observed reduction of spontaneous seizure frequency in the treated animals.

In the second half of this thesis, we investigated mechanisms by which the glial cell line-derived neurotrophic factor (GDNF) could suppress seizures, as shown in previous studies. We used electrophysiology to elucidate the specific actions of GDNF on principal neurons of the hippocampus. In both mouse and human hippocampal slices GDNF increased the inhibitory drive onto these cells, which we then attributed to a specific signalling pathway, including the GDNF family receptor alpha-1 (GFRα1) and the transmembrane receptor tyrosine kinase (Ret). We used this knowledge further and genetically modified mesenchymal stem cells (MSCs) to produce GDNF. MSCs have reportedly anti-inflammatory and neuroprotective properties and we therefore asked whether these cells, also releasing GDNF, could have anti-epileptogenic effects in an animal TLE model. We used a similar model as before, but this time transplanted the cells one day after the SE induction, targeting early epileptogenesis. Both the unmodified MSCs and the GDNF-MSCs altered the development of epilepsy, the former reduced the number of animals that developed spontaneous seizures and lowered seizure frequencies, while the latter decreased seizure incidence during the first two weeks after SE but not at the later stages. Certain behavioural alterations, such as short-term memory deficits or higher anxiety levels, were also ameliorated by both cell lines.

Taken together, these data provide several promising strategies towards developing novel treatments for epilepsy. This thesis explored the use of two distinct pathways, both focusing on increasing network inhibition, and offers valuable information that can be used to further advance the development of the proposed therapeutic approaches.

Populárně-vědecké shrnutí

Epilepsie je často stigmatizovaná nemoc postihující mozek. Pacienti s epilepsií trpí nejen nepředvídatelnými záchvaty, a právě tato nepředvídatelnost bývá často překážkou pro společenský život. U většiny pacientů však lze záchvaty potlačit specifickými léky. Přesto stále asi třetina z nich na tuto léčbu nereaguje a trpí nekontrolovatelnými epileptickými záchvaty. Tito pacienti ve většině případů trpí fokálními epilepsiemi, tedy epilepsiemi, jejichž zdrojem je konkrétní místo v mozku. V některých případech je účinným terapeutickým prostředkem chirurgická resekce epileptického ložiska, která však není dostupná pro každého a často zcela nezastaví výskyt záchvatů. Proto se pro tyto pacienty vyvíjejí další možnosti léčby, včetně buněčné a genové terapie.

Jedním z typů fokálních epilepsií je epilepsie spánkového laloku (temporal lobe epilepsy, TLE), u níž, jak již název napovídá, pocházejí záchvaty z této konkrétní oblasti mozku, a při níž je často postižen hipokampus, struktura zodpovědná za eg. ukládaní vzpomínek a prostorovou navigaci. Tento druh epilepsie je často způsoben poškozením mozku, kdy buněčné a molekulární změny v hipokampu po určité době vedou k nadměrné excitabilitě tkáně a snížení prahu záchvatů. Možné terapeutické intervence by tedy mohly být zavedeny ještě dříve, než se u pacienta objeví spontánní záchvaty, tedy v průběhu zmíněné latentní fáze po počátečním úrazu, která se nazývá epileptogeneze. V této disertační práci jsme použili zvířecí modely TLE a pokusili se zvýšit inhibici v hipokampu a buď potlačit spontánní záchvaty v chronické fázi epilepsie, nebo modifikovat procesy epileptogeneze.

Jako první terapeutickou možnost jsme v laboratoři vytvořili inhibiční neurony, tzv. GABAergní interneurony, z lidských embryonálních kmenových buněk (human embryonic stem cells, hESC). Tyto buňky jsou schopny inhibovat další neurony díky tomu, že uvolňují kyselinu gama-aminomáselnou (gamma-aminobutyric acid, GABA), která je hlavním inhibičním neurotransmiterem v mozku. Tyto buňky odvozené od hESC funkčně maturovaly *in vitro* v GABAergní interneurony schopné tvořit inhibiční synapse s dalšími lidskými neurony, které byly buď derivované z kortexů potracených plodů, nebo umístěné v mozkové tkáni získané z chirurgické resekce epileptických pacientů. Tyto výsledky nás nasměrovaly k tomu, abychom pokročili vpřed ke zkoumání potenciálu stejných buněk *in vivo*. K tomu jsme použili potkaní model TLE. U potkanů jsme vyvolali status epilepticus (SE) systémovými injekcemi kyseliny kainové a čtyři týdny poté jsme transplantovali GABAergní prekurzory odvozené od

hESC do hipokampů těchto zvířat. Transplantované buňky byly schopny integrace do hostitelské tkáně a časem dozrály ve funkční GABAergní interneurony. Jejich tvorba funkčních inhibičních synapsí směrem k hostitelským neuronům byla také potvrzena a my jsme se mohli domnívat, že to bylo důvodem k viditelnému snížení frekvence spontánních epileptických záchvatů u těchto zvířat.

V druhé polovině této práce jsme zkoumali inhibiční potenciál neurotrofního faktoru odvozeného z gliálních buněk (glial cell line-derived neurotrophic factor, GDNF). Bylo prokázáno, že tento neurotrofní faktor má vlastnosti redukující epileptické záchvaty u zvířecích modelů epilepsie; mechanismus jeho působení však nebyl plně pochopen. Použitím elektrofyziologie jsme se pokusili objasnit specifické účinky GDNF na hlavní excitační neurony hippocampu. V myších i lidských hipokampálních řezech měla aplikace GDNF za následek zvýšení inhibice na tyto buňky, což jsme následně přisoudili specifické signální dráze, která sestává mimo jiné z receptoru alfa-1 rodiny GDNF (GFRα1) a transmembránové receptorové tyrosinkinázy (Ret). Tyto poznatky jsme dále vytěžili a geneticky modifikovali mezenchymální kmenové buňky (mesenchymal stem cells, MSC) k produkci GDNF. MSC mají údajně protizánětlivé a neuroprotektivní vlastnosti, a proto jsme si položili otázku, zda by tyto buňky s adicí GDNF mohly mít antiepileptogenní účinky ve zvířecím modelu TLE. Použili jsme stejný model potkana jako dříve, ale tentokrát jsme buňky transplantovali jeden den po indukci SE se zaměřením na epileptogenezi. Jak nemodifikované MSC, tak GDNF-MSC pozměnily vývoj epilepsie, ty nemodifikované snížily počet zvířat, u kterých se vyvinuly spontánní záchvaty a snížily frekvenci záchvatů, oproti tomu GDNF buňky měly spíše brzký účinek a prodloužily intervaly mezi záchvaty. U obou buněčných linií byly také do určité míry korigovány změny chování asociované s epilepsií.

Celkově vzato existuje několik slibných strategií k vývoji nových způsobů léčby epilepsie. Tato práce zkoumala použití dvou odlišných cest, přičemž obě se zaměřovaly na zvýšení inhibice. V této práci poskytujeme cenná data, která lze použít k dalšímu pokroku ve vývoji těchto inovativních terapeutických přístupů.

Populärvetenskaplig sammanfattning

Epilepsi är ett ofta stigmatiserat tillstånd som påverkar hjärnan. Epilepsipatienter lider vanligtvis inte bara av anfall utan upplever ofta svårigheter i samhället. För de flesta patienter kan anfallen förhindras med anti-epileptiska mediciner. Dessa läkemedel är dock inte verksamma i ungefär en tredjedel av epilepsipatienter, vilka lider av okontrollerbara anfall. Majoriteten av dessa fall lider av fokala epilepsier, dvs att anfallen börjar från en specifik plats i hjärnan. I vissa fall kan dessa områden tas bort kirurgiskt, men detta är inte genomförbart för alla patienter och stoppar ofta inte anfallen fullständigt. Därför utvecklas nu alternativa behandlingsmetoder för dessa patienter, bland annat cell- och genterapier.

Temporallobsepilepsi (TLE) är en typ av fokal epilepsi där anfallen uppkommer i tinningloben och ofta leder till problem med nervkopplingarna i hippocampus, ett område som är viktigt för bland annat inlagring av långtidsminnen och navigering. TLE orsakas ofta av någon form av hjärnskada där cellulära och molekylära förändringar i hippocampus så småningom leder till hyperexcitabilitet. Denna hyperexcitabilitet kan sedan sänka tröskeln för initiering av epileptiska anfall. Möjliga terapier skulle därför kunna introduceras även innan patienten utvecklar spontana epilepsianfall, under den process som kallas epileptogenes. I denna avhandling har vi använt djurmodeller av TLE för att försöka öka inhibitoriska signaler i hippocampus och antingen hämma spontana epilepsianfall i kronisk epilepsi eller modifiera epileptogenesen.

Först genererade vi inhibitoriska neuron, så kallade GABAerga interneuron, från humana embryonala stamceller (hESCs). Dessa celler är kapabla att inhibera andra neuron på grund av deras frisättning av gamma-aminobutyrisk syra (GABA), som är den huvudsakliga inhibitoriska signalsubstansen i centrala nervsystemet. De genererade GABAerga cellerna mognade funktionellt i kultur och visade sig kapabla att forma inhibitoriska synapser på andra humana neuron, vilka antingen isolerats från humana embryon eller från vävnad som kirurgiskt avlägsnats från epileptiska patienter. Dessa resultat drev oss till att prova dessa cellers potential *in vivo.* För att göra detta använde vi oss av en råttmodell av TLE där man injicerar kainsyra systemiskt för att inducera status epilepticus, varefter hESC-genererade GABAerga prekursorceller transplanterades in i hippocampus fyra veckor efter injektionerna. Cellerna i transplantatet överlevde ympningsprocessen och mognade med tid till GABAerga neuron, vilka bekräftades forma inhibitoriska synapser med värdneuron. Vi antar att

detta resulterade i den minskning av mängden spontana epilepsianfall hos behandlade djur.

I den andra halvan av avhandlingen utforskar vi den inhibitoriska potentialen av gliacellinjederiverad neurotrofisk faktor (GDNF). Denna neurotrofiska faktor har visat sig ha anti-epileptiska egenskaper, vars mekanism ej är helt förstådd. Vi utnyttjade elektrofysiologi för att klargöra de specifika effekterna som GDNF har på de excitatoriska cellerna i hippocampus. I hjärnsnitt av hippocampus från både mus och människa har GDNF en ökande effekt på inhibitoriskt driv, vilket vi kunde attribuera till en specifik signaleringsväg. Denna signaleringsväg involverar receptorn GFRα1 samt tyrosinkinasreceptorn Ret. Vi använde denna kunskap ytterligare och utnyttjade genetiskt modifierade mesenkymala stamceller (MSCs) för att producera GDNF. MSCs har rapporterats ha anti-inflammatoriska och nervcellskyddande egenskaper och vi undrade därför huruvida celler som uttrycker GDNF skulle kunna ha anti-epileptogena effekter i en TLE-modell. Vi använde en liknande djurmodell som tidigare men transplanterade istället cellerna en dag efter SE, med målet att påverka epileptogenesen. Både de icke-modifierade och de modifierade MSCs påverkade utvecklingen av kronisk epilepsi. De icke-modifierade minskade mängden djur som utvecklade epilepsi samt minskade frekvensen mellan spontana anfall medan de modifierade hade en tidig effekt samt förlängde intervallen mellan anfall. Vissa beteendeförändringar korrigerades till viss del av båda cellinjer.

För att sammanfatta.

Det finns flera lovande behandlingstrategier som kan utvecklas till nya terapier för epilepsi. Denna avhandling har utforskat användandet av två distinkta vägar som båda fokuserar på att öka inhibition och bidrar med värdefulla data som kan användas för att utveckla nya cellbaserade terapier för epilepsi.

Original papers and manuscripts

I. Ana Gonzalez-Ramos, **Eliška Waloschková**, Apostolos Mikroulis, Zaal Kokaia, Johan Bengzon, Marco Ledri, My Andersson, Merab Kokaia. Human stem cell-derived GABAergic neurons functionally integrate into human neuronal networks. *Scientific Reports,* 11:22050 (2021)

II. **Eliška Waloschková**, Ana Gonzalez-Ramos, Apostolos Mikroulis, Jan Kudláček, My Andersson, Marco Ledri, Merab Kokaia. Human Stem Cell-Derived GABAergic Interneurons Establish Efferent Synapses onto Host Neurons in Rat Epileptic Hippocampus and Inhibit Spontaneous Recurrent Seizures. *International Journal of Molecular Sciences,* 22(24):13243 (2021)

III. Apostolos Mikroulis, **Eliška Waloschková**, Johan Bengzon, David Woldbye, Lars H. Pinborg, Bo Jespersen, Anna Sanchez Avila, Zsofia Laszlo, Christopher Henstridge, Marco Ledri, Merab Kokaia. GDNF increases inhibitory synaptic drive on principal neurons in the hippocampus via activation of the Ret pathway. *Manuscript*

IV. **Eliška Waloschková**, Esbjörn Melin, Camille Baumlin, My Andersson, Marco Ledri, Alberto Martínez Serano, Merab Kokaia. Alteration of epileptogenesis in a rat epilepsy model by transplanting human mesenchymal stem cells with and without GDNF release. *Manuscript*

Abbreviations

AAV	Adeno-associated virus
aCSF	Artificial cerebrospinal fluid
AHP	Afterhyperpolarisation
AMPA	Alpha-amino-3-hydroxy-5-methyl-4-isoxazole propionic acid
Ara-C	Cytosine-D-arabinofuranoside
ASMs	Anti-seizure medications
AP	Action potential / Anterior-posterior
BBB	Blood-brain barrier
BDNF	Brain-derived neurotrophic factor
CA	Cornu Ammonis
CB	Calbindin
ChR2	Channelrhodopsin-2
CNS	Central nervous system
Cm	Membrane capacitance
CR	Calretinin
Ctrl	Control
DAB	Diaminobenzidine
DALYs	Disability-adjusted life years
D-AP5	(2R)-amino-5-phosphonovaleric acid
DG	Dentate gyrus
DIV	Days *in vitro*
DV	Dorsal-ventral
EEG	Electroencephalogram

EC	Entorhinal cortex
ELISA	Enzyme-linked immunosorbent assay
ESCs	Embryonic stem cells
ETSP	Epilepsy Therapy Screening Program
FBS	Foetal bovine serum
FCD	Focal cortical dysplasia
FGF-2	Fibroblast growth factor 2
GABA	Gamma-aminobutyric acid
GDNF	Glial cell line-derived neurotrophic factor
GFP	Green fluorescent protein
GFRα1	GDNF family receptor alpha-1
hdInts	Human embryonic stem cell-derived interneurons
hiAD-MSCs	Human immortalised adipose-derived mesenchymal stem cells
hESCs	Human embryonic stem cells
ILAE	International League Against Epilepsy
iPSCs	Induced pluripotent stem cells
IPSCs	Inhibitory postsynaptic currents
ISIs	Inter-seizure intervals
KA	Kainic acid
LFP	Local field potential
MGE	Medial ganglionic eminence
ML	Medial-lateral
MSCs	Mesenchymal stem cells
NBQX	2,3-dihydroxy-6-nitro-7-sulfamoyl-benzo-quinoxaline-2,3-dione disodium salt
NCAM	Neural cell adhesion molecule
NMDA	N-methyl-D-aspartate
NSCs	Neural stem cells
NTFs	Neurotrophic factors

PBS	Phosphate-buffered saline
PDL	Poly-D-lysine
PFA	paraformaldehyde
PSCs	Pluripotent stem cells / Postsynaptic currents
PT	Post-transplantation
PTX	Picrotoxin
Ri	Input resistance
RMP	Resting membrane potential
Rs	Series resistance
RT	Room temperature
SE	Status epilepticus
sPSCs	Spontaneous postsynaptic currents
SRS	Spontaneous recurrent seizure
TBS	Tris-buffered saline
TEA	Tetraethylammonium.
TLE	Temporal lobe epilepsy
TTX	Tetrodotoxin
WHO	World Health Organization

Introduction

Epilepsy

Neurological disorders, i.e., disorders of the central nervous system (CNS), affect hundreds of millions of people worldwide. The Global Burden of Disease Study carried out by the World Health Organization (WHO) reports across the years, that neurological disorders cast the heaviest burden on people's lives out of all the diseases evaluated [1]. To assess this burden WHO uses a metric called disability-adjusted life years (DALYs) combining the time lived with a disability and the time lost due to premature mortality. Among the most common neurological disorders, epilepsy stands in fifth place, representing around 1% of all DALYs globally, surpassed only by stroke, migraine, dementia, and meningitis [1]. With an estimation of around 46 million people living with active epilepsy in 2016 [2], it has been reported that approximately 4-10 out of 1000 people suffer from this disease worldwide [3,4].

In addition to suffering from seizures, epilepsy patients often face other difficulties which can also affect their families and society in general. Epilepsy is associated with higher levels of depression and anxiety, people in some cases even fear leaving their homes not to experience a seizure in public [5]. Despite the efforts to destigmatize this condition, patients with epilepsy may still bear a psychosocial burden. In some countries people who suffer from epilepsy have troubles finding a spouse, they are denied employment even though their condition would not affect their performance, and children with epilepsy may be forced to skip school and have lower study scores [6,7]. These are just some examples of how this condition can affect the daily lives of patients and their close ones, casting some light on the prevailing global burden of epilepsy, and emphasizing the importance of disseminating knowledge about this common condition.

Although all patients with epilepsy experience seizures, not all people having seizures are diagnosed with epilepsy. The International League Against Epilepsy (ILAE) formulated the following definition [8]:

> "Epilepsy is a disease of the brain defined by any of the following conditions
>
> 1. At least two unprovoked (or reflex) seizures occurring >24 hours apart

2. One unprovoked (or reflex) seizure and a probability of further seizures similar to the general recurrence risk (at least 60%) after two unprovoked seizures, occurring over the next 10 years

3. Diagnosis of an epilepsy syndrome"

To understand this definition, we need to first understand what an unprovoked seizure is. The word "unprovoked" implies the absence of a temporary or reversible factor lowering the threshold and causing a seizure at that point in time [8], i.e., an unprovoked seizure is a seizure occurring in the absence of triggering factors, such as a potentially responsible clinical condition. In the presence of precipitating factors such as a brain injury or a tumour, closely temporally related seizures are defined as acute symptomatic seizures [9]. The definition above mentions also reflex seizures, which can be triggered by e.g., photic stimuli. Individuals with an enduring abnormal predisposition to have such seizures fall within the conceptual definition of epilepsy [8].

As implied, a seizure affects the brain. By definition, an epileptic seizure is "a transient occurrence of signs and/or symptoms due to abnormal excessive or synchronous neuronal activity in the brain" [10]. Seizures can affect the patient's emotional state, memory, consciousness, cognition, motor, and sensory functions, or behaviour. They are classified into several categories [11], based on their onset as either focal or generalised or as motor or non-motor, with each category having several subcategories (Figure 1).

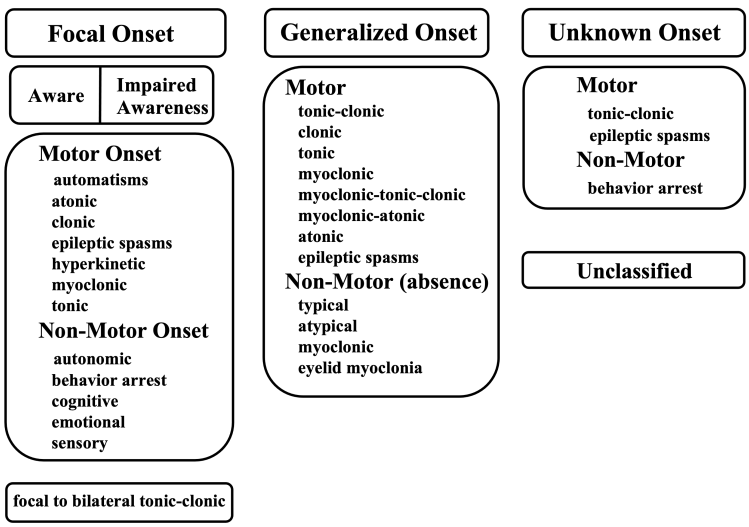

Figure 1. ILAE 2017 classification of seizure types. Seizures are classified by their onset to focal (with a region-specific localised onset), generalized (onset over wide areas of the brain), and unknown (the onset cannot be localised). Adapted from [11].

Available treatments

Due to the different types and origins of seizures, epilepsy cannot be perceived as a single specific disease but rather a complex of various disorders. Epilepsy therapy is therefore as complex as the disease itself and needs to be tailored to the specific patient. Up to this date, there is no definite cure for epilepsy and the goal of the treatment is therefore to reach seizure freedom. In most cases, this is achieved by anti-seizure medications (ASMs). Currently, there are around 30 ASMs available for epilepsy therapy [12]. They mostly act on either inhibitory or excitatory synapses between neurons, normalising the brain's electrical activity (Figure 2).

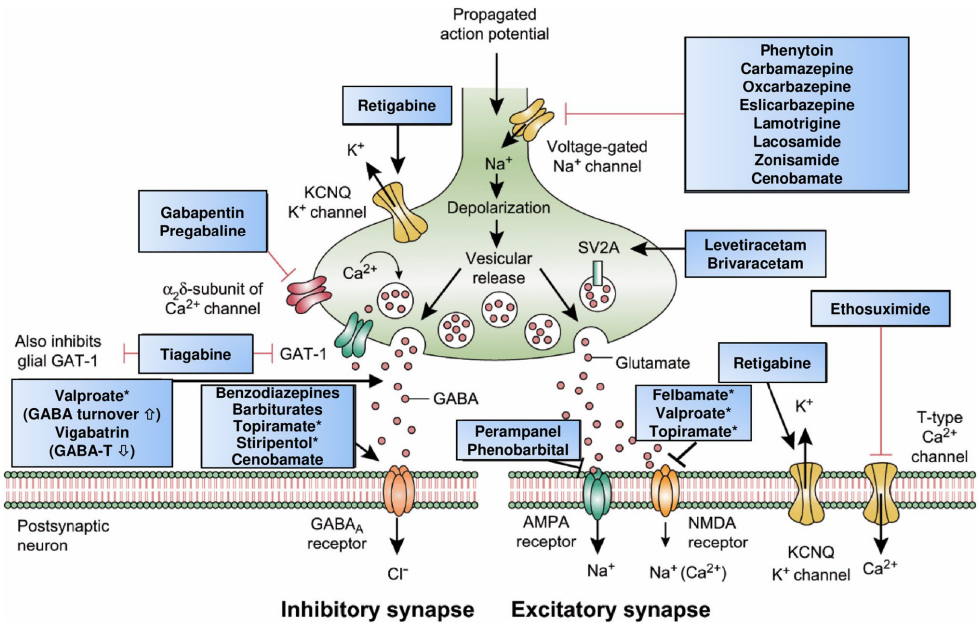

Figure 2. Mechanism of action of ASMs on synapses. Current ASMs act upon various targets within the presynaptic and postsynaptic regions, targeting e.g. specific ion channels, neurotransmitter receptors, and transporters. Asterisks indicate multiple mechanisms of action. AMPA, α-amino-3-hydroxy-5-methyl-4-isoxazole propionic acid; GABA γ-aminobutyric acid, GABA-T, GABA aminotransferase; GAT-1, GABA transporter 1; KCNQ, Kv7 potassium channel family; NMDA, N-methyl-D-aspartate; SV2A, synaptic vesicle protein 2A. Adapted from [12].

ASMs, however, are only a symptomatic treatment and can have adverse effects that influence the patient's relationship with the medication and quality of life [13]. Moreover, despite the continuous development of new ASMs, still, about one third of patients with epilepsy experience seizures that cannot be controlled [14–17]. This proportion of drug-resistant patients has unfortunately not changed during the decades of new drug development [14,18,19], suggesting that novel approaches towards epilepsy therapy should be investigated, possibly modifying the disease itself and not

only relieving its symptoms. The investigation of such approaches is the main aim of this thesis.

Temporal lobe epilepsy and the hippocampus

One of the epilepsies often refractory to ASMs is temporal lobe epilepsy (TLE), the most common type of focal epilepsy, where seizures originate in the temporal lobe. A majority of patients suffering from TLE are drug-resistant [20,21]. And in addition to suffering from seizures, they are prone to behavioural comorbidities, such as depression and anxiety or impairment of learning and memory [22]. For these patients, surgical resection of the epileptic focus is a well-established treatment method. However, the probability of reaching seizure freedom after undergoing temporal lobectomy declines over time, reaching as low as 40% after 15 years [23,24]. With relapse being so common, surgery might not be the ideal solution for TLE patients, although in some cases, it is the only option available.

One of the structures affected in TLE is the hippocampus. This specific structure within the temporal lobe has been widely studied over the decades for its involvement in memory formation. The interest in the hippocampus was sparked by the well-known case of patient H.M., who underwent experimental surgery for epilepsy in 1953, where the hippocampi in both hemispheres were removed. The patient was afterward not capable of forming new, declarative memories [25,26]. Since then, research of the hippocampus has led to the discovery of long-term potentiation [27], as well as different types of neurons associated with the spatial framework, such as place cells or head direction cells [28,29]. The hippocampus is believed to be responsible for storing an experience by combining its cognitive, sensory, and emotional components [30].

On the structural level, the hippocampus is formed as a polysynaptic circuit (Figure 3). Sensory inputs from the entorhinal cortex (EC) are lead through the perforant path to the granule cells in the dentate gyrus (DG), from here mossy fibres of the granule cells pass the information to the principal neurons in the cornu ammonis (CA)3 region. These cells then connect to the CA1 principal neurons, from where the information is then transmitted back to the deeper layers of the EC, either directly or through the subiculum [31].

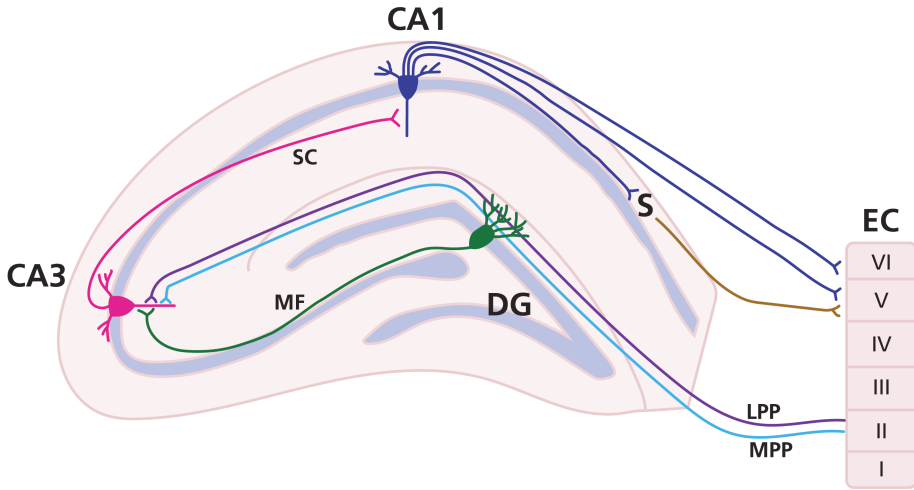

Figure 3. The hippocampal circuitry. A simplified illustration of the hippocampal pathways. Sensory inputs are led by the perforant pathway from the entorhinal cortex (EC) to the dentate gyrus (DG), from here to the CA3 and further to CA1, from where connections lead back to the EC directly or through the subiculum (S). CA, cornu ammonis; LPP, lateral perforant pathway; MPP, medial perforant pathway; MF, mossy fibers; SC, Schaffer collaterals.

Histopathology

Together with the excitatory glutamatergic neurons responsible for the circuit formation, inhibitory, gamma-aminobutyric acid (GABA)-ergic neurons are also present in the hippocampus and maintain the important balance between excitation and inhibition [32]. In TLE, both cell types can be affected. The most common histopathological abnormality found in patients with drug-resistant TLE is hippocampal sclerosis [33,34]. The main hallmark of hippocampal sclerosis is the loss of the principal excitatory neurons, which is additionally associated with astrogliosis, i.e., the presence of reactive astrocytes. The neuronal cell loss can affect any region of the hippocampus and based on the pattern of the neurodegeneration, the ILAE classified three different types of hippocampal sclerosis [33] (Figure 4). Another common histopathological feature of TLE is the loss or dysfunction of the inhibitory cells in the hippocampus, i.e., GABAergic interneurons [35–37]. This reorganization of the neural circuit results in diminished inhibition, structural alteration of synapses, and increased activity of the excitatory circuit, which may altogether contribute to a reduced seizure threshold [38–40]. In this thesis, we focused on increasing inhibition in the epileptic hippocampus, thereby possibly ameliorating the severity of the disease by decreasing seizure frequency.

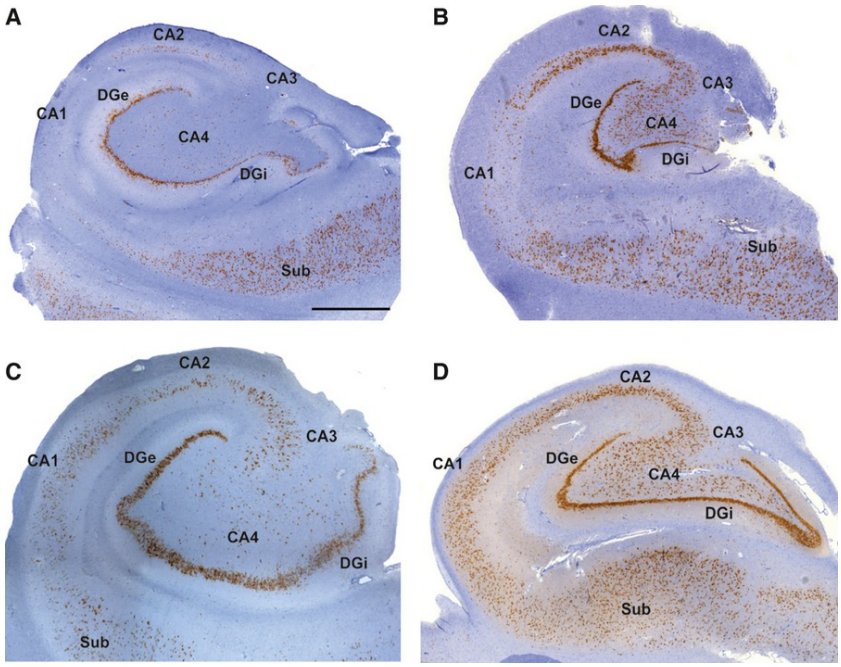

Figure 4. Examples of the histopathological subtypes of hippocampal sclerosis in patients with TLE defined by ILAE. (A) The most common type of hippocampal sclerosis. Significant specific pyramidal cell loss in CA4 and CA1. Damage to sectors CA3 and CA2 is also frequently visible. Note cell loss also in the dentate gyrus (DG), and preservation of cells in the subiculum (Sub). (B) CA1 predominant neuronal cell loss and gliosis (C) CA4 predominant neuronal cell loss and gliosis (D) No hippocampal sclerosis, gliosis only. Sections were stained for neuronal nuclei (NeuN) with hematoxylin counterstaining. DGe/DGi, external/internal limbs of dentate gyrus; Sub, subiculum. Scale bar 1000 µm. Adapted from [33].

Epileptogenesis

The histopathological features of TLE are often caused by an initial insult leading to the hippocampal reorganisation resulting in an enduring epileptogenic potential of the brain and the development of unprovoked seizures [41]. The seizure-free period between the insult and the onset of symptomatic epilepsy has been already noted in 1881, where Gowers described this interval to be several months- to years-long [42]. The process ongoing between the initial brain-damaging insult and the first unprovoked spontaneous seizure has however been studied only more recently, thanks to the development of animal models that resemble this latency period [43]. During this period, various changes occur in the brain that eventually leads to the development of chronic epilepsy. This process of molecular and cellular changes is called epileptogenesis. The insult triggering the transformation of a non-epileptic to an epileptic brain can for example be head trauma, infection, tumours, or prolonged acute symptomatic seizures such as status epilepticus (SE) [44]. However, epileptogenesis might not be limited by the occurrence of the first spontaneous seizure, but rather

continues if seizures are not well controlled as a consequence of the seizures themselves [45] (Figure 5). There are many cellular and molecular alterations ongoing during epileptogenesis, some may reflect the effort to repair the insult-induced damage, such as neurogenesis or activation of inflammatory cells. However, it is when the brain's attempt to self-repair fails that chronic epilepsy may develop [44,46]. Other detrimental changes include neurodegeneration, gliosis, mossy fibre sprouting, loss or reorganisation of dendrites, damage to the blood-brain barrier (BBB), and subsequent angiogenesis, or alteration in ion channel function [46] (Figure 5).

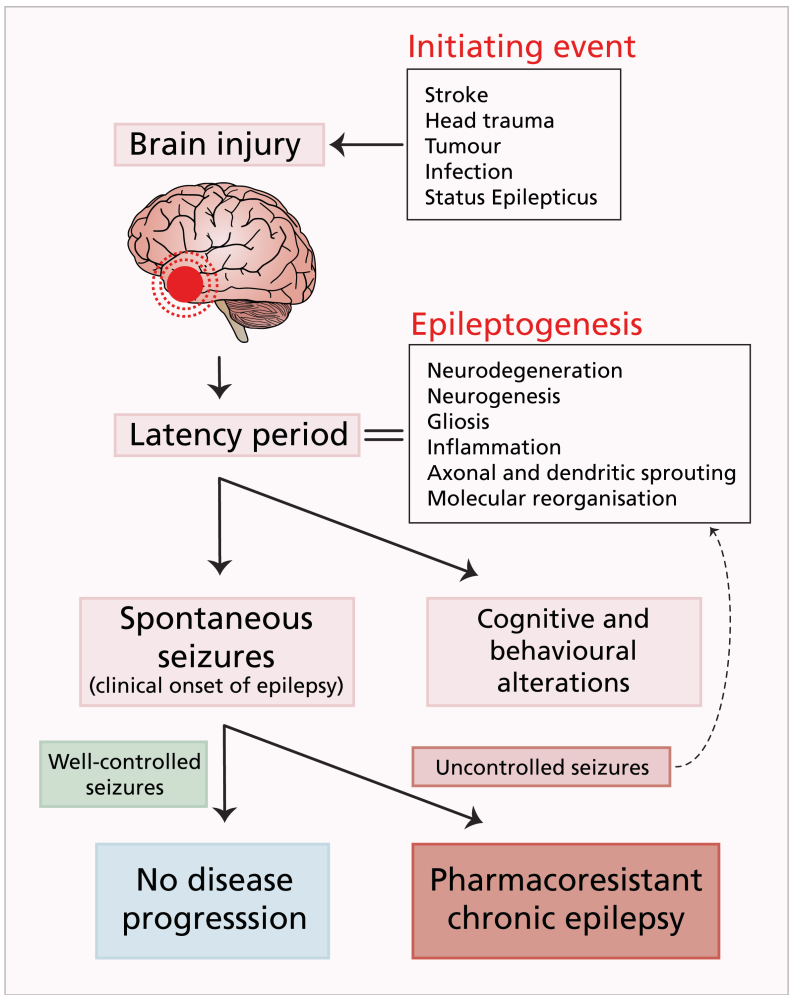

Figure 5. Steps in the development and progression of temporal lobe epilepsy. The process starts with a brain-damaging insult, which triggers the tissue reorganisation during epileptogenesis. After a latency period, spontaneous seizures occur, together with cognitive decline and behavioural alterations. If seizures are not well controlled, further progression of the process may result in the development of chronic epilepsy refractory to medication. Inspired by [44,45].

Targeting the process of epileptogenesis, and therefore preventing seizures or reducing the severity of the disease, is another pathway towards lessening the burden of epilepsy. However, no reliable biomarkers have been recognised yet, which would identify patients at risk of developing epilepsy [47]. Moreover, which of the many epileptogenesis processes are promising targets for therapy needs to be further investigated. As mentioned above, animal models of epilepsy largely contributed to the understanding of the epileptogenesis process. Using relevant models of TLE may therefore be the key in developing novel therapies targeting epileptogenesis as well as chronic epilepsy when it develops [48].

Animal models of TLE

Animal disease models are essential for both basic research and preclinical therapy development. For epilepsy, numerous models have been established and are being constantly developed and improved. Several new ASMs have been discovered by testing various novel compounds in animal models, which strongly supports the value of this type of research. This also implies that animal epilepsy models do indeed resemble human seizures in the response to ASMs [49].

Since this thesis is focused on TLE, non-relevant models will not be mentioned, but are reviewed in Löscher et al., 2017 [48]. The first developed model of drug-resistant TLE is thought to be the amygdala kindling model in rats, in which repeated electrical stimulations of the amygdala via a depth electrode lead to prevailing seizure susceptibility and other comorbidities resembling human TLE [50,51]. This amygdala kindling model contributed to the development of the ASM levetiracetam [52] and has been widely used for studying epileptogenesis, however, the kindled animals do not exhibit spontaneous seizures [44], and therefore, this model does not completely reflect symptomatic TLE in human patients. Among the most commonly used models of TLE are the post SE models, in which sustained SE is induced either by electrical stimulation or by chemoconvulsant administration. Sustained electrical stimulation of the amygdala or hippocampus leads to the development of spontaneously recurring seizures (SRSs) after a seizure-free latency period [53]. Similar outcomes are achieved after systemic injection of pilocarpine, from which rats develop SE and after approximately two weeks start showing SRSs. The rat pilocarpine model is the most frequently used post-SE TLE model, having similarities to human TLE in both chronic seizures and histopathological alterations [54,55]. Another widely used SE-inducing chemoconvulsant is kainic acid (KA), which activates a subset of glutamatergic receptors and therefore, induces excitation. KA can be injected either directly into the amygdala [56] or hippocampus of either rats [57] or mice [58] and cause more local damage, or used systemically for inducing SE, resulting in a more widespread bilateral brain damage. Two of these KA-SE TLE models are included in the Epilepsy Therapy

Screening Program (ETSP), a work frame established by the National Institute of Neurological Disorders and Stroke at the National Institutes of Health, which facilitates the discovery of new therapeutic agents for epilepsy [59]. One of these is the intrahippocampal KA mouse model, which has the advantage of exhibiting electrographic SRSs with a very high frequency [58]; the second is the systemic KA rat model, where after a latency period of days to weeks after SE, the rats show partial and generalised behavioural seizures [60]. In this thesis, this model has been used both to study a disease-modifying therapeutic intervention and to investigate a potential anti-epileptogenic treatment.

Emerging novel therapies

Currently available treatments of TLE are in a majority of cases only symptomatic, i.e., relieving patients from seizures but not targeting the cause of the disease itself. Moreover, the high incidence of drug resistance among TLE patients calls for the development of innovative non-pharmacological treatment options.

Cell therapy

One of the potential therapies currently being explored for epilepsy as well as other neurological conditions is cell therapy. This approach consists of the use of live-cell transplantation for therapeutic purposes. The final aim of cell therapy is either cell replacement in cases where a specific cell type is affected or reparation of the physiological function of the affected tissue [61]. For this purpose, stem cells are widely used, which are unspecialised cells capable of self-renewal, and importantly, they can differentiate into multiple cell types depending on their origin. Based on their ability to differentiate, stem cells can be either pluripotent, i.e., capable of generating virtually every cell in the human body, or multipotent, i.e., with a limited differentiation potential [62]. Examples of pluripotent stem cells (PSCs) are embryonic stem cells (ESCs), which are derived from the inner cell mass of the blastocyst stage embryo [63,64], or induced PCSs (iPSCs), which are cells derived from adult somatic cells genetically reprogrammed back to a pluripotent state [65–67]. Multipotent stem cells are for instance neural stem cells (NSCs), which are committed to the generation of cells of the CNS, such as neurons and glial cells [68], or mesenchymal stem cells (MSCs) which can give rise to cells of the mesenchymal lineage, such as osteocytes, chondrocytes, myocytes, and adipocytes [69].

GABAergic interneurons

The advantage of using stem cells for cell therapy is the possibility to generate a desired specific cell type. Within the development of novel therapies for TLE, this potential has been utilized to generate GABAergic interneurons with the prospect to inhibit the seizure-prone neuronal network [70]. This approach is addressing one of the previously mentioned pathological hallmarks of TLE, i.e., the loss or malfunction of GABAergic interneurons within the hippocampal network.

In animal models of epilepsy, different sources of GABAergic progenitor/precursor cells have been used in preclinical research. These cells are transplanted into the affected brain structures of the epileptic animals and the efficacy of the therapeutic intervention is assessed by looking at SRS frequency, histological outcomes, or effects on behaviour (Figure 6).

One of the earlier methods being explored is the transplantation of GABAergic progenitor cells derived from developing rodent embryos, specifically from the ganglionic eminence regions where GABAergic interneurons arise during development [71–76]. The transplantation of these cells proved to be effective in the pilocarpine mouse model, in which the authors observed a markedly reduced SRS frequency together with alleviation of behavioural comorbidities [75,76]. In the rat KA-SE model of chronic TLE, transplanted medial ganglionic eminence (MGE) derived NSCs gave rise to GABAergic interneurons in the rat hippocampus and reduced SRS frequency [76,77]. These studies represent a valuable proof of concept for the use of GABAergic interneurons for epilepsy treatment. However, more clinically relevant approaches are currently emerging.

The use of human cell sources allows for easier clinical translation of the proposed therapies. Although human foetal-derived NSCs have shown to be beneficial in a rat TLE model [78], the use of foetal cells comes with major ethical concerns. A more viable option is the use of human PSCs. To our knowledge, only two studies up to this date have investigated the therapeutic potential of human PCS-derived GABAergic interneurons in preclinical studies with rodent epilepsy models. In the first study [79] the pilocarpine mouse model was used, and MGE-like cells for transplantation were derived from a human embryonic stem cell (hESC) line by introducing small molecules into the cell culture media, directing the cells towards the MGE fate. The transplantation of these cells resulted in reduced SRS frequencies and improved outcomes in behavioural tests. The authors of the second, more recent study [80] used a human iPSC line as a cell source for producing MGE-like cells using a different small-molecule-based protocol for mimicking the differentiation process during brain development. After grafting into the hippocampi of rats with KA-induced TLE, these cells were also able to attenuate SRSs and behavioural and histological comorbidities. *Paper II* of this thesis is the third study reporting the therapeutic potential of human PSC-derived GABAergic interneurons in an epileptic rodent model, although using a

distinct method for cell differentiation. Yang and colleagues published in 2017 a simple protocol for generating GABAergic interneurons from PSCs by transcription factor reprogramming [81]. This is a more direct approach introducing two transcription factors determining the GABAergic fate into the cells' genetic information by using a lentiviral delivery system. The adaptation of this protocol to our conditions as described in *paper I* is where the story of this thesis began.

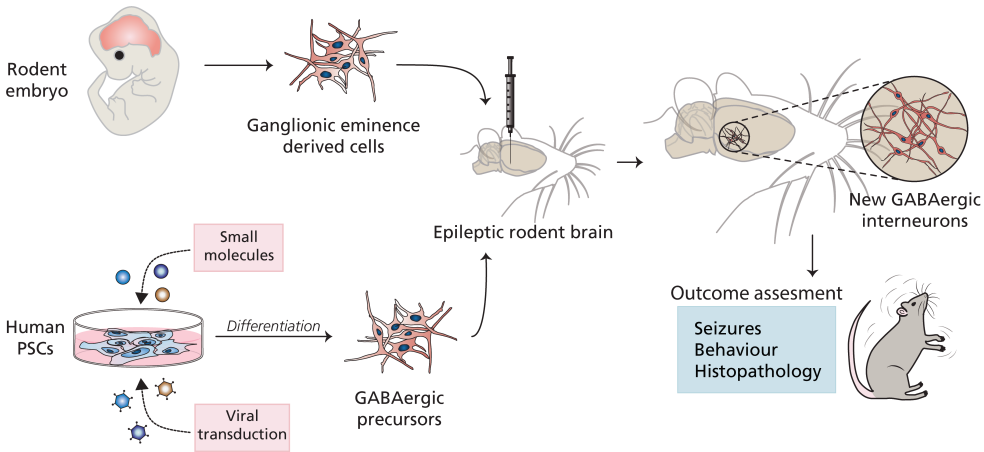

Figure 6. Strategies used for preclinical studies of GABAergic cell therapy for temporal lobe epilepsy. Cells derived from the ganglionic eminences of rodent embryos, either primary cells or neural stem cells, are used for transplantation into rodent models of TLE. As are the more clinically relevant human PSC-derived GABAergic interneuron precursors generated *in vitro* by differentiation. After transplantation, these cells mature into GABAergic interneurons and their therapeutic potential is assessed by evaluating SRSs, behavioural tests, and histology. GABA, gamma-aminobutyric acid; TLE, temporal lobe epilepsy; SRS, spontaneous recurrent seizures.

Mesenchymal stem cells

Among cell therapies not restricted to neurological diseases, the use of MSCs represents an interesting avenue towards epilepsy treatment. MSCs can be derived from a number of tissues. They were first identified in bone marrow aspirates [82,83], but other sources are now being utilised for MSC isolation, such as adipose tissue [84,85], umbilical cord [86], or placenta [87]. These tissues are easily harvestable and can be either replenished or are unwanted and would be otherwise discarded. The therapeutic potential of these cells lies in their immunomodulatory properties and their ability to promote endogenous tissue regeneration [88]. Indeed they are currently being investigated in a number of clinical trials with no reported serious adverse effects [89]. The consequences of MSC transplantation are currently being evaluated in animal models of several CNS disorders. In a stroke model, the cells were shown to be neuroprotective [90], as was also demonstrated in a model of multiple sclerosis, where the beneficial effects were attributed to immunomodulation as well [91]. They were shown to promote recovery after spinal cord injury in mice [92] or reduce dopaminergic cell death and promote

functional recovery in models of Parkinson's disease [93,94]. MSCs are thought to induce these beneficial effects not through their stemness per se but rather by releasing a wide variety of vesicles, exosomes, cytokines, and growth factors, which modulate the immune response or promote cell survival [95] (Figure 7).

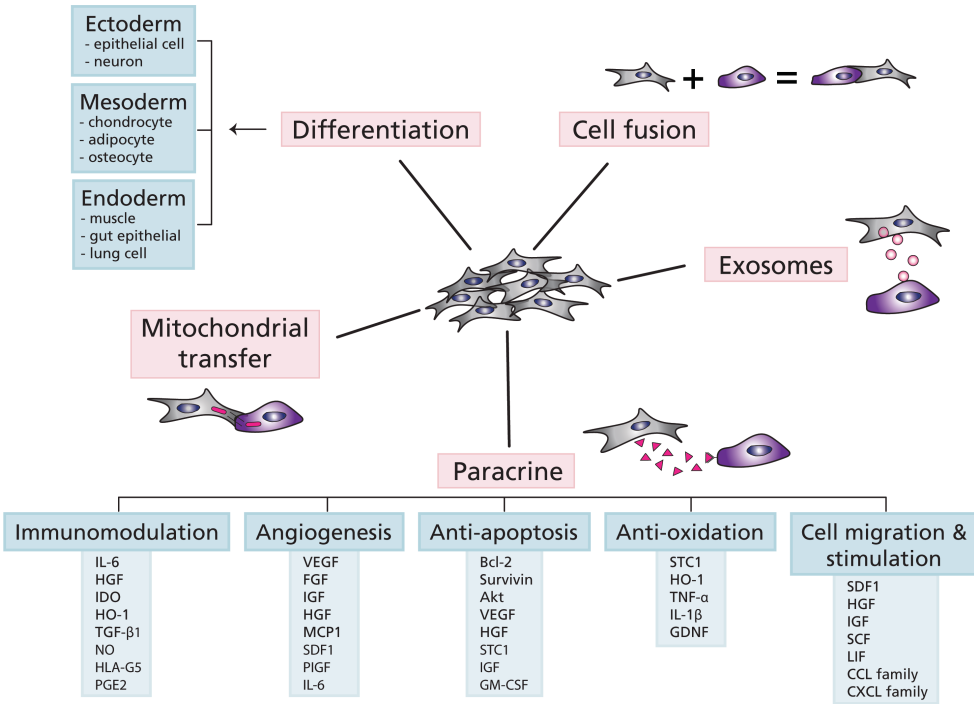

Figure 7. Modes of MSC action. MSCs can differentiate into cells of the ectodermal, mesodermal, and endodermal lineage, they can fuse with another cell, or through gap junctions, MSCs can transfer their mitochondria to neighboring cells. MSCs release vesicles/exosomes containing RNA, microRNA (miRNA), and/or proteins which can be engulfed by surrounding cells. They also secrete cytokines, chemokines, growth factors, and other molecules which affect immunomodulation, angiogenesis, anti-apoptosis, anti-oxidation, and cell migration/stimulation. IL-6, interleukin-6; HGF, hepatocyte growth factor; IDO, indoleamine 2,3-dioxygenase; HO-1, heme oxygenase 1; TGF, transforming growth factor; NO, nitric oxide; HLA-G5, human leukocyte antigen class I molecule G5; PGE2, prostaglandin E2; VEGF, vascular endothelial growth factor; FGF, fibroblast growth factor; IGF, insulin-like growth factor; MCP1, monocyte chemotactic protein 1; SDF1, stromal cell-derived factor 1; PIGF, placental growth factor; IL-6, interleukin 6; Bcl-2, B-cell lymphoma 2; Akt, v-akt murine thymoma viral oncogene homolog 1; STC1, stanniocalcin 1; GM-CSF, granulocyte-macrophage colony-stimulating factor; TNF, tumour necrosis factor; GDNF, glial-derived neurotrophic factor; SCF, stem cell factor; LIF, leukemia inhibitory factor; CCL, chemokine C-C motif ligand; CXCL, chemokine C-X-C motif ligand. Adapted from [95].

Not surprisingly, the use of MSCs has been investigated also for their therapeutic potential in epilepsy. Since inflammation and neurodegeneration take part in epileptogenesis [46,96], most of the studies using MSCs explored their potential for modulating the epileptogenic processes, as was also the case of our investigation in *paper IV*. Rodent MSCs have been used in the majority of cases, and studies report their beneficial effects when transplanted after SE in the rat pilocarpine TLE model [97–99],

with MSC-treated animals having fewer SRSs and better behavioural test scores, together with alleviating related histopathological features in the hippocampus, such as neuronal cell loss or aberrant mossy fibre sprouting. Transplantation of rodent MSCs in mice after KA-induced SE had similar effects on mossy fibre sprouting, in addition to the observed reduction of microglia activation and astrogliosis [100], which reflects the immunomodulatory properties of the cells. Rodent MSCs have also been investigated in chronic epilepsy, i.e., the cells were transplanted when SRSs had already developed. The results from these studies using the pilocarpine rat model suggest that this treatment may be effective in the later stages of the disease as well, since MSC transplanted animals displayed less epileptiform discharges [101] and a lesser extent of neurodegeneration [102], together with molecular changes such as reduction of pro-inflammatory cytokine and oxidative stress marker levels.

Again, human MSCs are not as widely used in preclinical studies but would be preferred from the translational point of view. Moreover, MSCs are thought to be immune-evasive, which allows xenogeneic and allogenic cells to possibly survive within the host tissues for several weeks without the need for immunosuppression [103–105]. In rats with pilocarpine-induced SE, human MSCs were studied for their effects on epileptogenesis, where they were deemed as neuroprotective and anti-inflammatory, reducing the SRS occurrence in treated animals [104].

In addition to the native therapeutic aspects of MSCs, they can be used as a delivery system for specific therapeutic agents [106] – a combination of cell and gene therapy, which will be discussed next.

Gene therapy

Gene therapy is a novel therapeutic approach, which utilises the possibility to introduce genes of interest into cells by inducing the production of a missing protein or a therapeutic agent. This can either be done directly *in vivo* by using viral particles for delivery and inducing the production of the protein of interest from endogenous cells, or *ex vivo*, where cells are firstly genetically modified *in vitro* and then used for *in vivo* transplantation as a delivery system of the desired protein.

In epilepsy, both gene therapy approaches have been studied, particularly in focal epilepsies such as TLE [107,108]. For the *in vivo* approach, the major factor that needs to be considered is the vector of the DNA delivery. The ideal vector needs to reach high enough safety levels to be translatable to the clinic, without the risk of mutagenesis, be readily manufacturable at a relevant scale, have a high efficiency of transduction, and a stable and sustained expression in target cells. Among the many other factors that should be considered are the cell type specificity, potential cytotoxicity, packaging capacity, and the ability to cross the BBB [108,109]. The most widely used type of

vector for targeting the CNS is the class of adeno-associated viruses (AAVs). AAVs are considered relatively safe, they induce a prolonged expression of the transgene with almost no integration into the host genome, and cause minimal inflammatory responses [110].

Various viral vectors have also been used in preclinical studies of gene therapy treatments for epilepsy. Among others, the delivery of neurotrophic factors (NTFs) has been widely investigated due to their trophic, neuroprotective, and other potentially beneficial effects. Fibroblast growth factor 2 (FGF-2) induces proliferation of neural progenitors and is neuroprotective, as is the brain-derived neurotrophic factor (BDNF), which in addition promotes neuronal differentiation [111]. In the pilocarpine rat TLE model, both these NTFs exhibited antiepileptogenic effects, such as reduction of SRSs and neurodegeneration together with increased neurogenesis [112]. BDNF has also been utilized in an *ex vivo* approach, where cells modified to release BDNF were encapsulated and inserted into the hippocampi of pilocarpine-treated rats after the development of SRSs. This intervention resulted in reduced SRS frequencies, better cognitive performance, a lesser extent of cell death, and elevated neurogenesis [113]. From the NTF family, another potential therapeutic agent has emerged – the glial cell line-derived neurotrophic factor (GDNF), which is investigated in this thesis and will therefore be discussed more thoroughly.

Glial cell line-derived neurotrophic factor

As its name implies, GDNF was first discovered by Lin et al. in 1991 as an NTF derived from glial cells, which promotes the survival and differentiation of dopaminergic neurons [114]. Since then it has been extensively studied as a potential therapeutic agent in Parkinson's disease [115,116], as well as in other CNS disorders such as spinal cord injury [117] and importantly, epilepsy.

Several studies showed the anti-seizure potential of GDNF, with both *in vivo* and *ex vivo* methods of delivery. Our group previously reported that direct *in vivo* injections of an AAV-GDNF vector suppressed acute seizures and increased seizure threshold [118]. Using the *ex vivo* route, implanting encapsulated GDNF-producing cells into the hippocampi, the earlier positive effects on seizure suppression were further supported. The encapsulated cells diminished seizures after electrical kindling [119], and their beneficial effects were also seen after implantation in the chronic phase of two post-SE TLE models. In rats with TLE, modelled by intrahippocampal KA injections, the unilateral implantation of encapsulated GDNF-releasing cells resulted in reduced numbers of SRSs [120]. In the pilocarpine rat model, the bilateral implants of the cells additionally resulted in the prevention of hippocampal volume loss and reduced neurodegeneration [121].

Apart from possible neuroprotection, *how* GDNF exerts these seizure-inhibiting effects is not yet fully understood. The main receptor binding GDNF and activating the

transmembrane receptor tyrosine kinase (Ret) intracellular signalling pathway is the GDNF family receptor alpha-1 (GFRα1) [122]. However, several alternative pathways have additionally been discovered. The GDNF-GFRα1 complex can act as a cell adhesion molecule and promote the formation of neuronal synapses in the hippocampus [123]. Other potential signalling pathways involve the neural cell adhesion molecule (NCAM) [124] or the heparin sulphate proteoglycan Syndecan-3, which was found to be expressed preferentially in GABAergic interneurons [125]. Since GDNF and the receptors involved in GDNF-mediated signalling are highly expressed in the principal neurons of the hippocampus [123,126,127], it is of interest to identify the molecular mechanisms of its inhibitory potential, as was also studied in *paper III* of this thesis.

Combining cell and gene therapy

The combination of the two above-described therapeutic approaches, cell therapy, and gene therapy, is not completely identical to *ex vivo* gene therapy. The cells used have a therapeutic potential on their own which is further enhanced by genetic modification [128]. An example of this combinatorial approach is the use of genetically modified NSCs, which by themselves have the potential in treating CNS disorders but can be additionally modified to deliver therapeutic agents of interest [129]. Another cell type commonly used for this purpose are MSCs. As described above, MSCs have immunomodulatory and neuroprotective properties, and combining these beneficial effects with introducing a desired transgene may be of use in various diseases [106].

Indeed, the therapeutic potential of genetically modified MSCs was investigated in a number of preclinical studies in animal models of CNS disorders. In stroke animal models, MSCs modified to produce NTFs, such as BDNF [130], FGF-2 [131], or GDNF [132], have shown promising results. MSCs overexpressing BDNF reduced neurodegeneration in a model of Huntington's disease [133]. GDNF-producing MSCs were shown to have a therapeutic potential in Parkinson's disease models [134,135]. In an epilepsy model, specifically the intra-amygdala KA mouse model, MSCs releasing adenosine were shown to have antiepileptogenic effects, ameliorating SRSs [136,137]. In this thesis, the potential of MSCs genetically modified to release GDNF transplanted into a rat epilepsy model was explored in *paper IV*.

Aims of the thesis

The overall aim of this thesis was to address the persisting gap in therapies available for patients with epilepsy, whose spontaneous seizures cannot be controlled by pharmaceutical treatments, and to explore the possibility of ameliorating the disease before spontaneous seizures occur. Specifically, the possibility to increase inhibition within the neuronal network and subsequently reduce the seizure burden in animal models of epilepsy was investigated.

Specific aims of the included papers were:

I. To efficiently generate functional mature GABAergic interneurons from hESCs, which are able to synaptically integrate into a human neuronal network.

II. To investigate whether the hESC-derived GABAergic interneurons can synaptically integrate into the epileptic rat hippocampus and reduce seizures in the KA-SE rat TLE model.

III. To investigate the reason behind the seizure-inhibiting properties of GDNF, focusing on the inhibitory drive in the mouse and human hippocampal network and the signalling pathways involved.

IV. To assess the antiepileptogenic potential of MSCs and genetically modified MSCs producing GDNF in the KA-SE rat TLE model.

Materials and methods

Animals

All animals used within the included studies were housed in the local animal facility under a 12-hour light/dark cycle with free access to food and water. Animals were housed in individually ventilated cages in groups of 2 or more, except when performing video/video-EEG monitoring, where animals were housed individually in adjusted open cages. All experimental procedures were approved by the local ethical committee for experimental animals (Ethical permit no. M47-15, M49-15 and 02998/2020) and conducted in agreement with the Swedish Animal Welfare Agency regulations and the EU Directive 2010/63/EU for animal experiments.

In *paper I,* C57Bl6/J mice were used for harvesting primary glial cells, and in *paper III*, the same strain was used for hippocampal slice preparation. For *in vivo* cell grafting, immunodeficient nude rats (NIH Nude rat, Charles River) were used in *paper II,* and Sprague Dawley rats (SD rats, Janvier Labs) in *paper IV*.

Status epilepticus induction

In *paper II* and *paper IV,* TLE was modelled by initiating KA-induced SE, which resulted in the development of SRSs. KA was injected subcutaneously in the neck region, starting with a higher initial dose (10 mg/kg of KA for nude rats, 5 mg/kg for SD rats). Subsequently, a lower dose (5 mg/kg for nude rats, 2.5 mg/kg for SD rats) was injected every hour until 4 or more stage 3, or higher, seizures per hour were detected (protocol illustrated in Figure 8). Seizures were monitored since the first injection and classified according to the modified Racine scale. Only stages 3 – 5 were documented: Stage 3 – unilateral forelimb clonus; Stage 4 – generalized seizure with rearing, body jerks, bilateral forelimb clonus; Stage 5 – generalized seizure with rearing, imbalance, falling, or wild running (Racine, 1972). After experiencing SE, animals were subcutaneously injected with a 1:1 Ringer/glucose (25 mg/ml) solution for rehydration and returned to housing cages supplemented with wet food. Animals were then weighed every day for 7 days after the SE induction and once per week henceforth to monitor their well-being.

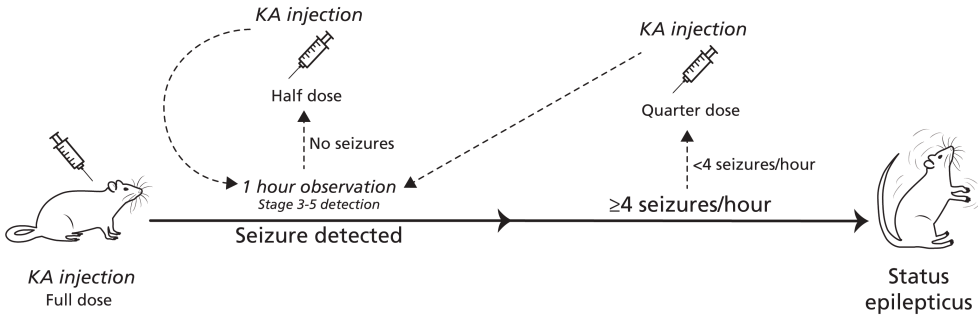

Figure 8. Schematic illustration of the protocol used for KA-SE inductions. Rats are firstly injected with a full dose of KA and subsequently observed for 1 hour. If no seizures are detected, a half dose of KA is administered. This continues until 4 or more seizures/hour are detected (SE has been reached). If less than 4 seizures/hour are detected an additional quarter dose of KA may be administered. KA, kainic acid; SE, status epilepticus.

In vitro methods

Cell cultures

Mouse primary glial cell cultures were used in *paper I* for co-culture in neuronal differentiations. The cells were harvested from the cerebral cortices of newborn mice at P3 to P5 by decapitation, brain extraction, and dissection. Separated cortices were cut, homogenised, and digested by trypsin. Cells were then dissociated mechanistically by a scalpel blade and then using a cell strainer, and subsequently plated onto T75 flask coated with poly-D-lysine (PDL; Sigma-Aldrich) in MEM (Gibco) additionally containing 5% foetal bovine serum (FBS; Sigma-Aldrich), 2% B-27 (Gibco), 1% GlutaMAX (Gibco), 1% Penicillin–Streptomycin and 0.4% D-Glucose (w/v; Sigma-Aldrich). The primary glial cells were passaged at least once before co-culturing, with a maximum of 5 passages.

For generating human embryonic stem cell-derived interneurons (hdInts) in *paper I* and *paper II,* H1 (WA01) ES cells were used. The cells were obtained from WiCell Research Resources (WiCell, WI, USA) and maintained in mTeSR1 medium (Stem Cell Technologies) on Matrigel-coated plates (Corning).

In *paper I,* hdInts were co-cultured with human primary cortical cells to investigate the formation of functional synapses. These cells were derived from cerebral cortices of aborted human foetuses at 8 weeks of age according to guidelines approved by the local ethical committee (Ethical permit number: Dnr 6.1.8-2887/2017), as previously described [138]. Briefly, the tissue was dissected, cut into small pieces, and then triturated with a pipette tip into a single-cell suspension. After washing with Neurobasal (Gibco) medium supplemented with B27, the cells were plated onto PDL/fibronectin

(Life Technologies) (both 10 µg/mL)-coated glass coverslips at a density of 50,000 cells/well and maintained in the same medium until co-culturing.

For *in vivo* grafting in *paper IV,* human immortalised adipose-derived MSCs (hiAD-MSCs; ASC52telo, hTERT immortalized Mesenchymal stem cells, ATCC SCRC4000, ATCC, VA, USA) were used. Two cell lines were generated from these cells using lentiviral transduction and subsequent fluorescence-activated cell sorting (for more detailed procedures see Materials and Methods section of *paper IV*). Briefly, the hiAD-MSCs were transduced with lentiviral particles containing either pCCL_EF1a-mCh or pCCL_EF1a-GDNF-mCh and sorted by flow cytometry, based on intense mCherry fluorescence. The sorted cells were cultured in T75 flasks in Mesenchymal Stem Cell Basal Medium (ATCC PCS-500-030, ATCC, VA, USA) supplemented with Mesenchymal Stem Cell Growth Kit (ATCC PCS-500-040, ATCC, VA, USA), Penicillin-Streptomycin (10 units/ml, Gibco), and Amphotericin B (25 ng/ml, Gibco). Cells were expanded as needed and cryopreserved so that the same passage could be used for all *in vivo* experiments.

Quality assessment of hiAD-MSC lines

To ensure that the properties of used MSCs remained unchanged across the experiments in *paper IV*, routine quality checks were performed. After *in vivo* grafting, the remaining cells were re-plated in 12-well plates (~13.000 cells/well), in the same culturing media as mentioned above. After 3 days in culture, the culturing media was collected for enzyme-linked immunosorbent assay (ELISA) measurements of GDNF release and replaced with differentiation media (StemPro Adipogenesis Differentiation Kit or StemPro Osteogenesis Differentiation Kit, both from Gibco). The cells were differentiated in the media for 21 days and afterwards fixed with 4% paraformaldehyde (PFA).

Human tissue

For experiments involving human tissue in *paper I* and *paper III*, human brain slices were cut from tissue received from surgical resections performed at Lund University Hospital and Rigshospitalet University Hospital, Copenhagen, and were maintained as previously described [139,140]. Tissue was obtained from patients undergoing surgical treatment for drug-resistant epilepsy (patient information is summarised in Table 1). All following procedures were approved by the local Ethical Committee in Lund (#212/2007) and Copenhagen (H-2-2011-104), respectively, and all experiments were performed in accordance with the Declaration of Helsinki. Written informed consent was obtained from all subjects prior to each surgery.

Briefly, resected tissue was collected in ice-cold sucrose-based cutting solution, containing (in mM): 200 sucrose, 21 $NaHCO_3$, 10 glucose, 3 KCl, 1.25 NaH_2PO_4, 1.6 $CaCl_2$, 2 $MgCl_2$, 2 $MgSO_4$ (all from Sigma-Aldrich), adjusted to 300–310 mOsm and 7.4 pH. In the same solution, 300 µm slices were cut using a vibratome (Leica VT1200S). For long-term organotypic cultures in *paper I,* the slices were subsequently transferred to a rinsing media, containing HBSS (Life Technologies), HEPES (4.76 mg/ml; Sigma-Aldrich), Glucose (2 mg/ml; Sigma-Aldrich) and Penicillin/Streptomycin (50 µl/ml; Life Technologies). After 15 min in the rinsing media, slices were transferred to membrane inserts (Millipore, PIHP03050) in 6-well plates containing BrainPhys medium (Stemcell Technologies) supplemented with B27, Glutamax (1:200), and Penicillin/Streptomycin (10 µl/ml; Life Technologies), and incubated in 5% CO_2 at 37 °C. The organotypic slices were used for *in vitro* grafting of hdInts, for which they were kept in culture for at least 1 day before seeding hdInts on the surface. For acute electrophysiological recordings in *paper III,* cut slices were transferred directly to a submerged incubation chamber filled with aCSF, containing (in mM): 129 NaCl, 21 $NaHCO_3$, 10 glucose, 3 KCl, 1.25 NaH_2PO_4, 2 $MgSO_4$, and 1.6 $CaCl_2$, adjusted to 300–310 mOsm, 7.4 pH, heated to 34 °C, and continuously bubbled with 95% O_2 and 5% CO_2. Slices were incubated submerged for 15-30 minutes before being transferred to cell culture membranes inside a humidified interface holding chamber containing the same aCSF, in which they were maintained for at least 24 hours before the start of the recordings.

Table 1. Patient information. TLE, temporal lobe epilepsy; FCD, focal cortical dysplasia.

Patient	Study	Resection	Age (years)	Sex
1	Paper I	TLE	49	Male
2	Paper I	FCD	27	Female
3	Paper III	TLE	18	Male
4	Paper III	TLE	4	Female
5	Paper III	TLE	43	Female

Lentiviral constructs and virus generation

In *paper I* and *paper II,* the following lentiviral constructs were used: lentivirus vector hSyn-hChR2(H134R)-mCherry-WPRE (obtained by cloning at the lab from Addgene #20945, a gift from Karl Deisseroth [141]); and for the doxycycline-inducible Tet-On system: lentivirus vector FUW-TetO-Ascl1-T2A-puromycin (Addgene #97329), lentivirus vector FUW-TetO-Dlx2-IRES-hygromycin (Addgene #97330), and lentivirus vector FUW-rtTA (Addgene #20342), all gift from Marius Werning [81]. The lentiviral particles were produced using PEI for transfection of 293T cells in a biosafety level 2 environment as previously described [142].

In *paper IV,* the pCCL_EF1a-mCh and pCCL_EF1a-GDNF-mCh plasmids were generated by Cristina Salado Manzano at CIEMAT (Madrid, Spain), and donated by

Dr. Josep M. Canals Coll from Universitat de Barcelona. The viral particles were produced at the Viral Vector service of Centro Nacional de Investigaciones Cardiovasculares (Madrid, Spain), by co-transfecting 293T cells with the lentiviral plasmid and a packaging plasmid.

Differentiation of hESCs into inhibitory GABAergic neurons

In *paper I* and *paper II,* GABAergic interneurons were derived from H1 ESCs, which were transduced with Tet-On system lentiviral particles and *ChR2-mCherry* lentivirus before differentiation. The induced GABAergic interneurons were generated as described in Yang et al. (2017) [81], with some modifications. Briefly, for starting the differentiation protocol, 60-70% confluent cells were treated with Accutase (Stem Cell Technologies) and plated as single cells in 6-well plates (~3–5x10^5 cells/well) at day *in vitro* (DIV) 0. Cells were seeded on plates coated with Matrigel (Corning), in mTeSR1 containing 10 mM Y-27632 (Stem Cell Technologies). On DIV 1, the culture medium was replaced with N2 medium consisting of DMEM/F12 supplemented with 1% N-2 Supplement (both Gibco), containing doxycycline (2 g/L, Sigma-Aldrich) to induce the Tet-On gene expression. The culture was kept in the same medium for one week. At 2 DIV, a drug-resistance selection period was started by adding puromycin (0.5 mg/mL, Gibco) and hygromycin (750 mg/mL, Invitrogen) to the fresh media. At 5 DIV antibiotics were removed and cytosine-D-arabinofuranoside (Ara-C, 4 M, Sigma-Aldrich) was added to fresh media. On day 7 of the differentiation, cells were detached into a single-cell suspension using Accutase or TrypLE Express Enzyme (Gibco) and used for either continued differentiation *in vitro*, co-culture with human primary cells and *in vitro* grafting in organotypic human slices (*paper I*), or *in vivo* grafting in nude rats (*paper II*). The different uses are summarised in Figure 9.

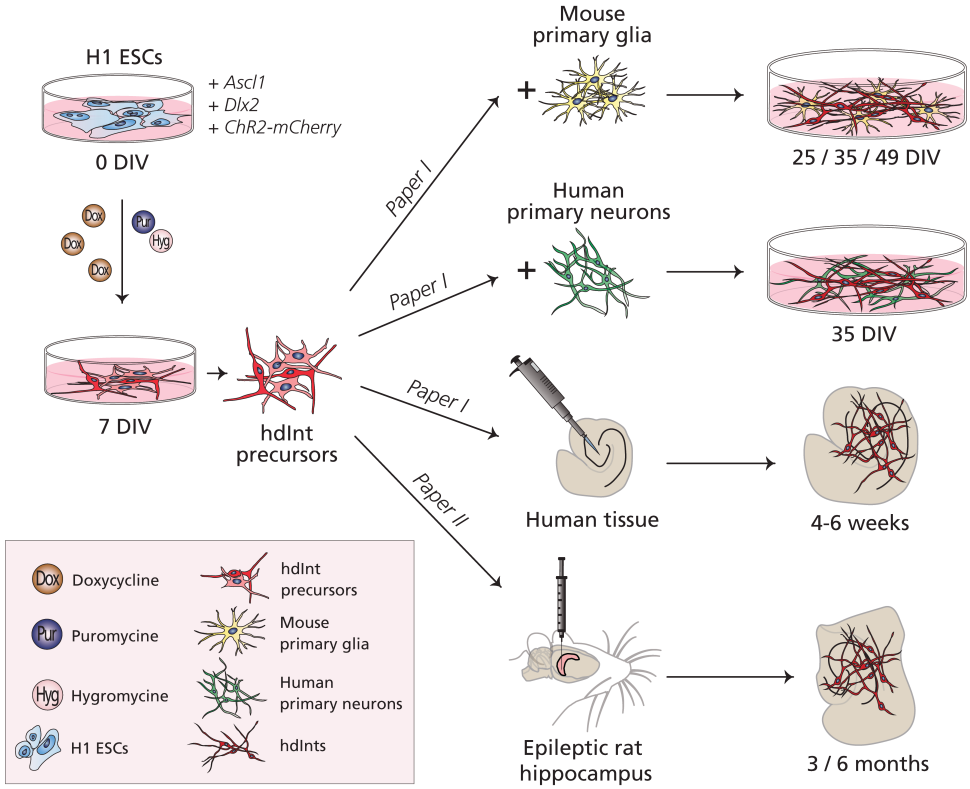

Figure 9. Illustration of the generation of hdInt precursors and their uses. H1 ESCs are transduced by lentiviral particles containing the transcription factors *Ascl1* and *Dlx2* together with the *ChR2-mCherry* lentivirus. After 7 days of differentiation induced by doxycycline, hdInt precursors are used either for continued differentiation *in vitro* with mouse primary glia or human primary cortical cells, or for grafting onto human tissue from patients with epilepsy or into the hippocampi of epileptic rats. ESCs, embryonic stem cells; DIV, days *in vitro*; ChR2, channelrhodopsin-2; hdInt, human ESC-derived interneuron.

For continued differentiation *in vitro*, detached cells were plated together with mouse primary glial cells on Matrigel-coated glass coverslips in 24-well plates (3-5x10^5 and 5x10^4 cells/well respectively). The medium was replaced with Growth medium consisting of Neurobasal medium supplemented with 5% FBS, 2% B27, and 1% GlutaMAX. The cultures were kept in the same medium until analysis at 25 DIV, 35 DIV, or 49 DIV, with half of the medium being exchanged every 2–3 days. Additionally, from ~10 DIV, Ara-C was added to the medium to inhibit glial cell proliferation, and from 15 DIV, BDNF (14 ng/ml, R&D Systems) was added. Importantly, doxycycline was withdrawn from the medium at 14 DIV. For co-culture, detached hdInt precursors were seeded onto human primary cortical cells at a density of 15x10^4 cells/well. Then, both cell types were cultured together following the same differentiation protocol for 4 weeks. For *in vitro* grafting, after seeding the cells, the human tissue organotypic cultures were kept for 30 min in the incubator in an air-

liquid interface, and afterwards, media was added on top to cover the surface. The cultures were kept in the BrainPhys based medium as mentioned above until the time point of analysis (4 to 6 weeks), with the addition of doxycycline for 1 week.

Stereotaxic surgeries

Cell grafting

Cell transplantation surgeries in *paper II* were performed 4 weeks post-SE. HdInt precursors were dissociated at 7 DIV using TrypLE Express Enzyme (Gibco), centrifuged, resuspended to a concentration of 100.000 cells/µl in HBSS (Gibco) containing 10 mM Y-27632 and DNase I Solution (1 g/ml, Stem Cell Technologies), and kept on ice until grafting. The cell suspension was then injected stereotaxically in the hippocampi of epileptic nude rats under isoflurane anaesthesia. Cells were injected bilaterally with the following coordinates from bregma: anterior-posterior (AP) -6.2 mm, medial-lateral (ML) ±5.2 mm, dorsal-ventral (DV) -6.0, -4.8 and -3.6 mm. In total, 3 µl of cell suspension per hippocampus were delivered; 1 µl at each DV coordinate (600.000 cells per animal). To continue the hdInt differentiation *in vivo*, animals were given doxycycline in drinking water (1 mg/ml, 0.5% sucrose) for two days before and four weeks post-transplantation (PT). Cells remaining after grafting were re-plated on Matrigel-coated coverslips in 24-well plates and cultured in N2 medium overnight, until being fixed with 4% PFA containing 0.25% glutaraldehyde, and analysed by immunocytochemistry.

For cell transplantations in *paper IV*, hiAD-MSCs were thawed and after 2 days in culture detached and resuspended, following the same procedures as above. The cell suspension was injected bilaterally into the hippocampi of Sprague Dawley rats 16-24 hours after SE. The injection procedure was identical to the one described above with a slight change in coordinates: AP -5.6 mm, ML ±5.0 mm, DV -6.0, -4.8 and -3.6 mm. Electrodes and a transmitter for video-EEG monitoring were implanted directly after cell transplantation during the same surgical procedure.

Electrode implantation

In *paper II* and *paper IV*, electrodes and transmitters for wireless video-EEG monitoring were implanted in a subset of animals. The procedure was performed mostly as described previously [143]. Briefly, the transmitter (F40-EET, Data Sciences International, MN, USA) was inserted in a subcutaneous pocket on the rat's back. One stainless steel electrode (Plastics One, Roanoke, VA, USA), soldered to the wire of the

transmitter, was implanted in the right hippocampus with the same coordinates as used for the cell injections. The second electrode was placed on top of the dura mater above the motor cortex. Two reference electrodes were placed on the dura mater, 2 mm rostral to the lambda. One stainless screw was attached to the skull bone to secure the electrode assembly by dental cement. After suturing and disinfecting the wound, the animals were injected with a Ringer/glucose (25 mg/ml) solution (1:1 ratio) and returned to housing cages supplied with wet food. Animals were weighed every day for a week after implantation and afterwards once per week.

Seizure monitoring

To start the video-EEG monitoring, the rat cages were individually placed on top of receiver units (Data Sciences International, MN, USA), and the wireless transmitters were activated by a magnet. Four cameras (Axis, Sweden) were used to continuously record video footage of the animal activity. Seizures were then detected offline in NeuroScore (Data Sciences International, MN, USA), where EEG traces were correlated to the video recordings. A scheme of the recording setup is illustrated in Figure 10.

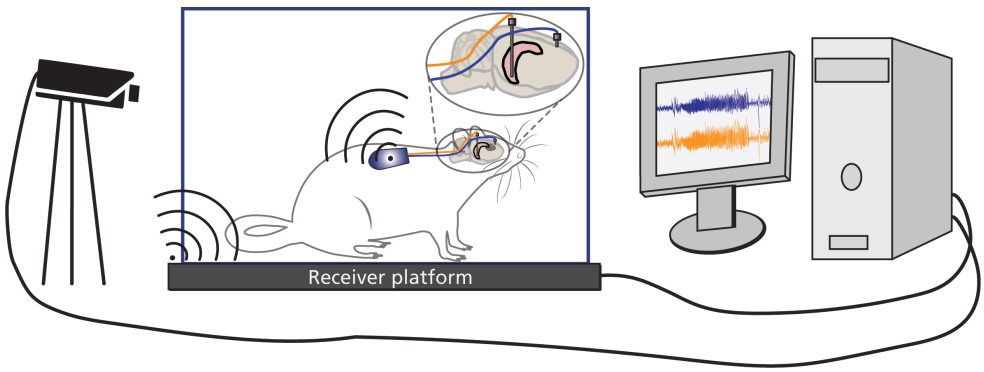

Figure 10. Video-EEG recording setup. The receiver platform wirelessly receives the EEG signal from the transmitter, which is activated by a magnet. The electrode placement in the rat's brain is depicted in the magnification – a depth electrode is placed in the hippocampus, a surface electrode is placed above the motor cortex. Cameras record the behaviour of the animals. The EEG and the video traces are recorded and stored together.

In *paper II,* seizures were detected mostly by only video monitoring (without EEG recordings). The same camera setup was used, and only behavioural seizures were retrospectively visually evaluated.

Behavioural analysis

In *paper IV,* several behavioural tests were performed to assess whether the therapeutic intervention with MSCs had a restoring effect on epilepsy-associated behavioural alterations. For performing and analysis of the tests, ANY-maze software (Stoelting) was used. The open-field test was used for anxiety and locomotion measurements. In 1x1 m, arenas the first 15 minutes of the test were analysed for anxiety related behaviour and the last 15 minutes for locomotion. The session was considered as a habituation stage for the simple novel object recognition test on the following day. During the learning phase, animals were placed in arenas containing two identical objects. After a 3-hour break, one of the two objects was exchanged for a novel one and the animals were placed back in the arena to monitor the time they spend exploring the different objects.

Electrophysiology

In *papers I, II* and *III,* various electrophysiological recordings were performed. For whole-cell patch-clamp recordings of cells grown in culture in *paper I*, glass coverslips were used for continuing the hdInt differentiations from DIV 7. The coverslips containing the cells were transferred to the recording chamber filled with artificial cerebrospinal fluid (aCSF) consisting of (in mM): 129 NaCl, 21 $NaHCO_3$, 10 glucose, 3 KCl, 1.25 NaH_2PO_4, 2 $MgSO_4$, and 1.6 $CaCl_2$ (all from Sigma-Aldrich), adjusted to 300–310 mOsm, pH 7.4, heated to 32 °C, and continuously bubbled with 95% O_2 and 5% CO_2.

For recordings performed in *paper II* and *paper III,* hippocampal slices were used. The animals were briefly anaesthetized with isoflurane and decapitated. Brains were rapidly removed and transferred to an ice-cold cutting aCSF solution containing (in mM): 75 sucrose, 67 NaCl, 26 $NaHCO_3$, 25 D-glucose, 2.5 KCl, 1.25 NaH_2PO_4, 0.5 $CaCl_2$, 7 $MgCl_2$ (all from Sigma-Aldrich), equilibrated with 95% O_2 and 5% CO_2), with a pH ~7.4 and osmolarity ~300 mOsm. The brains were cut in the ice-cold solution on a vibratome into 300 µm thick quasi-horizontal hippocampal slices, which were then transferred to recording aCSF containing (in mM): 118 NaCl, 2 $MgCl_2$, 2 $CaCl_2$, 2.5 KCl, 26 $NaHCO_3$, 1.25 NaH_2PO_4, 10 D-glucose. Slices were incubated in this solution for 30 min at 34 °C and then kept at room temperature (RT) until recording.

For studying the effect of GDNF in *paper III*, hippocampal slices were incubated for 1 hour in recording aCSF, either with or without including 2 nM of mouse GDNF (Sigma-Aldrich). Alternatively, the slices were incubated with 10 µM XIB4035 (Sigma-Aldrich), 1 µM PP2 (Tocris), 0.1% DMSO control aCSF, GDNF 2 nM with 0.1%

DMSO, or a combination of the above. After the incubation period, slices were immediately used for recordings or processed for protein extraction.

Whole-cell patch-clamp

The whole-cell patch-clamp recording method was used in *papers I, II* and *III*. This method allows investigation on a single-cell level, where one can study membrane properties, visualise currents flowing across the membrane, or assess the response of the cell to various drugs or stimulations in real-time. Briefly, a single cell is approached with a patch pipette filled with an electrolyte solution and a recording electrode connected to an amplifier. After forming a GΩ seal on the membrane surface of the cell, suction is applied through the pipette and the seal is ruptured, allowing access to the intracellular compartment.

The individual cells were visualized using infrared differential interference contrast video microscopy (BX51WI; Olympus). hdInts in *paper I* and *paper II* were identified under 520 nm fluorescent light for mCherry+, and for a subset of experiments in *paper I*, human primary neurons were identified by green fluorescent protein (GFP) expression. The tip resistance of the glass pipettes used for approaching the cells was in the range of 2-6 MΩ, these were filled with a specific intracellular solution. For recording from hdInts in *paper I* the solution consisted of (in mM): 122.5 K-gluconate, 17.5 KCl, 10 KOH-HEPES, 0.2 KOH-EGTA, 2 Mg-ATP, 0.3 Na_3GTP, and 8 NaCl (pH 7.2–7.4, ~300 mOsm; all from Sigma-Aldrich). For recording from human primary neurons, the solution contained (in mM): 140 KCl, 10 HEPES, 0.2 EGTA, 4 Mg-ATP, 0.4 Na_3GTP, and 10 NaCl (pH 7.2–7.4, ~300 mOsm). The same intracellular solution was used in *paper II* for all recordings. For recordings from mid-distal CA1 pyramidal neurons in *paper III,* the pipette solution contained (in mM): 135 CsCl, 8 NaCl, 0.2 CsOH-EGTA, 10 CsOH-HEPES, 2 MgATP, 0.3 Na_3GTP, 5 QX-314. Biocytin (0.5–1 mg/ml, Biotium) was additionally dissolved in all intracellular solutions for retrospective identification of the recorded cells. All recordings were performed using a HEKA EPC9 or EPC10 amplifier (HEKA Elektronik) and sampled at 10 kHz with a 3 kHz Bessel anti-aliasing filter while using PatchMaster software for data acquisition. For offline analysis, Igor Pro (Wavemetrics) and Python were used.

Passive membrane properties

In *paper I,* the resting membrane potential (RMP) was determined in current-clamp mode at 0 pA immediately after whole-cell configuration was established. Series resistance (Rs) and input resistance (Ri) were calculated from a 5-mV pulse of 100 ms duration, applied through the patch pipette. In *paper II* a series of these pulses was used to estimate RMP, Rs, Ri, and cell membrane capacitance (Cm). To determine the

ability to fire action potentials (APs), 500 ms current steps ranging from -40 pA to 200 pA in 10 pA steps were applied while holding the cell membrane potential at approximately -70 mV. To measure the AP properties, 1-s long linear ramp currents were injected into the cells, ranging from 0-25 pA up to 0-500 pA. Sodium and potassium currents were evoked by a series of 100-ms long voltage steps ranging from -90 mV to +40 mV in 10 mV steps.

Spontaneous synaptic activity

Spontaneous postsynaptic currents (sPSCs) were recorded at -70 mV. The events were then detected automatically and analysed offline using a custom Python script [144]. To avoid potential artefacts, events with a correlation coefficient to a generated PSC template lower than 0.6 were excluded from the analysis, as well as those with amplitude lower than 3 pA and rise-time higher than 5 ms. Additionally, in *paper I,* events with decay-time longer than 20 ms or shorter than 1.5 times the rise-time of the event were also excluded. In *paper III* events with 20-80% rise time longer than 5 ms and halfwidth shorter than the 20-80% rise time were excluded instead.

Optogenetics

Optogenetics was used to study the formation of functional efferent synapses from hdInts towards "host" neurons in culture or tissue. In both *paper I* and *paper II,* ChR2 was expressed in the hdInts under the synapsin promoter. ChR2 is a light-gated ion channel that upon exposure to blue-light acts as a cation channel. Its expression in neurons allows for specific activation of these cells. In both studies to depolarise the ChR2-expressing hdInts blue light (460 nm) was applied with a LED light source (Prizmatix, Israel). The light was delivered either for a duration of 500 ms or by 5 pulses of 3 milliseconds separated by 97 ms intervals. The efferent synaptic connection towards a recorded host cell was then detected as a postsynaptic current with a specific delay from the light pulse onset. See Figure 11 for a schematic illustration.

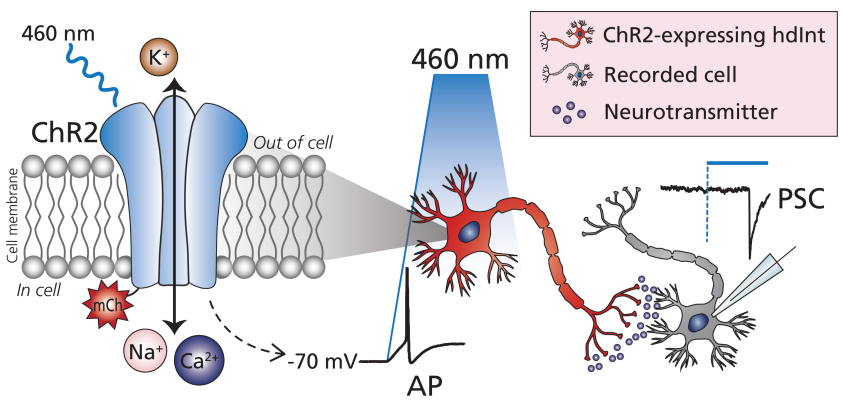

Figure 11. Use of optogenetics for the detection of efferent synapses from hdInts towards host neurons. The ChR2-expressing hdInt is activated by 460 nm (blue) light, which changes the conformation of the ChR2 molecule in the cell's membrane and allows the flow of cations across the membrane. This triggers depolarisation of the hdInt which leads to firing an AP. The AP propagates to the synaptic regions and causes the release of a neurotransmitter (in our case GABA), which then signals to the synaptically connected neuron. The connected neuron receives the signal through its neurotransmitter receptors (in our case GABAergic) expressed in the postsynaptic region, this then leads to the opening of ion channels on the cell membrane which we can detect as PSCs when recording from the cell. ChR2, channelrhodopsin-2; mCh, mCherry; AP, action potential; PSC, postsynaptic current.

Drugs

For whole-cell patch-clamp recordings various drugs were used to investigate synaptic activity and membrane properties of the recorded cells. The drugs and their concentrations are summarised in Table 2.

Table 2. Drugs and concentrations. PTX, picrotoxin; GABA, γ-amminobutyric acid; D-AP5, (2R)-amino-5-phosphonovaleric acid; NMDA, N-methyl-D-aspartate; NBQX, 2,3-dihydroxy-6-nitro-7-sulfamoyl-benzo-quinoxaline-2,3-dione disodium salt; AMPA, a-amino-3-hydroxy-5-methyl-4-isoxazole propionic acid; TTX, tetrodotoxin; TEA, tetraethylammonium.

Drug	Function	Concentration
PTX	GABA receptor blocker	100 µM
D-AP5	NMDA receptor blocker	50 µM
NBQX	AMPA receptor blocker	10 µM
TTX	Sodium channel blocker	1 µM
TEA	Potassium channel blocker	10 mM

Local field potential recordings of epileptiform activity

In *paper II* the effect of grafted hdInts on epileptiform activity was tested on hippocampal slices by blue-light application. The epileptiform activity was induced by either high-K^+ aCSF or zero-Mg^{2+} aCSF. The high-K^+ aCSF contained (in mM): 118 NaCl, 2 $MgCl_2$, 2 $CaCl_2$, 26 $NaHCO_3$, 1.25 NaH_2PO_4, 10 D-glucose and 7.5 to 9.5 KCl. The zero-Mg^{2+} was identical but contained no $MgCl_2$ and only 2.5 KCl. Local field potentials (LFPs) were recorded by glass pipettes with 1-3 MΩ of resistance filled by the same aCSF. The pipette was placed near the graft and where the epileptiform discharges were most prominent. The LFPs were recorded using the same amplifier and sampling rate as for whole-cell patch-clamp recordings. The epileptiform discharges were detected and analysed offline using a custom-made script in Matlab.

Immunological methods

Immunocytochemistry, immunohistochemistry, and imaging

We used immunostainings in all the studies included in the thesis for detecting various proteins of interest. For more detailed protocols see the methods sections of the respective papers.

Generally, when staining cells (*paper I, II* and *IV*), they were washed by phosphate-buffered saline (PBS) and fixed for 10-30 mins by 4% PFA before starting the procedure. When staining tissue sections either whole 300 μm slices from the vibratome were used after overnight fixation in 4% PFA (*paper I, II* and *III*), or they were sub-cut into 30 μm sections on a microtome (*paper II* and *III*). For all GABA stainings, 0.25% glutaraldehyde was added to the PFA solution. In *paper IV*, tissue was collected directly for these experiments. Rats were anaesthetised and perfused with 0.9% ice-cold saline, followed by ice-cold 4% PFA, the brains were extracted and fixed in the same PFA solution overnight. After at least 2 days of incubation in 25% sucrose, the brains were cut into 30 μm sections on a microtome. Sections not used directly for stainings were kept in a glycerol based anti-freeze solution at -20 °C.

For starting the staining procedures, after thorough washing, the samples were incubated in a blocking solution to prevent unspecific antibody binding. This solution consisted of 5-10% serum specific for the secondary antibody in PBS with 0.25% Triton-X. In some cases, permeabilization (*paper I*) or antigen retrieval (*paper III*) was performed before the blocking step. After 1-2 hours of blocking, samples were incubated with primary antibodies diluted in the same blocking solution, either overnight or for 48 hours at 4 °C (300 μm slices), for enzymatic stainings overnight at RT. After washing off the primary antibody solution, in some cases a second blocking step was included, otherwise, samples were incubated with secondary antibodies for 1.5-2 hours (or 24-48 hours at 4 °C for 300 μm slices) either fluorophore-conjugated to allow for fluorescent detection (AlexaFluor Plus 488/555/647, 1:500-1000, Thermo Fisher Scientific) or biotinylated for streptavidin amplification or diaminobenzidine (DAB) detection (1:200, Vector Laboratories). In some cases, for signal amplification and visualisation of patched biocytin-filled cells, streptavidin-conjugated fluorophores were used (1:2000, Jackson Immunoresearch). For DAB detection, sections were then incubated with peroxidase-conjugated avidin-biotin (ABC) kit solution for 1 hour (Vectastain ABC kit), washed thoroughly and then revealed by peroxide-catalysed DAB precipitation (ImmPACT DAB Peroxidase Substrate, both from Vector Laboratories). After washing, tissue sections were mounted on gelatine-coated slides. DAB-revealed sections were dehydrated in an ascending series of alcohols, cleared with xylene and coverslipped with Pertex mountant. Immunofluorescent samples were

mounted/coverslipped with PVA-DABCO. Cell nuclei were stained with Hoechst/DAPI either by including it in PBS in the last washing step before mounting or directly in the mounting media (1:1000). For detailed information of antibodies and dilutions used, see Table 3. Images were acquired either by confocal microscopy (Nikon Confocal A1RHD) or by epifluorescence or brightfield microscopy (Olympus BX61).

Table 3. Summary of primary antibodies.

Antibody	Host	Company	Cat. No.	Dilution
Oct4	Rabbit	Abcam	ab19857	1:500
MAP2	Chicken	Abcam	ab5392	1:2000
MAP2	Mouse	Sigma-Aldrich	M2320	1:500
mCherry	Chicken	Abcam	ab205402	1:2000
GABA	Rabbit	Sigma-Aldrich	A2052	1:2000
GAD65/67	Rabbit	Sigma-Aldrich	G5163	1:500-1000
CB	Rabbit	Swant	CB-38a	1:1000
CR	Rabbit	Swant	CR-7697	1:1000
PV	Mouse	Swant	PV235	1:1000
SST	Rat	Millipore	MAB354	1:100
NPY	Rabbit	Sigma-Aldrich	N9528	1:5000
CCK	Rabbit	Sigma-Aldrich	C2581	1:1000
GFAP	Mouse	Sigma-Aldrich	G3793	1:150
TH	Mouse	Millipore	MAB318	1:200
vGlut1	Mouse	Synaptic Systems	135511	1:200
KGA	Rabbit	Abcam	ab93434	1:1000
STEM121*	Mouse	Takara Bio	Y40410	1:400
Sox2	Rabbit	Abcam	ab97959	1:1000
Ki67	Rabbit	Novocastra	NCL-Ki67p	1:250
Nestin	Mouse	Abcam	ab6142	1:500
β-III-tubulin	Rabbit	Abcam	ab18207	1:1000
Gephyrin	Rabbit	Synaptic Systems	147011	1:500
Synaptophysin**	Mouse	Abcam	ab8049	1:50
Syndecan 3**	Rabbit	Proteintech	10886-1-AP	1:50
Ret***	Rabbit	Abcam	ab134100	1:200
Phospho-Ret***	Rabbit	Sigma-Aldrich	SAB4504530	1:200
Fyn***	Rabbit	Cell Signaling Tech.	4023	1:500
Phospho-Fyn***	Rabbit	Abcam	ab182661	1:500
CD68/ED1	Mouse	Bio-Rad	MCA341R	1:200

*, Streptavidin amplification used for immunofluorescence; **, used for array tomography; ***, used for western blot.

In *paper III,* array tomography was used for the detection of specific proteins expressed in the mouse hippocampus. The staining procedure varies from the one described above and is described in the Methods section of the paper.

For osteocyte and adipocyte stainings in *paper IV*, different staining procedures were used. After fixation cells were thoroughly washed with distilled water. For osteocyte staining, cells were incubated with 2% Alizarin-Red Staining Solution (Sigma-Aldrich) for 2-3 minutes, then rinsed well with water. For adipocyte staining, cells were

incubated with 60% isopropanol, then incubated with Oil Red O solution (Sigma-Aldrich) for 15 mins and washed thoroughly with water. Images were acquired on an inverted microscope (Olympus CKX53).

Image analysis was done using ImageJ (NIH) or Python. The specific procedures are described in the methods sections of the respective papers.

Western blot

In *paper III,* a subset of 300 µm vibratome slices which were incubated in different conditions (see electrophysiology section) was used for protein quantification by Western blot. Tissue was collected into cold N-PER Neuronal Protein Extraction Reagent containing Halt Protease and Phosphatase Inhibitor Cocktail (Thermo Scientific), homogenized, and kept on ice for 10 minutes. Afterwards, samples were centrifuged for 10 minutes at 10.000 g at 4°C, supernatants were collected, aliquoted and stored at -80°C.

To measure protein concentrations in the samples, a Pierce BCA Protein Assay Kit was used (Thermo Scientific). Samples were then denatured at 95 °C for 5 minutes in Bolt LDS Sample Buffer containing Bolt Sample Reducing Agent (Invitrogen). To run SDS-PAGE 30 ug of protein per sample loaded on Bolt 4-12% Bis-Tris Gels with Bolt MES SDS Running Buffer (Invitrogen) and PageRuler Plus Prestained Protein Ladder (Thermo Scientific). After electrophoresis, gels were blotted onto PVDF membranes using Trans-Blot Turbo Mini PVDF Transfer Packs and the Trans-Blot Turbo Transfer System (Bio-Rad) on a High MW program. The membranes were then directly fixed with 0.4% PFA for 30 minutes and then thoroughly rinsed with water. After washing with tris-buffered saline (TBS) containing 0.1% Tween 20 (TTBS), the membranes were blocked in TTBS containing 5% skim milk for 90 minutes at RT and then incubated with primary antibodies diluted in TTBS containing 1% Bovine Serum Albumin (BSA) overnight at 4°C. Primary antibodies and their used concentrations are summarized in Table 3. The next day membranes were washed, incubated in blocking solution containing anti-rabbit HRP-coupled secondary antibodies and Anti-beta Actin antibody (HRP-coupled; Abcam, ab49900) for 90 minutes at RT and thoroughly washed after. Membranes were then exposed to SuperSignal West Pico PLUS Chemiluminescent Substrate (Thermo Scientific) and signals were detected using a ChemiDoc Imaging System (Bio-Rad). In some cases, membranes were stripped using Restore PLUS Western Blot Stripping Buffer (Thermo Scientific) and re-stained with total protein antibodies. Levels of total and phosphorylated proteins were estimated by measuring band intensities with Image Lab Software (Bio-Rad). For Phospho-Ret and Ret analysis, the combination of the two bands was considered as total Ret, for Phospho-Fyn and Fyn analysis the Fyn band was considered as total Fyn due to the identical molecular weight. In all cases, beta-actin was used as a loading control.

Enzyme-linked immunosorbent assay

In *paper IV,* ELISA was used to measure the amount of GDNF release from the MSC lines. The culture media was collected 3 days after plating the cells leftover from cell injections. The levels of GDNF were quantified using a commercially available kit (GDNF Human ELISA Kit, Invitrogen).

Gene expression analysis

In *paper I,* the expression of certain genes related to different stages of neurodevelopment and neuronal subtypes was evaluated using RT-qPCR. RNA was extracted from cells using RNeasy mini kit (Qiagen) and then reversed to cDNA using Maxima First Strand cDNA Synthesis Kit for RT-qPCR (Thermo Fisher Scientific). The obtained cDNA was mixed with PowerUp SYBR Green Master Mix (Thermo Fisher) before running the qPCR. A complete list of the genes and primers used is available within the supplementary information of *paper I*. Data were represented using the ΔCt method, in which all gene expression values are calculated as the average change based on two different housekeeping genes (*ACTB* and *GAPDH*).

Data analysis and statistics

Statistical analysis was performed in Prism (GraphPad), Python (Intel) or Statistica (TIBCO). Generally, for data normally distributed an unpaired t-test was used, when the normality of data was not confirmed, the Mann-Whitney test was used instead. For paired data, the Wilcoxon test was used, while multiple paired comparisons were performed using the Friedman test with Dunn's post hoc test. The binomial test, the Chi-square test or the Fisher's exact test were used for proportion comparisons. Spearman correlation was used for exploring the relationship between two variables. One-way ANOVA with Tukey's post hoc test (for normally distributed data) or Kruskal-Wallis with Dunn's post-hoc test was used for comparing more than two groups together. Linear or non-linear regression was used for the comparison of data with fitted curves. For all these tests, the level of significance was set to $p<0.05$. For the Kolmogorov-Smirnov test, which was used to compare cumulative probability distributions, the level of significance was set to $p<0.01$.

Results

The overall aim of this thesis was to reduce seizure activity in animal models of epilepsy by increasing inhibition within the hippocampal circuitry. In the first half of the thesis, we investigated the inhibitory potential of hESC-derived GABAergic interneurons (*papers I* and *II*), and in the second half, we assessed the inhibitory effects of GDNF (*papers III* and *IV*). For more detailed results, I kindly refer the reader to the respective papers.

GABAergic interneurons generated from human ESCs integrate into human neuronal networks *in vitro*

In *paper I,* we established the protocol to generate GABAergic interneurons from hESCs in the lab by following a published method [81] and introducing some modifications. Firstly, we thoroughly examined the phenotype and electrophysiological properties of the generated cells across 49 days of differentiation. Secondly, we investigated whether they are able to form functional efferent synapses towards human neurons in primary culture and resected tissue from patients with epilepsy.

Human ESCs rapidly differentiate into GABAergic interneurons with electrophysiological properties maturing over time

Together with a clear morphological change of the cultured cells, the switch from a pluripotent stem cell state towards a neuronal phenotype was observed on the gene expression level. A fast reduction of pluripotency markers was observed during the first week of differentiation together with a steady increase in neuronal and GABAergic markers over the whole differentiation period. To accompany the gene expression results, immunocytochemistry at the final stages of the differentiation revealed that 87% of MAP2+ cells (a neuronal marker) were positive for GABA together with a similar number of cells being positive for GAD65/67, another marker of GABAergic neurons. A very small number of cells were deemed glutamatergic or dopaminergic. Within the whole GABAergic population, two interneuron subtypes were predominant, i.e., interneurons expressing calretinin (CR) and calbindin (CB). Cells expressing CR represented 29% of the population, while CB-expressing cells accounted

for 36% of the GABAergic cells. Other interneuron subtypes, such as somatostatin-, neuropeptide-Y- or parvalbumin-expressing interneurons, were rarely spotted (<1%).

To assess the functional maturation of the hdInts and confirm their GABAergic nature on the synaptic level, individual cells within the cultures were subjected to whole-cell patch-clamp recordings. The cells were examined at 25, 35 and 49 DIV and clear signs of their functional maturation over time *in vitro* were observed, such as higher resting membrane potentials (RMP) at the later timepoints or increased number of cells able to fire induced action potentials (APs), these having higher amplitudes, faster rise times and larger afterhyperpolarisation (AHP) amplitudes. The observed changes were correlated to an increased expression of functional voltage-dependent sodium and potassium channels on the cell membrane, as shown by larger induced currents at the later time points. In addition to the mentioned parameters, spontaneous postsynaptic currents were analysed. An increase in the number of detected postsynaptic events at the latest time point indicated continuous formation of new synapses within the neuronal network, and importantly, these currents were diminished by the application of picrotoxin (PTX), a GABA receptor blocker, while blocking glutamatergic receptors had no such effect. These results further support the claim that the generated cells are mostly GABAergic, as suggested by gene expression and immunocytochemistry analyses.

HdInts form functional efferent synapses onto human neurons in vitro

Synaptic integration of the hdInts into a previously established human neuronal network was investigated in two separate sets of experiments: (i) co-culture with human primary neurons from aborted foetuses and (ii) grafting onto cultured slices from brain resections from patients with epilepsy.

The hESCs used for hdInt generation were transduced by a *ChR2-mCherry* lentivirus prior to differentiation. This allowed us to specifically activate the hdInts with blue light while recording from a "host" cell nearby and detect efferent postsynaptic currents. Indeed, after delivering a blue-light pulse these postsynaptic currents were observed in human primary neurons after 4 weeks of co-culture with hdInts. The application of PTX blocked these synaptic responses indicating that the formed synapses were of an inhibitory nature. Correspondingly, when grafting the hdInts onto human tissue, already at 4 weeks post-transplantation (PT), similar postsynaptic currents emerging after blue-light activation of the hdInts were detected when recording from host neurons. These were then readily blocked by PTX as in the co-culture with human primary neurons. These results add to the previously described morphological and functional maturation of the hdInts into inhibitory neurons and demonstrate that they can integrate into human neuronal networks on a synaptic level. These cells could be therefore considered as a promising resource for the future development of cell-based therapies for epilepsy.

GABAergic interneurons generated from human ESCs suppress seizure activity in the epileptic rat brain

In the next study (*paper II*) we asked whether grafted hdInts could suppress spontaneous recurrent seizures (SRSs) in rats with modelled TLE. Additionally, we investigated their functional maturation and formation of efferent connections in the epileptic rat hippocampus over time and tested whether optogenetic activation of the cells is sufficient for reducing epileptiform activity in the rat hippocampal slices.

Grafted hdInts functionally mature in the epileptic rat hippocampus over time and form efferent synapses

As in *paper I,* whole-cell patch-clamp recordings were utilized to investigate the maturation of the hdInts over time. In this study, hdInt precursors were transplanted into the rat hippocampus 4 weeks after KA-SE, and the grafted cells were analyzed at two time points, 3 months PT and 6 months PT. Already at the earlier time point, all the recorded grafted hdInts were able to fire induced APs, however, the AP amplitudes were larger at 6 months PT, the threshold was lower, duration shorter and AHP amplitude higher. Together with the higher RMP of the recorded cells at the later time point, these changing properties indicated progressive functional maturation of the grafted hdInts in the epileptic rat hippocampus. Additionally, these changes corresponded to the increased sodium and potassium currents recorded at 6 months PT, which indicated a higher number of the functional ion channels on the cell membrane. Spontaneous postsynaptic currents were analyzed as well to explore the synaptic integration of the grafted cells into the rat hippocampal network. As expected, cells at the later timepoint received more synaptic inputs as shown by a higher frequency of events. These currents furthermore displayed faster rise times and higher amplitudes. Taken together these results show that over time the hdInts functionally mature in the epileptic hippocampus and integrate more into the neuronal network with time.

To complement these data, we used the expression of ChR2 in the grafted cells to investigate the formation of efferent synapses from the grafted hdInts onto host neurons within the rat hippocampal slices. As in *paper I,* postsynaptic currents induced by the blue-light mediated activation of hdInts were detected when recording from host neurons. These currents were more abundant at the later time point of analysis, suggesting that the grafted hdInts form more efferent synapses over time. Interestingly, these efferent connections were observed also between two hdInts, with the same progression of synapse formation across the two time points. Importantly, the GABAergic nature of the efferent synapses was verified. The application of PTX at both timepoints resulted in the currents being blocked whether it was a graft-to-host or graft-to-graft synaptic connection. These results show that the grafted hdInts functionally

connect with each other as well as with host neurons and that the formed efferent synapses are indeed inhibitory.

The hdInt population in the rat epileptic hippocampus comprises mostly of two interneuron subtypes

In addition to electrophysiological experiments, the hippocampal slices from epileptic rats were subjected to immunohistochemical analysis at both 3 and 6 months PT to further assess their phenotype. As mentioned in the results of *paper I*, the GABAergic cell population generated *in vitro* was comprised of mainly CB- and CR-expressing interneurons. Immunohistochemistry of the *in vivo* grafted hdInts revealed that also, in this case, these two interneuron subtypes represented the vast majority of the cell population at both time points of analysis, with slightly more CR+ cells at 6 months PT. At 3 months PT CB-expressing cells represented 37% of STEM121+ cells (human cell marker) and at 6 months PT 38%. CR-expressing cells accounted for 32% of STEM121+ cells at 3 months PT, while at 6 months PT the percentage was slightly higher, i.e., 38%. The hippocampal slices with hdInt grafts were also stained for GABA. As it was not possible to count individual cells in this case the overall fluorescence levels were examined with the graft area having clearly higher levels than the surrounding tissue. These data from immunohistochemistry contribute to the previous electrophysiology results, further supporting that the grafted cells mature into GABAergic interneurons *in vivo*.

Optogenetic activation of hdInts in hippocampal slices reduces epileptiform activity

Local field potential recordings were used at 6 months PT to investigate whether the grafted hdInts have an inhibitory effect after their optogenetic activation. Firstly, epileptiform discharges were induced in the tissue and then by administering a pulse of blue light the hdInts were activated. During these light stimulation periods, the rate of the epileptiform discharges was diminished suggesting that GABA release from the grafted interneurons has an inhibitory effect in the epileptic tissue.

Grafted hdInts reduce spontaneous seizure frequency in vivo

Lastly, we assessed the therapeutic effect of the cell transplantation in the TLE model used. This was done 4 months after inducing SE in rats by KA injections, with hdInt precursors being transplanted 4 weeks post-SE. To detect seizures, 7 days of 24/7 video recordings were analyzed. The results show that the therapeutic intervention reduced the frequency of SRSs in the epileptic animals by a median of 87%, compared to untreated controls, together with a significantly reduced total time spent in seizure.

Taken together, the results from *paper II* suggest that the functional maturation of the grafted hdInts in the epileptic rat hippocampus, their formation of efferent inhibitory synapses towards the host cells, and their release of GABA within the hippocampal

network inhibits seizure activity in rats with KA-induced TLE. This approach could be used in the future for developing novel cell-based therapies for patients with refractory epilepsy.

Glial cell line-derived neurotrophic factor increases inhibition in the hippocampus

In several animal models of epilepsy, GDNF has been shown to suppress seizures. The mechanisms of how GDNF contributes to synaptic inhibition in the hippocampus were studied in *paper III.* In this study, we used mouse hippocampal slices and human hippocampal slices resected from epilepsy patients. Using whole-cell patch-clamp, immunohistochemistry, and western blot we investigated the effect of GDNF on GABAergic inhibitory transmission within the hippocampal neuronal network.

GDNF increases inhibitory synaptic drive onto CA1 pyramidal neurons in the mouse and human hippocampus

To study the effects of GDNF, mouse hippocampal slices were firstly incubated with GDNF and afterwards whole-cell patch-clamp recordings were performed from CA1 pyramidal neurons. When comparing inhibitory postsynaptic currents (IPSCs) recorded from cells subjected to GDNF to those from control slices, an increased frequency and amplitude of these events was observed. Furthermore, GDNF seemed to increase the proportion of high amplitude/fast rise time events. This suggests an increase of inhibitory postsynaptic sites of the pyramidal neurons specifically in the perisomatic region. Similar results were obtained from human hippocampal slices from resections from patients with epilepsy, where a significant decrease in inter-event intervals was observed after GDNF incubation, however, with a slight decrease in the IPSC amplitudes.

Contributing to these findings are the results from immunohistochemistry performed on the mouse slices, where staining against gephyrin (a postsynaptic marker of inhibitory synapses) was shown to have a higher density in slices incubated with GDNF. On the contrary, staining against parvalbumin and GAD65/67 did not resemble these differences. This further adds to the electrophysiology data, indicating that GDNF does not have an effect on the number of GABAergic pre-synapses, but rather increases the number of perisomatic inhibitory postsynaptic sites.

The inhibitory effect of GDNF is mediated through the activation of the Ret pathway

For investigating the involvement of different intracellular signalling pathways in the GDNF-mediated increase of inhibition several drugs were utilised. Specifically for the

Ret pathway the drug used was XIB4035, which is a positive modulator of the GFRα1/Ret pathway. Adding XIB4035 to the GDNF incubation increased both the frequencies and amplitudes of recorded IPSCs. When incubating slices with a supposed Ret antagonist SPP86 and GDNF, a decrease in inter-event intervals was detected, however, the amplitudes were lower. We concluded that these contrasting results may be due to the non-specificity of SPP86, which acts on multiple targets [145].

In addition to the electrophysiology data, the involvement of the Ret pathway was studied by quantifying the levels of phosphorylated Ret in protein samples from GDNF-incubated slices. Western blot analysis revealed higher levels of phosphorylated Ret after GDNF incubation, which was not further increased by the positive modulator XIB4035. The addition of the Ret antagonist SPP86 however returned the GDNF-induced Ret phosphorylation to the control levels. Taken together, despite some contradictory outcomes, both the electrophysiology and western blot results point to the Ret pathway as the most likely mediator of the GDNF effect.

Two alternative signalling pathways were also investigated for their possible contribution to the GDNF-mediated effect on inhibitory synaptic transmission. However, none of them has proven to have a significant role. The first was the Syndecan-3 pathway since it has been shown that it is expressed mostly in inhibitory interneurons [125]. Results from array tomography showed no detectable levels of Syndecan-3 staining in perisomatic inhibitory synapses targeting CA1 pyramidal neurons, nor in the pyramidal neurons themselves. Together with the low affinity of GDNF to Syndecan-3, these results imply no significant contribution of this pathway to the GDNF-mediated effect. The second investigated pathway alternative to Ret was the NCAM pathway. Activated NCAM signals through the phosphorylation of Fyn, therefore, we used PP2, an antagonist of the Fyn kinase, to explore the involvement of this pathway. Incubation with GDNF and PP2 resulted in decreased IPSC inter-even-intervals and increased amplitudes, which would presumably be the opposite if the NCAM pathway was involved in the inhibitory effect of GDNF. Correspondingly, no significant differences were detected when comparing levels of phosphorylated Fyn in slices incubated with GDNF and GDNF with PP2. Taken together, in our experimental conditions these two signalling pathways don't show that they considerably contribute to the GDNF-mediated increase in the inhibitory synaptic drive on pyramidal neurons, further supporting the involvement of the Ret pathway instead.

To conclude the results from *paper III*, the data suggest that GDNF may be used in the future for developing novel treatment strategies for epilepsy based on its potentiating effect on GABAergic inhibitory transmission in the hippocampal network, which may counteract the increased excitability of an epileptic brain.

Epileptogenesis in rats is altered by human mesenchymal stem cells with and without GDNF release

Utilising the knowledge from *paper III*, that GDNF potentiates inhibition in the hippocampus, in *paper IV* we asked whether introducing it as soon as possible after SE could modify the epileptogenesis process by preventing, delaying, or reducing SRSs in the KA-SE rat TLE model. For delivering GDNF to the hippocampus of these animals we used human adipose-derived MSCs engineered to release GDNF (GDNF-MSCs), and since MSCs alone have a reported therapeutical effect, we used the unmodified cells as a control (Ctrl-MSCs).

Human mesenchymal stem cell transplantation attenuates seizure development during epileptogenesis and seizure frequency thereafter

The MSCs were transplanted bilaterally into the hippocampi of Sprague Dawley rats 16-24 hours after KA-SE induction, together with implanting cortical and hippocampal electrodes for recording EEG activity. This allowed us to monitor brain activity since the start of the epileptogenesis process. The animals were monitored for 35 days. During this time, both GDNF-MSCs and Ctrl-MSCs had inhibitory effects on seizure occurrence. The treated animal groups were always compared to Sham animals, which went through the same surgical procedure but received only the transplantation media without cells. The transplantation of Ctrl-MSCs decreased the number of animals developing SRSs during the recording period and decreased the seizure occurrence rate. None of these parameters was however modified by GDNF-MSC transplantation. Nevertheless, when analysing the seizure occurrence probability, the GDNF-MSCs had a beneficial effect in the first 2 weeks after transplantation, and on the contrary, the Ctrl-MSCs acted therapeutically in the last 3 weeks of the recording period. Therefore, the unmodified Ctrl-MSC transplantation resulted overall in a better outcome, since the beneficial effect of the GDNF-MSCs was limited only to the beginning of the epileptogenesis process.

Next, the frequency of spontaneous seizures was analysed when they started to occur. When comparing to the median of the Sham animals, the Ctrl-MSCs lowered the SRS frequency while the GDNF-MSCs had no such effect. However, when looking closer at the intervals between individual seizures (inter-seizure intervals, ISIs), the GDNF-MSC transplantation modified their distribution, prolonging a part of the ISIs.

Epilepsy-related behavioural alterations are partially corrected by human mesenchymal stem cell transplantation

When looking at the behaviour of MSC-treated and Sham animals, they were always compared to healthy rats, which did not undergo any procedure. The behavioural tests were performed after the 35 days of seizure recording. Sham animals had higher anxiety

levels compared to the healthy ones, whereas the anxiety levels of animals transplanted with MSCs, both Ctrl-MSCs and GDNF-MSCs did not differ from the healthy controls. However, the MSC treatment was not able to restore the locomotion alterations, such as higher distance travelled in the arena and faster speed. Nevertheless, the Ctrl-MSC transplantation did to some extent bring the short-term memory deficits back to healthy control levels. In summary, the behavioural tests used revealed that the unmodified Ctrl-MSCs partially normalised some epilepsy-associated alterations, particularly short-term memory deficits and higher anxiety levels, while the GDNF-MSCs had a therapeutic effect only on the latter.

Transplantation of human mesenchymal stem cells does not reduce microglia activation when cells are no longer present in the tissue

Since MSCs have an immunomodulatory effect, we investigated whether intervening early in the epileptogenesis process by Ctrl- or GDNF-MSC transplantation could diminish the epilepsy-related neuroinflammation in the hippocampus. For this purpose, immunohistochemical analysis has been performed on tissue collected 40 days PT. In Sham animals as well as in the MSC-treated groups the inflammation levels were increased compared to healthy controls, as shown by more staining against activated microglia (ED1/CD68). Therefore, neither the Ctrl-MSC nor the GDNF-MSC transplantation did not attenuate this particular pathological process. We furthermore assessed how long do the two cell lines survive in the tissue by staining against mCherry at 7, 14, 21 and 40 days PT. Surviving Ctrl-MSCs and GDNF-MSCs were observed up until 14 days PT in all the transplanted animals, with no remaining cells found at 21, nor 40 days PT.

Taken together, our results from *paper IV* demonstrate the beneficial effects of MSCs with or without GDNF release on seizures and behavioural alterations during the epileptogenesis process. The presented data hold potential in developing future therapies targeting epileptogenesis.

General discussion

This thesis adds valuable knowledge to the field of novel epilepsy therapies. We focused on TLE as one of the focal epilepsies most commonly pharmacoresistant. To address the hyperexcitability of the neuronal network in TLE we aimed to elevate network inhibition and hopefully suppress seizure activity in animal epilepsy models. In the first half of the work presented here, we focused on generating functionally mature GABAergic interneurons for this purpose. In the second half, we explored the possibilities of utilising GDNF, its' mechanisms of action and antiepileptogenic properties in combination with MSCs.

Enhancing network inhibition by GABAergic cell transplantation

In *paper I,* we generated GABAergic interneurons from hESCs which were able to mature over time *in vitro*. The advantage of the protocol used was its simplicity and high yield of a nearly pure GABAergic cell population. This was achieved by overexpressing just two transcription factors, *Ascl1* and *Dlx2*, which are essential for achieving the GABAergic neuronal phenotype [81]. Other protocols for differentiation of GABAergic interneurons from PSCs use small molecules which direct the fate of the cells. These protocols are usually laborious, with a need to often change the media composition, and take a long time before reaching a certain level of neuronal maturity [146–149]. Using the shorter, more direct path, the cells we differentiated were able to fire action potentials already at 25 DIV, thanks to their expression of functional sodium and potassium channels.

We generated these cells for the purpose of using them in preclinical studies of cell replacement therapy for epilepsy. Cell therapy is a rapidly evolving field being explored for the treatment of various CNS disorders. The desired scenario for successful replacement of the affected neurons is a functional integration of the transplanted neurons into the host neuronal network. The transplanted cells should be able to receive synaptic signals from surrounding neurons and importantly, form efferent synaptic connections towards the host neurons. To confirm this, electrophysiology is the preferred method. Histology may indicate the formation of synapses by staining against

presynaptic and postsynaptic proteins [80], moreover, using the rabies virus for monosynaptic tracing can reveal the connectivity of the grafted neurons [150]. However, with electrophysiology, we can confirm that these synapses are indeed functional. For this purpose, optogenetics proved to be an essential tool [151]. Multiple studies have used optogenetics *in vitro* and *in vivo* to show the formation of functional afferent synapses from host cells to grafted hPSC-derived neurons [152,153], while others observed functional efferent synapses formed by the grafted cells onto the host neurons [79,152,154]. In the context of epilepsy, Cunningham et al. reported that grafted hESC-derived GABAergic interneurons forming efferent synapses with host neurons were able to ameliorate the disease in a mouse pilocarpine TLE model [79].

The ultimate goal of developing novel therapies is to use them to treat human patients. Of course, animal disease models are essential in preclinical research, however, the human CNS poses naturally a different environment. It is therefore of interest to study the interactions of human-derived transplanted neurons to human "host" neurons in existing networks, even if this is possible only *in vitro*. It has been previously shown that human derived neurons are able to receive synaptic inputs from host neurons in human neuronal cultures [138,155], as we confirmed here as well. However, to our knowledge, the formation of functional efferent synapses from the derived neurons onto host human neurons has not been yet reported. In our study, we included such experiments using human foetal-derived neurons and human brain tissue resected from patients with epilepsy. In both cases, we confirmed the synaptic integration of our hESC-derived GABAergic interneurons into the pre-existing human neuronal network *in vitro*. Using optogenetics we proved that the differentiated interneurons formed functional efferent inhibitory synapses onto human host neurons. This *in vitro* platform of testing graft integration into a human neuronal environment could be used in parallel with animal studies to ensure easier clinical translation of developing novel therapies.

In *paper II* we then investigated the potential of these cells to reduce seizure activity using an animal TLE model. Previous studies in animal epilepsy models demonstrated that cell therapy may hold promising potential for the treatment of refractory epilepsy. However, in most of the cases, the authors used foetal-derived GABAergic precursors [71,72,76,77,156]. From the translational perspective, this is not a viable cell source. Using cells derived from foetal tissue not only poses major ethical concerns but also implies a concerning variability depending on the different origins of the tissue. Nevertheless, these studies provide the necessary proof of principle that GABAergic interneurons grafted into an epileptic brain may ameliorate epilepsy symptoms. Naturally, more recent efforts have been put into developing approaches using human cells, which could in the end be used for treating human patients. Human PSCs are inherently the preferred cell source for these types of studies, due to their pluripotent capacities. The two studies published so far, taking advantage of hPSCs for generating

GABAergic interneurons and transplanting them into the hippocampi of rodent TLE models, are the ones by Cunningham et al. from 2014 [79] and Upadhya et al. from 2019 [80]. Even though the results of these studies are very promising, one drawback could be seen in the very long times of the differentiation protocols prior to transplantation. Both studies used small-molecule protocols for deriving the GABAergic precursors from hPSCs, which as mentioned earlier are slow and laborious. In this case, it took several weeks of differentiation *in vitro* before the cells were used for transplantation. In the case of our study, where we used the more direct approach of overexpressing important transcription factors, we were able to transplant the GABAergic precursors safely already 7 days after the start of the differentiation, which may be an advantage for future clinical applications.

For investigating the anti-seizure properties of our hESC-derived GABAergic interneurons we used the well-established rat KA-SE TLE model, which resembles human acquired TLE in several aspects and is included within the framework of the ETSP [59]. Here we transplanted the cells into the hippocampi of the rats four weeks after KA-induced SE. Before evaluating the therapeutic outcome of this intervention, we asked whether the human cell-derived GABAergic interneurons mature and integrate into the rat hippocampus *in vivo*, as they did *in vitro* in the human neuronal networks. As mentioned before, the maturation and synaptic integration of cells used in cell-replacement therapies for CNS disorders is desired for this approach. The cells used in our study did indeed functionally mature *in vivo* in the epileptic rat hippocampus. Moreover, we report the continuing progress of the neuronal maturation from 3 to 6 months after the transplantation. Using electrophysiology to investigate the neuronal properties of the grafted cells we did not encounter a single cell not being able to fire induced APs even at the earlier time point.

To further validate the integration of the grafted cells into the hippocampal network, we needed to prove their synaptic integration as well. Only one of the above-mentioned studies with hPSC-derived GABAergic interneurons observed functional synaptic integration, including afferent and efferent synaptogenesis, using optogenetics and electrophysiology [79]. The more recent work by Upadhya et al. reports synaptic integration of the grafted cells as well, however only using histological methods [80]. It is important to mention here another study where authors used hPSCs to derive GABAergic interneurons and studied their antiepileptic potential in a mouse TLE model [157]. Unfortunately, these cells failed to suppress seizures in this model of epilepsy, despite the grafted interneurons exhibiting mature neuronal properties. The authors afterwards published a second study, investigating the maturation of the hPSC-derived GABAergic interneurons over time *in vivo*. Although they did report substantial morphological and electrophysiological maturation of these cells, they did not examine the formation of functional synapses between the grafted and the host neurons [158]. In our study we addressed this question thoroughly, using optogenetics

as we did in *paper I*. We showed that the grafted hESC-derived GABAergic interneurons were able to form functional inhibitory efferent synapses onto host neurons in the epileptic rat hippocampus already 3 months after being transplanted, and more synapse formation was seen after additional 3 months, indicating that the cells continue to mature and integrate into the host neuronal network.

To further develop this approach, the cell differentiation should be reproducible and yield a high proportion of the desired cell type. With the electrophysiology experiments, we confirmed that our grafted interneurons form inhibitory synapses, which supports the claim that they are indeed GABAergic. Moreover, we investigated which specific subtypes of interneurons are present within the graft population with histology. The majority of the grafted cells were in our case CR- and CB-expressing interneurons. This was not surprising since very similar percentages of these two cell types were present in the *in vitro* differentiated GABAergic population in *paper I*. We hypothesised that these two interneuron subtypes may have a therapeutic potential in epilepsy since it has been shown that they may be affected in the human epileptic hippocampus, where CR interneurons were reported to be reduced in numbers and an altered morphology has been observed of CB interneurons [36,159]. In rodent TLE models CR interneurons are reportedly also vulnerable, with their numbers being strongly decreased and their dendrites reduced and segmented [160,161]. Recently a study using the same transcription factors as we did, reprogrammed glial cells into mostly CR interneurons *in vivo* in the intrahippocampal KA mouse model of TLE. Using this approach, the authors observed a reduction in spontaneous seizures in the treated animals [162].

For the validation of our approach used in *paper II*, we used two different methods. Firstly, we took advantage of the optogenetic modification of the grafted cells and proved that they are able to inhibit epileptiform discharges in hippocampal slices from the epileptic animals *in vitro*. Secondly, we video-monitored the epileptic rats and quantified the number of spontaneous behavioural seizures. We've seen that the animals that received transplants of the hESC-derived GABAergic progenitors displayed a median decrease of 87% in motor seizures. We supported the use of only video recordings without recording the EEG activity by our previous results from this rat TLE model where 97% of all electrographic seizures had behavioural components and were clearly recognisable. This is in accordance with a previous report using the KA-SE rat TLE model where 94% of all electrographic seizures reached stage 5 of the Racine scale and where no seizure clustering affecting the weekly seizure frequencies was observed [80]. Still, however, there is a possibility that our transplants diminished the behavioural seizures in these animals to only electrographic seizures, which would not be detectable by eye. This could still be considered as a positive outcome of the treatment, nevertheless.

In summary, the results from *paper I* and *paper II* of this thesis, showing that hESC-derived GABAergic interneurons functionally integrate into human neuronal networks

in vitro and rat epileptic hippocampal networks *in vivo*, and confirming their ability to suppress seizure activity, represent an important step forward towards developing an innovative therapy alternative to current epilepsy treatments. This approach could in the future help those patients whose seizures can't be controlled by available medications.

Enhancing network inhibition by GDNF and mesenchymal stem cell transplantation

The many positive effects of GDNF on neurons have been observed in preclinical studies of various CNS disorders. In the field of epilepsy, both our group and others have reported the anti-seizure effects of GDNF in animal models, either by overexpressing it directly in host cells using *in vivo* gene therapy [118] or by implanting cells previously modified to produce GDNF *in vitro* [119–121]. What mechanisms stand behind these seizure-inhibitory properties of GDNF has however not yet been fully clarified. Nevertheless, some studies do provide certain clues. It has been shown that the migration of GABAergic interneuron precursors during the development of the olfactory bulb is guided by GDNF, with the participation of one of its receptors, NCAM [163]. Another one of the GDNF receptors, GFRα1, has been shown to be involved in promoting differentiation and migration of cortical GABAergic interneurons during development [164]. This study also found that the Ret and NCAM pathways were not involved in this process, which further led to the identification of the third alternative interneuron-specific GDNF receptor, Syndecan-3 [125]. It has been also reported that mice lacking GFRα1 had reduced numbers of parvalbumin interneurons and displayed a reduced seizure threshold [165]. Taken together, the beneficial effects of GDNF on GABAergic interneurons may be the reason behind its anti-seizure effects, since GABAergic interneurons are responsible for neuronal inhibition in the CNS and the alteration of their numbers or function is a well-documented pathology in patients with epilepsy and animal epilepsy models [35–40].

In *paper III* of this thesis, we investigated the effects of GDNF on CA1 principal excitatory neurons in the hippocampus, particularly, how it acts on their inhibitory synaptic inputs. After incubating hippocampal slices with GDNF, by using electrophysiology, we observed an increase in the inhibitory synaptic drive on the principal hippocampal neurons. This was apparent in mouse as well as human hippocampal slices. The specific pattern of both higher frequencies and amplitudes of the inhibitory postsynaptic events, as we detected in the mouse tissue, has been attributed to changes at the postsynaptic sites [166]. We further supported these electrophysiology findings by observing a denser gephyrin staining on cell soma

membranes of CA1 principal neurons in the GDNF incubated slices. Gephyrin is involved in clustering GABAA receptors on the postsynaptic membrane, therefore, this further supports that GDNF acts rather postsynaptically, possibly increasing GABAA receptor clustering and therefore the efficacy of inhibitory signalling on CA1 pyramidal neurons.

As mentioned above, GDNF acts through various receptors and signalling pathways. In *paper III* we further investigated which of these is involved in the observed effect of GDNF on inhibitory synaptic activity. We used electrophysiology, western blots, and immunohistochemistry to confirm or rule out the involvement of the respective signalling pathways. Enhancing the GFRα1/Ret signalling increased the inhibitory effect of GDNF. Furthermore, the phosphorylation of Ret was higher in GDNF-incubated slices, which then got normalised by inhibiting Ret signalling. All of these observations indicate that the Ret pathway is the one responsible for exerting the GDNF-mediated inhibitory effects on seizures. The other two options, the NCAM/Fyn and the Syndecan-3 pathways, were most probably not involved. We did not see any elevated Fyn phosphorylation levels after GDNF exposure, nor did we see any changes in the electrophysiological measures when inhibiting the Fyn kinase. No Syndecan-3 staining was detected on the somas of CA1 pyramidal neurons, and together with the reported lower affinity of GDNF to this receptor [125,167], we deemed it unlikely that Syndecan-3 has any role in the observed GDNF-mediated changes.

Together with our proposed scenario of how GDNF could suppress seizure activity in animal models of epilepsy, several other alternative mechanisms are possible. One of these is supported by the finding that albumin-mediated disruption of the BBB in mice triggers epileptogenesis and results in seizures [168]. Claudin-5 is a major component of maintaining the integrity of the BBB. The expression of this important molecule was found to be increased by GDNF [169], thus, the elevation of extracellular GDNF levels could alleviate the BBB damage and, in that way, contribute to seizure reduction. GDNF could also act therapeutically within the pathological inflammatory processes which are associated with epileptogenesis [96]. An *in vitro* study reported that astrocyte-derived GDNF can reduce microglial activation [170], therefore, GDNF could hypothetically diminish inflammation in epileptogenesis and ameliorate its outcome.

Taken together, our results from *paper III* suggest that GDNF increases inhibition on the principal neurons of the CA1 region of the hippocampus by inducing GABAA receptor clustering and that this is most probably mediated through the GFRα1/Ret signalling pathway. With this, we contributed to the understanding of how GDNF may exert its anti-seizure effect.

In *paper IV* we continued to investigate whether the GDNF-induced increase in inhibition and thereby seizure-suppression, could be achieved by transplanting

genetically modified GDNF-releasing human MSCs. For this purpose, we used human-derived MSCs as a delivery tool of GDNF and at the same time as a potentiator of the possible therapeutic outcomes. MSCs have shown to have a therapeutic potential in many CNS disorders [90–92] including epilepsy [97–101,104], even without GDNF release. Their beneficial effects are mostly attributed to their neuroprotective and anti-inflammatory properties. Within the epilepsy field, this is mostly utilised to possibly alleviate the inflammatory processes and neurodegeneration associated with epileptogenesis.

MSCs have been widely used in numerous preclinical studies and clinical trials due to the simplicity of their isolation and usage. These cells do not pose any ethical concerns, since they can be derived from adult tissue, which ads the option to use autologous cells for transplantation. Furthermore, they are immune-evasive [103], which reduces the need for immunosuppression when using xeno- or allogeneic transplants. Additionally, MSCs can be used as carriers for other therapeutic agents [171–173]. We utilised this option in our study to deliver GDNF to the rat hippocampi after KA-SE, since as mentioned several times before, GDNF was shown to have seizure-ameliorating effects in several animal epilepsy models [118–121]. Among all the advantages of using MSCs, there is also the possibility to deliver the cells intravenously. However, for the purpose of delivering the therapeutic agent in sufficient amounts to a specific location, we chose to inject them through the intraparenchymal route. Supporting our decision, a study that compared the two delivery routes reported more cells integrated into the hippocampus after intrahippocampal administration of the MSCs compared to the intravenous injections and further confirmed that this results in a better therapeutic outcome in the rat pilocarpine model of TLE [102].

A potential translational drawback of most of the studies which already reported positive effects of MSC transplantation in animal epilepsy models is the use of rodent cells. As already mentioned in the discussion of the GABAergic approach, the use of human cells is generally preferred for further translating cell therapies to human patients. Nevertheless, the studies with rodent MSCs provide useful data for the development of this approach. Most authors focus on how the MSC treatment affects the histopathology during epileptogenesis or in chronic epilepsy. The cells were reported to reduce neurodegeneration and inflammation in the pilocarpine rat TLE model both when used as an antiepileptogenic treatment [97,99] and when introduced after the development of spontaneous seizures [102]. It was shown that MSC transplantation one day after inducing KA-SE in mice resulted in reduced mossy fibre sprouting, astrogliosis and microglia activation one week after [100]. Although human MSCs are not yet used as frequently, similar antiepileptogenic outcomes of their transplantation in rodent epilepsy models were observed, including decreased neuronal loss and glial activation as a result of transplantation one day after pilocarpine-induced SE in rats [104].

Some of these studies include certain measures assessing seizure activity but their relevance should be considered with some reservations. Unlike our study where we monitored the animals continuously for five weeks with video-EEG recordings, most of the mentioned studies either did not use EEG recordings [97,99], therefore, possibly missing only electrographic seizures, or used very short episodic recording periods. For example, in [98] authors use only 2 hours of EEG recordings per week, and in [101] even shorter 15 minute-long EEG recordings were used. In the study with human MSCs, only 9 hours of video-EEG recordings per week were analysed [104]. From these recordings, the authors of the studies conclude that MSC transplantation reduces epileptiform or seizure activity in the treated animals. However, in all the cases where only episodic monitoring was utilised, the authors used the rat pilocarpine model of TLE, which is characterised by seizure clustering [174–176]. Therefore, it would be more relevant to monitor these animals for much longer periods of time to avoid the influence of possible seizure clusters on the results. Importantly, our results reported in *paper IV* are derived from long-term video-EEG recordings starting directly after the MSC transplantation, i.e., one day after KA-induced SE, and continuing for 35 days. This ensures more reliable and conclusive results.

By analysing the video-EEG recordings, we observed that both Ctrl-MSCs and GDNF-MSCs alter the probability of seizure occurrence, the former in the last 3 weeks of the monitoring, while the latter in the first 2 weeks. Moreover, the transplantation of the Ctrl-MSCs resulted in fewer animals developing seizures while the GDNF-MSC transplantation mostly prolonged the inter-seizure intervals. Both cell lines reduced anxiety levels in the epileptic rats but only the Ctrl-MSCs partially restored short-term memory deficits. We cannot attribute these observed differences to the variability of cell survival after transplantation between the two cell lines since both Ctrl-MSCs and GDNF-MSCs were detected in the tissue at 14 days after transplantation but not at 21 days. One could speculate that increased inhibition onto the principal neurons by GDNF releasing grafts was exerted while the cells were still surviving, while the anti-inflammatory and cell-protecting effects outlasted the graft survival. It is however still unclear why GDNF-releasing transplants were unable to exert the latter effects. Identification of how the two cell lines affect the epileptogenesis-associated processes, such as neurodegeneration or inflammation would possibly help to clarify these outcomes. We did analyse the level of microglial activation in the tissue, but this was done only at 40 days after the transplantations and no differences in these measures were seen between the groups. We could therefore speculate that the cells may have had a transient differential anti-inflammatory effect within the hippocampus while they were still surviving and that this might have been sufficient to ameliorate the outcomes of the disease progression.

In summary, *paper IV* provides a deeper insight into how seizures develop during the epileptogenesis process in rats after KA-SE and how the different attributes are affected

by MSC transplantation and by combining it with GDNF release. The positive results from this study may be of use when developing novel antiepileptogenic treatments. However, the differences between the two cell lines used and which specific aspects of epileptogenesis they influence should be further investigated.

Conclusions and future perspectives

In this thesis, we focused on a thorough investigation of different therapeutic approaches for treating TLE. Since patients suffering from this specific type of focal epilepsy often cannot be helped by current medications, the research of alternative treatments is of utmost importance.

In *papers I* and *II,* we focused on developing a cell therapy, aiming to inhibit neuronal networks with the transplantation of human-derived GABAergic interneurons. The advantage of our approach is that we studied the interactions of the hdInts within human neuronal networks *in vitro* and then in an epileptic rodent brain we confirmed that these cells have a seizure-inhibiting effect. The combination of multiple methods of assessing the therapeutic potential of a novel treatment, as was performed here, is an important step towards making a preclinical study more translational. Moreover, including a human *in vitro* platform in preclinical research is implied when the aim is to treat human patients in the future. To continue this path perhaps multicentre studies could be prompted, investigating the safety and therapeutic effects of these cells in multiple epilepsy models. The efficacy of the treatment in one model of the disease does not guarantee that it will act the same in different models. For example, the ETSP framework could be utilised here, as it is proposed in developing new pharmacological treatments for epilepsy [59]. Moreover, assessing the tumorigenicity of the transplant and its survival and efficacy in the long term should be further investigated. Here we demonstrate that the cell therapy reduces seizures at 3 months PT, studies showing that this effect lasts throughout the life of the animals could be performed. Other important aspects to consider when translating a cell-based treatment to the clinics are producing the cells in good manufacturing practice conditions and the possibility of upscaling to the needs of clinical use. For rodent disease models a small number of cells is sufficient, however, when transplanting into the human brain the amount would need to increase by several-fold.

In *paper III* we reported the effects of GDNF on inhibition of the principal neurons in the hippocampus which we associated with the GFRα1/Ret signalling pathway. We have shown that adding GDNF extracellularly increased the inhibitory drive onto these neurons. This we observed in mouse hippocampal slices as well as in resected human tissue from patients with epilepsy, which indicates that this inhibitory effect can be induced in human epileptic tissue as well. Our study therefore provides new insight into how GDNF may exhibit the seizure-inhibiting effects reported in several epilepsy models [118–121]. As for the investigation of the antiepileptogenic potential of GDNF

through the increased inhibition in *paper IV*, more research on GDNF signalling throughout epileptogenesis would possibly help elucidate at what timepoints would the introduction of GDNF be beneficial. In our study, we delivered GNDF into the hippocampi of rats one day after the induction of KA-SE using human-derived MSCs as a carrier. A beneficial effect of these GDNF-MSCs on seizure incidence was seen only for 2 weeks PT, i.e., when alive cells were present in the rat hippocampi. On the other hand, the transplantation of naïve MSCs resulted in seizure reduction at the later stages of epileptogenesis even with cells no longer present. The reason behind the observed differences between the two cell lines could be investigated at multiple time points throughout the epileptogenesis process, looking perhaps at neurodegeneration and inflammation in the hippocampus in more detail. MSCs are widely utilised for their protective, regenerative, and anti-inflammatory properties in a number of clinical trials; however, we must not forget that they are derived from various tissue sources and can differ in their therapeutic potential. In the case of using MSCs as an antiepileptogenic treatment multicentre studies exploring the efficacy and safety of different MSCs in multiple models of epileptogenesis would help move this therapeutic approach forward. From these efforts, a well-defined clinically translatable cell product could arise which could in the future be used for preventing the occurrence of seizures in patients at risk of developing epilepsy. Although there are currently no reliable biomarkers for identifying these patients, studying epileptogenesis and the possible therapeutic interventions preventing the disease is of importance, given that studies of biomarker identification are rapidly expanding.

To conclude, in this thesis, we provide important preclinical data which should encourage further development of the proposed novel alternative treatments for epilepsy. During this developmental process one should always keep the ultimate goal in mind: what we are creating in the lab should eventually be used for treating human patients. This mindset is crucial when translating the studied treatment from laboratory conditions to clinical practice.

Acknowledgements

Here I would like to express my immense gratitude to all the people who contributed to this long yet rewarding PhD journey.

First of all, I would like to thank my supervisor, **Merab Kokaia**, for giving me this chance to grow as a scientist, for the support during the years, for leading me towards a successful finish even during the difficult pandemic times. Thank you for giving me freedom in my ideas but guiding me when needed, thank you for believing in my skills but understanding that doctoral students are just humans too. You motivated me to learn so much during these years and for that I am eternally grateful. Of course, here I need to mention my co-supervisors, **Marco Ledri** and **My Andersson**. Marco, thank you for your valuable input in my projects, for always being there to discuss project planning, analysis, or anything that you could help with. Thank you for your honesty, it was always appreciated and kept me in the real world. My, thank you for always being so positive and excited about new ideas. Thank you for having your doors open to talk not only about scientific but also personal matters. Your input, guidance, and "you can do it" attitude helped me immensely to get through these years of hard work.

Secondly, I would like to acknowledge all the people in the lab, without whom I wouldn't reach the finish line. **Ana**, my fellow PhD student, officemate, and friend, I think only us two fully understand how challenging this journey was. Starting it with you by my side was an honour, thank you for teaching me valuable skills in the beginning and for being there to help during the years. Your never-ending enthusiasm, energy, and diligence always motivated me and pushed me to do my best. Working with you and beside you was always fun and I am very grateful it was you who was there from the beginning to the end. Thank you for all the chats in the office, for all the fikas together and above all for making me feel that I am not alone in this fight. **Ling**, you were such a great addition to the lab! Your excitement to learn new methods and help out in all aspects of lab work helped me to finalise everything I needed. Thank you for cutting the tremendous amount of rat brains, for helping out with stainings but also for the nice conversations while mounting or at fikas, and overall, for becoming a friend who I can talk to. **Esbjörn**, you are a great teacher, and I am grateful that I could work with you in the last years. You taught me to be creative, to have realistic expectations and to put the work in project planning. Thank you for that and for all the fun times in and out of the animal house. **Fredrik**, your creativity inspired me, thank you for your

valuable input and constructive criticism. **Ann-Katrin**, I appreciated all the help with administration, and I value it now that you are gone even more. You were always there to help and to have a nice conversation at fika. **Jenny**, seeing your journey as a scientist makes me believe that everything is possible. Thank you for both being there in the beginning as an inspiration and now in the end bringing new energy to the lab.

Among the people from the lab, I will also mention those who moved on to work elsewhere. **Valentina**, thank you for teaching me so many valuable lessons in the beginning and taking us under your wings. **Nora,** the surgery skills I have now I learnt thanks to you. **Susanne J.**, thank you for sharing your hands-on experience and all your useful tips in troubleshooting protocols. **Susanne G.**, without you I wouldn't have finished any of my *in vivo* projects. I am very grateful for your help with all the work in the animal house and I will always remember the fun times we had, spending whole days together in the basement talking about random things, from Eurovision to shopping dresses. **Apostolos**, you were a crucial part of my PhD journey, thanks to you I can call myself an electrophysiologist. Thank you for everything you taught me, for always being there to help out in the patch-clamp room or adjusting a script, and mostly for making everything more purple. **Honzo**, díky za připomenutí češtiny, za všechny ty muzikální večery i za všechny ty dny strávené v patch-clamp roomu. Ta energie, kterou jsi do laborky přinesl, nám bez tebe chybí. **Nádia**, foi um prazer conhecer-te e espero que nos encontraremos em breve!

To all the students going through the lab, I am grateful for bringing new enthusiasm and passion for science as well as interesting fika conversations. **Lucrezia**, you were a great student, and it was an honour to be your supervisor. Thank you for the challenging yet fun times and all the laughs we had together. **Kerstin**, you became a natural part of the lab, thank you for being there for talks and being so understanding and supportive. **Marine**, you made me feel welcomed in the beginning and made the start easier, thank you for the happy times in the lab and during travels. Also, thanks to all the others who made these years fun: **Bianca, Anja, Arianna, Antonino, Buse, Mohammed**, **Daniel, Adrien**, probably there are people who I forgot but I am grateful, nevertheless.

I would like to acknowledge also all the people from the Marie-Curie consortium I was a part of, Training4CRM. We travelled around Europe together and learnt so many new things from each other. Thanks to **Cristina, Robin, Theresa, Camille, Christine, Shashank, Alireza** and all the others for such good times, **Jenny** for the great coordination and **Josep Canals** for hosting me for a secondment in Barcelona and making me feel at home. I am also very grateful for the opportunity to collaborate with **Alberto** and **Camille**, and later on **Marta Pereira** on the last paper of the thesis.

I would have a hard time enduring this PhD journey without all the amazing people outside the lab. I am so grateful to have my Norsegirls: **Juli,** my work cousin, **Marija,**

my Slavic sister, and **Nadja,** my Swedish blondie. These past years you were the ones that kept me going, I look forward to our Tuesday yoga nights every week and I know you will always be there for me. Thank you for your love and friendship. Thank you also for going through this thesis and giving me valuable input. **Marija,** I believe you will be the best head toastmaster there ever was, thank you for taking on that responsibility. And of course, I won't forget the rest of our Norsemen family. **Fábio**, my Portuguese brother, I enjoyed the more than two years of living together, all the dinners and parties. I value your friendship, honesty, and willingness to help despite your busy work schedule. **Albert**, the half-Slav of the family, I enjoyed our movie nights and lazy days. Thank you for being a good friend and especially thanks for the unlimited supply of LOTR memes. **Isak**, I am always amazed by your ever-growing knowledge. History, languages, musical instruments, you know it all. I am glad to have you as a friend, kind-hearted and the best ramen cook in the world. **Elias**, thank you for sharing your crazy work stories and for being such an easy-going friend, always willing to help out.

To all the other people from the originally "**Be creative**", later "**Be festive**" groups and all the others I met during the years, I enjoyed having so many amazing people around and for sure I will miss some names now. Thank you, **Martino, Matilde, Marcus, Alex, Roberta, Maria, Caro, Tiago B., David, Edo, Jess, Lav, Chang, Kat, Laura, Marta, Nic, Scott, Henrique**, **Oskar, Franki, Vika, Mert, Carletto, Kritika,** and probably others that I forgot.

Next, I would like to thank my whole **family**. A nakonec bych chtěla poděkovat celé svojí **rodině**. Díky za podporu v celém tom dlouhém procesu vzdělávaní, při stěhování se do zahraničí a za to, že mě vždycky přijmete s otevřenou náručí, když už mám dost studeného Švédska a potřebuji dobít energii. Mám Vás ráda. Taky bych tady ráda zmínila moji milou **Markétku**, děkuji za Tvé přátelství na blízko i na dálku. Finally we can both call each other „The Doctor".

And finally, the person who is there for me every day even though from far away. **Tiago**, I am so grateful to have you, thank you for everything, from just listening to me complain or introducing me to Portuguese culture, to travelling together and just having a good time. Thank you for your encouragement during these last hard months and also for taking my mind off things when I was drowning in stress. I love you and can't wait for our future adventures together. Amo-te!

References

1. Feigin, V.L.; Nichols, E.; Alam, T.; Bannick, M.S.; Beghi, E.; Blake, N.; Culpepper, W.J.; Dorsey, E.R.; Elbaz, A.; Ellenbogen, R.G.; et al. Global, regional, and national burden of neurological disorders, 1990–2016: a systematic analysis for the Global Burden of Disease Study 2016. *Lancet Neurol.* **2019**, *18*, 459–480, doi:10.1016/S1474-4422(18)30499-X.
2. Beghi, E.; Giussani, G.; Abd-Allah, F.; Abdela, J.; Abdelalim, A.; Abraha, H.N.; Adib, M.G.; Agrawal, S.; Alahdab, F.; Awasthi, A.; et al. Global, regional, and national burden of epilepsy, 1990–2016: a systematic analysis for the Global Burden of Disease Study 2016. *Lancet Neurol.* **2019**, *18*, 357–375, doi:10.1016/S1474-4422(18)30454-X.
3. Sander, J.W. The epidemiology of epilepsy revisited : Current Opinion in Neurology. *Curr. Opin. Neurol.* **2003**, *16*, 165–170.
4. Beghi, E. The Epidemiology of Epilepsy. *Neuroepidemiology* **2020**, *54*, 185–191, doi: 10.1159/000503831.
5. de Boer, H.M.; Mula, M.; Sander, J.W. The global burden and stigma of epilepsy. *Epilepsy Behav.* **2008**, *12*, 540–546, doi:10.1016/j.yebeh.2007.12.019.
6. Wiebe, S.; Bellhouse, D.R.; Fallahay, C.; Eliasziw, M. Burden of epilepsy: The Ontario Health Survey. *Can. J. Neurol. Sci.* **1999**, *26*, 263–270, doi:10.1017/S0317167100000354.
7. Reynolds, E.H. The ILAE/IBE/WHO Global Campaign against Epilepsy: Bringing Epilepsy "Out of the Shadows." *Epilepsy Behav.* **2000**, *1*, S3–S8, doi:10.1006/ebeh.2000.0104.
8. Fisher, R.S.; Acevedo, C.; Arzimanoglou, A.; Bogacz, A.; Cross, J.H.; Elger, C.E.; Engel, J.; Forsgren, L.; French, J.A.; Glynn, M.; et al. ILAE Official Report: A practical clinical definition of epilepsy. *Epilepsia* **2014**, *55*, 475–482, doi:10.1111/epi.12550.
9. Hauser, W.A.; Beghi, E. First seizure definitions and worldwide incidence and mortality. *Epilepsia* **2008**, *49*, 8–12, doi:10.1111/j.1528-1167.2008.01443.x.
10. Fisher, R.S.; Van Emde Boas, W.; Blume, W.; Elger, C.; Genton, P.; Lee, P.; Engel, J. Epileptic seizures and epilepsy: Definitions proposed by the International League Against Epilepsy (ILAE) and the International Bureau for Epilepsy (IBE). *Epilepsia* **2005**, *46*, 470–472, doi: 10.1111/j.0013-9580.2005.66104.x.
11. Fisher, R.S.; Cross, J.H.; D'Souza, C.; French, J.A.; Haut, S.R.; Higurashi, N.; Hirsch, E.; Jansen, F.E.; Lagae, L.; Moshé, S.L.; et al. Instruction manual for the ILAE 2017 operational classification of seizure types. *Epilepsia* **2017**, *58*, 531–542, doi:10.1111/epi.13671.

12. Löscher, W.; Klein, P. The Pharmacology and Clinical Efficacy of Antiseizure Medications: From Bromide Salts to Cenobamate and Beyond. *CNS Drugs* **2021**, *35*, 935–963, doi: 10.1007/s40263-021-00827-8.

13. Eddy, C.M.; Rickards, H.E.; Cavanna, A.E. The cognitive impact of antiepileptic drugs. *Ther. Adv. Neurol. Disord.* **2011**, *4*, 385–407, doi:10.1177/1756285611417920.

14. Janmohamed, M.; Brodie, M.J.; Kwan, P. Pharmacoresistance – Epidemiology, mechanisms, and impact on epilepsy treatment. *Neuropharmacology* **2020**, *168*, 107790, doi: 10.1016/j.neuropharm.2019.107790.

15. Chen, Z.; Brodie, M.J.; Liew, D.; Kwan, P. Treatment outcomes in patients with newly diagnosed epilepsy treated with established and new antiepileptic drugs a 30-year longitudinal cohort study. *JAMA Neurol.* **2018**, *75*, 279–286, doi:10.1001/jamaneurol.2017.3949.

16. Kwan, P.; Brodie, M.J. Early Identification of Refractory Epilepsy. *N. Engl. J. Med.* **2000**, *342*, 314–319, doi:10.1056/nejm200002033420503.

17. Kalilani, L.; Sun, X.; Pelgrims, B.; Noack-Rink, M.; Villanueva, V. The epidemiology of drug-resistant epilepsy: A systematic review and meta-analysis. *Epilepsia* **2018**, *59*, 2179–2193, doi:10.1111/epi.14596.

18. Löscher, W.; Schmidt, D. Modern antiepileptic drug development has failed to deliver: Ways out of the current dilemma. *Epilepsia* **2011**, *52*, 657–678, doi: 10.1111/j.1528-1167.2011.03024.x.

19. Perucca, E.; Brodie, M.J.; Kwan, P.; Tomson, T. 30 years of second-generation antiseizure medications: impact and future perspectives. *Lancet Neurol.* **2020**, *19*, 544–556, doi: 10.1016/S1474-4422(20)30035-1.

20. Semah, F.; Picot, M.C.; Adam, C.; Broglin, D.; Arzimanoglou, A.; Bazin, B.; Cavalcanti, D.; Baulac, M. Is the underlying cause of epilepsy a major prognostic factor for recurrence? *Neurology* **1998**, *51*, 1256–1262, doi:10.1212/WNL.51.5.1256.

21. Stephen, L.J.; Kwan, P.; Brodie, M.J. Does the Cause of Localisation-Related Epilepsy Influence the Response to Antiepileptic Drug Treatment? *Epilepsia* **2001**, *42*, 357–362, doi:10.1046/J.1528-1157.2001.29000.X.

22. Marcangelo, M.J.; Ovsiew, F. Psychiatric Aspects of Epilepsy. *Psychiatr. Clin. North Am.* **2007**, *30*, 781–802, doi: 10.1016/j.psc.2007.07.005.

23. McIntosh, A.M.; Wilson, S.J.; Berkovic, S.F. Seizure outcome after temporal lobectomy: Current research practice and findings. *Epilepsia* **2001**, *42*, 1288–1307, doi:10.1046/j.1528-1157.2001.02001.x.

24. McIntosh, A.M.; Kalnins, R.M.; Mitchell, L.A.; Fabinyi, G.C.A.; Briellmann, R.S.; Berkovic, S.F. Temporal lobectomy: Long-term seizure outcome, late recurrence and risks for seizure recurrence. *Brain* **2004**, *127*, 2018–2030, doi:10.1093/brain/awh221.

25. Scoville, W.B.; Milner, B. Loss of recent memory after bilateral hippocampal lesions. *J. Neurol. Neurosurg. Psychiatry* **1957**, *20*, 11–21, doi:10.1136/jnnp.20.1.11.

26. Squire, L.R. The Legacy of Patient H.M. for Neuroscience. *Neuron* **2009**, *61*, 6–9, doi:10.1016/j.neuron.2008.12.023.

27. Bliss, T.V.P.; Lømo, T. Long-lasting potentiation of synaptic transmission in the

dentate area of the anaesthetized rabbit following stimulation of the perforant path. *J. Physiol.* **1973**, *232*, 331–356, doi:10.1113/jphysiol.1973.sp010273.

28. O'Keefe, J.; Dostrovsky, J. The hippocampus as a spatial map. Preliminary evidence from unit activity in the freely-moving rat. *Brain Res.* **1971**, *34*, 171–175, doi:10.1016/0006-8993(71)90358-1.
29. Taube, J.S.; Muller, R.U.; Ranck, J.B. Head-direction cells recorded from the postsubiculum in freely moving rats. I. Description and quantitative analysis. *J. Neurosci.* **1990**, *10*, 420–435, doi:10.1523/jneurosci.10-02-00420.1990.
30. Knierim, J.J. The hippocampus. *Curr. Biol.* **2015**, *25*, R1116–R1121, doi: 10.1016/j.cub.2015.10.049.
31. Duvernoy, H.M. *The Human Hippocampus*; Springer Berlin Heidelberg, **2005**, doi: 10.1007/b138576.
32. Freund, T.F.; Buzsáki, G. Interneurons of the hippocampus. *Hippocampus* **1996**, *6*, 347–470, doi: 10.1002/(SICI)1098-1063(1996)6:4<347::AID-HIPO1>3.0.CO;2-I.
33. Blümcke, I.; Thom, M.; Aronica, E.; Armstrong, D.D.; Bartolomei, F.; Bernasconi, A.; Bernasconi, N.; Bien, C.G.; Cendes, F.; Coras, R.; et al. International consensus classification of hippocampal sclerosis in temporal lobe epilepsy: A Task Force report from the ILAE Commission on Diagnostic Methods. *Epilepsia* **2013**, *54*, 1315–1329, doi:10.1111/epi.12220.
34. Cavanagh, J.B.; Meyer, A. Aetiological aspects of ammon's horn sclerosis associated with temporal lobe epilepsy. *Br. Med. J.* **1956**, *2*, 1403–1407, doi:10.1136/bmj.2.5006.1403.
35. Bausch, S.B. Axonal sprouting of GABAergic interneurons in temporal lobe epilepsy. *Epilepsy Behav.* **2005**, *7*, 390–400, doi: 10.1016/j.yebeh.2005.07.019.
36. Maglóczky, Z.S.; Wittner, L.; Borhegyi, Z.S.; Halász, P.; Vajda, J.; Czirják, S.; Freund, T.F. Changes in the distribution and connectivity of interneurons in the epileptic human dentate gyrus. *Neuroscience* **2000**, *96*, 7–25, doi:10.1016/S0306-4522(99)00474-1.
37. de Lanerolle, N.C.; Kim, J.H.; Robbins, R.J.; Spencer, D.D. Hippocampal interneuron loss and plasticity in human temporal lobe epilepsy. *Brain Res.* **1989**, *495*, 387–395, doi:10.1016/0006-8993(89)90234-5.
38. Sun, C.; Mtchedlishvili, Z.; Bertram, E.H.; Erisir, A.; Kapur, J. Selective loss of dentate hilar interneurons contributes to reduced synaptic inhibition of granule cells in an electrical stimulation-based animal model of temporal lobe epilepsy. *J. Comp. Neurol.* **2007**, *500*, 876–893, doi:10.1002/cne.21207.
39. Zhang, W.; Yamawaki, R.; Wen, X.; Uhl, J.; Diaz, J.; Prince, D.A.; Buckmaster, P.S. Surviving hilar somatostatin interneurons enlarge, sprout axons, and form new synapses with granule cells in a mouse model of temporal lobe epilepsy. *J. Neurosci.* **2009**, *29*, 14247–14256, doi:10.1523/JNEUROSCI.3842-09.2009.
40. Liu, Y.Q.; Yu, F.; Liu, W.H.; He, X.H.; Peng, B.W. Dysfunction of hippocampal interneurons in epilepsy. *Neurosci. Bull.* **2014**, *30*, 985–998, doi: 10.1007/s12264-014-1478-4.

41. French, J.A.; Williamson, P.D.; Thadani, V.M.; Darcey, T.M.; Mattson, R.H.; Spencer, S.S.; Spencer, D.D. Characteristics of medial temporal lobe epilepsy: I. Results of history and physical examination. *Ann. Neurol.* **1993**, *34*, 774–780, doi:10.1002/ANA.410340604.

42. Gowers, W. *Epilepsy and other chronic convulsive diseases their causes, symptoms, & treatment.*; London: Churchill, **1881**.

43. Pitkänen, A.; Engel, J. Past and Present Definitions of Epileptogenesis and Its Biomarkers. *Neurotherapeutics* **2014**, *11*, 231–241, doi:10.1007/s13311-014-0257-2.

44. Löscher, W.; Brandt, C. Prevention or modification of epileptogenesis after brain insults: Experimental approaches and translational research. *Pharmacol. Rev.* **2010**, *62*, 668–700, doi:10.1124/pr.110.003046.

45. Pitkänen, A.; Sutula, T.P. Is epilepsy a progressive disorder? Prospects for new therapeutic approaches in temporal-lobe epilepsy. *Lancet Neurol.* **2002**, *1*, 173–181, doi:10.1016/S1474-4422(02)00073-X.

46. Pitkänen, A.; Lukasiuk, K. Molecular and cellular basis of epileptogenesis in symptomatic epilepsy. *Epilepsy Behav.* **2009**, *14*, 16–25, doi:10.1016/j.yebeh.2008.09.023.

47. Engel, J.; Pitkänen, A. Biomarkers for epileptogenesis and its treatment. *Neuropharmacology* **2020**, *167*, 107735, doi:10.1016/j.neuropharm.2019.107735.

48. Löscher, W. Animal Models of Seizures and Epilepsy: Past, Present, and Future Role for the Discovery of Antiseizure Drugs. *Neurochem. Res.* **2017**, *42*, 1873–1888, doi:10.1007/s11064-017-2222-z.

49. Bialer, M.; White, H.S. Key factors in the discovery and development of new antiepileptic drugs. *Nat. Rev. Drug Discov.* **2010**, *9*, 68–82, doi:10.1038/nrd2997.

50. Goddard, G. V.; McIntyre, D.C.; Leech, C.K. A permanent change in brain function resulting from daily electrical stimulation. *Exp. Neurol.* **1969**, *25*, 295–330, doi:10.1016/0014-4886(69)90128-9.

51. Löscher, W.; Jäckel, R.; Czuczwar, S.J. Is amygdala kindling in rats a model for drug-resistant partial epilepsy? *Exp. Neurol.* **1986**, *93*, 211–226, doi:10.1016/0014-4886(86)90160-3.

52. Löscher, W.; Hönack, D.; Rundfeldt, C. Antiepileptogenic effects of the novel anticonvulsant levetiracetam (ucb L059)in the kindling model of temporal lobe epilepsy. *J. Pharmacol. Exp. Ther.* **1998**, *284*, 474–479.

53. Mazarati, A.M.; Thompson, K.W.; Suchomelova, L.; Sankar, R.; Shirasaka, Y.; Nissinen, J.; Pitkänen, A.; Bertram, E.H.; Wasterlain, C. Status Epilepticus: Electrical Stimulation Models. In *Models of Seizures and Epilepsy*; Academic Press, **2006**; pp. 449–464 ISBN 9780120885541, doi:10.1016/B978-012088554-1/50038-4.

54. Cavalheiro, E.A.; Leite, J.P.; Bortolotto, Z.A.; Turski, W.A.; Ikonomidou, C.; Turski, L. Long-Term Effects of Pilocarpine in Rats: Structural Damage of the Brain Triggers Kindling and Spontaneous I Recurrent Seizures. *Epilepsia* **1991**, *32*, 778–782, doi:10.1111/J.1528-1157.1991.TB05533.X.

55. Curia, G.; Longo, D.; Biagini, G.; Jones, R.S.G.; Avoli, M. The pilocarpine model of

temporal lobe epilepsy. *J. Neurosci. Methods* **2008**, *172*, 143–157, doi:10.1016/J.JNEUMETH.2008.04.019.

56. Ben-Ari, Y.; Tremblay, E.; Ottersen, O.P. Injections of kainic acid into the amygdaloid complex of the rat: An electrographic, clinical and histological study in relation to the pathology of epilepsy. *Neuroscience* **1980**, *5*, 515–528, doi:10.1016/0306-4522(80)90049-4.
57. Cavalheiro, E.A.; Riche, D.A.; Le Gal La Salle, G. Long-term effects of intrahippocampal kainic acid injection in rats: A method for inducing spontaneous recurrent seizures. *Electroencephalogr. Clin. Neurophysiol.* **1982**, *53*, 581–589, doi:10.1016/0013-4694(82)90134-1.
58. Riban, V.; Bouilleret, V.; Pham-Lê, B.T.; Fritschy, J.M.; Marescaux, C.; Depaulis, A. Evolution of hippocampal epileptic activity during the development of hippocampal sclerosis in a mouse model of temporal lobe epilepsy. *Neuroscience* **2002**, *112*, 101–111, doi:10.1016/S0306-4522(02)00064-7.
59. Kehne, J.H.; Klein, B.D.; Raeissi, S.; Sharma, S. The National Institute of Neurological Disorders and Stroke (NINDS) Epilepsy Therapy Screening Program (ETSP). *Neurochem. Res.* **2017**, *42*, 1894–1903, doi:10.1007/s11064-017-2275-z.
60. Bertoglio, D.; Amhaoul, H.; Van Eetveldt, A.; Houbrechts, R.; Van De Vijver, S.; Ali, I.; Dedeurwaerdere, S. Kainic acid-induced post-status epilepticus models of temporal lobe epilepsy with diverging seizure phenotype and neuropathology. *Front. Neurol.* **2017**, *8*, 588, doi:10.3389/fneur.2017.00588.
61. Gage, F.H. Cell therapy. *Nature* **1998**, *392*, 18–24.
62. Zakrzewski, W.; Dobrzyński, M.; Szymonowicz, M.; Rybak, Z. Stem cells: Past, present, and future. *Stem Cell Res. Ther.* **2019**, *10*, 1–22, doi:10.1186/s13287-019-1165-5.
63. Thomson, J.A. Embryonic stem cell lines derived from human blastocysts. *Science (80-.).* **1998**, *282*, 1145–1147, doi:10.1126/science.282.5391.1145.
64. Reubinoff, B.E.; Pera, M.F.; Fong, C.Y.; Trounson, A.; Bongso, A. Embryonic stem cell lines from human blastocysts: Somatic differentiation in vitro. *Nat. Biotechnol.* **2000**, *18*, 399–404, doi:10.1038/74447.
65. Takahashi, K.; Yamanaka, S. Induction of Pluripotent Stem Cells from Mouse Embryonic and Adult Fibroblast Cultures by Defined Factors. *Cell* **2006**, *126*, 663–676, doi:10.1016/j.cell.2006.07.024.
66. Takahashi, K.; Tanabe, K.; Ohnuki, M.; Narita, M.; Ichisaka, T.; Tomoda, K.; Yamanaka, S. Induction of Pluripotent Stem Cells from Adult Human Fibroblasts by Defined Factors. *Cell* **2007**, *131*, 861–872, doi:10.1016/j.cell.2007.11.019.
67. Yu, J.; Vodyanik, M.A.; Smuga-Otto, K.; Antosiewicz-Bourget, J.; Frane, J.L.; Tian, S.; Nie, J.; Jonsdottir, G.A.; Ruotti, V.; Stewart, R.; et al. Induced pluripotent stem cell lines derived from human somatic cells. *Science (80-.).* **2007**, *318*, 1917–1920, doi:10.1126/science.1151526.
68. Gage, F.H. Mammalian neural stem cells. *Science (80-.).* **2000**, *287*, 1433–1438.
69. Dominici, M.; Le Blanc, K.; Mueller, I.; Slaper-Cortenbach, I.; Marini, F.C.; Krause,

D.S.; Deans, R.J.; Keating, A.; Prockop, D.J.; Horwitz, E.M. Minimal criteria for defining multipotent mesenchymal stromal cells. The International Society for Cellular Therapy position statement. *Cytotherapy* **2006**, *8*, 315–317, doi:10.1080/14653240600855905.

70. Shetty, A.K.; Upadhya, D. GABA-ergic cell therapy for epilepsy: Advances, limitations and challenges. *Neurosci. Biobehav. Rev.* **2016**, *62*, 35–47, doi:10.1016/j.neubiorev.2015.12.014.

71. Hattiangady, B.; Rao, M.S.; Shetty, A.K. Grafting of striatal precursor cells into hippocampus shortly after status epilepticus restrains chronic temporal lobe epilepsy. *Exp. Neurol.* **2008**, *212*, 468–481, doi:10.1016/j.expneurol.2008.04.040.

72. Baraban, S.C.; Southwell, D.G.; Estrada, R.C.; Jones, D.L.; Sebe, J.Y.; Alfaro-Cervello, C.; Garcia-Verdugo, J.M.; Rubenstein, J.L.R.; Alvarez-Buylla, A. Reduction of seizures by transplantation of cortical GABAergic interneuron precursors into Kv1.1 mutant mice. *Proc. Natl. Acad. Sci.* **2009**, *106*, 15472–15477, doi:10.1073/pnas.0900141106.

73. Gallego, J.M.; Sancho, F.J.; Vidueira, S.; Ortiz, L.; Gómez-Pinedo, U.; Barcia, J.A. Injection of embryonic median ganglionic eminence cells or fibroblasts within the amygdala in rats kindled from the piriform cortex. *Seizure* **2010**, *19*, 461–466, doi:10.1016/j.seizure.2010.06.001.

74. de la Cruz, E.; Zhao, M.; Guo, L.; Ma, H.; Anderson, S.A.; Schwartz, T.H. Interneuron Progenitors Attenuate the Power of Acute Focal Ictal Discharges. *Neurotherapeutics* **2011**, *8*, 763–773, doi:10.1007/s13311-011-0058-9.

75. Hunt, R.F.; Girskis, K.M.; Rubenstein, J.L.; Alvarez-Buylla, A.; Baraban, S.C. GABA progenitors grafted into the adult epileptic brain control seizures and abnormal behavior. *Nat. Neurosci.* **2013**, *16*, 692–697, doi:10.1038/nn.3392.

76. Casalia, M.L.; Howard, M.A.; Baraban, S.C. Persistent seizure control in epileptic mice transplanted with gamma-aminobutyric acid progenitors. *Ann. Neurol.* **2017**, *82*, 530–542, doi:10.1002/ana.25021.

77. Waldau, B.; Hattiangady, B.; Kuruba, R.; Shetty, A.K. Medial ganglionic eminence-derived neural stem cell grafts ease spontaneous seizures and restore GDNF expression in a rat model of chronic temporal lobe epilepsy. *Stem Cells* **2010**, *28*, 1153–1164, doi:10.1002/stem.446.

78. Lee, H.; Yun, S.; Kim, I.S.; Lee, I.S.; Shin, J.E.; Park, S.C.; Kim, W.J.; Park, K.I. Human fetal brain-derived neural stem/progenitor cells grafted into the adult epileptic brain restrain seizures in rat models of temporal lobe epilepsy. *PLoS One* **2014**, *9*, e104092, doi:10.1371/journal.pone.0104092.

79. Cunningham, M.; Cho, J.-H.; Leung, A.; Savvidis, G.; Ahn, S.; Moon, M.; Lee, P.K.J.; Han, J.J.; Azimi, N.; Kim, K.-S.; et al. hPSC-derived maturing GABAergic interneurons ameliorate seizures and abnormal behavior in epileptic mice. *Cell Stem Cell* **2014**, *15*, 559–73, doi:10.1016/j.stem.2014.10.006.

80. Upadhya, D.; Hattiangady, B.; Castro, O.W.; Shuai, B.; Kodali, M.; Attaluri, S.; Bates, A.; Dong, Y.; Zhang, S.C.; Prockop, D.J.; et al. Human induced pluripotent stem cell-derived MGE cell grafting after status epilepticus attenuates chronic epilepsy and comorbidities via synaptic integration. *Proc. Natl. Acad. Sci. U. S. A.* **2019**, *116*, 287–

296, doi:10.1073/pnas.1814185115.

81. Yang, N.; Chanda, S.; Marro, S.; Ng, Y.H.; Janas, J.A.; Haag, D.; Ang, C.E.; Tang, Y.; Flores, Q.; Mall, M.; et al. Generation of pure GABAergic neurons by transcription factor programming. *Nat. Methods* **2017**, *14*, 621–628, doi:10.1038/nmeth.4291.

82. Haynesworth, S.E.; Goshima, J.; Goldberg, V.M.; Caplan, A.I. Characterization of cells with osteogenic potential from human marrow. *Bone* **1992**, *13*, 81–88, doi:10.1016/8756-3282(92)90364-3.

83. Pittenger, M.F.; Mackay, A.M.; Beck, S.C.; Jaiswal, R.K.; Douglas, R.; Mosca, J.D.; Moorman, M.A.; Simonetti, D.W.; Craig, S.; Marshak, D.R. Multilineage potential of adult human mesenchymal stem cells. *Science (80-.).* **1999**, *284*, 143–147, doi:10.1126/science.284.5411.143.

84. Halvorsen, Y.C.; Wilkison, W.O.; Gimble, J.M. Adipose-derived stromal cells—their utility and potential in bone formation. *Int. J. Obes.* **2000**, *24*, S41–S44, doi:10.1038/sj.ijo.0801503.

85. Zuk, P.A.; Zhu, M.; Mizuno, H.; Huang, J.; Futrell, J.W.; Katz, A.J.; Benhaim, P.; Lorenz, H.P.; Hedrick, M.H. Multilineage cells from human adipose tissue: Implications for cell-based therapies. In Proceedings of the Tissue Engineering; Mary Ann Liebert, Inc., **2001**; Vol. 7, pp. 211–228, doi:10.1089/107632701300062859.

86. Romanov, Y.A.; Svintsitskaya, V.A.; Smirnov, V.N. Searching for Alternative Sources of Postnatal Human Mesenchymal Stem Cells: Candidate MSC-Like Cells from Umbilical Cord. *Stem Cells* **2003**, *21*, 105–110, doi:10.1634/stemcells.21-1-105.

87. in 't Anker, P.S.; Scherjon, S.A.; Kleijburg-van der Keur, C.; de Groot-Swings, G.M.J.S.; Claas, F.H.J.; Fibbe, W.E.; Kanhai, H.H.H. Isolation of Mesenchymal Stem Cells of Fetal or Maternal Origin from Human Placenta. *Stem Cells* **2004**, *22*, 1338–1345, doi:10.1634/stemcells.2004-0058.

88. Pittenger, M.F.; Discher, D.E.; Péault, B.M.; Phinney, D.G.; Hare, J.M.; Caplan, A.I. Mesenchymal stem cell perspective: cell biology to clinical progress. *npj Regen. Med. 2019 41* **2019**, *4*, 1–15, doi:10.1038/s41536-019-0083-6.

89. Rodríguez-Fuentes, D.E.; Fernández-Garza, L.E.; Samia-Meza, J.A.; Barrera-Barrera, S.A.; Caplan, A.I.; Barrera-Saldaña, H.A. Mesenchymal Stem Cells Current Clinical Applications: A Systematic Review. *Arch. Med. Res.* **2021**, *52*, 93–101, doi:10.1016/j.arcmed.2020.08.006.

90. Toyoshima, A.; Yasuhara, T.; Kameda, M.; Morimoto, J.; Takeuchi, H.; Wang, F.; Sasaki, T.; Sasada, S.; Shinko, A.; Wakamori, T.; et al. Intra-arterial transplantation of allogeneic mesenchymal stem cells mounts neuroprotective effects in a transient ischemic stroke model in rats: Analyses of therapeutic time window and its mechanisms. *PLoS One* **2015**, *10*, doi:10.1371/journal.pone.0127302.

91. Barhum, Y.; Gai-Castro, S.; Bahat-Stromza, M.; Barzilay, R.; Melamed, E.; Offen, D. Intracerebroventricular transplantation of human mesenchymal stem cells induced to secrete neurotrophic factors attenuates clinical symptoms in a mouse model of multiple sclerosis. *J. Mol. Neurosci.* **2010**, *41*, 129–137, doi:10.1007/s12031-009-9302-8.

92. Hofstetter, C.P.; Schwarz, E.J.; Hess, D.; Widenfalk, J.; El Manira, A.; Prockop, D.J.;

Olson, L. Marrow stromal cells form guiding strands in the injured spinal cord and promote recovery. *Proc. Natl. Acad. Sci. U. S. A.* **2002**, *99*, 2199–2204, doi:10.1073/pnas.042678299.

93. Li, Y.; Chen, J.; Wang, L.; Zhang, L.; Lu, M.; Chopp, M. Intracerebral transplantation of bone marrow stromal cells in a 1-methyl-4-phenyl-1,2,3,6-tetrahydropyridine mouse model of Parkinson's disease. *Neurosci. Lett.* **2001**, *316*, 67–70, doi:10.1016/S0304-3940(01)02384-9.

94. McCoy, M.K.; Martinez, T.N.; Ruhn, K.A.; Wrage, P.C.; Keefer, E.W.; Botterman, B.R.; Tansey, K.E.; Tansey, M.G. Autologous transplants of Adipose-Derived Adult Stromal (ADAS) cells afford dopaminergic neuroprotection in a model of Parkinson's disease. *Exp. Neurol.* **2008**, *210*, 14–29, doi:10.1016/j.expneurol.2007.10.011.

95. Liang, X.; Ding, Y.; Zhang, Y.; Tse, H.F.; Lian, Q. Paracrine mechanisms of mesenchymal stem cell-based therapy: Current status and perspectives. *Cell Transplant.* **2014**, *23*, 1045–1059, doi:10.3727/096368913X667709.

96. Vezzani, A.; Friedman, A.; Dingledine, R.J. The role of inflammation in epileptogenesis. *Neuropharmacology* **2013**, *69*, 16–24, doi: 10.1016/j.neuropharm.2012.04.004.

97. Abdanipour, A.; Tiraihi, T.; Mirnajafi-Zadeh, J. Improvement of the pilocarpine epilepsy model in rat using bone marrow stromal cell therapy. *Neurol. Res.* **2011**, *33*, 625–632, doi:10.1179/1743132810Y.0000000018.

98. Long, Q.; Qiu, B.; Wang, K.; Yang, J.; Jia, C.; Xin, W.; Wang, P.; Han, R.; Fei, Z.; Liu, W. Genetically engineered bone marrow mesenchymal stem cells improve functional outcome in a rat model of epilepsy. *Brain Res.* **2013**, *1532*, 1–13, doi:10.1016/j.brainres.2013.07.020.

99. Fukumura, S.; Sasaki, M.; Kataoka-Sasaki, Y.; Oka, S.; Nakazaki, M.; Nagahama, H.; Morita, T.; Sakai, T.; Tsutsumi, H.; Kocsis, J.D.; et al. Intravenous infusion of mesenchymal stem cells reduces epileptogenesis in a rat model of status epilepticus. *Epilepsy Res.* **2018**, *141*, 56–63, doi:10.1016/j.eplepsyres.2018.02.008.

100. Voulgari-Kokota, A.; Fairless, R.; Karamita, M.; Kyrargyri, V.; Tseveleki, V.; Evangelidou, M.; Delorme, B.; Charbord, P.; Diem, R.; Probert, L. Mesenchymal stem cells protect CNS neurons against glutamate excitotoxicity by inhibiting glutamate receptor expression and function. *Exp. Neurol.* **2012**, *236*, 161–170, doi:10.1016/j.expneurol.2012.04.011.

101. Huicong, K.; Zheng, X.; Furong, W.; Zhouping, T.; Feng, X.; Qi, H.; Xiaoyan, L.; Xiaojiang, H.; Na, Z.; Ke, X.; et al. The imbalanced expression of adenosine receptors in an epilepsy model corrected using targeted mesenchymal stem cell transplantation. *Mol. Neurobiol.* **2013**, *48*, 921–930, doi:10.1007/s12035-013-8480-0.

102. Salem, N.A.; El-Shamarka, M.; Khadrawy, Y.; El-Shebiney, S. New prospects of mesenchymal stem cells for ameliorating temporal lobe epilepsy. *Inflammopharmacology* **2018**, *26*, 963–972, doi:10.1007/s10787-018-0456-2.

103. Ankrum, J.A.; Ong, J.F.; Karp, J.M. Mesenchymal stem cells: Immune evasive, not immune privileged. *Nat. Biotechnol.* **2014**, *32*, 252–260, doi:10.1038/nbt.2816.

104. Huang, P.Y.; Shih, Y.H.; Tseng, Y. jhan; Ko, T.L.; Fu, Y.S.; Lin, Y.Y. Xenograft of human umbilical mesenchymal stem cells from Wharton's jelly as a potential therapy for rat pilocarpine-induced epilepsy. *Brain. Behav. Immun.* **2016**, *54*, 45–58, doi:10.1016/j.bbi.2015.12.021.

105. Das, M.; Mayilsamy, K.; Tang, X.; Han, J.Y.; Foran, E.; Willing, A.E.; Mohapatra, S.S.; Mohapatra, S. Pioglitazone treatment prior to transplantation improves the efficacy of human mesenchymal stem cells after traumatic brain injury in rats. *Sci. Rep.* **2019**, *9*, 1–13, doi:10.1038/s41598-019-49428-y.

106. D'souza, N.; Rossignoli, F.; Golinelli, G.; Grisendi, G.; Spano, C.; Candini, O.; Osturu, S.; Catani, F.; Paolucci, P.; Horwitz, E.M.; et al. Mesenchymal stem/stromal cells as a delivery platform in cell and gene therapies. *BMC Med.* **2015**, *13*, 1–15, doi:10.1186/s12916-015-0426-0.

107. Simonato, M. Gene therapy for epilepsy. *Epilepsy Behav.* **2014**, *38*, 125–130, doi:10.1016/j.yebeh.2013.09.013.

108. Falcicchia, C.; Simonato, M.; Verlengia, G. New tools for epilepsy therapy. *Front. Cell. Neurosci.* **2018**, *12*, 147, doi:10.3389/fncel.2018.00147.

109. Chira, S.; Jackson, C.S.; Oprea, I.; Ozturk, F.; Pepper, M.S.; Diaconu, I.; Braicu, C.; Raduly, L.Z.; Calin, G.A.; Berindan-Neagoe, I. Progresses towards safe and efficient gene therapy vectors. *Oncotarget* **2015**, *6*, 30675, doi:10.18632/ONCOTARGET.5169.

110. Bessis, N.; GarciaCozar, F.J.; Boissier, M.C. Immune responses to gene therapy vectors: influence on vector function and effector mechanisms. *Gene Ther. 2004 111* **2004**, *11*, S10–S17, doi:10.1038/sj.gt.3302364.

111. Simonato, M.; Zucchini, S. Are the neurotrophic factors a suitable therapeutic target for the prevention of epileptogenesis? In Proceedings of the Epilepsia; John Wiley & Sons, Ltd, **2010**; Vol. 51, pp. 48–51, doi:10.1111/j.1528-1167.2010.02609.x.

112. Paradiso, B.; Marconi, P.; Zucchini, S.; Berto, E.; Binaschi, A.; Bozac, A.; Buzzi, A.; Mazzuferi, M.; Magri, E.; Mora, G.N.; et al. Localized delivery of fibroblast growth factor-2 and brain-derived neurotrophic factor reduces spontaneous seizures in an epilepsy model. *Proc. Natl. Acad. Sci. U. S. A.* **2009**, *106*, 7191–7196, doi:10.1073/pnas.0810710106.

113. Falcicchia, C.; Paolone, G.; Emerich, D.F.; Lovisari, F.; Bell, W.J.; Fradet, T.; Wahlberg, L.U.; Simonato, M. Seizure-Suppressant and Neuroprotective Effects of Encapsulated BDNF-Producing Cells in a Rat Model of Temporal Lobe Epilepsy. *Mol. Ther. - Methods Clin. Dev.* **2018**, *9*, 211–224, doi:10.1016/j.omtm.2018.03.001.

114. Lin, L.F.H.; Doherty, D.H.; Lile, J.D.; Bektesh, S.; Collins, F. GDNF: A glial cell line - Derived neurotrophic factor for midbrain dopaminergic neurons. *Science (80-.).* **1993**, *260*, 1130–1132, doi:10.1126/science.8493557.

115. De Tassigny, X.D. anglemon.; Pascual, A.; Lopez-Barneo, J. GDNF-based therapies, GDNF-producing interneurons, and trophic support of the dopaminergic nigrostriatal pathway. Implications for parkinson's disease. *Front. Neuroanat.* **2015**, *9*, 1–15, doi:10.3389/fnana.2015.00010.

116. Björklund, A. GDNF Therapy: Can We Make It Work? *J. Parkinsons. Dis.* **2021**, *11*, 1019–1022, doi:10.3233/JPD-212706.

117. Walker, M.J.; Xu, X.M. History of glial cell line-derived neurotrophic factor (GDNF) and its use for spinal cord injury repair. *Brain Sci.* **2018**, *8*, 109, doi:10.3390/brainsci8060109.

118. Kanter-Schlifke, I.; Georgievska, B.; Kirik, D.; Kokaia, M. Seizure suppression by GDNF gene therapy in animal models of epilepsy. *Mol. Ther.* **2007**, *15*, 1106–1113, doi:10.1038/sj.mt.6300148.

119. Kanter-Schlifke, I.; Fjord-Larsen, L.; Kusk, P.; Ängehagen, M.; Wahlberg, L.; Kokaia, M. GDNF released from encapsulated cells suppresses seizure activity in the epileptic hippocampus. *Exp. Neurol.* **2009**, *216*, 413–419, doi:10.1016/j.expneurol.2008.12.021.

120. Nanobashvili, A.; Melin, E.; Emerich, D.; Tornøe, J.; Simonato, M.; Wahlberg, L.; Kokaia, M. Unilateral ex vivo gene therapy by GDNF in epileptic rats. *Gene Ther.* **2019**, *26*, 65–74, doi:10.1038/s41434-018-0050-7.

121. Paolone, G.; Falcicchia, C.; Lovisari, F.; Kokaia, M.; Bell, W.J.; Fradet, T.; Barbieri, M.; Wahlberg, L.U.; Emerich, D.F.; Simonato, M. Long-Term, Targeted Delivery of GDNF from Encapsulated Cells Is Neuroprotective and Reduces Seizures in the Pilocarpine Model of Epilepsy. *J. Neurosci.* **2019**, *39*, 2144–2156, doi:10.1523/JNEUROSCI.0435-18.2018.

122. Treanor, J.J.S.; Goodman, L.; De Sauvage, F.; Stone, D.M.; Poulsen, K.T.; Beck, C.D.; Gray, C.; Armanini, M.P.; Pollock, R.A.; Hefti, F.; et al. Characterization of a multicomponent receptor for GDNF. *Nature* **1996**, *382*, 80–83, doi:10.1038/382080a0.

123. Ledda, F.; Paratcha, G.; Sandoval-Guzmán, T.; Ibã̃ez, C.F. GDNF and GFRα1 promote formation of neuronal synapses by ligand-induced cell adhesion. *Nat. Neurosci. 2007 103* **2007**, *10*, 293–300, doi:10.1038/nn1855.

124. Paratcha, G.; Ledda, F.; Ibáñez, C.F. The neural cell adhesion molecule NCAM is an alternative signaling receptor for GDNF family ligands. *Cell* **2003**, *113*, 867–879, doi:10.1016/S0092-8674(03)00435-5.

125. Bespalov, M.M.; Sidorova, Y.A.; Tumova, S.; Ahonen-Bishopp, A.; Magalhães, A.C.; Kulesskiy, E.; Paveliev, M.; Rivera, C.; Rauvala, H.; Saarma, M. Heparan sulfate proteoglycan syndecan-3 is a novel receptor for GDNF, neurturin, and artemin. *J. Cell Biol.* **2011**, *192*, 153–169, doi:10.1083/jcb.201009136.

126. Pochon, N.A.M.; Menoud, A.; Tseng, J.L.; Zurn, A.D.; Aebischer, P. Neuronal GDNF expression in the adult rat nervous system identified by in situ hybridization. *Eur. J. Neurosci.* **1997**, *9*, 463–471, doi:10.1111/j.1460-9568.1997.tb01623.x.

127. Burazin, T.C.D.; Gundlach, A.L. Localization of GDNF/neurturin receptor (c-ret, GFRα-1 and α-2) mRNAs in postnatal rat brain: Differential regional and temporal expression in hippocampus, cortex and cerebellum. *Mol. Brain Res.* **1999**, *73*, 151–171, doi:10.1016/S0169-328X(99)00217-X.

128. Rafi, M.A. Gene and stem cell therapy: Alone or in combination? *BioImpacts* **2011**, *1*,

213–218, doi:10.5681/bi.2011.030.

129. Jandial, R.; Singec, I.; Ames, C.P.; Snyder, E.Y. Genetic modification of neural stem cells. *Mol. Ther.* **2008**, *16*, 450–457, doi:10.1038/sj.mt.6300402.

130. Kurozumi, K.; Nakamura, K.; Tamiya, T.; Kawano, Y.; Kobune, M.; Hirai, S.; Uchida, H.; Sasaki, K.; Ito, Y.; Kato, K.; et al. BDNF Gene-Modified Mesenchymal Stem Cells Promote Functional Recovery and Reduce Infarct Size in the Rat Middle Cerebral Artery Occlusion Model. *Mol. Ther.* **2004**, *9*, 189–197, doi:10.1016/J.YMTHE.2003.10.012.

131. Ikeda, N.; Nonoguchi, N.; Ming, Z.Z.; Watanabe, T.; Kajimoto, Y.; Furutama, D.; Kimura, F.; Dezawa, M.; Coffin, R.S.; Otsuki, Y.; et al. Bone marrow stromal cells that enhanced fibroblast growth factor-2 secretion by herpes simplex virus vector improve neurological outcome after transient focal cerebral ischemia in rats. *Stroke* **2005**, *36*, 2725–2730, doi:10.1161/01.STR.0000190006.88896.d3.

132. Horita, Y.; Honmou, O.; Harada, K.; Houkin, K.; Hamada, H.; Kocsis, J.D. Intravenous administration of glial cell line-derived neurotrophic factor gene-modified human mesenchymal stem cells protects against injury in a cerebral ischemia model in the adult rat. *J. Neurosci. Res.* **2006**, *84*, 1495–1504, doi:10.1002/JNR.21056.

133. Dey, N.D.; Bombard, M.C.; Roland, B.P.; Davidson, S.; Lu, M.; Rossignol, J.; Sandstrom, M.I.; Skeel, R.L.; Lescaudron, L.; Dunbar, G.L. Genetically engineered mesenchymal stem cells reduce behavioral deficits in the YAC 128 mouse model of Huntington's disease. *Behav. Brain Res.* **2010**, *214*, 193–200, doi:10.1016/j.bbr.2010.05.023.

134. Glavaski-Joksimovic, A.; Virag, T.; Mangatu, T.A.; McGrogan, M.; Wang, X.S.; Bohn, M.C. Glial cell line-derived neurotrophic factor-secreting genetically modified human bone marrow-derived mesenchymal stem cells promote recovery in a rat model of Parkinson's disease. *J. Neurosci. Res.* **2010**, *88*, 2669–2681, doi:10.1002/jnr.22435.

135. Moloney, T.C.; Rooney, G.E.; Barry, F.P.; Howard, L.; Dowd, E. Potential of rat bone marrow-derived mesenchymal stem cells as vehicles for delivery of neurotrophins to the Parkinsonian rat brain. *Brain Res.* **2010**, *1359*, 33–43, doi:10.1016/J.BRAINRES.2010.08.040.

136. Ren, G.; Li, T.; Lan, J.Q.; Wilz, A.; Simon, R.P.; Boison, D. Lentiviral RNAi-induced downregulation of adenosine kinase in human mesenchymal stem cell grafts: A novel perspective for seizure control. *Exp. Neurol.* **2007**, *208*, 26–37, doi:10.1016/j.expneurol.2007.07.016.

137. Boison, D. Engineered adenosine-releasing cells for epilepsy therapy: Human mesenchymal stem cells and human embryonic stem cells. *Neurotherapeutics* **2009**, *6*, 278–283, doi:10.1016/j.nurt.2008.12.001.

138. Miskinyte, G.; Devaraju, K.; Grønning Hansen, M.; Monni, E.; Tornero, D.; Woods, N.B.; Bengzon, J.; Ahlenius, H.; Lindvall, O.; Kokaia, Z. Direct conversion of human fibroblasts to functional excitatory cortical neurons integrating into human neural networks. *Stem Cell Res. Ther.* **2017**, *8*, 1–18, doi:10.1186/s13287-017-0658-3.

139. Wickham, J.; Brödjegård, N.G.; Vighagen, R.; Pinborg, L.H.; Bengzon, J.; Woldbye, D.P.D.; Kokaia, M.; Andersson, M. Prolonged life of human acute hippocampal slices

from temporal lobe epilepsy surgery. *Sci. Reports 2018 81* **2018**, *8*, 1–13, doi:10.1038/s41598-018-22554-9.

140. Wickham, J.; Ledri, M.; Bengzon, J.; Jespersen, B.; Pinborg, L.H.; Englund, E.; Woldbye, D.P.D.; Andersson, M.; Kokaia, M. Inhibition of epileptiform activity by neuropeptide Y in brain tissue from drug-resistant temporal lobe epilepsy patients. *Sci. Reports 2019 91* **2019**, *9*, 1–11, doi:10.1038/s41598-019-56062-1.

141. Zhang, F.; Wang, L.P.; Brauner, M.; Liewald, J.F.; Kay, K.; Watzke, N.; Wood, P.G.; Bamberg, E.; Nagel, G.; Gottschalk, A.; et al. Multimodal fast optical interrogation of neural circuitry. *Nature* **2007**, *446*, 633–639, doi:10.1038/nature05744.

142. Lockowandt, M.; Günther, D.M.; Quintino, L.; Breger, L.S.; Isaksson, C.; Lundberg, C. Optimization of production and transgene expression of a retrogradely transported pseudotyped lentiviral vector. *J. Neurosci. Methods* **2020**, 108542, doi:10.1016/j.jneumeth.2019.108542.

143. Nikitidou Ledri, L.; Melin, E.; Christiansen, S.H.; Gøtzsche, C.R.; Cifra, A.; Woldbye, D.P.D.; Kokaia, M. Translational approach for gene therapy in epilepsy: Model system and unilateral overexpression of neuropeptide Y and Y2 receptors. *Neurobiol. Dis.* **2016**, *86*, 52–61, doi:10.1016/J.NBD.2015.11.014.

144. GitHub - AMikroulis/xPSC-detection: Template correlation-based detection of postsynaptic currents. Available online: https://github.com/AMikroulis/xPSC-detection.

145. Dinér, P.; Alao, J.P.; Söderlund, J.; Sunnerhagen, P.; Grøtli, M. Preparation of 3-substituted-1-isopropyl-1 H-pyrazolo[3,4-d]pyrimidin-4- amines as RET kinase inhibitors. *J. Med. Chem.* **2012**, *55*, 4872–4876, doi:10.1021/jm3003944.

146. Maroof, A.M.; Keros, S.; Tyson, J.A.; Ying, S.W.; Ganat, Y.M.; Merkle, F.T.; Liu, B.; Goulburn, A.; Stanley, E.G.; Elefanty, A.G.; et al. Directed differentiation and functional maturation of cortical interneurons from human embryonic stem cells. *Cell Stem Cell* **2013**, *12*, 559–572, doi:10.1016/j.stem.2013.04.008.

147. Nicholas, C.R.; Chen, J.; Tang, Y.; Southwell, D.G.; Chalmers, N.; Vogt, D.; Arnold, C.M.; Chen, Y.J.J.; Stanley, E.G.; Elefanty, A.G.; et al. Functional maturation of hPSC-derived forebrain interneurons requires an extended timeline and mimics human neural development. *Cell Stem Cell* **2013**, *12*, 573–586, doi:10.1016/j.stem.2013.04.005.

148. Liu, Y.; Liu, H.; Sauvey, C.; Yao, L.; Zarnowska, E.D.; Zhang, S.C. Directed differentiation of forebrain GABA interneurons from human pluripotent stem cells. *Nat. Protoc.* **2013**, *8*, 1670–1679, doi:10.1038/nprot.2013.106.

149. Au, E.; Ahmed, T.; Karayannis, T.; Biswas, S.; Gan, L.; Fishell, G. A modular gain-of-function approach to generate cortical interneuron subtypes from ES cells. *Neuron* **2013**, *80*, 1145–1158, doi:10.1016/j.neuron.2013.09.022.

150. Wickersham, I.R.; Lyon, D.C.; Barnard, R.J.O.; Mori, T.; Finke, S.; Conzelmann, K.K.; Young, J.A.T.; Callaway, E.M. Monosynaptic Restriction of Transsynaptic Tracing from Single, Genetically Targeted Neurons. *Neuron* **2007**, *53*, 639–647, doi:10.1016/j.neuron.2007.01.033.

151. Habibey, R.; Sharma, K.; Swiersy, A.; Busskamp, V. Optogenetics for neural transplant manipulation and functional analysis. *Biochem. Biophys. Res. Commun.* **2020**, *527*, 343–349, doi:10.1016/j.bbrc.2020.01.141.

152. Tønnesen, J.; Parish, C.L.; Sørensen, A.T.; Andersson, A.; Lundberg, C.; Deisseroth, K.; Arenas, E.; Lindvall, O.; Kokaia, M. Functional integration of grafted neural stem cell-derived dopaminergic neurons monitored by optogenetics in an in vitro Parkinson model. *PLoS One* **2011**, *6*, e17560, doi:10.1371/journal.pone.0017560.

153. Avaliani, N.; Sørensen, A.T.; Ledri, M.; Bengzon, J.; Koch, P.; Brüstle, O.; Deisseroth, K.; Andersson, M.; Kokaia, M. Optogenetics reveal delayed afferent synaptogenesis on grafted human-induced pluripotent stem cell-derived neural progenitors. *Stem Cells* **2014**, *32*, 3088–3098, doi:10.1002/stem.1823.

154. Weick, J.P.; Liu, Y.; Zhang, S.C. Human embryonic stem cell-derived neurons adopt and regulate the activity of an established neural network. *Proc. Natl. Acad. Sci. U. S. A.* **2011**, *108*, 20189–20194, doi:10.1073/pnas.1108487108.

155. Grønning Hansen, M.; Laterza, C.; Palma-Tortosa, S.; Kvist, G.; Monni, E.; Tsupykov, O.; Tornero, D.; Uoshima, N.; Soriano, J.; Bengzon, J.; et al. Grafted human pluripotent stem cell-derived cortical neurons integrate into adult human cortical neural circuitry. *Stem Cells Transl. Med.* **2020**, sctm.20-0134, doi:10.1002/sctm.20-0134.

156. Henderson, K.W.; Gupta, J.; Tagliatela, S.; Litvina, E.; Zheng, X.; Van Zandt, M.A.; Woods, N.; Grund, E.; Lin, D.; Royston, S.; et al. Long-Term Seizure Suppression and Optogenetic Analyses of Synaptic Connectivity in Epileptic Mice with Hippocampal Grafts of GABAergic Interneurons. *J. Neurosci.* **2014**, *34*, 13492–13504, doi:10.1523/JNEUROSCI.0005-14.2014.

157. Anderson, N.C.; Van Zandt, M.A.; Shrestha, S.; Lawrence, D.B.; Gupta, J.; Chen, C.Y.; Harrsch, F.A.; Boyi, T.; Dundes, C.E.; Aaron, G.; et al. Pluripotent stem cell-derived interneuron progenitors mature and restore memory deficits but do not suppress seizures in the epileptic mouse brain. *Stem Cell Res.* **2018**, *33*, 83–94, doi:10.1016/J.SCR.2018.10.007.

158. Shrestha, S.; Anderson, N.C.; Grabel, L.B.; Naegele, J.R.; Aaron, G.B. Development of electrophysiological and morphological properties of human embryonic stem cell-derived GABAergic interneurons at different times after transplantation into the mouse hippocampus. *PLoS One* **2020**, *15*, e0237426, doi:10.1371/journal.pone.0237426.

159. Tóth, K.; Ero'ss, L.; Vajda, J.; Halász, P.; Freund, T.F.; Maglóczky, Z. Loss and reorganization of calretinin-containing interneurons in the epileptic human hippocampus. *Brain* **2010**, *133*, 2763–2777, doi:10.1093/brain/awq149.

160. Zhang, S.; Khanna, S.; Tang, F.R. Patterns of hippocampal neuronal loss and axon reorganization of the dentate gyrus in the mouse pilocarpine model of temporal lobe epilepsy. *J. Neurosci. Res.* **2009**, *87*, 1135–1149, doi:10.1002/jnr.21941.

161. Tóth, K.; Maglóczky, Z. The vulnerability of calretinin-containing hippocampal interneurons to temporal lobe epilepsy. *Front. Neuroanat.* **2014**, *8*, 100, doi:10.3389/fnana.2014.00100.

162. Lentini, C.; D'Orange, M.; Marichal, N.; Trottmann, M.-M.; Vignoles, R.; Foucault,

L.; Verrier, C.; Massera, C.; Raineteau, O.; Conzelmann, K.-K.; et al. Reprogramming reactive glia into interneurons reduces chronic seizure activity in a mouse model of mesial temporal lobe epilepsy. *Cell Stem Cell* **2021**, doi:10.1016/j.stem.2021.09.002.

163. Paratcha, G.; Ibáñez, C.F.; Ledda, F. GDNF is a chemoattractant factor for neuronal precursor cells in the rostral migratory stream. *Mol. Cell. Neurosci.* **2006**, *31*, 505–514, doi:10.1016/j.mcn.2005.11.007.

164. Pozas, E.; Ibáñez, C.F. GDNF and GFRalpha1 promote differentiation and tangential migration of cortical GABAergic neurons. *Neuron* **2005**, *45*, 701–13, doi:10.1016/j.neuron.2005.01.043.

165. Canty, A.J.; Dietze, J.; Harvey, M.; Enomoto, H.; Milbrandt, J.; Ibáñez, C.F. Regionalized loss of parvalbumin interneurons in the cerebral cortex of mice with deficits in GFRα1 signaling. *J. Neurosci.* **2009**, *29*, 10695–10705, doi:10.1523/JNEUROSCI.2658-09.2009.

166. Markram, H.; Tsodyks, M. Redistribution of synaptic efficacy between neocortical pyramidal neurons. *Nature* **1996**, *382*, 807–810, doi:10.1038/382807a0.

167. Cik, M.; Masure, S.; Lesage, A.S.J.; Van Der Linden, I.; Van Gompel, P.; Pangalos, M.N.; Gordon, R.D.; Leysen, J.E. Binding of GDNF and neurturin to human GDNF family receptor α 1 and 2: Influence of cRET and cooperative interactions. *J. Biol. Chem.* **2000**, *275*, 27505–27512, doi:10.1074/jbc.M000306200.

168. Weissberg, I.; Wood, L.; Kamintsky, L.; Vazquez, O.; Milikovsky, D.Z.; Alexander, A.; Oppenheim, H.; Ardizzone, C.; Becker, A.; Frigerio, F.; et al. Albumin induces excitatory synaptogenesis through astrocytic TGF-β/ALK5 signaling in a model of acquired epilepsy following blood-brain barrier dysfunction. *Neurobiol. Dis.* **2015**, *78*, 115–125, doi:10.1016/j.nbd.2015.02.029.

169. Shimizu, F.; Sano, Y.; Saito, K.; Abe, M.A.; Maeda, T.; Haruki, H.; Kanda, T. Pericyte-derived glial cell line-derived neurotrophic factor increase the expression of claudin-5 in the blood-brain barrier and the blood-nerve barrier. *Neurochem. Res.* **2012**, *37*, 401–409, doi:10.1007/s11064-011-0626-8.

170. Rocha, S.M.; Cristovão, A.C.; Campos, F.L.; Fonseca, C.P.; Baltazar, G. Astrocyte-derived GDNF is a potent inhibitor of microglial activation. *Neurobiol. Dis.* **2012**, *47*, 407–415, doi:10.1016/j.nbd.2012.04.014.

171. Sasaki, M.; Radtke, C.; Tan, A.M.; Zhao, P.; Hamada, H.; Houkin, K.; Honmou, O.; Kocsis, J.D. BDNF-hypersecreting human mesenchymal stem cells promote functional recovery, axonal sprouting, and protection of corticospinal neurons after spinal cord injury. *J. Neurosci.* **2009**, *29*, 14932–14941, doi:10.1523/JNEUROSCI.2769-09.2009.

172. Li, T.; Ren, G.; Kaplan, D.L.; Boison, D. Human mesenchymal stem cell grafts engineered to release adenosine reduce chronic seizures in a mouse model of CA3-selective epileptogenesis. *Epilepsy Res.* **2009**, *84*, 238–241, doi:10.1016/j.eplepsyres.2009.01.002.

173. Glavaski-Joksimovic, A.; Virag, T.; Mangatu, T.A.; McGrogan, M.; Wang, X.S.; Bohn, M.C. Glial cell line-derived neurotrophic factor-secreting genetically modified human bone marrow-derived mesenchymal stem cells promote recovery in a rat model of

Parkinson's disease. *J. Neurosci. Res.* **2010**, *88*, 2669–2681, doi:10.1002/jnr.22435.

174. Arida, R.M.; Scorza, F.A.; De Araujo Peres, C.; Cavalheiro, E.A. The course of untreated seizures in the pilocarpine model of epilepsy. *Epilepsy Res.* **1999**, *34*, 99–107, doi:10.1016/S0920-1211(98)00092-8.

175. Goffin, K.; Nissinen, J.; Van Laere, K.; Pitkänen, A. Cyclicity of spontaneous recurrent seizures in pilocarpine model of temporal lobe epilepsy in rat. *Exp. Neurol.* **2007**, *205*, 501–505, doi:10.1016/j.expneurol.2007.03.008.

176. Bortel, A.; Lévesque, M.; Biagini, G.; Gotman, J.; Avoli, M. Convulsive status epilepticus duration as determinant for epileptogenesis and interictal discharge generation in the rat limbic system. *Neurobiol. Dis.* **2010**, *40*, 478–489, doi:10.1016/j.nbd.2010.07.015.

Paper I

scientific reports

Check for updates

OPEN

Human stem cell-derived GABAergic neurons functionally integrate into human neuronal networks

Ana Gonzalez-Ramos[1]✉, Eliška Waloschková[1], Apostolos Mikroulis[1], Zaal Kokaia[2], Johan Bengzon[3], Marco Ledri[1], My Andersson[1] & Merab Kokaia[1]✉

Gamma-aminobutyric acid (GABA)-releasing interneurons modulate neuronal network activity in the brain by inhibiting other neurons. The alteration or absence of these cells disrupts the balance between excitatory and inhibitory processes, leading to neurological disorders such as epilepsy. In this regard, cell-based therapy may be an alternative therapeutic approach. We generated light-sensitive human embryonic stem cell (hESC)-derived GABAergic interneurons (hdIN) and tested their functionality. After 35 days in vitro (DIV), hdINs showed electrophysiological properties and spontaneous synaptic currents comparable to mature neurons. In co-culture with human cortical neurons and after transplantation (AT) into human brain tissue resected from patients with drug-resistant epilepsy, light-activated channelrhodopsin-2 (ChR2) expressing hdINs induced postsynaptic currents in human neurons, strongly suggesting functional efferent synapse formation. These results provide a proof-of-concept that hESC-derived neurons can integrate and modulate the activity of a human host neuronal network. Therefore, this study supports the possibility of precise temporal control of network excitability by transplantation of light-sensitive interneurons.

GABA-releasing interneurons comprise a highly abundant cell type in the central nervous system. Although they represent a minority of the total neuronal population (only 20% in comparison to 80% of the excitatory neurons), they exert a strong inhibitory effect on principal glutamatergic neurons, controlling network excitability. Furthermore, interneurons modulate cortical maturation, synchronous network oscillations and network plasticity[1,2]. GABAergic interneurons are highly heterogeneous, forming different subpopulations based on their function, morphology and connectivity[3–5]. Dysfunction of interneurons has been implicated in neurological disorders, including schizophrenia, autism, and epilepsy[6,7]. For instance, in temporal lobe epilepsy, the dysfunction and decreased numbers of interneurons in the hippocampus leads to a disruption of the normal hippocampal circuitry resulting in a hyperexcitable neuronal network and seizures[8].

Human pluripotent stem cells are a powerful tool for both modelling brain development and disease, as well as development of cell therapies. The possibility to differentiate patient-specific stem cells to mature regional- and transmitter- specific subtypes of particular human interneuron populations provides an exceptional platform for studying pathophysiology as well as a potential therapeutic approach for diseases. To this goal, several studies have focused on generating GABAergic neurons from human stem cells (hSC), both induced pluripotent stem cells and ESCs[9–11]. Moreover, due to the limited endogenous regeneration capacity of the human brain, transplantation of neural SCs or hSC-derived neurons into a diseased or injured brain is a promising therapeutic approach to restore neuronal population and function. In the past, several studies have shown that transplanted fetal rodent medial ganglionic eminence (MGE)-derived GABAergic progenitor cells can integrate into host tissue and restore function of lost interneurons in animal models of epilepsy[12,13]. Despite the high value of these studies, translation to the clinic requires a human cell source, generating a robust and consistent yield of GABAergic neurons, and proof of functional cell integration. In this regard, hSCs offer great potential as an unlimited source of derived neurons for cell-based therapeutic strategies.

[1]Epilepsy Center, Department of Clinical Sciences, Lund University Hospital, 22184 Lund, Sweden. [2]Lund Stem Cell Center, Department of Clinical Sciences, Lund University Hospital, 22184 Lund, Sweden. [3]Department of Clinical Sciences, Lund University, Skånes Universitetssjukhus, 22184 Lund, Sweden. ✉email: ana.gonzalez_ramos@med.lu.se; merab.kokaia@med.lu.se

In this study, we used a reprogramming approach based on the transgene expression of transcription factors *Ascl1* and *Dlx2* to induce the differentiation of hESCs into a pure population of interneurons in a short time[14]. The functional maturation of the derived neurons during the differentiation process was also assessed electrophysiologically at various time points. Furthermore, hESC were genetically modified using optogenetics to permit modulation of activity of hdINs by light. Using optogenetics, we demonstrate for the first time that hdINs can integrate into a human neuronal network by forming functional efferent synapses onto human primary neurons. We further confirm integration of hdINs in human epileptic brain slices obtained from surgeries for drug-resistant epilepsy, and thereby provide opportunity to modulate disease-altered human neuronal networks.

Results

Human ESC-derived neurons exhibit a GABAergic phenotype and express calretinin and calbindin markers. Previous studies have demonstrated the possibility to generate highly enriched GABAergic neuronal cultures from hESCs[9–11,14]. Here, hESCs were differentiated into GABAergic neurons using a single-step method overexpressing the transcription factors *Ascl1* and *Dlx2*, which are key factors for this lineage determination (Fig. 1A, B)[14]. The phenotype and electrophysiological properties of the hdINs were assessed at 25, 35, and 49 DIV (Fig. 1A). First, a clear gradual change in morphology was observed in the cell cultures during differentiation, accompanied by a change in gene expression, displayed by a reduction of the pluripotency marker OCT4, encoded by *POU5F1* gene, and the pluripotency and neural precursor marker *SOX2* (Fig. 1K). *POU5F1* had a maximal expression level at 1 DIV, which was decreased at 4 DIV, until not being detected from 7 DIV onwards. *SOX2* gene expression was high at 1 and 4 DIV with a marked reduction from the 7 DIV time point. On the other hand, the *MAP2* gene (neuronal marker) expression was already detected at 4 DIV and showed a tendency to increase its expression over time (Fig. 1C and K). Similarly, *SYN1* displayed a gradual increase of expression from 7 to 35 DIV, at which time point the maximal expression was reached indicating the onset of synaptic maturation of differentiated neurons (Fig. 1K). The slight reduction of *SYN1* expression at 49 DIV could be explained by the decrease of cell density due to reduced viability of astrocytes after long-term culturing in media containing Ara-C. Altogether, these changes indicated a fast, transitional dynamic switch from the expression of pluripotency towards neuronal markers around 4 and 7 DIV. Importantly, the differentiation protocol did not generate astrocytes or oligodendrocyte precursors from hESCs since human *GFAP* and human *PDGFRα* expression levels were hardly detectable (Fig. 1K and Figure S1).

Within the neuronal population, most of the hdINs were positive for GABA, 86.66 ± 2.14% positive cells out of MAP2 + (85.48 ± 2.98% at 35 DIV and 88.23 ± 3.46% at 49 DIV) (Fig. 1D and F). The GABAergic identity of the neuronal population was confirmed by expression of GAD65/67, 88.95 ± 3.55% positive cells out of MAP2 + (89.87 ± 2.11% at 35 DIV and 88.03 ± 4.3% at 49 DIV) (Fig. 1F) and *GAD1* gene expression levels (which encodes for GAD67) that increased over the differentiation timeline (Fig. 1K). These results demonstrate a predominantly GABAergic phenotype of cells over glutamatergic (VGLUT1/KGA, 0.41 ± 0.19% positive cells out of MAP2 +, Fig. 1E and F) or dopaminergic ones (TH, 4.1 ± 0.78% positive cells out of MAP2 +, Fig. 1F). The *SLC17A7* gene, encoding for VGLUT1, was barely detectable by RT-qPCR (Fig. 1K). Furthermore, within the GABAergic neuronal population, the most abundant subtypes were calbindin (CB)- and calretinin (CR)-expressing interneurons, representing 36.38 ± 0.82% (36.23 ± 1.3% at 35 DIV and 35.25 ± 0.25% at 49 DIV) and 28.83 ± 3.08% (35.37 ± 1.3% at 35 DIV and 22.3 ± 1.73% at 49 DIV) respectively (Fig. 1G, H and J). Among other interneuron subtypes tested, there were cells found expressing somatostatin (SST, 0.79 ± 0.19%, Fig. 1I–J) and neuropeptide-Y (NPY, 0.71 ± 0.17%, Fig. 1J), while almost none of them were positive for either parvalbumin (PV, 0.28 ± 0.28%) or cholecystokinin (CCK, 0%) (Fig. 1J). Results from the immunostaining were supported by gene expression data, where also *VIP* and *NKX2.1* (MGE marker) gene expression were included (Figure S1). *NKX2.1* gene expression started appearing at 4 DIV maintaining stable levels and increasing slightly at 25 until 49 DIV. These results support the possibility of having some early-stage neurons in the cultures. Moreover, expression of *PPP1R1B* gene that encodes for DARPP-32, a marker for striatal medium spiny neurons, which are GABAergic projecting neurons, was not present at 35 DIV and 49 DIV (Figure S1).

Maturation of intrinsic electrophysiological properties of hdINs over time in culture and functional confirmation of their GABAergic nature. Electrophysiological properties of the hdINs at different time points were investigated to correlate functional maturation with the progress of their morphological changes during the differentiation process. Whole-cell patch-clamp recordings were performed at 25 DIV (blue), 35 DIV (green) and 49 DIV (red) (Fig. 2). Input resistance was similar at all time points analyzed (Fig. 2I and Table S1). Small differences in resting membrane potential in cells at both 35 and 49 DIV compared to 25 DIV were observed (− 34.27 ± 2.87 mV at 25 DIV, − 47.20 ± 1.84 mV at 35 DIV and − 44.85 ± 1.94 mV at 49 DIV) (Fig. 2H and Table S1). Already at 25 DIV, hdINs were able to fire multiple action potentials upon depolarization (Fig. 2K) and displayed both a fast-inward sodium ion current and a sustained outward potassium (K^+) ion current (Fig. 2P–W). The percentage of hdINs firing to ramp depolarizing current was increased over time and action potentials displayed higher amplitudes, faster rise times and larger after-hyperpolarization at 35–49 DIV compared to 25 DIV (Fig. 2A–F and J–O, and Table S1). However, no statistically significant differences in these parameters were observed between the 35 DIV and the 49 DIV time points. These observed changes reflect an increase in functional voltage-dependent Na^+ and K^+ channels, supported by larger inward and outward current peaks at later time points (Fig. 2S and W). Altogether, these differences in intrinsic properties demonstrate a clear functional maturation of hdINs over time in culture, reaching a more mature state already at 35 DIV. The firing patterns observed were single, regular or clustered spiking, with no sustained spiking beyond 62 Hz observed.

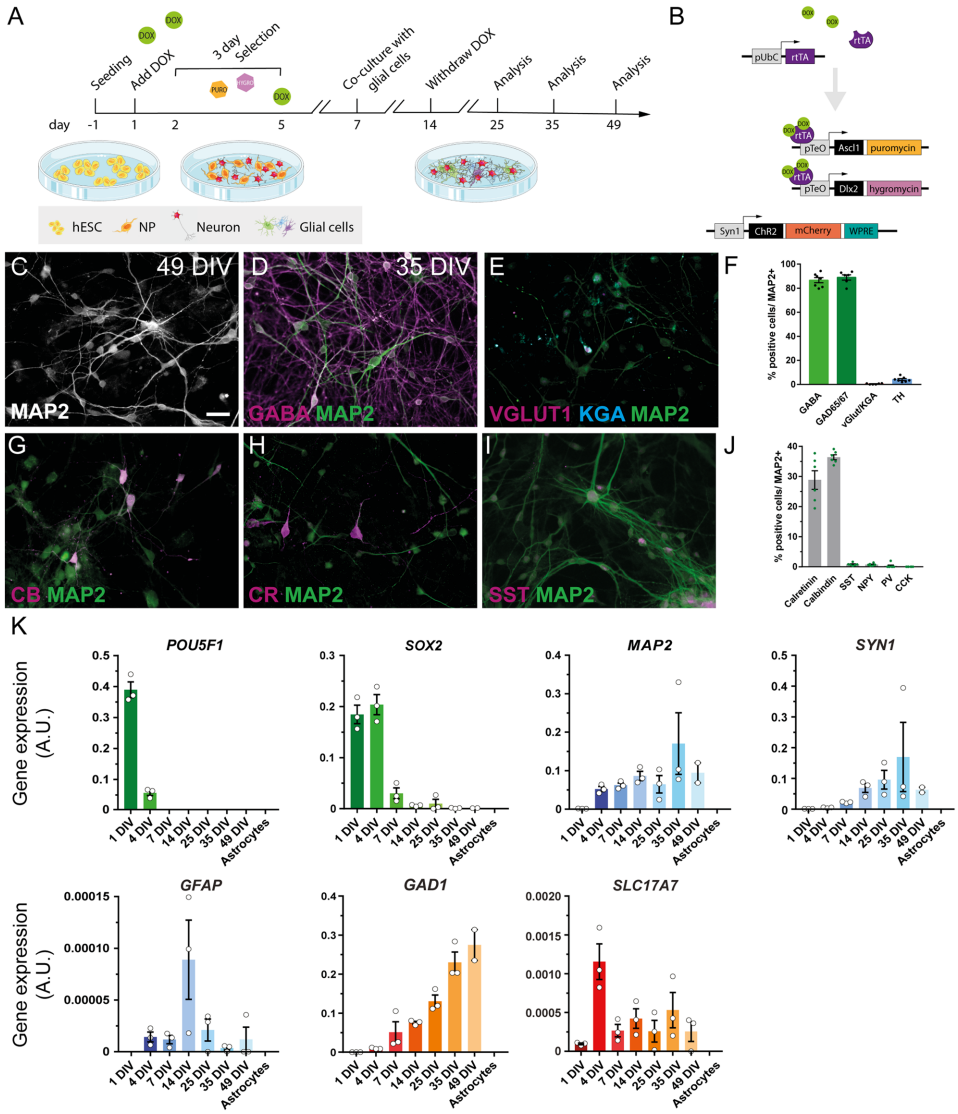

Figure 1. Transgene expression of the transcription factors *Ascl1* and *Dlx2* by Tet-On system triggers the differentiation of hESC to GABAergic neurons. (**A**) Differentiation protocol used for the generation of hdINs. (**B**) Schematic view of the constructs carried by the lentiviral particles used in the differentiation protocol (Tet-On system), and for the expression of ChR2. (**C**) Immunocytochemistry for the neuronal marker MAP2 + of the derived neurons at 49 DIV. (**D**, **E**) Immunocytochemistry of hdINs at 35 DIV for GABAergic (GABA) and glutamatergic (VGLUT1 and KGA) markers. (**F**) Quantification of the percentage of GABA +, GAD65/67 +, vGlut1 +/ KGA + and TH + cells over MAP2 + cells as an average of both time points, 35 and 49 DIV. (**G**–**I**) Representative images of hdINs showing the presence of the interneuron markers CB, CR, and SST. (**J**) Quantification of the percentage of CR +, CB +, SST +, NPY +, PV + and CCK + subtypes over MAP2 + cells. (**K**) Gene expression profile during the differentiation. Values for the pluripotency gene *POU5F1* that encodes for OCT4, and *SOX2* gene in green. Genes expressed in mature cell populations such as *MAP2* and *SYN1* in neurons, and human *GFAP* in astrocytes where also analyzed and indicated in blue. Key genes of the two main neuronal populations in the brain were also studied and shown in orange, quantifying *GAD1* gene which is expressed in GABAergic neurons and *SLC17A7* gene which encodes for VGLUT1 and it is expressed in glutamatergic neurons. NP, neural precursor. Scale bar: 100 µm. Mean ± SEM. Schematics were generated and adapted using resources from Servier Medical Art[35].

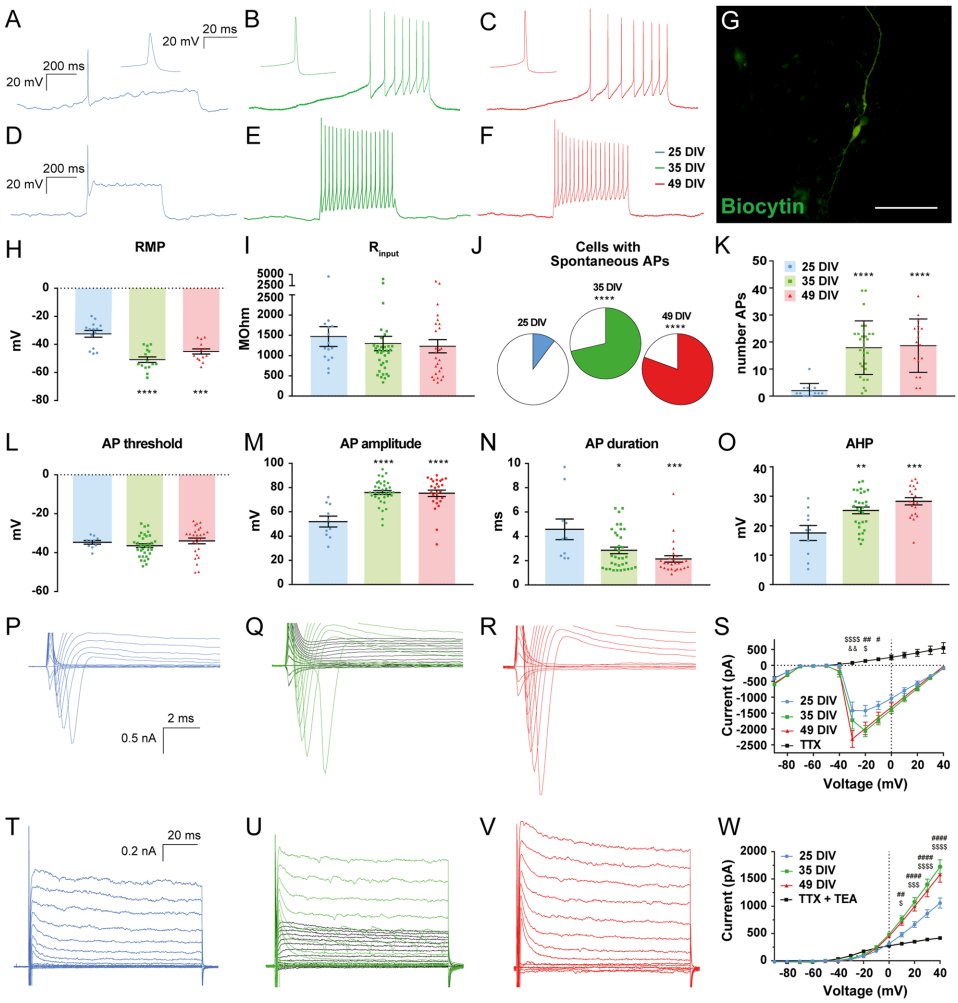

Figure 2. Electrophysiological properties of hdINs during maturation process over time in culture. Differential cell response (**A**–**C**) to 0–25 pA ramps of depolarizing current and (**D**–**F**) 50 pA depolarizing current pulses at different time points. (**G**) hdIN filled with biocytin. (**H**–**I**) RMP and Ri at different time points. (**J**) Increased proportion of cells with spontaneous APs (colored area) over time. (**K**) Maximum number of APs that cells fired in response to 500 ms current pulses. (**L**–**O**) Distribution of AP threshold (**L**), amplitude (**M**), duration (**N**) and afterhyperpolarization (**O**) at different time points. (**P**–**R**) Expanded current traces illustrating the sodium current and (**T**–**V**) the potassium current activated during voltage pulses ranging from −90 to + 40 mV in 10 mV steps at different time points. Sodium and potassium currents were blocked by TTX (1 µM) and TTX + TEA (10 mM) respectively (black lines). Sodium (**S**) and potassium (**W**) current peak plotted against the voltage steps. Scale bar: 100 µm. Mean ± SEM. One-way ANOVA with Tukey's post hoc test and Fisher's exact test (25 DIV n = 15 in blue, 35 DIV n = 36 in green, and 49 DIV n = 26 in red). *$p < .05$; **$p < .01$; ***$p < .001$; ****$p < .0001$; compared to 25 DIV group. Two-way ANOVA with Tukey's post-hoc test. #, 25DIV vs 35DIV; $, 25DIV vs 49DIV; &, 35DIV vs 49DIV (25 DIV n = 15 in blue, 35 DIV n = 28 in green, and 49 DIV n = 33 in red). AP, action potential; AHP, afterhyperpolarization; RMP, resting membrane potential; Ri, input resistance.

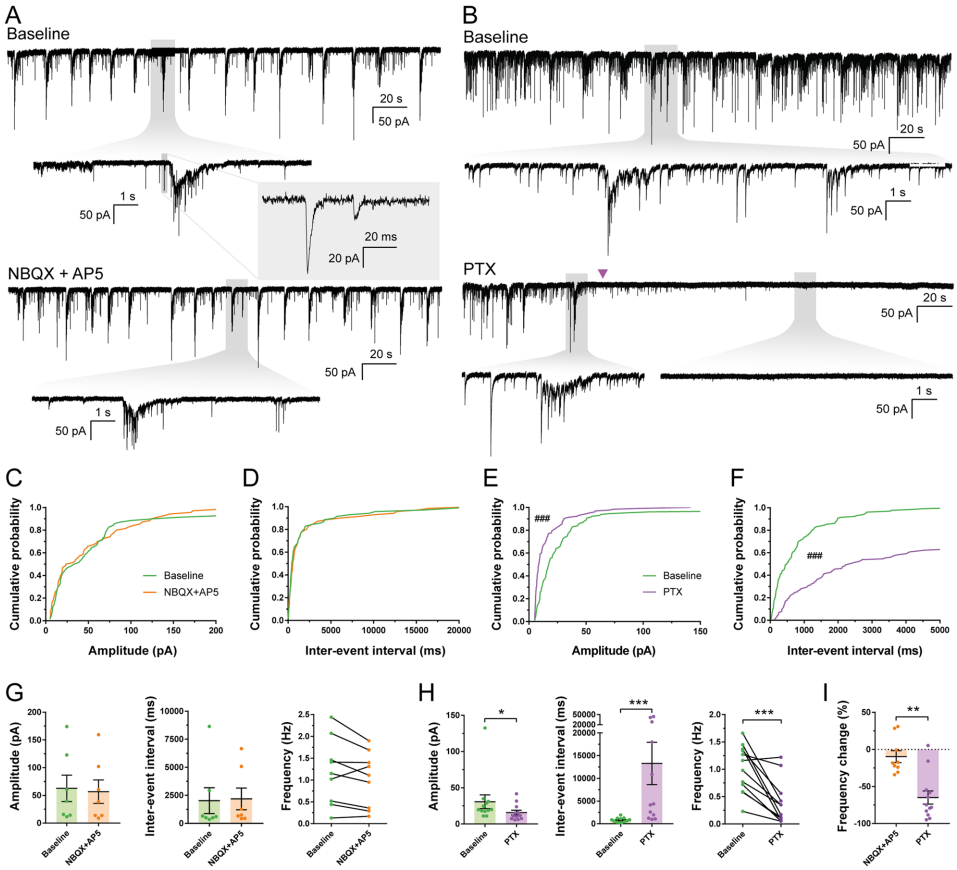

Figure 3. Spontaneous synaptic currents recorded in hdINs are GABAergic. hdINs exhibited spontaneous synaptic currents at 35 and 49 DIV (**A**, **B**). These spontaneous currents were reduced or abolished by the addition of PTX (1 mM, purple arrow) (**B** and **E**–**F**), but were not affected by NBQX (5 µM) and AP5 (50 µM) (**A** and **C**–**D**). Cumulative probability curves comparing the events during baseline and addition of the drugs for both amplitude (**C** for NBQX + AP5, and **E** for PTX) and inter-event interval (**D** for NBQX + AP5, and **F** for PTX). (**G**) Distribution of the mean amplitude, inter-event interval and frequency for spontaneous synaptic currents recorded from cells during baseline and after the addition of (**G**) NBQX and AP5, or (**H**) PTX. (**I**) Average frequency change after the addition of each drug in comparison to the baseline. Mean ± SEM. Kolmogorov–Smirnov test for cumulative distributions and Mann–Whitney test for comparison of means (NBQX + AP5 n = 7 and PTX n = 14; 10 events per cell and condition). Kolmogorov–Smirnov test: $^{###}p < .0001$. Mann–Whitney test: $^{*}p < .01$; $^{**}p < .001$; $^{***}p < .0001$; $^{****}p < .00001$.

To further explore the neuronal identity and functionality of hdINs, spontaneous synaptic currents were recorded and analyzed. These were more abundant at the latest time point, 49 DIV, indicating continuous synaptogenesis over the time points analyzed (Table S1 and Figure S2A–D). Furthermore, when blocking AMPA and NMDA glutamate receptors by applying NBQX and AP-5, respectively (Fig. 3A), no changes were observed in either amplitude (62.76 ± 11.19 pA for the baseline and 56.73 ± 10.37 pA for NBQX + AP5) (Fig. 3C and G) or inter-event interval (2027.08 ± 497.39 ms for the baseline and 2183.74 ± 514.15 ms for NBQX + AP5) (Fig. 3D and G). However, blocking $GABA_A$ receptors by adding Picrotoxin (PTX) (Fig. 3B) to the artificial cerebrospinal fluid (aCSF) resulted in a significant decrease in amplitude (29.61 ± 3.46 pA for the baseline and 15.97 ± 1.67 pA for PTX) (Fig. 3E and H) and increase in the inter-event interval of post-synaptic currents (829.43 ± 86.66 ms for the baseline and 12,641.96 ± 2345.03 ms for PTX) (Fig. 3F and H). PTX increased the inter-event interval (Fig. 3F and H), reducing their frequency by 64.52 ± 8.23% on average (1.01 ± 0.12 Hz for the baseline and 0.37 ± 0.11 Hz

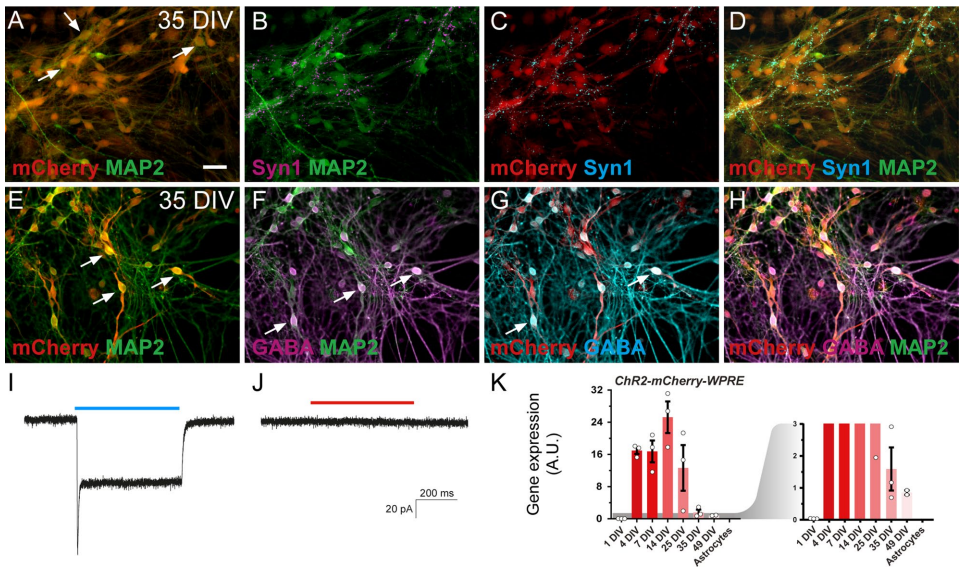

Figure 4. ChR2 is expressed in hdINs, enabling them to respond to blue light. (**A**–**D**) Immunocytochemistry of hdINs at 35 DIV for the neuronal marker MAP2 + in combination with the fluorescent reporter for ChR2, mCherry +, and a mature neuronal marker Syn1 + in simple differentiation cultures. (**E**–**H**) Immunocytochemistry indicating the co-expression of GABA + and mCherry + in some hdINs at 35 DIV. White arrows are examples of double positive cells for the indicated markers. ChR2-mCherry + neurons responded to blue light pulse stimulation (**I**), but not to a red-light pulse stimulation (**J**). (**K**) *ChR2-mCherry-WPRE* expression at different time points of the differentiation, shown in red. A magnified graph for *ChR2-mCherry-WPRE* values is shown in red as well on the right of the previous graph. Scale bar: 100 µm. Blue light, 460 nm. Red light, 595 nm. Blue and red line, light stimulation for the specific wavelength.

for PTX) (Fig. 3H and I), and decreased the overall amplitude of the events, mostly by reducing the number of higher amplitude events (Fig. 3E and H). Hence, the majority of synaptic inputs were blocked by PTX but not by NBQX and AP-5 (1.18 ± 0.25 Hz for the baseline and 1.02 ± 0.21 Hz for NBQX + AP5, Fig. 3G), supporting the predominantly GABAergic nature of the synaptic network, and thereby confirming functionally the inhibitory phenotype observed with immunocytochemistry and gene expression analysis.

Synaptic integration of hdINs with human primary cortical neurons in vitro. Next, we investigated whether hdINs could integrate into a human neuronal circuit in vitro and thereby modulate neuronal activity of host neurons. For this purpose, lentiviral transduction of *ChR2-mCherry* was performed before starting the differentiation of hESCs. Subsequent analyses revealed that 74.1 ± 1.35% of MAP2-positive cells also expressed mCherry (Fig. 4A–H and K), and that expressing cells were readily depolarized by exposure to ChR2-activating blue light (460 nm wavelength) similarly at 35 and 49 DIV, but not to red light (Fig. 4I–J). These results ensured that it was possible to specifically activate hdINs and study their efferent synaptic integration in human neuronal cultures. Human primary neuronal cultures were obtained from brain tissue of 8 weeks old aborted fetuses, and used as established human neuronal network after 7 DIV[15]. After four weeks in culture, human primary cortical neurons were mostly glutamatergic (Fig. 5G and I–K) with few GABAergic neurons (Fig. 5H), and displayed spontaneous synaptic bursting indicating network activity[16]. The hdINs and human primary neurons were first co-cultured for four weeks (from 7 to 35 DIV), and then whole-cell patch-clamp recordings were performed to assess the functionality and integration of hdINs in the network (Fig. 5A–D). At this time point, 35 DIV, hdINs represented 2.71% of the total number of cells within the co-culture (Fig. 5E–F) and received functional afferent connections from the human primary neurons (Fig. 5I), which had a strong glutamatergic component (Fig. 5J–K). Moreover, the activation of hdINs using blue light induced postsynaptic currents in recorded human primary neurons (Fig. 6B and D–I). For each cell, these synaptic responses occurred at a certain latency from the light stimulation onset which varied from cell to cell (Fig. 6G–I). Thus, in the recorded cells the light responses were not generated by light per se since in that case, the response would have been instantaneous without any latency period (like in the mCherry + hdIN example (Fig. 6A and C). For each recorded cell, the response latency (relative to the light pulse onset) was consistent for all repeated stimulations (Fig. 6H–I) confirming stable functional synaptic connections onto human primary cortical neurons after 4 weeks of co-culture.

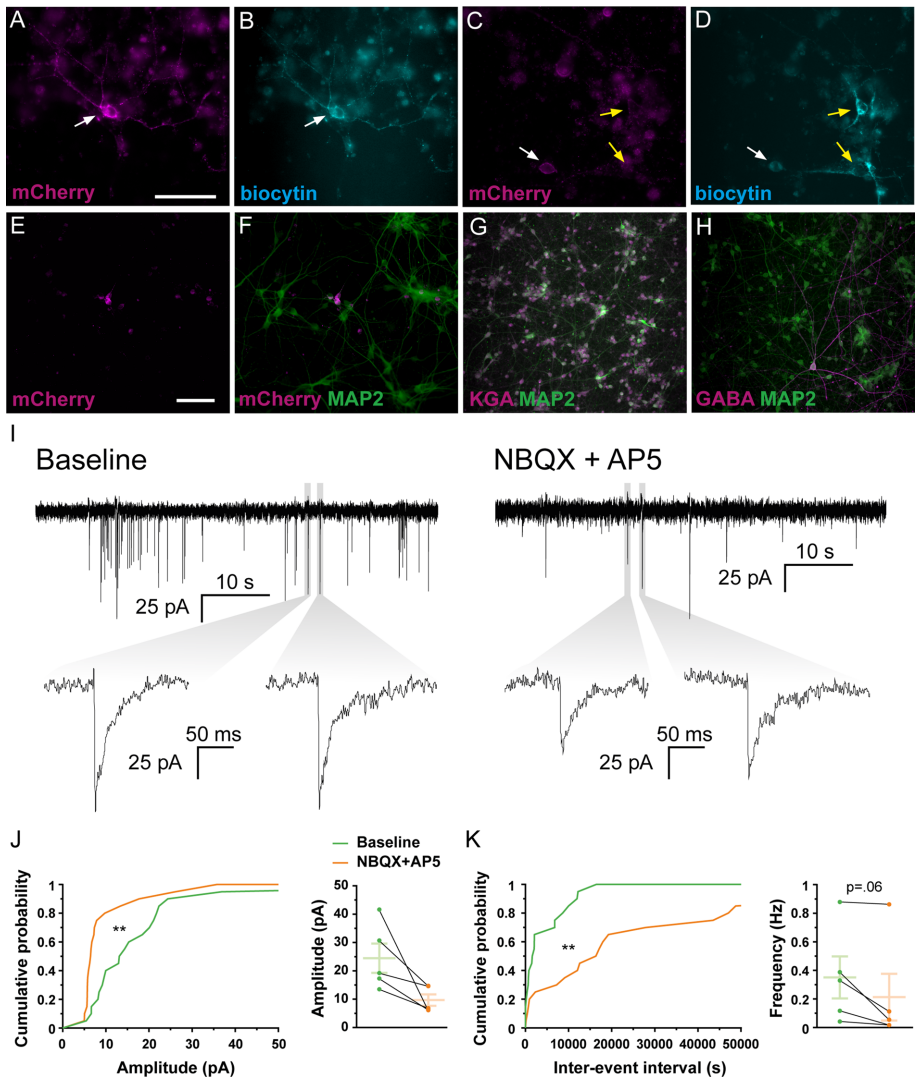

Figure 5. Co-cultures of human primary neurons and hdINs at 35 DIV demonstrate afferent synaptic connections from the primary neurons to the hdINs. Immunohistochemistry of co-cultures of hdINs and human primary neurons used for electrophysiological analysis at 35 DIV. Some of the recorded neurons (biocytin +, **B** and **D**) were also hdINs mCherry + (white arrows, **A** and **C**), and some were mCherry-, indicating that the latter were primary neurons (yellow arrows, **C**–**D**). (**E**, **F**) The ratio of mCherry + /MAP2 + cells to human primary neurons mCherry-/MAP2 +. (**G**, **H**) Human primary neurons were mostly glutamatergic (KGA +, **G**) and very few GABAergic (GABA +, **H**). (**I**) Spontaneous synaptic currents in whole-cell voltage-clamp mode showing afferent connections to the hdINs at 35 DIV. Some of the events disappeared when NBQX and AP5 where applied (right). (**J**, **K**) Cumulative probability curves comparing the events during baseline (green) and addition of the drugs (orange) for both amplitude (**J**, left) and inter-event interval (**K**, left). Distribution of the mean amplitude (**J**, right) and frequency (**K**, right) for spontaneous synaptic currents. Scale bar: 100 µm. Mean ± SEM. Kolmogorov–Smirnov test for cumulative distributions and Wilcoxon test for comparison of paired means (n = 5). Kolmogorov–Smirnov test: $^{**}p < .005$.

Figure 6. Effect of ChR2 activation on the human primary neurons co-cultured with hdINs at 35 DIV. hdINs were co-cultured at 7 DIV with primary neurons from an 8-week-old human fetus for 4 weeks. Both (**A**) hdINs, expressing mCherry as a reporter for ChR2, and (**B**) human primary neurons were recorded (n = 18 and n = 6, respectively). (**C**) The activation of ChR2 by blue light in hdINs triggered an inward current, unaffected by either NBQX + AP5 or PTX. (**D**–**F**) Light activation of ChR2 in hdINs also generated a delayed synaptic response in the surrounding primary neurons, indicating synaptic integration of those cells in the pre-existing neuronal network. Light responses were assessed during (**D**) 500 ms light pulse in voltage-clamp, (**E**) light train of 5 pulses of 3 ms with 97 ms of interval between pulses in voltage-clamp, and (**F**) 500 ms light pulse in current-clamp. These responses in the primary cells were blocked by PTX (right column, **D**–**F**), but not by NBQX + AP5 (middle column, **D**–**F**), confirming their GABAergic nature. Note that the GABAergic currents are depolarizing in the primary neurons recorded because a high chloride internal solution was used in the patch pipette. (**G**) On the left, bright-field image of a primary neuron being recorded. In the middle, same cell showing GFP + expression. On the right, the primary neuron is mCherry- (negative). (**H**) Histogram of latencies of synaptic responses for each neuron recorded. Only the first event for each trace is included in the analysis. (**I**) Two examples of primary cells displaying delayed light-induced synaptic responses. On the top, traces in voltage clamp showing the synaptic responses to blue light stimulation (blue line) and, on the bottom, histogram of latencies of increased frequency of synaptic responses for each neuron recorded. P-value for Poisson test is indicated for the highest frequency distribution time. Blue line, light stimulation. Schematics were generated and adapted using resources from Servier Medical Art[35].

Moreover, the delayed synaptic response was blocked by PTX (Fig. 6D–F, right column), but not by NBQX and AP-5 (Fig. 6D–F, middle column), demonstrating the GABAergic nature of the synaptic connections originating from the light response of transplanted cells, and confirming to the morphological evidence that hdINs were indeed of GABAergic phenotype even when co-cultured with human primary neurons.

Survival, differentiation, and synaptic integration of hdINs transplanted into human tissue from brain resections of drug-resistant epileptic patients. To determine if survival and synaptic integration of dhINs was possible in chronic epileptic tissue, we grafted hdINs onto cultured slices obtained from patients undergoing surgery for drug-resistant epilepsy. The hdINs were transplanted after 7 DIV onto organotypic cultures of resected adult brain from one temporal lobe epilepsy patient (cortical slices, n = 4 and hippocampal slices, n = 3) and one focal cortical dysplasia patient (cortical slices, n = 3), and kept in culture for 4 to 6 weeks. The grafted hdINs expressed the neuronal marker MAP2 + (Fig. 7A and C) and exhibited extensive arborizations (Fig. 7A) after 4 weeks in culture. hdINs were functional and showed intrinsic properties comparable to mature neurons at both 4 and 6 weeks after ex vivo transplantation (Figure S3 A–D). Moreover, hdINs responded to blue light with photocurrents (Figure S3 E–G) and received afferent synaptic inputs from the neighboring cells (Figure S3 H–I, n = 28 cells). In some of the hdINs, delayed inward synaptic currents were observed during the 500 ms light pulse (after the direct light response, Figure S3 J, red arrow), presumably generated by afferent synaptic connections from other hdINs (Figure S3 J, green arrows). Optogenetic activation of hdINs induced postsynaptic currents in host neurons already at 4 weeks AT (Fig. 7A–B and D–E, n = 7), which were blocked by PTX but not NBQX + AP5 (Fig. 7F; n = 4), as observed in the co-cultures with human primary neurons. These experiments demonstrate that hdINs survive and differentiate into GABAergic phenotype even when transplanted into epileptic human brain tissue.

Taken together, our findings demonstrate the capacity of the hdINs to differentiate into mature functional neurons, integrate into a human neuronal network by receiving functional afferent connections and, most importantly, by forming efferent synaptic connections with neighboring human host neurons enabling precise spatiotemporal modulation of the human neuronal network, including epileptic tissue.

Discussion

Here we demonstrate, for the first time to our knowledge, that hESC-derived GABAergic neurons can form functional *efferent* synaptic connections onto human primary neurons in vitro, and to host neurons in human epileptic tissue after transplantation.

By validating and adapting the differentiation protocol published by Yang, et al. (2017)[14] to overexpress only two transcription factors critical for the GABAergic fate (*Ascl1* and *Dlx2*), we obtained cultures with high yield of GABAergic neurons. This protocol also required a shorter time of differentiation compared to those published elsewhere based on the use of small molecules[9–11,17]. Human ESCs differentiated to functional neurons, exhibiting a fast TTX-sensitive sodium current and a sustained TEA-sensitive potassium current, allowing cells to fire action potentials already at 25 DIV. Efferent synaptogenesis was apparent at 35 DIV and proved to be predominantly GABAergic since it was blocked by PTX, but not affected by NBQX and AP-5.

One of the potential future applications of these cells is cell-based replacement therapy. As mentioned before, GABA-releasing interneurons are responsible for the modulation of neuronal network activity in the brain, and therefore their alteration or absence disrupts the excitatory-inhibitory balance in the neuronal circuits leading to neurological disorders[8]. The substitution and/or replacement of those aberrant or missing interneurons could become a potential therapeutic approach for disorders such as schizophrenia, autism, and epilepsy. A translational development of this approach towards the clinical applications will require homogeneity and reproducibility of the cell differentiation. In this regard, the present study achieved high yield of GABAergic interneurons of two major subtypes expressing CB and CR, respectively, as well as forebrain markers such as FOXG1[14]. The markers

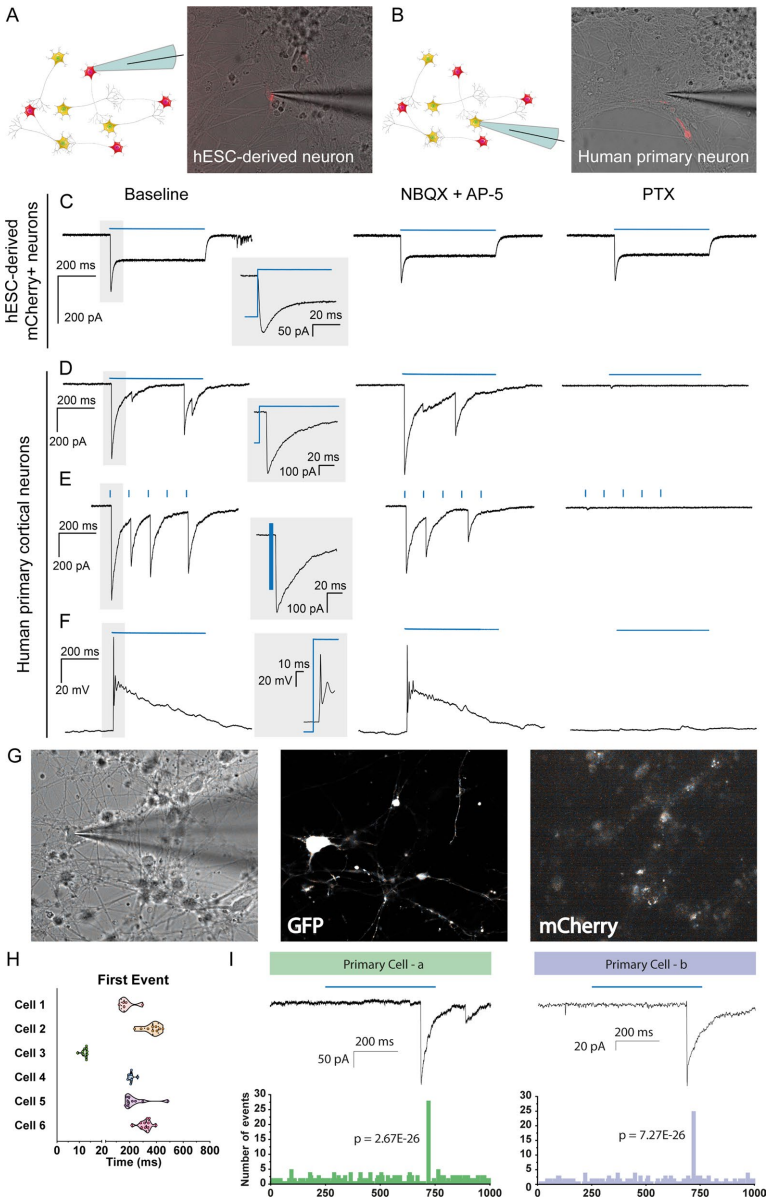
A
hESC-derived neuron
B
Human primary neuron
Baseline
NBQX + AP-5
PTX
C
hESC-derived mCherry+ neurons
200 ms
200 pA
20 ms
50 pA
D
Human primary cortical neurons
200 ms
200 pA
20 ms
100 pA
E
200 ms
200 pA
20 ms
100 pA
F
200 ms
20 mV
10 ms
20 mV
G
GFP
mCherry
H
First Event
Cell 1
Cell 2
Cell 3
Cell 4
Cell 5
Cell 6
0 10 20 200 400 600 800
Time (ms)
I
Primary Cell - a
Primary Cell - b
200 ms
50 pA
200 ms
20 pA
Number of events
p = 2.67E-26
p = 7.27E-26
0 250 500 750 1000

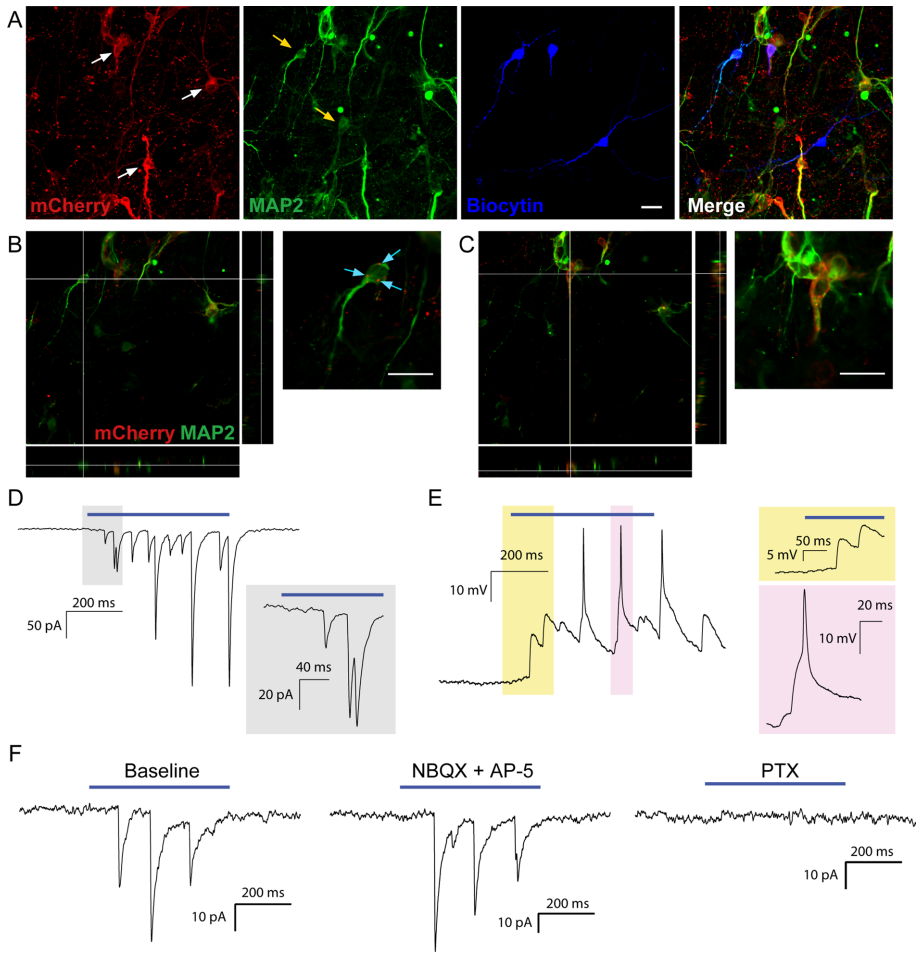

Figure 7. Grafted hdINs established functional efferent synaptic connections to the host adult human neurons. (**A**) hdINs survive and differentiate after transplantation onto human organotypic brain cultures for 4–6 weeks AT. hdIN-mCherry + neurons are indicated with white arrows, and host neurons are marked with yellow arrows (mCherry-/MAP2 +). (**B**) Orthogonal projection of a host neuron and magnification on the right. There are mCherry + processes surrounding the host neuron (cyan arrows). (**C**) Orthogonal projection of a hdIN mCherry + neuron, which is also MAP2 +. (**D**) Delayed synaptic response in voltage-clamp mode of the host neuron after optogenetic stimulation of the hdINs by a 500 ms light pulse, indicating synaptic integration of those cells in the pre-existing neuronal network at 4 weeks AT. (**E**) Delayed synaptic response in current-clamp mode of the host neuron after optogenetic stimulation of the hdINs, illustrating changes of the membrane potential (magnification in yellow), that eventually leads to the generation of an AP (magnification in pink). Note that the $GABA_A$ receptor-generated currents are depolarizing in the host recorded cell because a high chloride solution was used in the patch pipette. These responses in the host neurons were blocked by PTX (right column in **F**), but not by NBQX + AP5 (middle column in **F**), confirming their GABAergic nature. Scale bar: 20 µm.

of striatal GABAergic projection neurons CTIP2 and DARPP-32 were absent, suggesting exclusive generation of forebrain GABAergic interneurons.

Another important aspect is the validation of animal data in human-derived tissue to ensure that outcomes are not specific just to the rodent brain. Currently, however, most of the translational research is being focused on animal models. This may have contributed to the failure of some therapies when tested in human clinical trials. It is believed that for cell replacement therapy, a functional integration of transplanted neurons into the existing brain circuitry is needed. Previous studies have used optogenetics for addressing this issue[18–21]. For example, Cunningham, et al. (2014) transplanted human stem cell-derived GABAergic interneurons expressing ChR2 into the hippocampus of a pilocarpine mouse model of epilepsy, and suppressed seizures and behavioral abnormalities either by spontaneous firing or by optogenetic stimulation[22]. Weick, et al. (2011) also used optogenetics to demonstrate functional synaptic integration in vitro of hESC-derived excitatory neurons into a pre-existing mouse neuronal circuit[16]. Using an optogenetic approach, we demonstrate that in cultured human primary cortical neurons and in an adult epileptic human neural circuitry, grafted hESC-derived GABAergic neurons integrate, forming functional efferent synapses. The human cell co-culture paradigm and the ex vivo transplantation onto human epileptic organotypic cultures shown here for testing the efferent synaptic integration of derived neurons could be considered as a useful platform incorporated into the roadmap of clinical translation.

One interesting aspect demonstrating efferent synaptic integration of the derived GABAergic neurons is the response pattern recorded in co-cultured human primary neurons (Fig. 6D–F). Light responses occurred with a consistent latent period upon light stimulation (Fig. 6G–I), that differed from cell to cell. The consistent latent period for each cell indicates that the effect is light dependent, rather than spontaneous (Fig. 6G–I). The variability between cells could be due to multiple causes: (i) Varied length of a polysynaptic chain between the hdINs and recorded primary neurons. This is enabled by GABA being an excitatory neurotransmitter at this stage of neuronal development, due to higher intracellular concentration of chloride, which depolarizes the membrane upon $GABA_A$ receptor activation[23–29]. In support, Dzhala et al. (2005) demonstrated that the peak of *SLC12A2* expression (encoding NKCC1) in human brain occurs at 35 postconceptional weeks (PCW), decreasing rapidly during the first year of life (54–92 PCW). It is in early childhood (92–210 PCW, approximately 1–3.3 years) when *SLC12A5* expression levels (encoding for KCC2 protein) takes over[30]. (ii) The differential expression of ChR2 in the hdINs that leads to variability in timing to the first action potential. (iii) Variability of neurotransmitter release from grafted cells by direct depolarization of presynaptic terminals by light.

Various types of derived neurons engrafted in human neuronal cultures receiving functional afferent synaptic connections, as also shown here, have been reported previously[31,32]. However, evidence for functional efferent connections from the converted neurons to the human fetal primary cortical neurons or the organotypic human brain slices has been lacking. Our study provides the first evidence to our knowledge that hESC-derived neurons are capable of forming functional efferent synaptic connections to human neurons, and thereby possess the potential to modulate activity and network excitability of the human neuronal network.

Methods

Stem cell maintenance. H1 (WA01) ESC were obtained from WiCell Research Resources (Wicell, WI). Human ESC were maintained as feeder-free cells on Matrigel-coated (Corning) plates using Essential 8 Flex medium (E8F; Gibco) and passaged as colonies using ReLeSR (Stem Cell Technologies).

Mouse primary glial cell culture. All animals were bred at the local animal facility and kept in 12 h light/dark cycle with access to food and water ad libitum. All procedures were approved by the Malmö/Lund Animal Research Ethics Board, ethical permit number 02998/2020.

Mouse primary glial cells were harvested from the cerebral cortex of newborn C57Bl6/J mice at P3 to P5. Briefly, mice pups were separated from the mum and decapitated without anesthesia using scissors. Thus, the brain was extracted and dissected, and the cerebral cortex was cut, homogenized, and digested with trypsin for 30 min at 37 °C. Cells were dissociated mechanically, passed through a cell strainer, and plated onto T75 flasks coated with poly-D-lysine (PDL; Sigma-Aldrich) in MEM (Gibco) supplemented with 5% fetal bovine serum (FBS; Sigma), 0.4% D-Glucose (w/v; Sigma), 2% B-27 (Gibco), 1% GlutaMAX (Gibco) and 1% Penicillin–Streptomycin. Primary glial cells were maintained and passaged at confluency using trypsin until a maximum of 5 passages, being passaged at least once before being used for co-culture with the hdINs.

Lentiviral constructs and virus generation. High-titer of third-generation lentiviral particles was produced using PEI for transfection of the 293 T cells in biosafety level 2 environment[33]. Lentiviral particles were obtained for the following constructs: hSyn1-ChR2(H134R)-mCherry-WPRE (obtained by cloning at the lab, from Addgene #20945), and the TetOn system consisting on FUW-rtTA (Addgene #20342), FUW-TetO-Ascl1-T2A-puromycin (Addgene #97329) and FUW-TetO-Dlx2-IRES-hygromycin (Addgene #97330).

Differentiation of hESC-derived neurons. Before starting the differentiation procedure, hESC were transduced with lentiviral particles carrying hSyn1-ChR2(H134R)-mCherry-WPRE, and the TetOn system rtTA/Ascl1-puro/Dlx2-hygro at MOI 5/2.5/2.5 respectively; in fresh E8F medium containing 10 μM ROCK inhibitor Y-27632 (Y; Stem Cell Technologies).

hdINs were generated as described in Yang *et al.* (2017)[14], with the addition of some modifications. Human ESC were passaged as single cells using Accutase (Stem Cell Technologies). Cells were plated in six-well plates coated with Matrigel at a density of 3×10^5 cells/well in E8F containing Y on −1 DIV. At 1 DIV, the cultured medium was replaced with N2 medium consisting of DMEM/F12 (Gibco) supplemented with N2 Supplement (1:100; Gibco) and containing doxycycline (DOX; 2 g/l; Sigma-Aldrich) to induce the TetO gene

expression. DOX was added to the media for 14 days. At 2 DIV, an antibiotic-resistance selection period was started by adding puromycin (puro; 0.5 µg/ml; Gibco) and hygromycin (hygro; 750 µg/ml; Invitrogen) to the fresh media. At 5 DIV, the selection period ended and cells were cultured in N2 medium containing DOX and cytosine β-D-arabinofuranoside (Ara-C; 4 µM, Sigma). After a week in culture, at 7 DIV, cells were detached into a single-cell suspension using Accutase and plated together with mouse primary glial cells on Matrigel-coated glass coverslips in a 24-well plate ($3–5 \times 10^5$ and 5×10^4 cells/well respectively). At this point, the medium was replaced with Growth medium consisting of Neurobasal medium supplemented with 2% B27, 1% GlutaMAX and 5% FBS. From 7 DIV until the day of the analysis (25 DIV, 35 DIV, and 49 DIV), half of the medium was replaced for fresh one every 2–3 days. Additionally, from approximately 10 DIV onwards Ara-C was added to the medium to inhibit glial cell proliferation, and from 15 DIV until the last time point BDNF (14 ng/ml, R&D Systems) was also added. Importantly, DOX was withdrawn from the medium at 14 DIV.

Derivation of human fetal primary cortical cells and co-culture with hdINs. Human primary cortical cells were derived from the cerebral cortex of aborted human fetuses (8 weeks of age) according to guidelines approved by the Lund-Malmö Ethical Committee (Ethical permit number: Dnr 6.1.8-2887/2017) as described in Miskinyte et al. (2017)[31]. The tissue was carefully dissected, minced into small pieces, and then triturated with a pipette tip into a single-cell suspension. The cells were washed with Neurobasal (Gibco)-based medium supplemented with B27, and plated onto poly-D-lysine (Sigma-Aldrich)/fibronectin (Life Technologies) (both 10 µg/mL)-coated glass coverslips at a density of 50,000 cells/well and maintained in the same medium until co-culturing. For a subset of experiments, human primary neurons were transduced with lentiviral vectors carrying EF1α-GFP prior to the co-culture (Fig. 6G).

hdIN precursors were detached at day 7 of differentiation and seeded onto human primary cortical cells at a density of 15×10^4 cells/well. Then, both cell types were cultured together following the differentiation protocol described above for 4 weeks (reaching 35 DIV for hdINs). Due to the proliferative nature of the neuronal precursors from the human fetuses, at 35 DIV hdINs represented a 2.71% of the total number of cells in the culture, calculated by counting 2.01 ± 0.27% mCherry + cells which are the 74.1 ± 1.35% of the total hdINs. So, probability of recording from hdIN mCherry- cells instead of human primary neurons was less than 1%. Those values are in coherence with the number of cells we would expect from previous counting at 35 DIV in a regular differentiation with 500.000 seeding cells at 7 DIV. The number of cells were 61.5 ± 5.42 cells in an area of 680 × 510 µm, and in the co-culture scenario where the seeding cells at 7 DIV were 15×10^4 cells/well (3.3 times less) the number was 7.83 for the same area. Hence, the co-culture environment does not affect the survival of the differentiated cells.

Organotypic cultures of adult human brain tissue and transplantation of the hdINs. Resected neocortical and hippocampal tissue were obtained from patients undergoing surgical treatment for drug-resistant epilepsy (n = 2). The use of resected patient tissue and following procedures were approved by the local Ethical Committee in Lund (#212/2007) and were performed in accordance with the Declaration of Helsinki. Written informed consent was obtained from all subjects prior to each surgery. Patient information:

Patient 1: TLE resection, male, age 49 years, duration of epilepsy 4 years; approximately 3 seizures/week; medication at time of surgery: lamotrigine; pathology: signs of previous limbic encephalitis.

Patient 2: FCD resection, female, age 27 years, duration of epilepsy 16 years; approximately 3–5 seizures/month; medication at time of surgery: lamotrigine and Trileptal®; pathology: FCD type IIId.

The tissue slices were derived and handled as previously described[34]. Briefly, tissue was transported from the surgery room to the electrophysiology laboratory in an ice-cold sucrose-based slushed cutting solution, containing in mM: 200 sucrose, 21 $NaHCO_3$, 10 glucose, 3 KCl, 1.25 NaH_2PO_4, 1.6 $CaCl_2$, 2 $MgCl_2$, 2 $MgSO_4$ (all from Sigma-Aldrich, Sweden), adjusted to 300–310 mOsm, 7.4 pH. At the laboratory, the tissue was then transferred into the same type of solution, continuously bubbled with 95% O_2 and 5% CO_2. The 300 µm slices were cut with a vibratome (Leica VT1200S) and transferred to a rinsing media, containing: HBSS (Life Technologies), HEPES (4.76 mg/ml; Sigma), Glucose (2 mg/ml; Sigma), Penicillin/Streptomycin solution (50 ul/ml; Life Technologies). After 15 min in the rinsing media, slices were transferred to membrane inserts (Millipore, PIHP03050) in six well plates filled with slice culture medium: BrainPhys medium (Stemcell Technologies) supplemented with B27, Glutamax (1:200), Penicillin/Streptomycin solution (10 ul/ml; Life Technologies), and incubated in 5% CO_2 at 37 °C. The organotypic slices were kept in culture for at least 1 day before hdINs were detached at 7 DIV and seeded onto the tissue. Organotypic cultures were kept for 30 min in the incubator after seeding the cells in an air-liquid interface, then media was added on top to cover the surface.

Immunocytochemistry. Both hdINs and human primary neurons, plated on glass coverslips were rinsed with phosphate-buffered saline (PBS), fixed in 4% paraformaldehyde (PFA) for 20 min at room temperature (RT), and washed three times in KPBS. For GABA detection, coverslips were fixed with 0.25% glutaraldehyde in 4% PFA instead. Then, coverslips were pre-incubated in blocking solution for 1 h (10% normal serum and 0.25% Triton X-100 in KPBS). Primary antibodies diluted in the blocking solution were incubated overnight at 4 °C (Table S2). Coverslips were washed three times in KPBS and further incubated with Alexa Fluor 488, 555 and 647 conjugated donkey or goat secondary antibodies (1:1000, Jackson Immunoresearch, PA) against the respective primary antibodies, diluted in blocking solution for 1.5 h at RT. Nuclei were counterstained with Hoechst 33342 (1:1000) diluted in the last rinsing with PBS before mounting with Dabco mounting media. Images were acquired by an epifluorescence microscope (Olympus BX61).

For staining human organotypic cultures, slices were fixed overnight at 4 °C with 4% PFA and changed to KPBS after. Then, slices were incubated for 1 h at RT in permeabilization solution (0.02% BSA + 1% Triton X-100 in PBS) and 2 h at RT in blocking solution (5% normal serum + 1% BSA + 0.2% Triton X-100 in PBS). Primary

antibodies were diluted in blocking solution and incubated for 48 h at 4 °C. Then, slices were incubated again in blocking solution 2 h at RT. Secondary antibodies were applied in blocking solution for 48 h at 4 °C. Finally, nuclei were stained with Hoechst for 20 min at RT before sections were mounted. Images were acquired by confocal microscopy (Nikon Confocal A1RHD microscope).

Gene expression analysis. RNA was extracted from cells using RNeasy mini kit (Qiagen) and then reversed to cDNA using Maxima First Strand cDNA Synthesis Kit for RT-qPCR (Thermo Fisher Scientific). For quantitative PCR, cDNA was prepared with PowerUp SYBR Green Master Mix (Thermo Fisher). Candidate genes related to different stages of neurodevelopment and neuronal subtypes were selected for gene expression analysis. A complete list of the primers used is shown in Table S3. Three different biological replicates from different batches of differentiation were used for each time point. All the samples were run in technical triplicates, and the average Ct-values were used for calculations. Data was represented using the ΔCt method, in which all gene expression values are calculated as the average change based on two different housekeeping genes (*ACTB* and *GAPDH*).

Electrophysiology. Human dIN precursors were grown on coverslips from day 7 of differentiation when they were co-cultured with mouse primary glial cells. For in vitro recordings, the coverslips were transferred to the recording chamber containing aCSF (in mM): 129 NaCl, 21 $NaHCO_3$, 10 glucose, 3 KCl, 1.25 NaH_2PO_4, 2 $MgSO_4$, and 1.6 $CaCl_2$, adjusted to 300–310 mOsm, pH 7.4, heated to 32 °C and continuously bubbled with carbogen (95% O_2 and 5% CO_2).

Target cells were identified under fluorescent light (520 nm) for $mCherry^+$ and all the recorded cells were visualized for whole-cell patch-clamp recordings using infrared differential interference contrast video microscopy (BX51WI; Olympus). The glass capillary patch pipette (tip resistance between 2.5 and 6 MΩ) was backfilled with a solution containing in mM: 122.5 K-gluconate, 17.5 KCl, 10 KOH-HEPES, 0.2 KOH-EGTA, 2 Mg-ATP, 0.3 Na_3GTP, and 8 NaCl, pH 7.2–7.4 (mOsm 290–300; all from Sigma-Aldrich). Moreover, biocytin (0.5–1 mg/ml, Biotium) was dissolved in the pipette solution for *post-hoc* identification of recorded cells. All recordings were performed using an EPC10 double patch-clamp amplifier (HEKA Elektronik, Germany), sampled at 10 kHz with a 3 kHz Bessel anti-aliasing filter and using PatchMaster software for data acquisition.

After the formation of a GΩ seal, the patch was ruptured giving direct access to the intracellular compartment. Resting membrane potential (RMP) was determined in current-clamp mode at 0 pA immediately after establishing the whole-cell configuration. Series resistance (Rs) and input resistance (Ri) were calculated from a 5 mV voltage pulse applied through the patch pipette and monitored throughout the experiment. A series of square current steps of 500 ms duration from − 40 to 200 pA in 10 pA steps, were applied at a membrane potential of approximately − 70 mV with holding current as needed, to determine the cells' ability to generate action potentials (AP). Sodium and potassium currents were evoked by a series of 100 ms long voltage steps ranging from − 90 to + 40 mV in 10 mV steps and their sensitivity to 1 µM TTX and 10 mM TEA was determined. AP characteristics were assessed by administration of a depolarizing ramp current over 1 s, from a holding potential of − 70 mV, starting with a 0–25 pA ramp and up to a 0–300 pA ramp in various cells. Spontaneous postsynaptic currents were recorded at − 70 mV.

Drugs and concentrations. Drugs and concentrations: All the used drugs were applied in an aCSF solution perfusing the recording chamber, with the following concentrations: *N*-Methyl-D-aspartic acid (NMDA) receptor blocker (2R)-amino-5-phosphonovaleric acid (D-AP5) 50 µM (Abcam); a-amino-3-hydroxy-5-methyl-4-isoxazolepropionic (AMPA) receptor blocker 2,3-dihydroxy-6-nitro-7-sulfamoyl-benzo[f]quinoxaline-2,3-dione (NBQX) 5 µM (Abcam Biochemicals); $GABA_A$-receptor blocker picrotoxin (PTX) 100 µM (Tocris); Tetrodotoxin (TTX) 1 µM (Abcam); and tetraethylammonium (TEA) 10 mM (Abcam).

Optogentics. For the optogenetic activation of ChR2-expressing cells, blue light of 460 nm wavelength was applied with a LED light source (Prizmatix, Modiin Ilite, Israel) connected to the microscope via a waveguide, illuminating the slice through the water immersion 40 × microscope objective. Red light (595 nm) was applied as a negative control. The frequency and duration of light pulses were programmed and controlled within the Patchmaster software. Stimulation of ChR2-expressing cells was done either by continuous application of the blue light for 500 ms (pulse) or 5 pulses of 3 ms separated by 97 ms intervals (train).

Human primary neuron and host neurons from the human tissue recordings. Human primary neurons and host neurons from the human organotypic cultures were identified by infrared differential interference contrast microscopy, not expressing mCherry under fluorescent light. For a subset of experiments, these cells were identified by GFP + expression (Fig. 6G). The patch pipette was backfilled with a solution containing in mM: 140 KCl, 10 HEPES, 0.2 EGTA, 4 Mg-ATP, 0.4 Na_3GTP, and 10 NaCl, pH 7.2–7.4 (mOsm 290–300; all from Sigma-Aldrich).

Statistical analysis. Quantification of the number of immunoreactive cells was performed in five randomly selected 20 × visual fields for each coverslip from at least three independent cell differentiations. Results for the different markers were expressed as a percentage of the total number of MAP2 + cells. The number of MAP2 + cells varied between 26 to 130 cells in each area counted, with a mean of 52.25 ± 1.78 cells/area, and a minimum of 600 cells were counted for each marker and time point.

Whole-cell patch-clamp recordings were analyzed offline with Igor Pro (Wavemetrics) and Python. AP amplitude was measured on ramp recordings from threshold to peak and AP duration was measured as the width at the threshold. The amplitude of the afterhyperpolarization (AHP) was measured on depolarizing square current steps as the difference between the AHP peak and the AP threshold. Spontaneous postsynaptic currents were detected and analyzed using a custom Python script (https://github.com/AMikroulis/xPSC-detection). Voltage-clamp recordings were low-pass filtered at 400 Hz. An averaged postsynaptic current template generated from hdINs recordings was used for the detection (Figure S2E). Events with a correlation coefficient to the template of 0.6 or greater were included in the analysis (Figure S2F). The rise and decay times were measured as the interval between 20 and 80% of the maximum amplitude. Before the statistical analysis, four exclusion criteria were applied: (1) events with < 5 pA of amplitude were excluded (due to the amplifier's intrinsic noise floor at 4 pA p-p); (2) events with rise-time > 3 ms were excluded; (3) events with decay-time > 20 ms were excluded; and (4) events with decay-time shorter than 1.5 times the rise-time of the event were also excluded. For an equal statistical representation of the different neurons analyzed, an equal number of events were analyzed for all neurons.

Statistical analysis of the data was performed using Prism 7 (GraphPad). The Mann–Whitney test was used for comparison of medians, one-way ANOVA with Tukey's post hoc test for multiple comparisons of means and Wilcoxon test for comparison of paired data. Fisher's exact test was used for comparison of proportions. The level of significance for the tests was set at $p < 0.05$. The Kolmogorov–Smirnov test was used for distribution comparisons of spontaneous currents and the significance was set to $p < 0.01$. All data is presented in the figures as Mean ± SEM. Outlier detection test was applied for the analysis of spontaneous synaptic activity in Fig. 3 and Figure S2, detecting only one outlier that was discarded from the analysis although it did not affect the statistical significance.

Received: 20 July 2021; Accepted: 26 October 2021
Published online: 11 November 2021

References

1. Ouellet, L. & de Villers-Sidani, E. Trajectory of the main GABAergic interneuron populations from early development to old age in the rat primary auditory cortex. *Front. Neuroanat.* **8**, 40. https://doi.org/10.3389/fnana.2014.00040 (2014).
2. Lehmann, K., Steinecke, A. & Bolz, J. GABA through the ages: Regulation of cortical function and plasticity by inhibitory interneurons. *Neural Plast.* **2012**, 892784. https://doi.org/10.1155/2012/892784 (2012).
3. Tremblay, R., Lee, S. & Rudy, B. GABAergic interneurons in the neocortex: From cellular properties to circuits. *Neuron* **91**, 260–292. https://doi.org/10.1016/j.neuron.2016.06.033 (2016).
4. Markram, H. *et al.* Interneurons of the neocortical inhibitory system. *Nat. Rev. Neurosci.* **5**, 793–807. https://doi.org/10.1038/nrn1519 (2004).
5. Ascoli, G. A. *et al.* Petilla terminology: Nomenclature of features of GABAergic interneurons of the cerebral cortex. *Nat. Rev. Neurosci.* **9**, 557–568. https://doi.org/10.1038/nrn2402 (2008).
6. Steinecke, A., Gampe, C., Valkova, C., Kaether, C. & Bolz, J. Disrupted-in-Schizophrenia 1 (DISC1) is necessary for the correct migration of cortical interneurons. *J. Neurosci.* **32**, 738–745. https://doi.org/10.1523/jneurosci.5036-11.2012 (2012).
7. Magloire, V., Mercier, M. S., Kullmann, D. M. & Pavlov, I. GABAergic interneurons in seizures: Investigating causality with optogenetics. *Neuroscientist* **25**, 344–358. https://doi.org/10.1177/1073858418805002 (2019).
8. Liu, Y. Q., Yu, F., Liu, W. H., He, X. H. & Peng, B. W. Dysfunction of hippocampal interneurons in epilepsy. *Neurosci. Bull.* **30**, 985–998. https://doi.org/10.1007/s12264-014-1478-4 (2014).
9. Maroof, A. M. *et al.* Directed differentiation and functional maturation of cortical interneurons from human embryonic stem cells. *Cell Stem Cell* **12**, 559–572. https://doi.org/10.1016/j.stem.2013.04.008 (2013).
10. Nicholas, C. R. *et al.* Functional maturation of hPSC-derived forebrain interneurons requires an extended timeline and mimics human neural development. *Cell Stem Cell* **12**, 573–586. https://doi.org/10.1016/j.stem.2013.04.005 (2013).
11. Liu, Y. *et al.* Directed differentiation of forebrain GABA interneurons from human pluripotent stem cells. *Nat. Protoc.* **8**, 1670–1679. https://doi.org/10.1038/nprot.2013.106 (2013).
12. Baraban, S. C. *et al.* Reduction of seizures by transplantation of cortical GABAergic interneuron precursors into Kv1.1 mutant mice. *Proc. Natl. Acad. Sci. USA* **106**, 15472–15477. https://doi.org/10.1073/pnas.0900141106 (2009).
13. Casalia, M. L., Howard, M. A. & Baraban, S. C. Persistent seizure control in epileptic mice transplanted with gamma-aminobutyric acid progenitors. *Ann. Neurol.* **82**, 530–542. https://doi.org/10.1002/ana.25021 (2017).
14. Yang, N. *et al.* Generation of pure GABAergic neurons by transcription factor programming. *Nat. Methods* **14**, 621–628. https://doi.org/10.1038/nmeth.4291 (2017).
15. Chalmers-Redman, R. M. E., Priestley, T., Kemp, J. A. & Fine, A. In vitro propagation and inducible differentiation of multipotential progenitor cells from human fetal brain. *Neuroscience* **76**, 1121–1128. https://doi.org/10.1016/S0306-4522(96)00386-7 (1997).
16. Weick, J. P., Liu, Y. & Zhang, S. C. Human embryonic stem cell-derived neurons adopt and regulate the activity of an established neural network. *Proc. Natl. Acad. Sci. USA* **108**, 20189–20194. https://doi.org/10.1073/pnas.1108487108 (2011).
17. Au, E. *et al.* A modular gain-of-function approach to generate cortical interneuron subtypes from ES cells. *Neuron* **80**, 1145–1158. https://doi.org/10.1016/j.neuron.2013.09.022 (2013).
18. Avaliani, N. *et al.* Optogenetics reveal delayed afferent synaptogenesis on grafted human-induced pluripotent stem cell-derived neural progenitors. *Stem Cells (Dayton, Ohio)* **32**, 3088–3098. https://doi.org/10.1002/stem.1823 (2014).
19. Habibey, R., Sharma, K., Swiersy, A. & Busskamp, V. Optogenetics for neural transplant manipulation and functional analysis. *Biochem. Biophys. Res. Commun.* https://doi.org/10.1016/j.bbrc.2020.01.141 (2020).
20. Tonnesen, J. *et al.* Functional integration of grafted neural stem cell-derived dopaminergic neurons monitored by optogenetics in an in vitro Parkinson model. *PLoS ONE* **6**, e17560. https://doi.org/10.1371/journal.pone.0017560 (2011).
21. Andersson, M. *et al.* Optogenetic control of human neurons in organotypic brain cultures. *Sci. Rep.* **6**, 24818. https://doi.org/10.1038/srep24818 (2016).
22. Cunningham, M. *et al.* hPSC-derived maturing GABAergic interneurons ameliorate seizures and abnormal behavior in epileptic mice. *Cell Stem Cell* **15**, 559–573. https://doi.org/10.1016/j.stem.2014.10.006 (2014).
23. Watanabe, M. & Fukuda, A. Development and regulation of chloride homeostasis in the central nervous system. *Front. Cell Neurosci.* **9**, 371. https://doi.org/10.3389/fncel.2015.00371 (2015).
24. Wang, C. *et al.* Developmental changes in KCC1, KCC2, and NKCC1 mRNA expressions in the rat brain. *Brain Res. Dev. Brain Res.* **139**, 59–66. https://doi.org/10.1016/s0165-3806(02)00536-9 (2002).

25. Owens, D. F. & Kriegstein, A. R. Is there more to GABA than synaptic inhibition?. *Nat. Rev. Neurosci.* **3**, 715–727. https://doi.org/10.1038/nrn919 (2002).
26. Rahmati, N., Hoebeek, F. E., Peter, S. & De Zeeuw, C. I. Chloride homeostasis in neurons with special emphasis on the olivocerebellar system: Differential roles for transporters and channels. *Front. Cell Neurosci.* **12**, 101. https://doi.org/10.3389/fncel.2018.00101 (2018).
27. Achilles, K. *et al.* Kinetic properties of Cl uptake mediated by Na+-dependent K+-2Cl cotransport in immature rat neocortical neurons. *J. Neurosci.* **27**, 8616–8627. https://doi.org/10.1523/jneurosci.5041-06.2007 (2007).
28. Yamada, J. *et al.* Cl- uptake promoting depolarizing GABA actions in immature rat neocortical neurones is mediated by NKCC1. *J. Physiol.* **557**, 829–841. https://doi.org/10.1113/jphysiol.2004.062471 (2004).
29. Li, H., Tornberg, J., Kaila, K., Airaksinen, M. S. & Rivera, C. Patterns of cation-chloride cotransporter expression during embryonic rodent CNS development. *Eur. J. Neurosci.* **16**, 2358–2370. https://doi.org/10.1046/j.1460-9568.2002.02419.x (2002).
30. Dzhala, V. I. *et al.* NKCC1 transporter facilitates seizures in the developing brain. *Nat. Med.* **11**, 1205–1213. https://doi.org/10.1038/nm1301 (2005).
31. Miskinyte, G. *et al.* Direct conversion of human fibroblasts to functional excitatory cortical neurons integrating into human neural networks. *Stem Cell Res. Ther.* **8**, 207. https://doi.org/10.1186/s13287-017-0658-3 (2017).
32. Grønning Hansen, M. *et al.* Grafted human pluripotent stem cell-derived cortical neurons integrate into adult human cortical neural circuitry. *Stem Cells Transl. Med.* **9**, 1365–1377. https://doi.org/10.1002/sctm.20-0134 (2020).
33. Dull, T. *et al.* A third-generation lentivirus vector with a conditional packaging system. *J. Virol.* **72**, 8463–8471 (1998).
34. Wickham, J. *et al.* Prolonged life of human acute hippocampal slices from temporal lobe epilepsy surgery. *Sci. Rep.* **8**, 4158. https://doi.org/10.1038/s41598-018-22554-9 (2018).
35. *Servier Medical Art*. https://smart.servier.com/.

Acknowledgements

This project was funded by the European Union Horizon 2020 Programme (H2020-MSCA-ITN-2016) under the Marie Skłodowska-Curie Innovative Training Network, project Training4CRM Grant Agreement No. 722779. This project was also funded by the Swedish Research Council (Grant Number: Projekt-id: 2017-00921, MA Grant Number: 2016-02605), The Swedish Brain Foundation (MA) and Crafoord Foundation (MA). We thank Sara Palma-Tortosa and Emmanuela Monni, senior postdoctoral researcher and research engineer at the Laboratory of Stem Cells and Restorative Neurology in the University Hospital of Lund, (Sweden) and Sopiko Kartsivadze, MD and PhD student at Tbilisi State University (Georgia), for providing the foetal human primary neurons and their culturing expertise. Mohanad Hayatleh, Master thesis' student in the lab, for cell counting of immunofluorescent images for different markers. We also thank Jessica Giacomoni, PhD student at the Developmental and Regenerative Neurobiology group at Lund University (Sweden) for kindly sharing some primers and antibodies, and Jordi Rodó for the advice and help on gene expression analysis. Schematics were generated using resources from Servier Medical Art (smart.servier.com).

Author contributions

A.G.-R. designed the study; generated the lentiviral particles; transduced the hESC; collected data performed cell culture differentiation, including human primary cortical neurons and human brain tissue organotypic cultures, gene expression analysis, whole-cell patch-clamp recordings, and immunocytochemistry. Furthermore, A.G.-R. analysed all the data collected, created the figures, and drafted the manuscript. E.W. contributed to data collection regarding cell culture differentiation (excluding human primary cortical neurons and human brain tissue organotypic cultures), whole-cell patch-clamp and immunocytochemistry. A.M. wrote the script in Python for the spontaneous postsynaptic current analysis. Z.K. provided the human primary cortical neurons and respective ethical permits. J.B. neurosurgeon that extracted and provided the human brain tissue resections and respective ethical permits. M.L., M.A., and M.K. designed and supervised the study, produced, and revised the final version of the manuscript.

Funding

Open access funding provided by Lund University.

Competing interests

The authors declare no competing interests.

Additional information

Supplementary Information The online version contains supplementary material available at https://doi.org/10.1038/s41598-021-01270-x.

Correspondence and requests for materials should be addressed to A.G.-R. or M.K.

Supplemental items

Figure S1

Gene expression profile during the cell differentiation. RT-qPCR analysis for the gene expression of oligodendrocyte precursors marker (*PDGFRα*, blue), the MGE marker (*NKX2.1*, orange), and the main interneuron subtypes markers (pink) together with *PPP1R1B* gene (pink), which is expressed in the striatal GABAergic projecting neurons known as medial spiny neurons. Mean ± SEM (n = 3 differentiation batches for condition / time point).

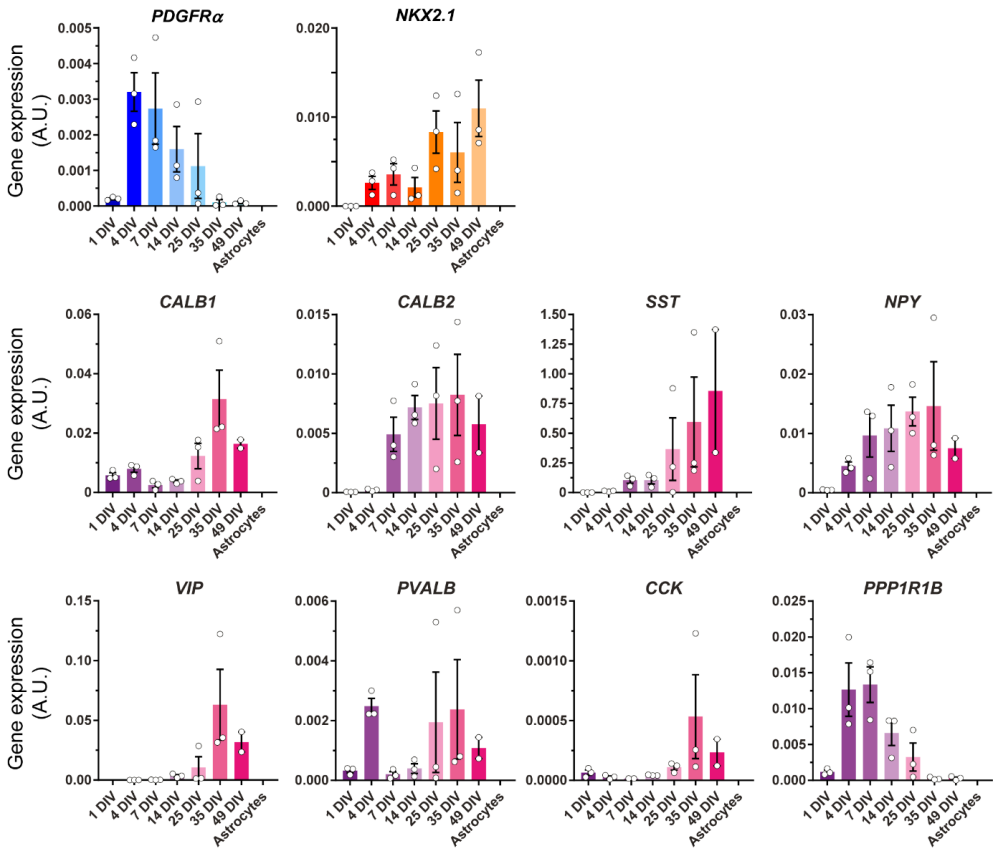

Figure S2

Spontaneous synaptic currents recorded in hdINs at 35 and 49 DIV. hdINs exhibited spontaneous synaptic currents at 35 and 49 DIV. Approximately 80% of the events at 49 DIV had larger amplitudes than at 35 DIV (A). This was accompanied by a higher number of events at 49 DIV (C) compared to 35 DIV. Nevertheless, distribution of the means for both amplitude (B) and inter-event interval (D) were similar between 35 and 49 DIV. (E) Template used for detecting events. (F) Example of event detection using a 0.6 correlation coefficient to the model (E), before further filtering using exclusion criteria. Above in black there is the recording in voltage-clamp and below in red is the automated event detection indicated with red arrows. Mean ± SEM. Kolmogorov-Smirnov test for cumulative distributions and Mann-Whitney test for comparison of means (35 DIV n=13 and 49 DIV n=8, 10 events per cell and condition). ##, p<.001.

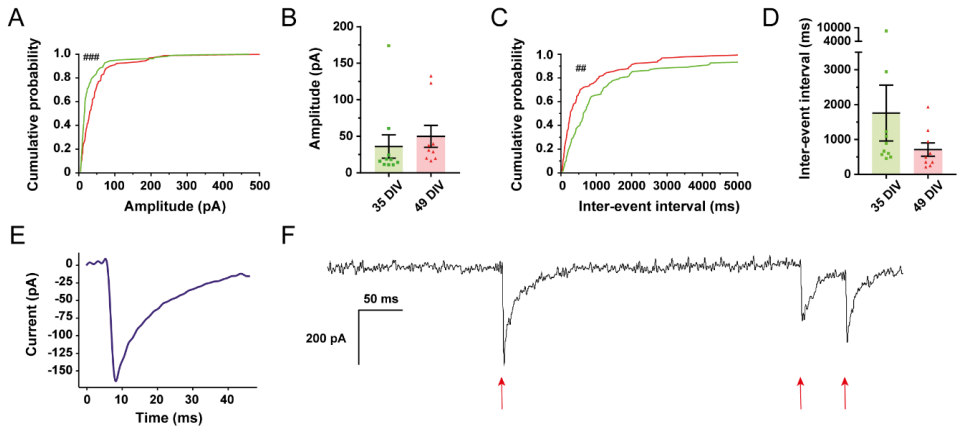

Figure S3

Electrophysiological properties and spontaneous synaptic currents in dhINs 4-6 weeks after *ex vivo* transplantation onto adult human organotypic brain cultures. Grafted hdINs were able to respond with multiple action potentials to depolarizing current pulses (A) and ramps of depolarizing current (B), comparable to mature neurons. Magnification of a current induced action potential in green. (C) Expanded current traces illustrating the sodium current and (D) the potassium current activated during voltage pulses ranging from -90 mV to +40 mV in 10 mV steps. (E-G) Optogenetic stimulation of ChR2 in hdINs triggered inward currents. Light responses were assessed during (E) 500 ms light pulse in voltage-clamp, (F) light train of 5 pulses of 3 ms with 97 ms of interval between pulses in voltage-clamp, and (G) 500 ms light pulse in current-clamp. (H, I) Spontaneous synaptic currents in whole-cell voltage-clamp (H) and current-clamp (I) mode showing afferent synaptic activity in the hdINs. (J) Optogenetic stimulation of ChR2 in hdINs triggered immediate inward currents (red arrow) and, in some cells, also delayed light responses (green arrow) later in the light pulse generated most likely by another hdINs connecting to the recorded one. Blue line, light stimulation.

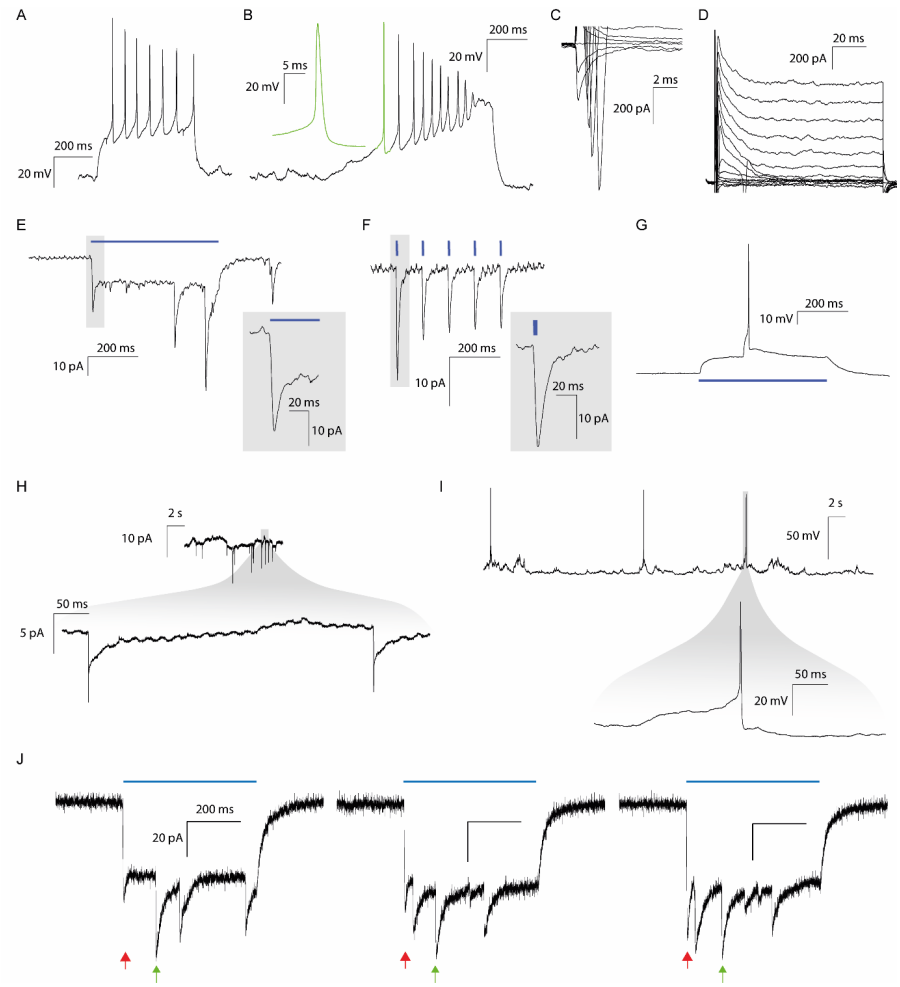

Table S1

Electrophysiological properties of hdINs. The upper table shows the intrinsic electrophysiological properties of hdINs at different time points. The lower table summarizes the properties of the spontaneous synaptic currents of hdINs at the two latest time points. ([a]) Ratio of cells. Mean ± SEM. One-way ANOVA with Tukey's post hoc test for multiple comparisons of means and Fisher's exact test for comparison of proportions (25 DIV n=15, 35 DIV n=36, and 49 DIV n=26) in the upper table. Mann-Whitney test for comparison of medians (35 DIV n=11 and 49 DIV n=8) and Fisher's exact test for comparison of proportions (35 DIV n=26 and 49 DIV n=25) in the bottom table. *, p<.05; **, p<.01; ***, p<.001; ****, p<.0001; indicates a statistically significant difference in comparison to the 25 DIV group in the top table and to the 35 DIV group in the bottom one. AP, action potential; RMP, resting membrane potential; Ri, input resistance.

Intrinsic electrophysiological properties

	hESC-derived Neurons		
	25 DIV	35 DIV	49 DIV
Spontaneous APs [a]	2/15	25/36 ****	21/26 ****
RMP (mV)	**-34.27** ± 2.87	**-47.20** ± 1.84 ****	**-44.85** ± 1.94 ***
R_i (MOhm)	**1470** ± 244.67	**1296.13** ± 178.03	**1205.86** ± 158.35
Fire to Ramps [a]	9/13	35/36 *	25/26 *
Action Potential			
Threshold (mV)	**-34.62** ± 0.94	**-36.39** ± 0.95	**-33.90** ± 1.49
Amplitude (mV)	**51.98** ± 4.36	**75.87** ± 1.7 ****	**75.27** ± 2.62 ****
Duration (ms)	**4.58** ± 0.85	**2.85** ± 0.27 *	**2.14** ± 0.26 ***
AHP amplitude (mV)	**17.58** ± 2.54	**25.16** ± 1.15 **	**28.28** ± 1.23 ***
Max. number	**2** ± 0.73	**17.9** ± 1.80 ****	**18.64** ± 2.39 ****

Electrophysiological properties of spontaneous synaptic currents

	hESC-derived Neurons	
	35 DIV	49 DIV
Spontaneous synaptic activity [a]	13/26	23/25 **
Amplitude (pA)	**34.33** ± 5.82	**49.63** ± 7.39
Inter-event interval, IEI (ms)	**1688.46** ± 322.5	**711.02** ± 107.02
Rising time (ms)	**1.1** ± 0.04	**1.06** ± 0.05
Decay time (ms)	**14.87** ± 0.55	**15.1** ± 0.55

Table S2

Primary antibodies used for immunocytochemistry. Antibodies used for immunocytochemistry detection of different markers for cellular characterization.

Antibody	Host species	Dilution	Company
Oct4	Rabbit	1:500	Abcam ab19857
MAP2	Chicken	1:2000	Abcam ab5392
MAP2	Mouse	1:500	Sigma Aldrich M2320
mCherry	Chicken	1:2000	Abcam ab205402
GABA	Rabbit	1:2000	Sigma Aldrich A2052
GAD65/67	Rabbit	1:500	Sigma Aldrich G5163
Calretinin (CR)	Rabbit	1:1000	Swant CR7697
Calbindin (CB)	Rabbit	1:1000	Swant CB-38a
PV	Mouse	1:1000	Swant PV235
SST	Rat	1:100	Millipore MAB354
NPY	Rabbit	1:5000	Sigma Aldrich N9528
CCK	Rabbit	1:1000	Sigma Aldrich C2581
GFAP	Mouse	1:150	Sigma Aldrich G3793
TH	Mouse	1:200	Millipore MAB318
vGlut1	Mouse	1:200	Synaptic Systems 135511
KGA	Rabbit	1:1000	Abcam ab93434

Table S3

Primer sequences used for gene expression analysis. List of primer sequences used for RT-qPCR detection of specific genes for cellular characterization.

TARGET GENE	PRIMERS	
	Forward	Reverse
h-*ACTB*	CCTTGCACATGCCGGAG	GCACAGAGCCTCGCCTT
h-*GAPDH*	TTGAGGTCAATGAAGGGGTC	GAAGGTGAAGGTCGGAGTCA
h-*POU5F1* (OCT4)	TCTCCAGGTTGCCTCTCACT	GTGGAGGAAGCTGACAACAA
h-*SOX2*	CATGGCAATCAAAATGTCCA	TTTCACGTTTGCAACTGTCC
h-*MAP2*	CCGTGTGGACCATGGGGCTG	GTCGTCGGGGTGATGCCACG
h-*SYN1*	CCCGTGGTTGTGAAGATGGGGC	TGCCACGACACTTGCGATGTCC
h-*NKX2.1*	AGGGCGGGGCACAGATTGGA	GCTGGCAGAGTGTGCCCAGA
h-*GAD1* (GAD67)	GCCAGACAAGCAGTATGATGT	CCAGTTCCAGGCATTTGTTGAT
h-*PVALB*	TGCAGGATGTCGATGACAGA	TTTCTTCAGGCCGACCATTT
h-*SST*	CCCCAGACTCCGTCAGTTTCT	CATTCTCCGTCTGGTTGGGT
h-*CALB1* (CB)	TGGATCAGTATGGGCAAAGAGA	ATCGGAAGAGCAGCAGGAAAT
h- *CALB2* (CR)	TGGAAGCACTTTGACGCAGAC	CAGAGCCTTTCCTTGCCTTCT
h-*VIP*	TCTCACAGACTTCGGCATGG	TCATTTGCTCCCTCAAAGGGT
h-*NPY*	TGTTCCCAGAACTCGGCTTG	TGCATTGGTAGGATGGGTGG
h-*CCK*	AGGGTATCGCAGAGAACGGA	CTTATCCTGTGGCTGGGGTC
h-*PPP1R1B* (DARPP32)	GAGAGCCTCAGGAGAGGGGCAC	AGGTGGTGTGTAGGCACAGGGG
h-*SLC17A7* (VGLUT1)	AATAACAGCACGACCCACCGCG	AGCCGTGTATGAGGCCGACAGT
h-*GFAP*	AGATCCGCACGCAGTATGA	AGTCGTTGGCTTCGTGCTT
h-*PDGFRA*	CCTTGGTGGCACCCCTTAC	TCCGGTACCCACTCTTGATCTT
m-*Actb*	CATTGCTGACAGGATGCAGAAGG	TGCTGGAAGGTGGACAGTGAGG
m-*Gapdh*	AACTTTGGCATTGTGGAAGG	ACACATTGGGGGTAGGAACA
m-*Gfap*	ACCAGCTTACGGCCAACAGT	TACGCAGCCAGGTTGTTCTC
WPRE	GTCCTTTCCATGGCTGCTC	CCGAAGGGACGTAGCAGA

Paper II

International Journal of
Molecular Sciences

MDPI

Article

Human Stem Cell-Derived GABAergic Interneurons Establish Efferent Synapses onto Host Neurons in Rat Epileptic Hippocampus and Inhibit Spontaneous Recurrent Seizures

Eliška Waloschková [1,*], Ana Gonzalez-Ramos [1], Apostolos Mikroulis [1], Jan Kudláček [1,2], My Andersson [1], Marco Ledri [1] and Merab Kokaia [1,*]

[1] Epilepsy Center, Department of Clinical Sciences, Lund University Hospital, 221 84 Lund, Sweden; ana.gonzalez_ramos@med.lu.se (A.G.-R.); apostolos.mikroulis@med.lu.se (A.M.); jan.kudlacek@lfmotol.cuni.cz (J.K.); my.andersson@med.lu.se (M.A.); marco.ledri@med.lu.se (M.L.)
[2] Department of Physiology, Second Faculty of Medicine, Charles University, 150 06 Prague, Czech Republic
* Correspondence: eliska.waloschkova@med.lu.se (E.W.); merab.kokaia@med.lu.se (M.K.)

Abstract: Epilepsy is a complex disorder affecting the central nervous system and is characterised by spontaneously recurring seizures (SRSs). Epileptic patients undergo symptomatic pharmacological treatments, however, in 30% of cases, they are ineffective, mostly in patients with temporal lobe epilepsy. Therefore, there is a need for developing novel treatment strategies. Transplantation of cells releasing γ-aminobutyric acid (GABA) could be used to counteract the imbalance between excitation and inhibition within epileptic neuronal networks. We generated GABAergic interneuron precursors from human embryonic stem cells (hESCs) and grafted them in the hippocampi of rats developing chronic SRSs after kainic acid-induced status epilepticus. Using whole-cell patch-clamp recordings, we characterised the maturation of the grafted cells into functional GABAergic interneurons in the host brain, and we confirmed the presence of functional inhibitory synaptic connections from grafted cells onto the host neurons. Moreover, optogenetic stimulation of grafted hESC-derived interneurons reduced the rate of epileptiform discharges in vitro. We also observed decreased SRS frequency and total time spent in SRSs in these animals in vivo as compared to non-grafted controls. These data represent a proof-of-concept that hESC-derived GABAergic neurons can exert a therapeutic effect on epileptic animals presumably through establishing inhibitory synapses with host neurons.

Keywords: human embryonic stem cells; GABA; interneurons; optogenetics; epilepsy; cell integration; synaptic integration

Citation: Waloschková, E.; Gonzalez-Ramos, A.; Mikroulis, A.; Kudláček, J.; Andersson, M.; Ledri, M.; Kokaia, M. Human Stem Cell-Derived GABAergic Interneurons Establish Efferent Synapses onto Host Neurons in Rat Epileptic Hippocampus and Inhibit Spontaneous Recurrent Seizures. *Int. J. Mol. Sci.* **2021**, 22, 13243. https://doi.org/10.3390/ijms222413243

Academic Editor: Aleksey Zaitsev

Received: 23 November 2021
Accepted: 5 December 2021
Published: 8 December 2021

1. Introduction

Epilepsy is a neurological disorder affecting around 50 million people worldwide [1]. Patients suffering from epilepsy have access to a variety of symptomatic pharmacological treatments [2–5]. However, despite the growing number of these anti-seizure medications (ASMs), there are no established preventive or disease-modifying treatments available [6]. Moreover, long-term intake of ASMs is associated with adverse side effects [7–9], and most importantly, available medications are not effective in 30% of patients who become drug-resistant [10,11]. Most commonly these patients suffer from temporal lobe epilepsy (TLE), which is characterised by focal spontaneous recurrent seizures (SRSs) originating in the mesial temporal lobe often with secondary generalization. Many TLE patients also exhibit comorbidities, such as depression, anxiety, psychosis, and impairment of learning and memory [12]. For some of these drug-resistant patients, surgical resection of the epileptogenic focus may be an effective treatment, nonetheless, this therapeutic approach is possible only in a relatively small number of individuals due to the location of the seizure focus in, e.g., eloquent brain areas [13].

One of the structures affected in TLE is the hippocampus, where alterations of its neuronal circuitry lead to hyperexcitability [14]. One of the causes of hyperexcitability

is dysfunction and/or degeneration of inhibitory GABAergic interneurons [15,16] which express and release the inhibitory neurotransmitter γ-amino-butyric acid (GABA) [17]. The loss of these neurons can lead to decreased inhibition in the neuronal networks, shifting the balance towards increased excitability, and reduced threshold for seizure initiation [18–20]. Therefore, there is an increased interest in developing cell therapies for epilepsy based on transplanting GABAergic progenitor cells in the seizure focus, thus enhancing inhibitory neurotransmission, which could normalize increased excitability of the local networks and thereby suppress SRSs. Several studies in animal models of TLE focused on medial ganglionic eminence (MGE)-derived GABAergic progenitor cells. After in vivo transplantation, these cells can differentiate into subclasses of interneurons typical for the hippocampus, migrate extensively, are capable of integration into the hippocampal circuitry, and most importantly, significantly diminish SRSs [21–26]. However, in all the studies, foetal rodent tissue has been used as the source of MGE-derived GABAergic progenitor cells. Although this approach provides a proof-of-concept for this idea, it lacks the translational potential for treating human patients. It is therefore not surprising that recent research has focused on the use of cells derived from human pluripotent stem cells (hPSCs), as a renewable resource for cell-based therapies. Studies using MGE-like GABAergic progenitors derived from hPSCs indicated seizure attenuation several months after transplantation in two rodent TLE models [27,28] suggesting that this strategy may be a promising approach for new therapy development.

In our previous study [29], we successfully generated optogenetically regulatable GABAergic interneurons from hESCs in vitro in a relatively short time, by adapting a protocol based on overexpressing two transcription factors, *Dlx2* and *Ascl1* [30]. Using optogenetic activation of these cells, we demonstrated the establishment of functional efferent synapses onto other human neurons in vitro [29]. In the current study, we asked whether these cells would also generate such synapses when grafted in vivo into the epileptic hippocampus. We transplanted these cells into the hippocampi of immunodeficient rats with kainate-induced TLE. We demonstrated that the hESC-derived GABAergic interneurons (hdInts) can functionally mature and form inhibitory synapses onto the host cells in the hippocampus already at three months and more prominently at six months post-transplantation (PT). Importantly, we observed a significant reduction of SRS frequency and total time spent in seizures in treated animals compared to untreated controls four months after status epilepticus (SE) induction. Taken together, our results provide evidence that hESC-derived interneurons suppress SRSs in epileptic animals by establishing inhibitory synaptic connections onto the host neurons and contribute to a better understanding of the potential mechanisms by which novel cell-based therapy would counteract refractory epilepsy.

2. Results

2.1. Kainic Acid-Induced Status Epilepticus and Development of Spontaneous Recurrent Seizures

To assess kainic acid-induced SE (KA-SE), animals were observed since the first KA injection (Figure S1, Video S1). With a median dose of 15 mg/kg of KA, all animals developed SE (n = 25). The mortality rate for KA-SE was 8% (two out of 25 animals). Animals were divided in two groups, (i) non-grafted (controls; n = 8) and (ii) cell-grafted (n = 16). To establish the frequency of motor SRSs, eight animals from both groups were video monitored for seven days continuously, starting four months after SE (i.e., three months PT, Figures 1A and 10A, Video S2). From the cell-grafted group, seven animals were used for electrophysiology and immunohistochemistry at three months PT, and eight animals were kept for six-month PT experiments. Motor SRSs were not detected in two rats from the control non-grafted group and were therefore excluded from the study. Video-EEG monitoring of three non-grafted rats used as a pilot, confirmed that 96.8% of electrographic SRSs were generalised motor SRSs (Figure S2A), therefore, only video recordings were used for the rest of the study to analyse SRS frequency and duration

(Rat #1—16 motor seizures out of 17 total; Rat #2—17 motor seizures out of 18 total; Rat #3—27 motor seizures out of 27 total; Figure S2B1,B2).

2.2. hESC-Derived Interneuron Precursors Functionally Mature in the Epileptic Rodent Hippocampus

As described before, hPSC-derived interneurons can mature and integrate into the rodent hippocampus [27,28]. In this study, GABAergic interneuron precursors were generated from hESCs by overexpressing *Ascl1* and *Dlx2* [30] and were transplanted already at seven days in vitro (DIV; Figure 1A), with their differentiation continuing in vivo by administering doxycycline to the animals in the drinking water (see Section 4.3). Spare hdInt precursors from transplantation surgeries were replated directly on the same day and fixed 24 h after. Immunocytochemistry of hdInt precursors confirmed successful patterning of the cells (GABA+ and β-III-tubulin+, Figure S3D,E) and their loss of the proliferative state (Ki67-, Figure S3B). Cells did not express Sox2 (Figure S3A), a stem cell marker, nor Nestin, a marker of neural precursors at the stage of radial glia (Figure S3C). A more detailed characterization of hdInts in vitro was described in our previous study [29].

To be able to investigate the formation of synapses onto the host neurons, the grafted cells were transduced by channelrhodopsin-2 (ChR2)-carrying lentiviral particles. First, their ability to respond to blue light (460 nm) was assessed by whole-cell patch-clamp recordings. These experiments were performed both at three months PT (n = 27 cells) and six months PT (n = 42 cells, Figure 1B). The transplanted cells generated action potentials (APs) in response to the light, and the proportion of cells being able to generate APs was significantly higher at six months (n = 24 out of 42) compared to three months PT (n = 10 out of 27, p = 0.0098; Figure 1D, Table S1). However, the peak current of the response (3 months PT: 115.6 ± 20.97 pA, 6 months PT: 80.52 ± 13.98 pA), as well as the steady-state current (3 months PT: 50.23 ± 10.3 pA, 6 months PT: 41.50 ± 7.9 pA) did not differ between the two time points (p = 0.2287 and p = 0.8427, respectively; Figure 1E, Table S1).

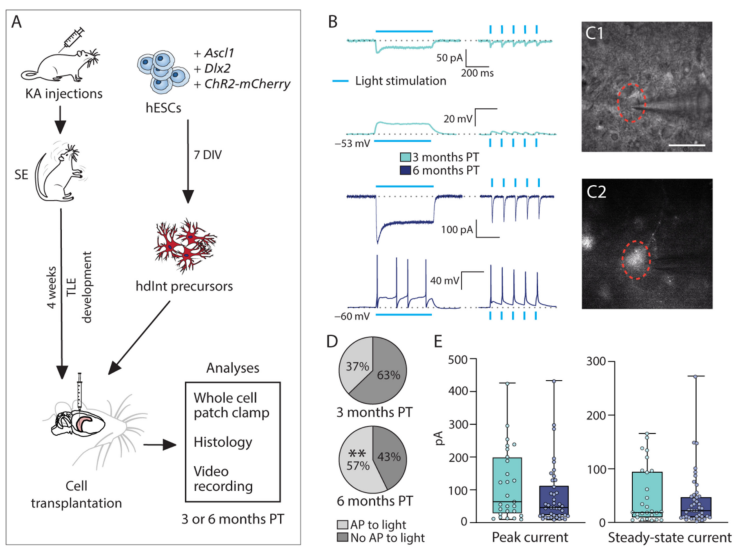

Figure 1. Experimental timeline and optogenetic properties of grafted hdInts. (**A**) Schematic representation of the timeline of the study. (**B**) Voltage- and current-clamp traces from ChR2-expressing hdInts

indicate the direct response to 460 nm light stimulation. Two types of stimulation were used: continuous 500 ms pulse (left column) and brief 3 ms pulses at 10 Hz (right column). (**C1**) Grafted hdInt being approached by a patch-clamp pipette after identified as mCherry+ (shown on (**C2**); i.e., expressing ChR2). Red dotted circle outlines the patched cell. (**D**) Significantly higher proportion of cells was able to generate APs in response to light stimulation at six months PT. (**E**) Neither the peak current nor the steady-state current significantly changed over time. **, $p < 0.01$; Binomial test was used to compare proportions in (**D**); Mann-Whitney test was used to compare medians in (**E**). Scale bar 20 µm. KA, kainic acid; SE, status epilepticus; TLE, temporal lobe epilepsy; ChR2, channelrhodopsin-2; hESCs, human embryonic stem cells; DIV, days in vitro; hdInt, hESC-derived GABAergic interneuron; PT, post-transplantation; AP, action potential.

Electrophysiological properties of the grafted cells were analysed to assess their functional maturation in the tissue environment of the epileptic hippocampus at three months PT (n = 27 cells) and six months PT (n = 42 cells). The input resistance (Ri) was significantly lower at six months PT (3 months PT: 974.0 ± 75.23 MΩ, 6 months PT: 746.4 ± 62.4 MΩ, $p = 0.0164$) while resting membrane potential (RMP) was significantly more negative at six months PT in the grafted cells (3 months PT: −52.64 ± 1.86 mV, 6 months PT: −59.77 ± 1.26 mV, $p = 0.0016$), better resembling the values of mature neurons (Figure 2A, Table S1). There was no significant difference in membrane capacitance (Cm, 3 months PT: 188.7 ± 24.01 pF, 6 months PT: 205.8 ± 16.37 pF, $p = 0.4493$) and series resistance (Rs, 3 months PT: 9.91 ± 1.35 MΩ, 6 months PT: 8.48 ± 1.08 MΩ, $p = 0.1853$; Figure 2A, Table S1). However, all AP properties showed a more mature neuronal phenotype at six months PT compared to the earlier time point, with the amplitude being larger (3 months PT: 54.56 ± 3.53 mV, 6 months PT: 76.79 ± 1.94 mV, $p < 0.0001$), the threshold lower (3 months PT: −31.82 ± 1.61 mV, 6 months PT: −36.5 ± 1.05 mV, $p = 0.0134$), the duration shorter (3 months PT: 3.11 ± 0.21 ms, 6 months PT: 1.95 ± 0.1 ms, $p < 0.0001$), and after-hyperpolarisation (AHP) amplitude larger (3 months PT: 22.28 ± 1.06 mV, 6 months PT: 28.39 ± 0.91 mV, $p < 0.0001$, Figure 2B, Table S1). All cells were able to fire depolarization-induced APs at both timepoints. In addition, a significant increase in sodium and potassium currents was observed at six months PT (Figure 2C,D). All the above-mentioned parameters indicate functional maturation of the grafted cells in the rat epileptic brain over time.

To investigate afferent synapses formed onto the grafted hdInts, we recorded spontaneous postsynaptic currents (sPSCs) in voltage-clamp mode at the holding potential of −70 mV (Figure 3A). sPSCs were then detected using a custom-made python script offline. The measured characteristics of the sPSCs were then compared between the cells at three- and six-months PT (n = 42 events/cell for distribution comparisons; for median comparisons: 3 months PT-n = 26 cells; 6 months PT-n = 42 cells). The median rise time of the detected events was significantly shorter at six months PT (3 months PT: 2.0 ± 0.06 ms, 6 months PT: 1.69 ± 0.04 ms, $p < 0.0001$), also clearly seen on the distribution curves (Figure 3B). Together with the significantly larger amplitude (3 months PT: 8.14 ± 0.77 pA, 6 months PT: 15.32 ± 1.6 pA, $p < 0.0001$), increased frequency (3 months PT: 1.36 ± 0.24 Hz, 6 months PT: 2.52 ± 0.2 Hz, $p < 0.0001$) and decreased inter-event intervals (IEIs) of the sPSCs at the later time point (Figure 3B), these changes indicate increased synaptic integration of the grafted hdInts into the host neural network over time (values summarized in Table S1).

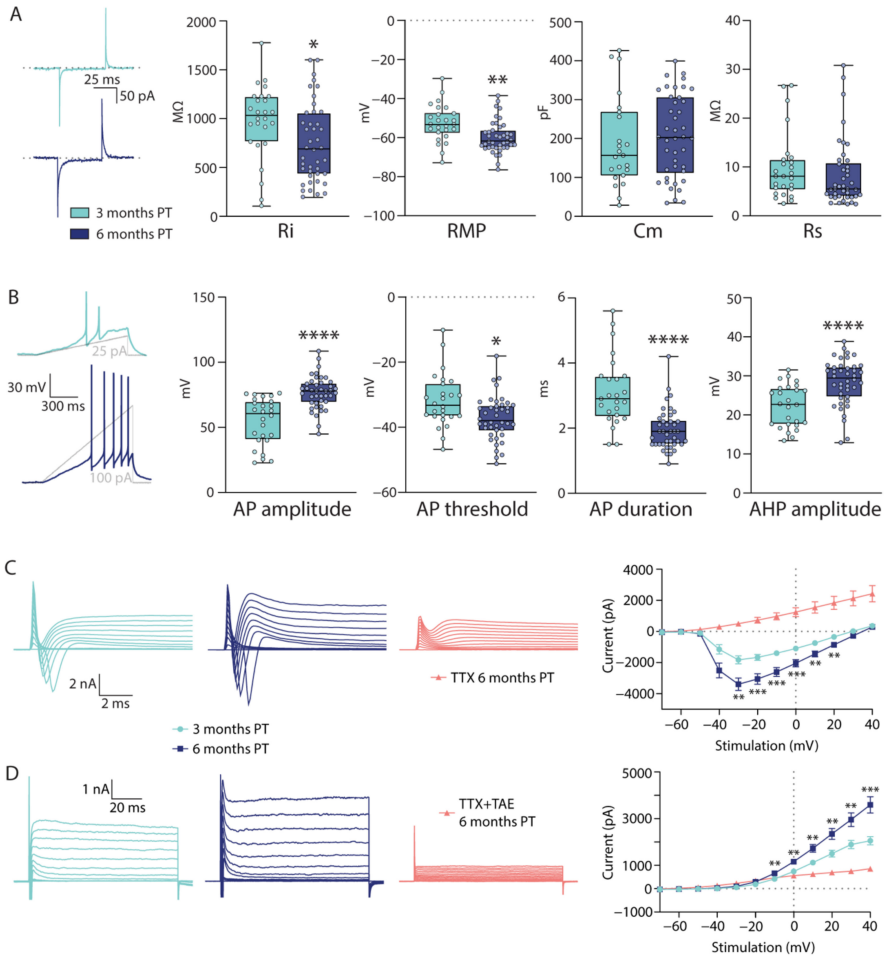

Figure 2. Electric membrane properties of grafted hdInts and their change over time. (**A**) Cell membrane properties of hdInts calculated from a series of 5 mV pulses applied through the patch pipette at three- and six-months PT. The Ri was lower and RMP higher, getting closer to mature neuronal characteristics at the later timepoint. (**B**) AP properties measured from induced APs. All changes between the two time points were significant and indicate neuronal maturation of the grafted cells. (**C**) TTX-sensitive evoked sodium currents were higher at six months PT. (**D**) TAE-sensitive evoked potassium currents were higher at six months PT. *, $p < 0.05$; **, $p < 0.01$; ***, $p < 0.001$; ****, $p < 0.0001$. Mann-Whitney test was used to compare medians in (**A**,**B**); Multiple unpaired *t*-tests were used to compare means in (**C**) and (**D**). Dotted grey line represents the baseline (0 mV/0 pA) from which reported values have been measured. Ri, input resistance; RMP, resting membrane potential; Cm, membrane capacitance; Rs, series resistance; AHP, after-hyperpolarisation; TTX, tetrodotoxin; TAE, tetraethylammonium.

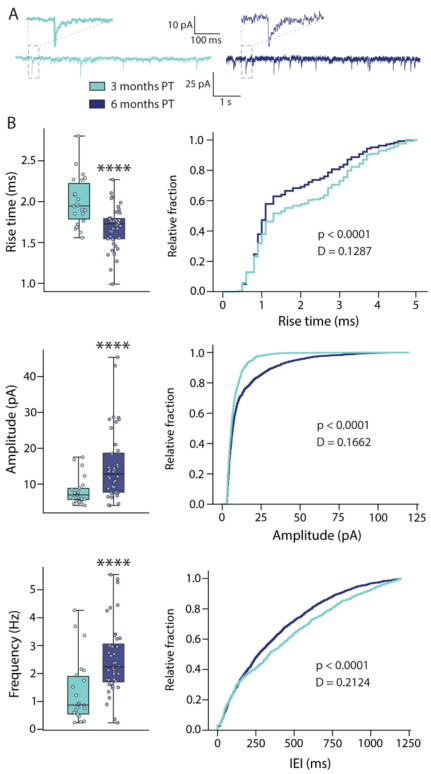

Figure 3. Spontaneous synaptic events in grafted hdInts. (**A**) Representative traces of voltage-clamp recordings from grafted hdInts in which sPSCs were detected. (**B**) Comparisons of sPSC characteristics between three- and six-months PT demonstrate the differences between medians and distributions. The rise time of the detected events is significantly shorter, amplitude significantly larger and frequency significantly higher at six months PT indicating improved synaptic integration at this later time point. ****, $p < 0.0001$. A Mann-Whitney test was used to compare medians in box plots, Kolmogorov-Smirnoff test was used for comparison of distributions. IEI, inter-event interval.

2.3. hESC-Derived Interneurons form Inhibitory Synapses between Each Other and onto Host Neurons

An important aspect of neuronal maturation and integration into the neuronal network is the ability of the transplanted cells to form efferent synapses onto the surrounding neurons. To investigate this, we took advantage of the optogenetic modification of the grafted hdInts. While recording from ChR2-expressing hdInts and illuminating the hippocampal slices with a 460 nm light pulse (Figure 4A), apart from the direct response to the light stimulation, delayed synaptic currents were also observed (with a delay from the light pulse onset; Figures 4B and S5). The delayed onset of the PSCs was most likely due to the time required for the synaptic transmission, as well as the reach time needed for the depolarization of the presynaptic hdInt cells to the level of AP generation (Figures S6 and S7). To verify that the delayed currents were indeed inhibitory synaptic connections from surrounding hdInts, the same light stimulation recordings were performed by adding picrotoxin (PTX), a GABA receptor blocker. Indeed, the delayed currents were no longer visible after PTX

treatment (n = 6 cells, Figure 4B), supporting the GABAergic nature of the graft-to-graft synapses. These graft-to-graft synapses were higher in proportion at six months PT (n = 13 out of 42 cells) compared to three months PT (n = 4 out of 27 cells, p = 0.0073) which suggests an increase in such synapses over time (Figure 4C). The ChR2-expression of grafted hdInts was identified before patching the cells by mCherry fluorescence and was confirmed retrospectively by staining against mCherry (Figure 4D,E).

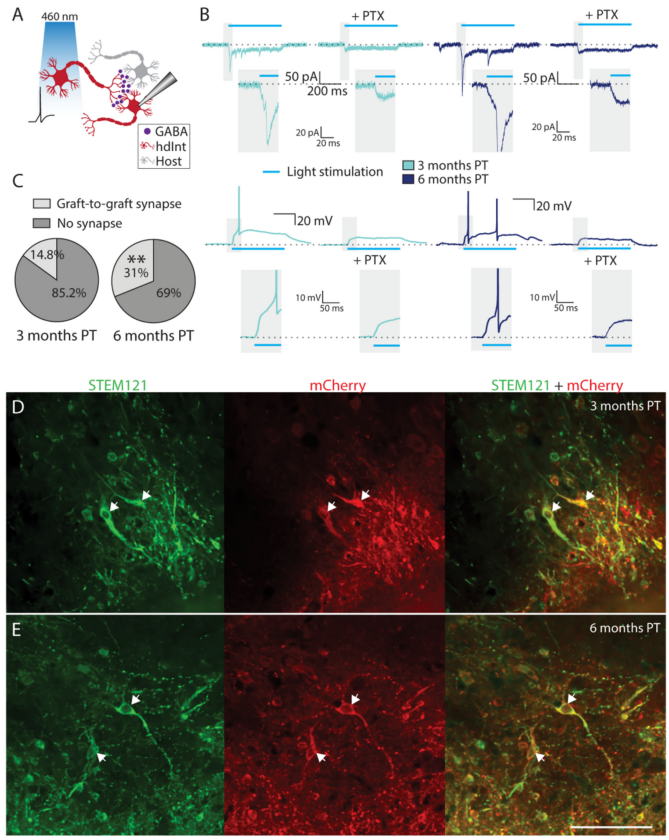

Figure 4. Graft-to-graft synaptic connectivity. (**A**) Cartoon representing a recording from a grafted hdInt receiving inhibitory synapses from another grafted hdInt (a graft-to-graft synapse) activated by blue light. (**B**) Representative traces from recorded hdInts in voltage- and current-clamp mode while illuminating slices by a 500 ms blue light pulse. Note a delayed synaptic response, which is then blocked by PTX, confirming the GABAergic nature of the synaptic connections. These PSCs were observed both at three- and six-months PT. (**C**) The proportion of cells with an observed graft-to-graft synapse was significantly higher at six months, compared to three months PT. (**D**,**E**) Immunofluorescent staining of slices used for electrophysiology experiments confirming the expression of mCherry in grafted hdInts. The cells exhibit staining for the human cell marker STEM121 (green) and mCherry (red). **, $p < 0.01$. The binomial test was used for the comparison of proportions in (**C**). Scale bar 100 µm. PTX, picrotoxin.

Similar experiments were performed to identify efferent synaptic connections from grafted hdInts onto the host neurons. Whole-cell patch-clamp recordings were performed from neurons not expressing ChR2 in the vicinity of a ChR2-expressing hdInt (Figure 5A). When a light pulse was delivered to the slice, there was no direct light-induced current observed (Figure 5B). However, in some cells delayed synaptic responses were detected instead (Figures 5B and S5). These currents were readily blocked in all cells by PTX application (n = 5 cells), again confirming that the synaptic connections were GABAergic (Figure 5B). In contrast, no change was observed in the delayed synaptic responses when 2,3-dihydroxy-6-nitro-7-sulfamoyl-benzo-quinoxaline-2,3-dione disodium salt (NBQX) and (2R)-amino-5-phosphonovaleric acid (D-AP5) were applied to block glutamatergic synaptic responses (Figure S4). Similar, to the above-mentioned graft-to-graft synapses, the graft-to-host synapses were observed in a higher proportion of cells at the later time point (3 months PT: n = 3 out of 25 cells, 6 months PT: n = 11 out of 37 cells, p = 0.0032, Figure 5C). All recorded host neurons with delayed synaptic responses were retrospectively confirmed as host neurons by confocal microscopy, by not expressing mCherry nor the human cell marker STEM121 (Figure 5D,E).

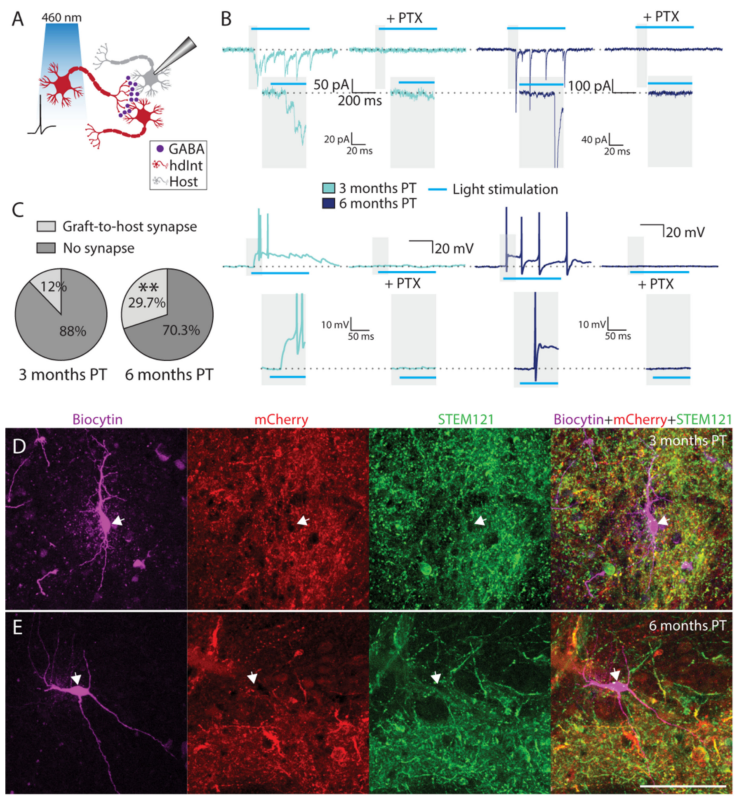

Figure 5. Graft-to-host synaptic connectivity. (**A**) Cartoon representing a recording from a host neuron receiving inhibitory synapses from a grafted hdInt (a graft-to-host synapse) activated by blue light. (**B**) Representative traces from recorded host neurons in voltage- and current-clamp mode while

illuminating slices by a 500 ms blue light pulse. Note a delayed synaptic response, which is then blocked by PTX, confirming the GABAergic nature of the synaptic connections. These PSCs were observed both at three- and six-months PT. (**C**) The proportion of cells with an observed graft-to-host synapse was significantly higher at six months, compared to three months PT. (**D**,**E**) Immunofluorescent staining of slices used for electrophysiology experiments, the patched biocytin-filled cells (magenta) do not exhibit staining for STEM121 (green) nor mCherry (red). **, $p < 0.01$. A binomial test was used for the comparison of proportions. Scale bar 100 μm.

To get a better understanding of the nature and origin of the delayed synaptic responses, time was measured from the onset of the light pulse to the base of the first delayed synaptic event. These measurements revealed a relatively narrow time window in which these events occurred in each cell (Figure S5). This finding indicates that the observed synaptic events were less likely to be random sPSCs but were rather delayed synaptic responses caused by light stimulation of a nearby ChR2-expressing hdInt. Notably, there was a quite wide range in the observed delayed synaptic responses between cells, especially at six months PT (Figure S5). To test whether one of the reasons could be a delayed AP generation in presynaptic hdInts after light onset, time was measured from the onset of the light pulse to the threshold of the first light-induced AP (only in cells with no graft-to-graft connections). A broad range of AP onset times was observed; thus a correlation analysis was performed which revealed that both light-induced peak current and steady-state current amplitudes correlated negatively with AP onset time ($r = -0.7647$, $p = 0.0009$; $r = -0.7412$, $p = 0.0015$, respectively; Figures S6A,B and S7).

2.4. hESC-Derived GABAergic Interneurons Express Interneuron Markers Calretinin and Calbindin

The grafted hdInts have proven to be GABAergic in our previous in vitro study [29]. The present electrophysiological experiments suggested that even after in vivo grafting these cells become GABAergic as judged by their efferent synaptic connections. To further consolidate their phenotype, the hippocampal slices used for whole-cell patch-clamp recordings were used for immunohistochemistry. Firstly, the expression of GABA in the tissue was examined, and indeed, the grafted areas expressed significantly higher fluorescence levels of GABA staining than the surrounding tissue both at three months PT ($n = 17$ slices, $p < 0.0001$) as well as at six months PT ($n = 19$ slices, $p < 0.0001$; Figure 6A1,A2). Summarized data are presented in Figure 6B.

To further specify the interneuron phenotype, we examined slices for calretinin (CR) and calbindin (CB) immunoreactivity. These stainings revealed that the expression of CB in the grafted hdInts was colocalized with the expression of the human cytoplasm marker STEM121 in a proportion of cells (Figure 7A1,A2), which was similar at both time points of analysis ($n = 21$ slices/timepoint, three months PT: 37.48 ± 1.98%, 6 months PT: 38.0 ± 3.18%, $p = 0.8904$; Figure 7C). Examples of double labelled cells with CB and STEM121, as well as STEM121 and Hoeschst are presented in Figure 7B.

Cells expressing both CR and the human cytoplasm marker STEM121 were identified in the graft as well (Figure 8A1,A2), with the percentage of cells co-expressing both markers being significantly higher at the six-month PT timepoint as compared to three months PT ($n = 21$ slices/timepoint, three months PT: 32.42 ± 1.66%, 6 months PT: 38.07 ± 2.17%, $p = 0.0455$; Figure 8C). Examples of double labelled cells with CR and STEM121, as well as STEM121 and Hoeschst are presented in Figure 8B.

In summary, hdInt precursors grafted into the rat epileptic hippocampus mature into GABAergic interneurons mostly with a CB and CR phenotype.

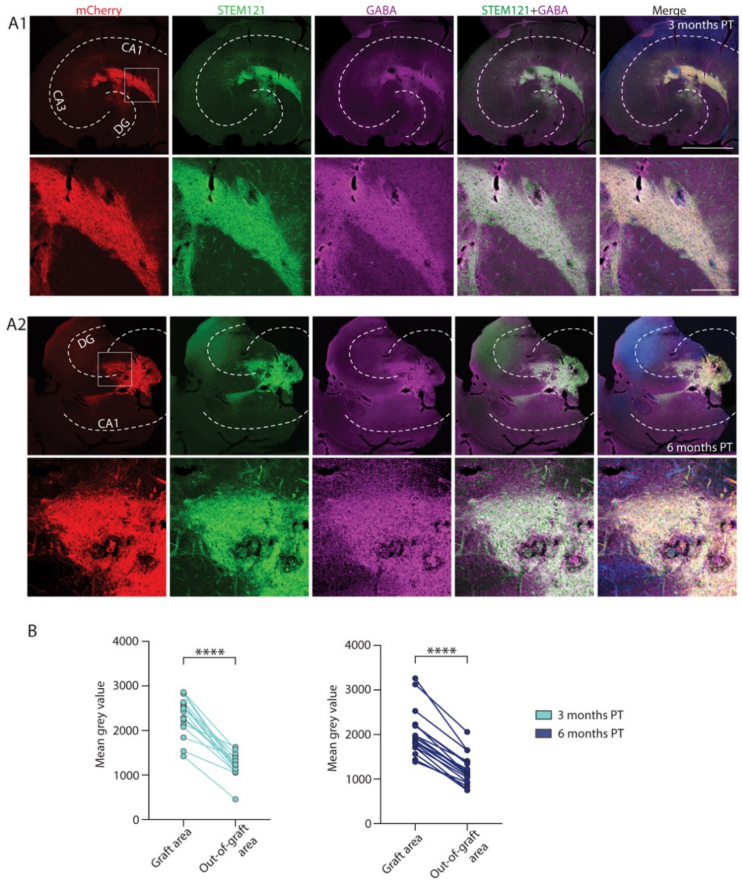

Figure 6. Histological analysis of GABA expression within and outside the graft. (**A**) Immunofluorescent staining of hippocampal sections with grafted hdInts for mCherry (marker for ChR2; red), human cytoplasm (STEM121; green), and GABA (magenta), merged with Hoechst (blue) in the last right column. GABA expression within the graft was well seen at both three months PT (**A1**) and six months PT (**A2**). (**B**) Quantification of GABA fluorescence intensity of the graft area compared with surrounding tissue at both timepoints. ****, $p < 0001$. Wilcoxon test was used in (**B**). Dashed white line in (**A1**,**A2**) represents the anatomical structure of the hippocampus. Scale bars 1 mm and 200 µm. DG, dentate gyrus.

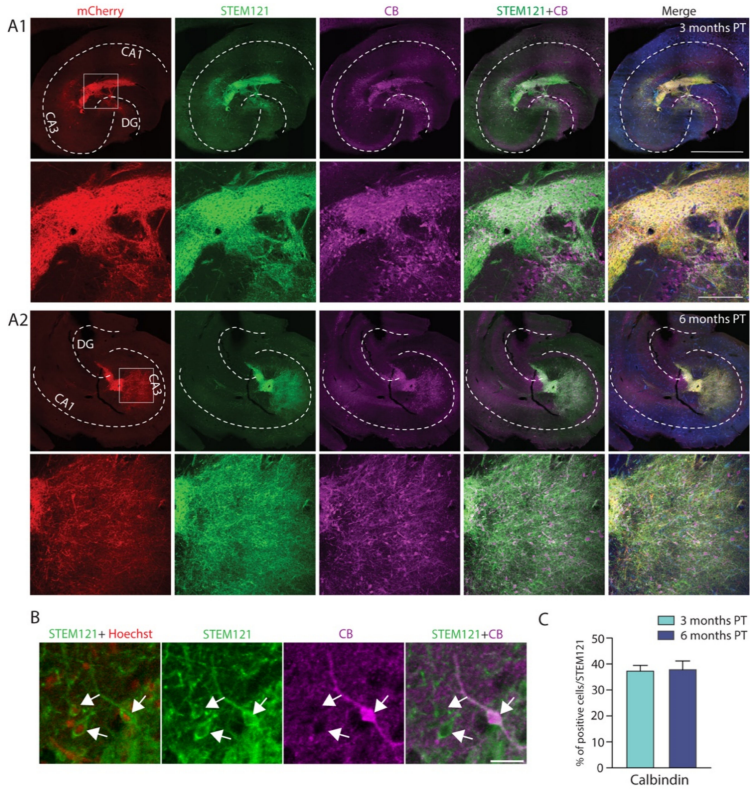

Figure 7. Grafted hdInts express calbindin, a marker of a GABAergic interneuron subpopulation. (**A**) Immunofluorescent images of hippocampal sections with grafted hdInts stained for mCherry (marker for ChR2; red), human cytoplasm (STEM121; green), and calbindin (CB; magenta), merged with Hoechst (blue) in the last right column. CB expression within the graft was observed at both three months PT (**A1**) and six months PT (**A2**). (**B**) A merged image of STEM121 and Hoechst was used for counting all STEM121+ cells, while the merged image of STEM121 and CB staining was used for counting STEM121+CB+ double-positive cells. Arrowheads indicate examples of counted cells. (**C**) Quantification of cells stained for STEM121 and CB. The percentage of cells co-expressing both CB and the human cytoplasm marker was similar at both timepoints. Unpaired *t*-test was used for comparison of means in C. Dashed white line in (**A1**,**A2**) represents the anatomical structure of the hippocampus. Scale bars: 1 mm ((**A1**,**A2**) upper row), 200 μm ((**A1**,**A2**) lower row), and 20 μm (**B**).

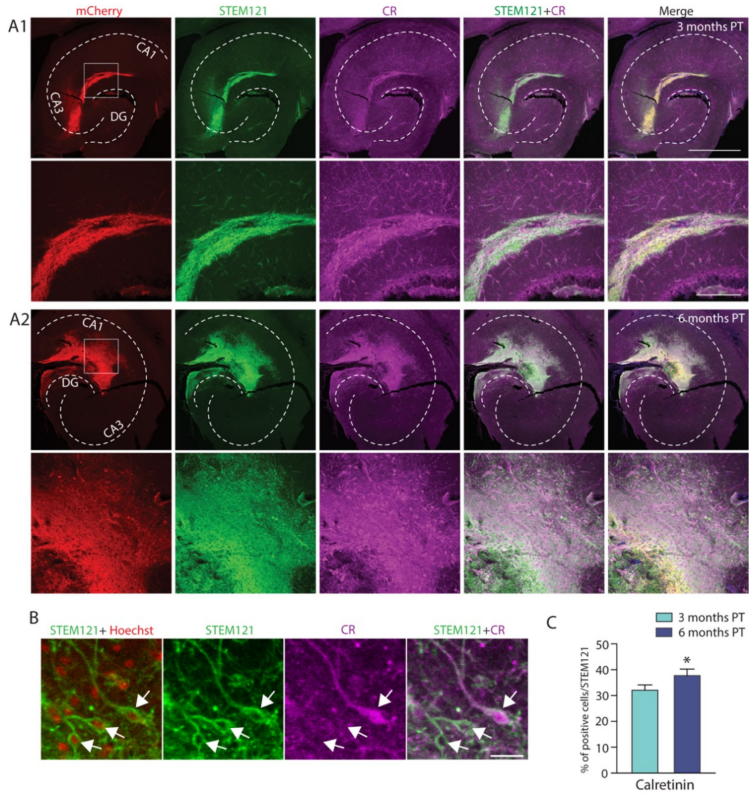

Figure 8. Grafted hdInts express the interneuron subpopulation marker calretinin. (**A**) Grafted hippocampal sections stained for mCherry (marker for ChR2; red), human cytoplasm (STEM121; green), and calretinin (CR; magenta), merged with Hoechst (blue) in the last right column. STEM121+ cells expressing CR were observed at both three months PT (**A1**) and six months PT (**A2**). (**B**) A merged image of STEM121 and Hoechst was used for counting all STEM121+ cells, merged image of STEM121 and CR staining was used for counting STEM121+CR+ double-positive cells. Arrowheads indicate counted cells. (**C**) Quantification of cells stained for STEM121 and CR. Note that the percentage of cells co-expressing both CR and the human cytoplasm marker was significantly higher at six months PT compared to three months PT. *, $p < 0.05$. Unpaired *t*-test was used for comparison of means in (**C**). Dashed white line in (**A1**,**A2**) represents the anatomical structure of the hippocampus. Scale bars: 1 mm ((**A1**,**A2**) upper row), 200 μm ((**A1**,**A2**) lower row) and 20 μm (**B**).

2.5. Optogenetic Activation of Grafted hESC-Derived Interneurons Reduces the Rate of Epileptiform Discharges In Vitro

To investigate whether GABA released from the synaptic terminals of transplanted hdInts may exert any effect on network activity in the hippocampus we took advantage of the ChR2 expression in these cells. A blue light was illuminated on the slices during ongoing pseudo-regular epileptiform discharges induced by high-K^+ or zero-Mg^{2+} artificial cerebrospinal fluid (aCSF). Examples of the raw and filtered epileptiform discharges recorded in the slices and their detection rate are presented in Figure 9A–C. The mean frequency of these discharges was estimated as 0.47 Hz, peak-to-peak amplitude 168 μV, peak power 8.08 μV2, and coastline index 2.78 μV. The light pulse trains at 30 Hz frequency

applied to the slices did not lead to any change in the epileptiform discharges. The 5 s continuous light exposure, however, slightly but statistically significantly reduced the rate of the epileptiform discharges by 0.041 ± 0.012 (−0.026) Hz and increased the peak-to-peak amplitude by 7.3 ± 3.7 (2.1) µV (n = 9 hippocampal slices, p = 0.0039, p = 0.0117, respectively). There was no change in the power and the coastline index (Figure 9D). These data show that GABA release from the transplanted neurons can interfere with ongoing synchronized epileptiform discharges, suggesting that they might have functional effects on seizure activity in vivo as well.

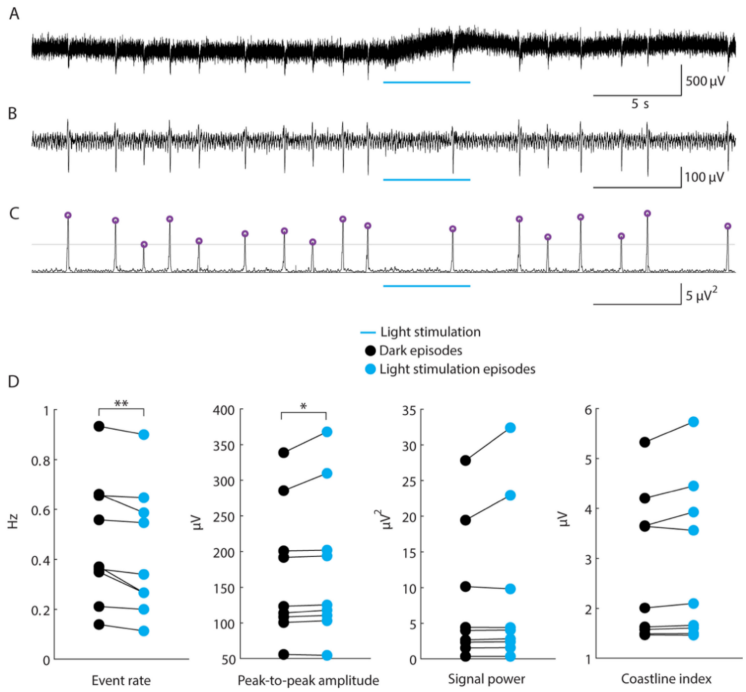

Figure 9. Light-induced activation of grafted hdInts reduces the rate of induced epileptiform discharges. (**A**) Example of a raw local field potential (LFP) recording with epileptiform discharges. (**B**) Filtered LFP trace. (**C**) Power of the filtered signal calculated in 50 ms windows shifted sample by sample. Grey horizontal line marks the detection threshold while purple circles mark the detections. (**D**) Parameters of the epileptiform discharges during dark periods and during light stimulations. *, $p < 0.05$; **, $p < 0.01$. The Wilcoxon signed-rank test was used for comparisons in (**D**).

2.6. Grafting of hESC-Derived Interneuron Precursors Reduces Seizure Frequency in Epileptic Rats

To investigate whether these cells also inhibit SRSs in vivo, we analysed behavioural motor SRSs at four months post SE based on continuous seven-day video recordings of non-grafted and grafted rats (n = 8 rats/group, Figure 10A). Seizure frequency, total time spent in seizure, average seizure duration, and severity were evaluated (Figure 10B). Grafted animals showed a statistically significant decrease in the motor SRS frequency compared to the non-grafted group (median decrease 87%, p = 0.0200, Figure 10B, left panel). Furthermore, the grafted animals exhibited significantly shorter total time spent in motor seizures (10.53 ± 3.84 min) compared to controls (32.48 ± 7.47 min, p = 0.0123,

Figure 10B, right panel). In contrast, neither average motor SRS duration (non-grafted: 22.83 ± 2.57 s, grafted: 24.14 ± 1.78 s, $p > 0.9999$) nor their severity (non-grafted: 4.62 ± 0.13 grade, grafted: 4.66 ± 0.09 grade, $p = 0.8252$) differed between the two groups (Figure 10B). It is worth noticing that this seizure-suppressant effect of transplanted hdInts was exerted without optogenetic activation of these cells.

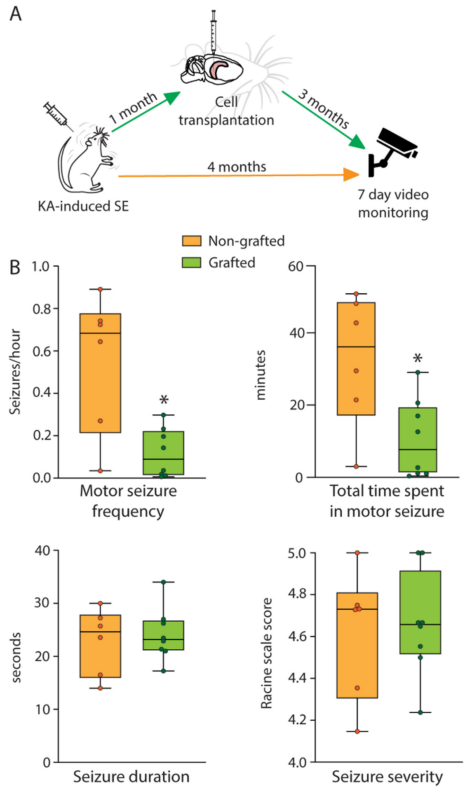

Figure 10. Effect of hdInt grafts on SRSs four months post SE. (**A**) Timeline of the experiments. ((**B**) upper panels) Graphs demonstrating median motor SRS frequency and total time in motor SRSs in control epileptic animals (non-grafted) and epileptic animals grafted with hdInts. ((**B**) lower panels) Graphs demonstrating median motor SRS duration and motor SRS severity in control epileptic animals (non-grafted) and epileptic animals grafted with hdInts. Note that motor SRS frequency and total time spent in motor SRS were significantly lower in the hdInt grafted group. *, $p < 0.05$. A Mann-Whitney test was used for comparison of medians in (**B**).

In summary, these results indicate a seizure-suppressant effect of grafted hESC-derived GABAergic interneurons in rats with KA-induced TLE. This positive outcome is probably the result of the grafted cells integrating into the hippocampal network by forming inhibitory synapses and releasing GABA, which inhibits seizure activity in the epileptic network of the hippocampus.

3. Discussion

In the presented study, we demonstrate that the transplanted hESC-derived GABAergic neurons mature and integrate into the epileptic rat hippocampal network by forming afferent and efferent synaptic connections with the host cells. Furthermore, we show that these cells inhibit epileptiform discharges in hippocampal slices in vitro when activated optogenetically and reduce the frequency of motor seizures in chronically epileptic rats in vivo.

The rationale for transplanting GABAergic neurons, derived from different sources, into the epileptic brain is based on an assumption that seizures arise due to increased excitability of neuronal circuits caused by an imbalance between excitatory and inhibitory synaptic processes. This imbalance is thought to be a consequence of the impairment of GABAergic synaptic transmission as a consequence of interneuron degeneration documented in a number of studies [18–20]. Thus, supplementing GABAergic interneurons by transplantation is supposed to ameliorate the impaired excitability and thereby counteract seizures. Indeed, several animal studies have demonstrated the beneficial effects of grafting foetal GABAergic neuron precursors in the epileptic hippocampus [21–26]. Although proving the principle in experimental conditions, foetal progenitors have limited if any translational value and cannot be applied clinically due to ethical concerns and variability in the quality of cell sources. A more viable source of cells for clinical application is hPSCs and their differentiation into MGE-like cells. Transplantation of these cells has proven to inhibit SRSs and behavioural comorbidities in various TLE models [27,28]. From the clinical perspective, a potential limitation of the approach used in these studies is a relatively slow differentiation rate of the cells taking five or even seven weeks to be ready for grafting. In our study, we transplanted hESC-derived neuronal precursors after only seven days in culture, while overexpressing *Ascl1* and *Dlx2*, two transcription factors necessary for determining their GABAergic fate [30]. Importantly, already at this early time point, the cells expressed neither stem cell nor mitotic markers, thus decreasing the risk of tumour formation (Figure S3). This short and simple protocol gives a significant advantage in terms of sustainability, lower demand on resources, and relatively high reproducibility [29,31].

Our present study demonstrates the maturation of hESC-derived interneurons over time from three months up to six-months after transplantation. All recorded cells were able to generate APs, with the properties maturing over time, reflecting corresponding increases in voltage-dependent sodium and potassium currents. Moreover, spontaneous synaptic activity was increased at the later timepoint PT, indicating improved integration into the neural network, by receiving more afferent synapses. Importantly, we demonstrate that the transplanted cells form efferent inhibitory synapses onto the host neurons providing a possibility of increased GABA release within the hippocampal network. In previous studies, synaptic integration of hPSC-derived interneurons into the epileptic rodent hippocampus was reported at five months PT histologically [28]. Functional maturation and efferent synapse formation of grafted hPSC-derived interneurons were also shown previously [27] although authors did not investigate whether these efferent connections were increasing over time. In yet another recent study authors report electrophysiological and morphological maturation of transplanted hPSC-derived interneurons from 16 to 24 weeks PT, however, without studying functional efferent synapse formation [32]. These cells failed to suppress SRSs in a mouse TLE model [33]. In our study, we report the continuing maturation of the grafted hdInts from three- to six-months PT with an increase in efferent synapse formation over time.

Interestingly, the time range of the delayed graft-derived synaptic responses, measured from the switch-on of the light illumination of the slices, was quite broad (Figure S5). Several factors may contribute to such variation (Figure S6). One possible explanation could be diverse wiring of the connections, ranging from direct synaptic input from a grafted hdInt to the patched cell, to a multisynaptic pattern with a variable number of intermediate neurons activated by the hdInt efferents before the patched cell is finally responding, which would explain the long delay times. The latter scenario is only possible

when assuming altered chloride homeostasis in the epileptic tissue converting GABA from hyperpolarising to a depolarising excitatory neurotransmitter [34,35] or as a consequence of neuronal damage induced during the slice preparation [36]. In addition, the longer delay times can also be a consequence of a delayed light-induced AP onset in the optogenetically stimulated hdInts (Figures S6B and S7), presumably depending on a variable level of ChR2 expression within the hdInt population in different cells.

Apart from the GABAergic phenotype of the grafted cells assessed by electrophysiology and immunohistochemistry, the predominant subtypes of the grafted hdInts were consistent with those expressing CR and CB as was also the case in our in vitro study [29]. Unfortunately, around 30% of the grafted cells remained unidentified, due to the lack of sufficient hippocampal sub-slices remaining after electrophysiological experiments for immunohistochemistry staining. Thus, there is a possibility that other subtypes of interneurons, such as somatostatin-, parvalbumin- or neuropeptide Y-expressing interneurons have been missed in these 30%. Nevertheless, one could argue that the presence of CR and CB interneurons observed in the grafts could be sufficient for a beneficial effect, since it has been shown for example that in the human epileptic hippocampus CB interneurons display an altered morphology, and the number of CR interneurons is significantly reduced [37]. Additionally, in rodent epilepsy models, CR interneurons appear to be vulnerable to excitotoxic damage [38]. In line with these observations, a recent study with reprogrammed glial cells into predominantly CR interneurons using the same transcription factors reported a reduction in chronic SRSs in a mouse model of epilepsy [39].

One obvious question regarding our study is whether video monitoring (without EEG recordings) for one week is sufficient as a reliable outcome measure of the effect of the grating of hdInts on SRSs. As mentioned previously in Section 2.1, when animals were monitored with both EEG and video, on average 97% of the SRSs were generalised, with clear motor components that were similar to those analysed in the experimental cohort with only video monitoring (Figure S2). Moreover, it has been reported in a similar KA-SE rat TLE model that 94% of all seizures detected by combined video-EEG monitoring were stage 5, thus detectable on video [28]. In the same study, grafting of hPSC-derived interneurons resulted in a 72% decrease of motor SRSs over a three-week recording period at the fifth month after SE. Importantly, this seizure-suppressing effect remained stable during the course of these 3 weeks. The authors also reported a significant reduction in total time spent in seizures, while no difference in the average duration of individual seizures was observed [28]. Taken together, these data support our assumption that the observed decrease (87%) in motor SRSs in our study reflects the alterations in almost all seizures that these animals experienced. However, we cannot exclude that transplanted hdInts may have converted motor SRSs into milder, only electrographic non-generalised SRSs. Even if this would be the case, this result on its own could be considered as a major positive outcome of the treatment.

In conclusion, our new data provide proof-of-concept of seizure-suppressant effects of grafted hdInts generated by a simple, fast, and efficient protocol for interneuron differentiation. This protocol proved to provide a reliable and renewable source of hdInts showing positive outcomes on various epileptic phenotype read-outs, including optogenetic inhibition of epileptiform discharges in vitro and SRSs in vivo. Although certain aspects of hdInt transplantation, such as more detailed histological analysis and EEG characterisation, need further investigation, this study can be considered as an important milestone in the development of a cell-based therapy for treating drug-resistant epilepsy.

4. Materials and Methods

4.1. Animals

Immunodeficient nude rat males (RNU rat, Charles River, Wilmington, MA, USA) were housed under a 12/12-h light cycle with ad libitum access to water and food in individually ventilated cages. A total of 25 rats were used.

The experimental procedures performed were approved by the local ethical committee for experimental animals (Ethical permit no. M47-15 and M49-15) and conducted in agreement with the Swedish Animal Welfare Agency regulations and the EU Directive 2010/63/EU for animal experiments.

4.2. Lentiviral Constructs and Virus Generation

The following lentivirus constructs were used: lentivirus vector hSyn-hChR2(H134R)-mCherry-WPRE (obtained by cloning at the lab from Addgene #20945, a gift from Karl Deisseroth [40]) for expressing channelrhodopsin-2 (ChR2) coupled with mCherry; and for the doxycycline-inducible Tet-On system: lentivirus vector FUW-TetO-Ascl1-T2A-puromycin (Addgene #97329) for expressing Ascl1-T2A-puromycin cassette; lentivirus vector FUW-TetO-Dlx2-IRES-hygromycin (Addgene #97330) for expressing Dlx2-IRES-hygromycin cassette; and lentivirus vector FUW-rtTA (Addgene #20342) containing rtTA, all gift from Marius Werning [30]. The lentiviral particles were produced as described elsewhere [41].

4.3. Cell Culture

H1 (WA01) ES cells were obtained from WiCell Research Resources (WiCell, Madison, WI, USA). hESCs were maintained as feeder-free cultures in mTeSR1 medium (Stem Cell Technologies, Vancouver, BC, Canada) and Matrigel-coated plates (Corning, Corning, NY, USA).

4.3.1. Generation of Induced GABAergic Interneuron Precursors from hESCs

H1 ESCs were transduced with Tet-On system lentiviral particles and ChR2-mCherry lentivirus. Cells were then expanded as needed, frozen down, and kept at −150 °C as a stock for starting differentiation.

The induced GABAergic interneurons were generated as described in Gonzalez-Ramos et al., 2021. Briefly, Tet-On-ChR2-H1 ESCs were thawed and expanded as needed. For starting the differentiation protocol, 60–70% of confluent cells were treated with Accutase (Stem Cell Technologies, Vancouver, BC, Canada) and plated as dissociated cells in six well plates (~3–5 × 10^5 cells/well) on day 0. Cells were plated on plates coated with Matrigel (Corning, Corning, NY, USA), in mTeSR1 containing 10 mM Y-27632 (Stem Cell Technologies, Vancouver, BC, Canada). On day 1, the culture medium was replaced with N2 Medium consisting of DMEM/F12 supplemented with 1% N-2 Supplement (both Gibco, Waltham, MA, USA), containing doxycycline (2 g/L, Sigma Aldrich, St. Louis, MO, USA) to induce Tet-On gene expression. The culture was retained in the medium for one week. On day 2, a drug-resistance selection period was started by adding puromycin (0.5 mg/mL, Gibco, Waltham, MA, USA) and hygromycin (750 mg/mL, Invitrogen, Waltham, MA, USA) to the fresh media. On day 4, the medium was replaced containing all antibiotics and on day 5, antibiotics were removed and cytosine β-D-arabinofuranoside (Ara-C, 4 μM, Sigma Aldrich, St. Louis, MO, USA) was added. On day 7, cells were used for in vivo grafting.

4.3.2. Cell Transplantation

Cell transplantation was performed four weeks post SE. Neuronal precursors were dissociated at 7 DIV using Tryple Express Enzyme (Gibco, Waltham, MA, USA), centrifuged, resuspended to a concentration of 100.000 cells/uL in HBSS (Gibco, Waltham, MA, USA) containing 10 mM Y-27632 and DNase I Solution (1 μg/mL, Stem Cell Technologies, Vancouver, BC, Canada) and kept on ice until grafting. Cells were then injected stereotaxically in the hippocampus of epileptic RNU rats under isoflurane anaesthesia. Cells were injected bilaterally in both hippocampi with the following coordinates from bregma: anterior-posterior (AP) −6.2 mm, medial-lateral (ML) ±5.2 mm, dorsal-ventral (DV) −6.0, −4.8 and −3.6 mm, 3 μL in total per hippocampus (1 μL at each DV coordinate). Animals were given doxycycline in drinking water (1 mg/mL, 0.5% sucrose) for two days before and four weeks PT to continue the cell differentiation in vivo. Cells remaining after grafting

were re-plated on Matrigel-coated coverslips in 24-well plates and cultured in N2 medium overnight, until being fixed with 4% paraformaldehyde containing 0.25% glutaraldehyde and used for immunocytochemistry.

4.4. Induction of Status Epilepticus

Male immunodeficient RNU rats (7–8-week-old) were injected subcutaneously in the neck region with an initial dose of 10 mg/kg of KA and subsequently with 5 mg/kg every hour until the first stage 3 or higher seizure grade was observed (scheme of the process is illustrated in Figure S1). Seizures were classified according to the modified Racine scale registering only stages 3 and higher: (3) unilateral forelimb clonus; (4) generalized seizure with rearing, body jerks, bilateral forelimb clonus; (5) generalized seizure with rearing, imbalance, falling, or wild running [42] (Video S1). SE was defined as at least four seizures per hour. After SE, the animals were injected with a Ringer/glucose (25 mg/mL) solution (1:1 ratio) and returned to housing cages. Animals were weighed every day for a week after SE induction and subsequently once per week. Cell transplantation was performed four weeks after SE induction.

4.5. Video Recordings and Video-EEG Recordings

To assess the frequency of motor SRSs, animals were video monitored continuously for four months after SE induction. During the dark (night) hours, infrared lamps were used to illuminate the cages. Videos were manually analysed retrospectively and animals not showing SRSs were excluded from the study. Only motor SRSs were detected, noting the time of seizure occurrence, duration of the seizure, and seizure severity (Video S2). Duration of seizures and seizure severity was averaged for each animal, seizure frequency was calculated as a number of seizures per hour for each animal and these values were then used for statistical analyses.

Furthermore, three non-grafted animals underwent implantation of electrodes and transmitters for wireless video-EEG monitoring five months after SE induction. This was done to determine if this rat strain tolerates the procedure and the implants and for further characterisation of their seizures. The whole procedure was performed as described previously [43]. Firstly, the rats were anesthetized with 4% isoflurane and placed in the stereotaxic frame while kept on 2% isofluorane. The transmitter (F40-EET, Data Sciences International, St. Paul, MN, USA) was placed in a subcutaneous pocket on the rats' backs. One stainless steel electrode (Plastics One, Roanoke, VA, USA), soldered to the wire of the transmitter, was implanted at the following coordinates: AP −6.2 mm, ML +5.2 mm, DV −6.0 mm. The second electrode was placed on top of dura mater above the motor cortex ipsilateral to the depth electrode. Two reference electrodes were placed on the dura mater, 2 mm rostral to the lambda. Two stainless screws were attached to the skull bone to secure the electrode assembly by dental cement. Animals were weighed every day for a week after implantation and consequently once per week henceforth. To begin the video-EEG monitoring, the wireless transmitter was activated by a magnet and the cage was placed on top of a receiver unit (Data Sciences International, St. Paul, MN, USA). Two cameras (Axis, Lund, Sweden) were used to continuously record video of the animal activity for 30 h, and seizures were then detected off-line in NeuroScore (Data Sciences International, St. Paul, MN, USA).

4.6. Electrophysiology

4.6.1. Whole-Cell Patch-Clamp Recordings in Hippocampal Slices

RNU rats at three- or six-months PT were briefly anesthetized with isoflurane and decapitated. Brains were transferred to an ice-cold modified artificial cerebrospinal fluid (aCSF) solution containing in mM: 75 sucrose, 67 NaCl, 26 $NaHCO_3$, 25 D-glucose, 2.5 KCl, 1.25 NaH_2PO_4, 0.5 $CaCl_2$, 7 $MgCl_2$ (all from Sigma Aldrich, St. Louis, MO, USA), equilibrated with carbogen (95% O_2/5% CO_2), with pH 7.4 and osmolarity ~300 mOsm. The brains were cut on a vibratome (VT1200S, Leica Microsystems, Wetzlar, Germany) into

300 µm thick quasi-horizontal hippocampal slices, which were transferred to aCSF containing in mM: 118 NaCl, 2 $MgCl_2$, 2 $CaCl_2$, 2.5 KCl, 26 $NaHCO_3$, 1.25 NaH_2PO_4, 10 D-glucose. Slices were incubated in this solution for 30 min at 34 °C, and subsequently at room temperature until recordings were performed. The individual cells in the slices were visualized for whole-cell patch-clamp recordings using infrared differential interference contrast video microscopy (BX51WI; Olympus, Shinjuku, Tokyo, Japan). Recordings were performed from grafted (identified under fluorescence with 520 nm light for mCherry+) and host cells (mCherry−) at 32 °C using a glass pipette filled with a solution containing (in mM): 140 KCl, 10 NaCl, 10 HEPES, 0.2 EGTA, 4 MgATP, and 0.4 Na_3GTP (~300 mOsm, pH 7.2; all from Sigma Aldrich, St. Louis, MO, USA). This solution inverts the polarity of chloride currents inward while increasing their amplitude, making them easier to detect. Average pipette resistance was between 2 and 4 MΩ, pipette capacitance was compensated for during cell-attached configuration. Biocytin (0.5–1 mg/mL, Biotium, Fremont, CA, USA) was included in the pipette solution to retrospectively identify recorded cells. All recordings were done using a HEKA EPC10 amplifier (HEKA Elektronik, Lambrecht, Germany) and sampled at 10 kHz with a 3 kHz Bessel anti-aliasing filter and using PatchMaster software for data acquisition.

4.6.2. Passive Membrane Properties of Transplanted Cells

Estimated resting membrane potential (RMP), series resistance (Rs), input resistance (Ri), and cell membrane capacitance (Cm) were calculated from a series of 5 mV pulses of 100 ms duration, applied through the patch pipette immediately after whole-cell configuration was established. The membrane capacitance was calculated from the charge integration of the transient response to the test pulse. To determine the ability to fire action potentials (APs), 500 ms current steps ranging from −40 pA to 200 pA in 10 pA steps were applied while holding the cell membrane potential at approximately −70 mV. From the same holding potential, 1-s linear ramp currents were injected into the cells to determine the AP threshold. AP amplitude was measured from threshold to peak, and duration was measured as the width at the threshold. The amplitude of the afterhyperpolarization (AHP) was measured as the difference between the AHP peak and the AP threshold. Sodium and potassium currents were evoked by a series of 100 ms long voltage steps ranging from −90 mV to +40 mV in 10 mV steps. In addition, their sensitivity to 1 µM tetrodotoxin (TTX, Abcam, Cambridge, UK) and 10 mM tetraethylammonium (TEA, Abcam, Cambridge, UK) was assessed.

4.6.3. Optogenetics

For optogenetic depolarization of ChR2-expressing cells, blue light was applied at 460 nm wavelength with a LED light source (Prizmatix, Holon, Israel) and delivered through a water immersion 40× microscope objective. Blue light was delivered for a duration of 500 milliseconds, or by 5 pulses of 3 milliseconds repeated at 10 Hz. For detection of graft-to-host synaptic connections, the same stimulation was used during recoding from a "host" cell in the vicinity of a ChR2-expressing cell.

4.6.4. Spontaneous Synaptic Activity

Spontaneous postsynaptic currents (sPSCs) were recorded at −70 mV. Whole-cell patch-clamp recordings of sPSCs were analysed offline with Igor Pro (Wavemetrics, Portland, OR, USA) and Python. sPSCs were detected automatically and analysed using a custom Python script [44]. A postsynaptic current template was generated from the voltage-clamp recordings which were low-pass filtered at 400 Hz and was used for the detection algorithm. Events with a correlation coefficient to the template lower than 0.6 were excluded from the analysis, as well as those with amplitude <3 pA and rise-time >5 ms. For distribution comparisons, an equal number of events was analysed from all recorded neurons, while for median comparisons all events were considered.

4.6.5. Drugs and Concentrations

For the blocking of GABAA and GABAC receptors, picrotoxin (PTX, 100 μM, Tocris, Bristol, UK) was used, although it might act on glycine and 5-HT_3 receptors [45,46]. However, the used concentration of PTX is considered to be insufficient to block the signalling through serotonin receptors [47]. (2R)-amino-5-phosphonovaleric acid (D-AP5, 50 μM, Abcam, Cambridge, UK) and 2,3-dihydroxy-6-nitro-7-sulfamoyl-benzo-quinoxaline-2,3-dione disodium salt (NBQX, 10 μM, Alomone Labs, Jerusalem, Israel) were used to block NMDA and AMPA receptors, respectively. TTX (1 μM, Abcam, Cambridge, UK) and TEA (10 mM, Abcam, Cambridge, UK) were used to block sodium and potassium channels, respectively.

4.6.6. Epileptiform Activity and Local Field Potential Recordings

To test the effect of grafted hdInts on epileptiform activity in vitro, we used local field potential (LFP) recordings in hippocampal slices from six-month PT rats. The slices were perfused by either high-K^+ aCSF or zero-Mg^{2+} aCSF. The high-K^+ aCSF contained in mM: 118 NaCl, 2 $MgCl_2$, 2 $CaCl_2$, 26 $NaHCO_3$, 1.25 NaH_2PO_4, 10 D-glucose and 7.5 to 9.5 KCl. The zero- Mg^{2+} was the same but contained 2.5 KCl and no $MgCl_2$. LFPs were recorded by a pipette of 1–3 MΩ resistance filled by the same aCSF. The pipette was placed in the vicinity of the graft and where the epileptiform discharges were most prominent. The LFPs were amplified and sampled at 10 kHz. To assess whether hdInts could suppress the epileptiform discharges, we activated them by blue light stimulation. We tested 3 stimulation protocols separated by 2 min of baseline (no light): (1) Five-second continuous light pulse separated by 35 s of a dark period, repeated 30 times. (2) Five-second pulse train at 30 Hz and 3 ms pulse width separated by 35 s of a dark period, repeated 30 times. (3) Three-minute pulse train at 30 Hz and 3 ms pulse width.

The epileptiform discharges were detected and analysed offline using a custom-made script in Matlab. Briefly, the signal was filtered between 2 and 400 Hz, comb-filtered to remove power line noise, and down-sampled to 1 kHz. Then, the signal power was computed in a 50 ms window, sliding sample-by-sample. The threshold for detection was determined as $4 \times median \times \sqrt{kurtosis}$ of the power and detections were marked at the maxima of the regions exceeding the threshold.

We analysed the frequency of occurrence of the events and, using the filtered signal, we computed 3 parameters for each event: peak-to-peak amplitude, peak signal power, and coastline index according to the formula: $\text{Coastline} = \frac{1}{N}\sum_{n=1}^{N-1}|y(n+1) - y(n)|$, where y is the filtered signal, N is the number of samples and n is the index of the sample. For the statistical analysis, the mean of these parameters was computed for the dark period and light stimulation period in each of the 30 runs of the given protocol in the given slice. Then, the runs were averaged and the resulting two numbers per slice (dark and light) were subtracted. The differences were then evaluated by Wilcoxon signed-rank test.

4.7. Immunohistochemistry, Immunocytochemistry, Imaging, and Quantification

For immunohistochemistry, 300 μm slices used for electrophysiological experiments were collected from aCSF and immediately fixed in 4% paraformaldehyde containing 0.25% glutaraldehyde. After overnight fixation at 4 °C, slices were transferred to 20% sucrose in 0.1 M sodium phosphate-buffered saline and kept at 4 °C for at least two days until further processing. The slices were either immediately stained or cut on a microtome into 30 μm thick sections and stored in a glycerol-based antifreeze solution at −20 °C until stained. For staining, sections were washed thoroughly with PBS, then blocked in 5% serum of the species specific to the secondary antibody, in PBS containing 0.25% Triton-X and incubated with primary antibodies overnight (or for 48 h for 300 μm slices) in the same solution at 4 °C. Following primary antibody incubation, sections were washed with PBS and blocked again with the same serum solution as above. Then, sections were incubated with secondary antibodies for 2 h (or 24 h for 300 μm slices) either fluorophore-conjugated to allow for fluorescent detection (AlexaFluor Plus 488/555/647, 1:1000, Thermo Fisher Scientific, Waltham, MA, USA), or biotinylated for streptavidin amplification (1:200, Vector

Laboratories, Burlingame, CA, USA). In some cases, for signal amplification and for visualisation of patched biocytin-filled cells, streptavidin-conjugated fluorophores were used (1:2000, Jackson Immunoresearch, West Grove, PA, USA). Immunofluorescent sections were coverslipped with PVA-DABCO containing 1:1000 Hoechst. For detailed information of antibodies and dilutions used, see Table S2. Images were acquired either by confocal microscopy (Nikon Confocal A1RHD microscope, Nikon, Minato, Tokyo, Japan) or by epifluorescence microscopy (Olympus BX61, Olympus, Shinjuku, Tokyo, Japan). For immunocytochemistry, the same staining process was used, omitting the second-day blocking step.

For all quantifications ImageJ software (NIH, Annapolis, MD, USA) was used. For quantification of GABA immunostaining, mean fluorescence intensity was measured in confocal Z-stack images taken at 20× magnification using maximal intensity projection from 13 stacks (1 µm distance). In each slice, the area of the graft was outlined based on the STEM121 immunostaining, and the median grey value was measured in the GABA-staining channel. Together with the graft area, an area outside of the graft was outlined and fluorescence intensity was measured. The two values in each slice were then compared. For quantification of CR and CB stainings, similar Z-stack images were composed. Firstly, all cells positive for the human cytoplasm marker (STEM121+ cells) were counted, and Hoechst was used to visualise the nuclei and identify individual cells. Secondly, cells double positive for STEM121 and CB or CR, respectively, were counted. A percentage of double-positive cells out of all STEM121+ cells was calculated for each slice and used for statistical analyses.

4.8. Statistical Analyses

Statistical analysis of the data was performed using Prism 9 software (GraphPad, San Diego, CA, USA). A Mann-Whitney test was used for comparison of medians, an unpaired *t*-test was used for comparison of means when data were normally distributed, the Wilcoxon test was used for paired data, and the binomial test was used for comparison of proportions. Spearman correlation was used for exploring the relationship of two variables. The level of significance for these tests was set at $p < 0.05$. The Kolmogorov-Smirnov test was used for distribution comparisons and the level of significance was set to $p < 0.01$ and $D > 0.1$. In box plots, the centre line represents the median, the box edges represent interquartile range, and whiskers the complete range of the values. The individual values are plotted as dots. In the rest of the graphs, the mean ± SEM is shown, which is also used to represent values in the main text.

Supplementary Materials: The following are available online at https://www.mdpi.com/article/10.3390/ijms222413243/s1.

Author Contributions: Conceptualization, E.W., M.L., M.A. and M.K.; methodology, E.W.; software, A.M., J.K.; validation, E.W.; formal analysis, E.W., J.K.; investigation, E.W., A.G.-R., J.K.; resources, M.K.; data curation, E.W.; writing—original draft preparation, E.W.; writing—review and editing, A.G.-R., A.M., J.K., M.L., M.A., M.K.; visualization, E.W.; supervision, M.L., M.A., M.K.; project administration, E.W.; funding acquisition, M.K. All authors have read and agreed to the published version of the manuscript.

Funding: This project was funded by the European Union Horizon 2020 Program (H2020-MSCA-ITN-2016) under the Marie Skłodowska-Curie Innovative Training Network, project Training4CRM, Grant Agreement No. 722779. This project was also funded by the Swedish Research Council (Grant Numbers: 2017-00921 and 2016–02605), the Swedish Brain Foundation (Grant Number: F02021-0369) and the grant of the Ministry of Health of the Czech Republic AZV NU 21-08-00533.

Institutional Review Board Statement: The experimental procedures performed were approved by the local ethical committee for experimental animals (Ethical permit no. M47-15 and M49-15) and conducted in agreement with the Swedish Animal Welfare Agency regulations and the EU Directive 2010/63/EU for animal experiments.

Informed Consent Statement: Not applicable.

Data Availability Statement: Data used for this study is available on request from the corresponding authors.

Acknowledgments: The authors would like thank Ling Cao for all the help with processing tissue and performing immunofluorescent stainings, Susanne Geres and Nora Pernaa for help with animal work, the Lund University Bioimaging Centre for access to the confocal microscope and Adam Mårs and Karim Ismael for help with video-recording analysis.

Conflicts of Interest: The authors declare no conflict of interest. The funders had no role in the design of the study; in the collection, analyses, or interpretation of data; in the writing of the manuscript, or in the decision to publish the results.

References

1. Beghi, E.; Giussani, G.; Abd-Allah, F.; Abdela, J.; Abdelalim, A.; Abraha, H.N.; Adib, M.G.; Agrawal, S.; Alahdab, F.; Awasthi, A.; et al. Global, regional, and national burden of epilepsy, 1990–2016: A systematic analysis for the Global Burden of Disease Study 2016. *Lancet Neurol.* **2019**, *18*, 357–375. [CrossRef]
2. Toda, Y.; Kobayashi, K.; Hayashi, Y.; Inoue, T.; Oka, M.; Ohtsuka, Y. Effects of intravenous diazepam on high-frequency oscillations in EEGs with CSWS. *Brain Dev.* **2013**, *35*, 540–547. [CrossRef] [PubMed]
3. Peng, B.-W.; Justice, J.A.; Zhang, K.; Li, J.; He, X.; Sanchez, R.M. Gabapentin promotes inhibition by enhancing hyperpolarization-activated cation currents and spontaneous firing in hippocampal CA1 interneurons. *Neurosci. Lett.* **2011**, *494*, 19–23. [CrossRef] [PubMed]
4. Braga, M.F.M.; Aroniadou-Anderjaska, V.; Li, H.; Rogawski, M.A. Topiramate reduces excitability in the basolateral amygdala by selectively inhibiting GluK1 (GluR5) kainate receptors on interneurons and positively modulating GABAA receptors on principal neurons. *J. Pharmacol. Exp. Ther.* **2009**, *330*, 558–566. [CrossRef]
5. Ylinen, A.; Valjakka, A.; Lahtinen, H.; Miettinen, R.; Freund, T.F.; Riekkinen, P. Vigabatrin pre-treatment prevents hilar somatostatin cell loss and the development of interictal spiking activity following sustained simulation of the perforant path. *Neuropeptides* **1991**, *19*, 205–211. [CrossRef]
6. O'Brien, T.J.; Ben-Menachem, E.; Bertram, E.H.; Collins, S.D.; Kokaia, M.; Lerche, H.; Klitgaard, H.; Staley, K.J.; Vaudano, E.; Walker, M.C.; et al. Proposal for a "phase II" multicenter trial model for preclinical new antiepilepsy therapy development. *Epilepsia* **2013**, *54*, 70–74. [CrossRef]
7. Chen, B.; Choi, H.; Hirsch, L.J.; Katz, A.; Legge, A.; Buchsbaum, R.; Detyniecki, K. Psychiatric and behavioral side effects of antiepileptic drugs in adults with epilepsy. *Epilepsy Behav.* **2017**, *76*, 24–31. [CrossRef]
8. Strine, T.W.; Kobau, R.; Chapman, D.P.; Thurman, D.J.; Price, P.; Balluz, L.S. Psychological Distress, Comorbidities, and Health Behaviors among U.S. Adults with Seizures: Results from the 2002 National Health Interview Survey. *Epilepsia* **2005**, *46*, 1133–1139. [CrossRef]
9. Cramer, J.A.; Steinborn, B.; Striano, P.; Hlinkova, L.; Bergmann, A.; Bacos, I.; Baukens, C.; Buyle, S. Non-interventional surveillance study of adverse events in patients with epilepsy. *Acta Neurol. Scand.* **2011**, *124*, 13–21. [CrossRef]
10. Duncan, J.S.; Sander, J.W.; Sisodiya, S.M.; Walker, M.C. Adult epilepsy. *Lancet* **2006**, *367*, 1087–1100. [CrossRef]
11. Engel, J. Epilepsy in the world today: The medical point of view. *Epilepsia* **2002**, *43*, 12–13. [CrossRef]
12. Marcangelo, M.J.; Ovsiew, F. Psychiatric Aspects of Epilepsy. *Psychiatr. Clin. N. Am.* **2007**, *30*, 781–802. [CrossRef]
13. Engel, J.; McDermott, M.P.; Wiebe, S.; Langfitt, J.T.; Stern, J.M.; Dewar, S.; Sperling, M.R.; Gardiner, I.; Erba, G.; Fried, I.; et al. Early surgical therapy for drug-resistant temporal lobe epilepsy: A randomized trial. *JAMA J. Am. Med. Assoc.* **2012**, *307*, 922–930. [CrossRef]
14. Yilmazer-Hanke, D.M.; Wolf, H.K.; Schramm, J.; Elger, C.E.; Wiestler, O.D.; Blümcke, I. Subregional Pathology of the Amygdala Complex and Entorhinal Region in Surgical Specimens from Patients with Pharmacoresistant Temporal Lobe Epilepsy. *J. Neuropathol. Exp. Neurol.* **2000**, *59*, 907–920. [CrossRef]
15. Ziburkus, J.; Cressman, J.R.; Barreto, E.; Schiff, S.J. Interneuron and pyramidal cell interplay during in vitro seizure-like events. *J. Neurophysiol.* **2006**, *95*, 3948–3954. [CrossRef]
16. Bausch, S.B. Axonal sprouting of GABAergic interneurons in temporal lobe epilepsy. *Epilepsy Behav.* **2005**, *7*, 390–400. [CrossRef]
17. Freund, T.F.; Buzsáki, G. Interneurons of the hippocampus. *Hippocampus* **1998**, *6*, 347–470. [CrossRef]
18. Liu, Y.Q.; Yu, F.; Liu, W.H.; He, X.H.; Peng, B.W. Dysfunction of hippocampal interneurons in epilepsy. *Neurosci. Bull.* **2014**, *30*, 985–998. [CrossRef]
19. Zhang, W.; Yamawaki, R.; Wen, X.; Uhl, J.; Diaz, J.; Prince, D.A.; Buckmaster, P.S. Surviving hilar somatostatin interneurons enlarge, sprout axons, and form new synapses with granule cells in a mouse model of temporal lobe epilepsy. *J. Neurosci.* **2009**, *29*, 14247–14256. [CrossRef]
20. Sun, C.; Mtchedlishvili, Z.; Bertram, E.H.; Erisir, A.; Kapur, J. Selective loss of dentate hilar interneurons contributes to reduced synaptic inhibition of granule cells in an electrical stimulation-based animal model of temporal lobe epilepsy. *J. Comp. Neurol.* **2007**, *500*, 876–893. [CrossRef]
21. Hunt, R.F.; Girskis, K.M.; Rubenstein, J.L.; Alvarez-Buylla, A.; Baraban, S.C. GABA progenitors grafted into the adult epileptic brain control seizures and abnormal behavior. *Nat. Neurosci.* **2013**, *16*, 692–697. [CrossRef]

22. Waldau, B.; Hattiangady, B.; Kuruba, R.; Shetty, A.K. Medial ganglionic eminence-derived neural stem cell grafts ease spontaneous seizures and restore GDNF expression in a rat model of chronic temporal lobe epilepsy. *Stem Cells* **2010**, *28*, 1153–1164. [CrossRef]
23. Casalia, M.L.; Howard, M.A.; Baraban, S.C. Persistent seizure control in epileptic mice transplanted with gamma-aminobutyric acid progenitors. *Ann. Neurol.* **2017**, *82*, 530–542. [CrossRef]
24. Henderson, K.W.; Gupta, J.; Tagliatela, S.; Litvina, E.; Zheng, X.; Van Zandt, M.A.; Woods, N.; Grund, E.; Lin, D.; Royston, S.; et al. Long-Term Seizure Suppression and Optogenetic Analyses of Synaptic Connectivity in Epileptic Mice with Hippocampal Grafts of GABAergic Interneurons. *J. Neurosci.* **2014**, *34*, 13492–13504. [CrossRef]
25. Baraban, S.C.; Southwell, D.G.; Estrada, R.C.; Jones, D.L.; Sebe, J.Y.; Alfaro-Cervello, C.; Garcia-Verdugo, J.M.; Rubenstein, J.L.R.; Alvarez-Buylla, A. Reduction of seizures by transplantation of cortical GABAergic interneuron precursors into Kv1.1 mutant mice. *Proc. Natl. Acad. Sci. USA* **2009**, *106*, 15472–15477. [CrossRef]
26. Hattiangady, B.; Rao, M.S.; Shetty, A.K. Grafting of striatal precursor cells into hippocampus shortly after status epilepticus restrains chronic temporal lobe epilepsy. *Exp. Neurol.* **2008**, *212*, 468–481. [CrossRef]
27. Cunningham, M.; Cho, J.-H.; Leung, A.; Savvidis, G.; Ahn, S.; Moon, M.; Lee, P.K.J.; Han, J.J.; Azimi, N.; Kim, K.-S.; et al. hPSC-derived maturing GABAergic interneurons ameliorate seizures and abnormal behavior in epileptic mice. *Cell Stem Cell* **2014**, *15*, 559–573. [CrossRef]
28. Upadhya, D.; Hattiangady, B.; Castro, O.W.; Shuai, B.; Kodali, M.; Attaluri, S.; Bates, A.; Dong, Y.; Zhang, S.C.; Prockop, D.J.; et al. Human induced pluripotent stem cell-derived MGE cell grafting after status epilepticus attenuates chronic epilepsy and comorbidities via synaptic integration. *Proc. Natl. Acad. Sci. USA* **2019**, *116*, 287–296. [CrossRef]
29. Gonzalez-Ramos, A.; Waloschková, E.; Mikroulis, A.; Kokaia, Z.; Bengzon, J.; Ledri, M.; Andersson, M.; Kokaia, M. Human stem cell-derived GABAergic neurons functionally integrate into human neuronal networks. *Sci. Rep.* **2021**, *11*, 1–16. [CrossRef]
30. Yang, N.; Chanda, S.; Marro, S.; Ng, Y.H.; Janas, J.A.; Haag, D.; Ang, C.E.; Tang, Y.; Flores, Q.; Mall, M.; et al. Generation of pure GABAergic neurons by transcription factor programming. *Nat. Methods* **2017**, *14*, 621–628. [CrossRef]
31. Allison, T.; Langerman, J.; Sabri, S.; Otero-Garcia, M.; Lund, A.; Huang, J.; Wei, X.; Samarasinghe, R.A.; Polioudakis, D.; Mody, I.; et al. Defining the nature of human pluripotent stem cell-derived interneurons via single-cell analysis. *Stem Cell Rep.* **2021**, *16*, 2548–2564. [CrossRef]
32. Shrestha, S.; Anderson, N.C.; Grabel, L.B.; Naegele, J.R.; Aaron, G.B. Development of electrophysiological and morphological properties of human embryonic stem cell-derived GABAergic interneurons at different times after transplantation into the mouse hippocampus. *PLoS ONE* **2020**, *15*, e0237426. [CrossRef]
33. Anderson, N.C.; Van Zandt, M.A.; Shrestha, S.; Lawrence, D.B.; Gupta, J.; Chen, C.Y.; Harrsch, F.A.; Boyi, T.; Dundes, C.E.; Aaron, G.; et al. Pluripotent stem cell-derived interneuron progenitors mature and restore memory deficits but do not suppress seizures in the epileptic mouse brain. *Stem Cell Res.* **2018**, *33*, 83–94. [CrossRef] [PubMed]
34. Palma, E.; Amici, M.; Sobrero, F.; Spinelli, G.; Di Angelantonio, S.; Ragozzino, D.; Mascia, A.; Scoppetta, C.; Esposito, V.; Miledi, R.; et al. Anomalous levels of Cl- transporters in the hippocampal subiculum from temporal lobe epilepsy patients make GABA excitatory. *Proc. Natl. Acad. Sci. USA* **2006**, *103*, 8465–8468. [CrossRef]
35. Huberfeld, G.; Wittner, L.; Clemenceau, S.; Baulac, M.; Kaila, K.; Miles, R.; Rivera, C. Perturbed chloride homeostasis and GABAergic signaling in human temporal lobe epilepsy. *J. Neurosci.* **2007**, *27*, 9866–9873. [CrossRef] [PubMed]
36. Bregestovski, P.; Bernard, C. Excitatory GABA: How a correct observation may turn out to be an experimental artifact. *Front. Pharmacol.* **2012**, *3*, 65. [CrossRef] [PubMed]
37. Maglóczky, Z.S.; Wittner, L.; Borhegyi, Z.S.; Halász, P.; Vajda, J.; Czirják, S.; Freund, T.F. Changes in the distribution and connectivity of interneurons in the epileptic human dentate gyrus. *Neuroscience* **2000**, *96*, 7–25. [CrossRef]
38. Tóth, K.; Maglóczky, Z. The vulnerability of calretinin-containing hippocampal interneurons to temporal lobe epilepsy. *Front. Neuroanat.* **2014**, *8*, 100. [CrossRef]
39. Lentini, C.; D'Orange, M.; Marichal, N.; Trottmann, M.-M.; Vignoles, R.; Foucault, L.; Verrier, C.; Massera, C.; Raineteau, O.; Conzelmann, K.-K.; et al. Reprogramming reactive glia into interneurons reduces chronic seizure activity in a mouse model of mesial temporal lobe epilepsy. *Cell Stem Cell* **2021**, *28*, 2104–2121.e10. [CrossRef]
40. Zhang, F.; Wang, L.P.; Brauner, M.; Liewald, J.F.; Kay, K.; Watzke, N.; Wood, P.G.; Bamberg, E.; Nagel, G.; Gottschalk, A.; et al. Multimodal fast optical interrogation of neural circuitry. *Nature* **2007**, *446*, 633–639. [CrossRef]
41. Lockowandt, M.; Günther, D.M.; Quintino, L.; Breger, L.S.; Isaksson, C.; Lundberg, C. Optimization of production and transgene expression of a retrogradely transported pseudotyped lentiviral vector. *J. Neurosci. Methods* **2020**, *336*, 108542. [CrossRef]
42. Racine, R.J. Modification of seizure activity by electrical stimulation: II. Motor seizure. *Electroencephalogr. Clin. Neurophysiol.* **1972**, *32*, 281–294. [CrossRef]
43. Nikitidou Ledri, L.; Melin, E.; Christiansen, S.H.; Gøtzsche, C.R.; Cifra, A.; Woldbye, D.P.D.; Kokaia, M. Translational approach for gene therapy in epilepsy: Model system and unilateral overexpression of neuropeptide Y and Y2 receptors. *Neurobiol. Dis.* **2016**, *86*, 52–61. [CrossRef]
44. GitHub—AMikroulis/xPSC-Detection: Template Correlation-Based Detection of Postsynaptic Currents. Available online: https://github.com/AMikroulis/xPSC-detection (accessed on 22 November 2021).
45. Pistis, M.; Belelli, D.; Peters, J.A.; Lambert, J.J. The interaction of general anaesthetics with recombinant GABA(A) and glycine receptors expressed in Xenopus laevis oocytes: A comparative study. *Br. J. Pharmacol.* **1997**, *122*, 1707–1719. [CrossRef]

46. Das, P.; Bell-Horner, C.L.; Machu, T.K.; Dillon, G.H. The GABAA receptor antagonist picrotoxin inhibits 5-hydroxytryptamine type 3A receptors. *Neuropharmacology* **2003**, *44*, 431–438. [CrossRef]
47. Das, P.; Dillon, G.H. Molecular determinants of picrotoxin inhibition of 5-hydroxytryptamine type 3 receptors. *J. Pharmacol. Exp. Ther.* **2005**, *314*, 320–328. [CrossRef]

Transplanted human stem cell-derived GABAergic interneurons establish efferent synapses with host neurons in rat epileptic hippocampus and inhibit spontaneous recurrent seizures

Supplementary materials

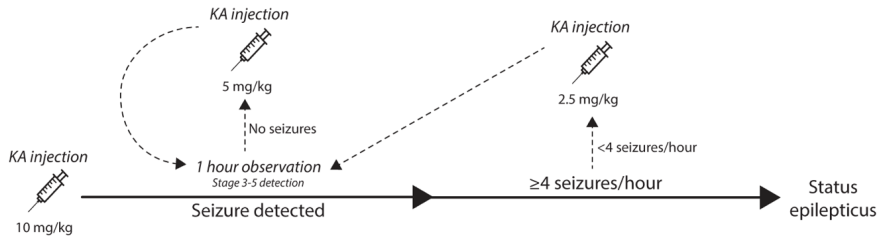

Figure S1. Schematic illustration of SE induction by KA. Rats were first injected with 10 mg/kg of KA, followed by a 1-hour observational period. If a stage 3 or higher seizure grade was detected, the rats were observed for another hour to determine the seizure frequency. If at least 4 seizures/hour were observed, rats were considered as having SE. If after the first KA injection, the rats did not develop seizures within an hour, a 5 mg/kg KA injection was added with the follow-up observation time as before. If during the assessment of seizure frequency less than 4 seizures/hour were observed, a 2.5 mg/kg dose of KA was added, followed by the same observation time until reaching the desired number of at least 4 generalised seizures per hour.

Video S1. Example of seizures detected during SE induction. Rat on the left displays a stage 5 seizure with rearing, loosing balance and falling. Rat on the left displays a stage 4 seizure with rearing, body jerks and bilateral forelimb clonus.

Video S2. Example of seizures detected during video-recordings 4 months post SE. (**A**) Rat #7 (lower right) displays a stage 5 seizure with rearing, loosing balance and falling. (**B**) Rat #6 (lower left) displays a stage 5 seizure with rearing, loosing balance and falling. (**C**) Rat #6 (lower left) displays a stage 4 seizure with rearing, body jerks and bilateral forelimb clonus.

Table S1. Summary of primary antibodies and dilutions used.

ANTIBODY	HOST	COMPANY	CAT. NO.	DILUTION
mCherry	Chicken	Abcam	Ab205402	1:2000
GABA	Rabbit	Sigma Aldrich	A2052	1:2000
Calbindin	Rabbit	Swant	CB-38a	1:1000
Calretinin	Rabbit	Swant	CR-7697	1:1000
STEM121*	Mouse	Takara Bio	Y40410	1:400

Sox2	Rabbit	Abcam	Ab97959	1:1000
Ki67	Rabbit	Novocastra	NCL-Ki67p	1:250
Nestin	Mouse	Abcam	Ab6142	1:500
β-III-tubulin	Rabbit	Abcam	Ab18207	1:1000

*Streptavidin amplification was used for immunofluorescence

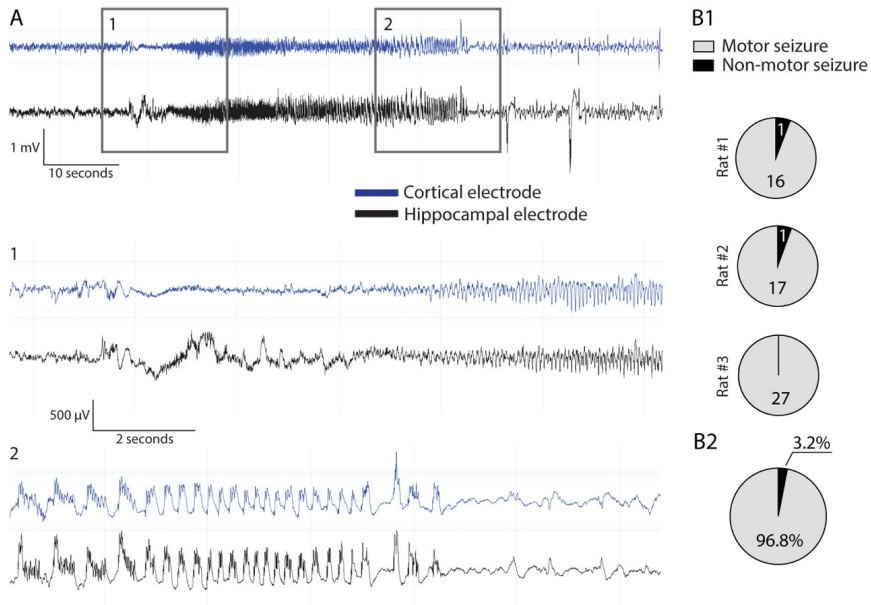

Figure S2. Electrographic characterisation of SRSs in KA induced epileptic rats 4-months post SE induction. (**A**) Representative EEG trace of a SRSs. Magnification 1 shows the beginning of the seizure, illustrating its origin in the hippocampus and the spread to the motor cortex. Magnification 2 indicates the end of the seizure and return to normal EEG activity. (**B1**) Quantification of the proportion of motor SRSs out of all detected electrographic SRSs in 3 rats. (**B2**) Pooled data from rats in B1 represented as percentages. Vast majority of all SRSs were generalised motor seizures.

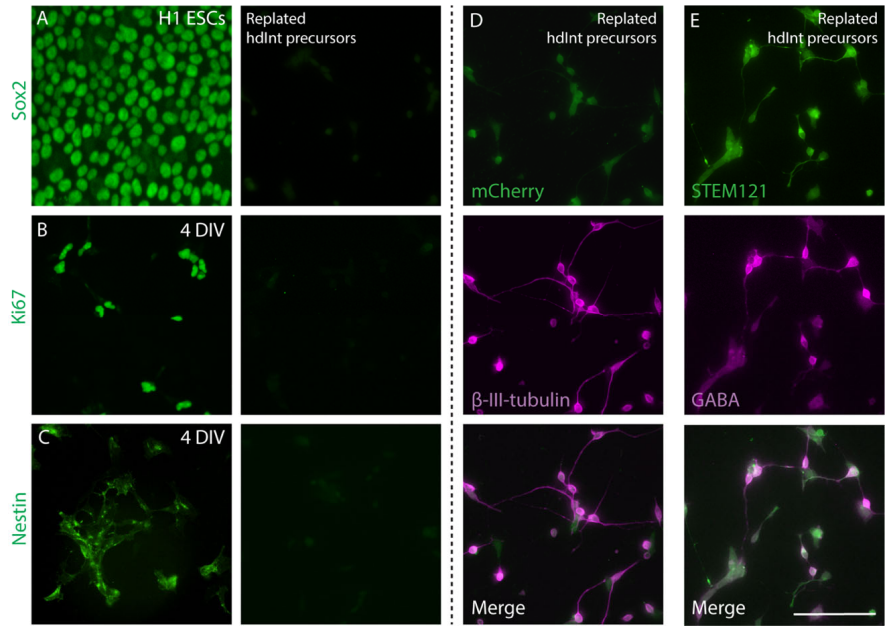

Figure S3. Stainings of left-over hdInt precursor cells remaining after grafting. (**A**) At time of transplantation hdInt precursors did not express Sox 2; H1 ESCs were used as a positive control. (**B, C**) hdInt precursors at time of transplantation did not express Ki67 nor Nestin. 4 DIV hdInt precursors were used as a positive control. (**D**) hdInt precursors expressing mCherry (in green) and β-III-tubulin (in magenta) at the time of transplantation. (**E**) Staining of hdInt precursors with STEM121 (in green), a human cytoplasm marker, and GABA (in magenta). Scale bar 100 μm.

Table S2. Electrophysiological properties of grafted hdInts. Table comparing the electrophysiological properties of grafted cells at 3 months (n = 26 cells) and 6 months (n = 42 cells) PT regarding their response to blue light, their intrinsic properties, and properties of recorded spontaneous postsynaptic events. Values are represented as mean ± SEM. Binomial test was used to compare proportions, Mann-Whitney test for comparison of medians. *, p<.05; **, p<.01; ****, p<.0001. AP, action potential; Ri, input resistance RMP, resting membrane potential; Cm, membrane capacitance; Rs, series resistance; AHP, afterhyperpolarization.

Light response properties

	3 months PT	6 months PT
APs to light	37%	57%**
Peak current (pA)	115.6 ± 20.97	80.52 ± 13.98
Steady state current (pA)	50.23 ± 10.3	41.5 ± 7.9

Intrinsic properties

	3 months PT	6 months PT
Ri (MW)	974 ± 75.23	746.4 ± 62.4*
RMP (mV)	-52.64 ± 1.86	-59.77 ± 1.26**
Cm (pF)	188.7 ± 24.01	205.8 ± 16.37
Rs (MW)	9.91 ± 1.35	8.48 ± 1.08
AP amplitude (mV)	54.56 ± 3.53	76.79 ± 1.95****
AP threshold (mV)	-31.82 ± 1.62	-36.5 ± 1.05*
AP duration (ms)	3.35 ± 0.32	2.04 ± 0.13****
AHP amplitude (mV)	22.28 ± 1.06	28.39 ± 0.91****

Properties of spontaneous postsynaptic currents

	3 months PT	6 months PT
Rise time (ms)	2.0 ± 0.06	1.69 ± 0.04****
Amplitude (pA)	8.14 ± 0.77	15.32 ± 1.6****
Frequency (Hz)	1.36 ± 0.24	2.52 ± 0.2****

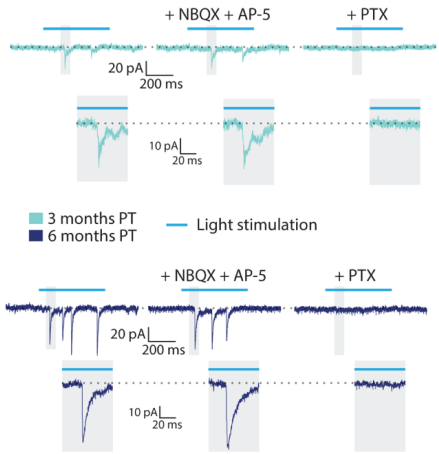

Figure S4. GABAergic nature of hdInt-mediated efferent synaptic connections. Voltage-clamp recordings from patched host cells at 3 months and 6 months PT. Blue light illumination of the slices resulted in delayed synaptic responses which were not affected by NBQX and AP-5 application, while were completely blocked by PTX.

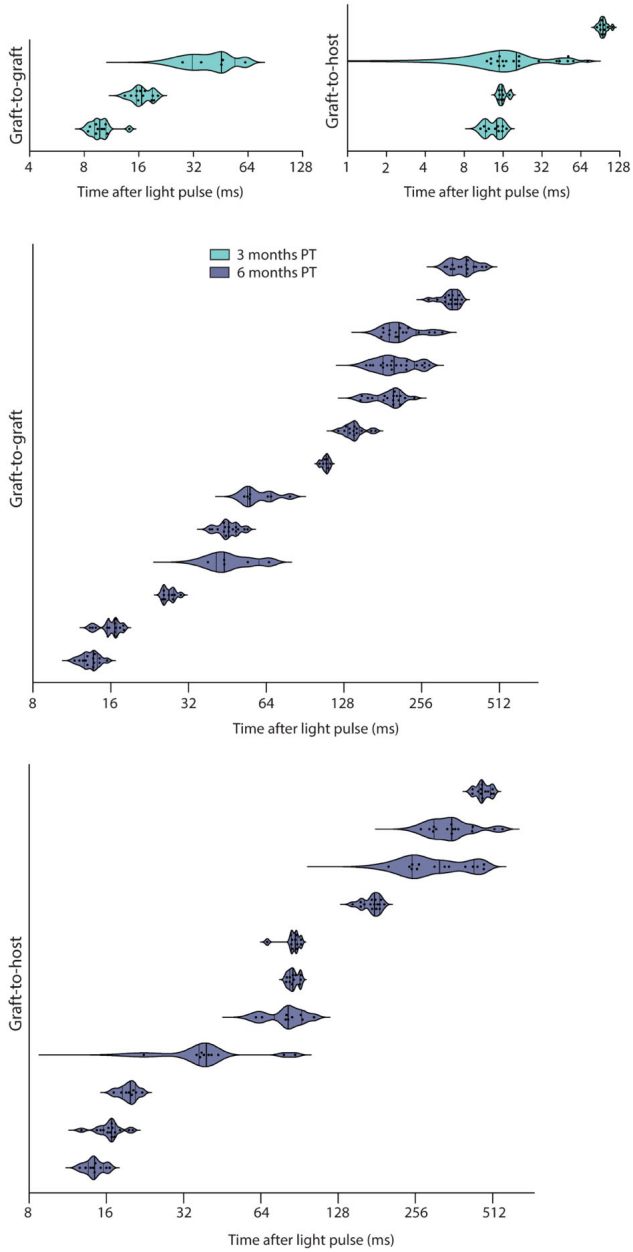

Figure S5. Individual light-induced delayed synaptic responses from each recorded cell. The time was measured from the beginning of the 500 ms light pulse to the base of the first synaptic event afterwards. Each violin plot represents an individual cell, dots are individually measured delays from each recorded trace. Thicker midline represents the median and thinner lines the interquartile range. Time axis is in exponential scale.

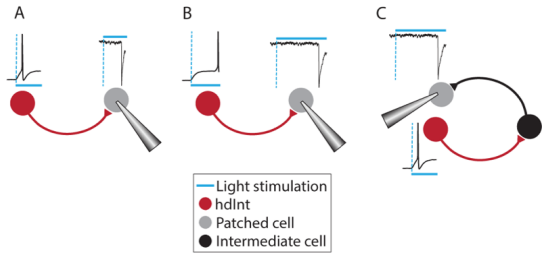

Figure S6. Cartoon of possible synaptic connections between grafted presynaptic cells and patched cells. (**A**) A direct connection between 2 cells with a short light-induced AP onset of the grafted hdInt resulting in a short delayed synaptic response in the patched neuron. (**B**) A direct connection between 2 cells with a delayed light-induced AP onset of the grafted hdInt resulting in a longer delay in the synaptic response in the patched neuron. (**C**) A multi-synaptic connection resulting in a longer delay in the synaptic response of the patched cell.

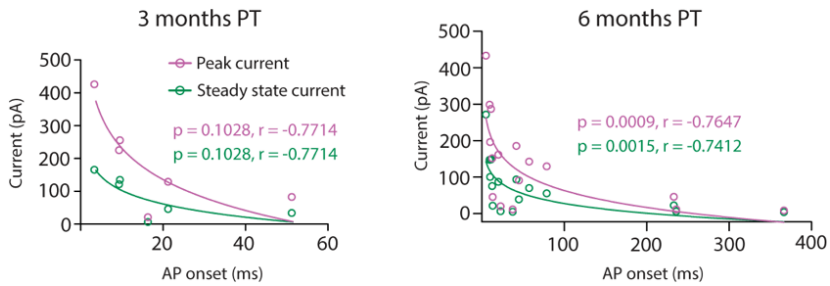

Figure S7. Light-induced currents of grafted hdInts correlated to the light-induced AP onset. The time was measured from the beginning of the 500 ms light pulse to the threshold of the first action potential. Only cells with no observed graft-to-graft connection were analysed. Correlation was not confirmed at 3 months PT (n = 6 cells) but was observed at 6 months PT (n = 16 cells) between both the peak and the steady state current and the AP onset. The higher the current the shorter AP onset. Non-parametric Spearman correlation was used, semilog line was fit in the graphs.